Synthesis of transition metal acetylide complexes and studies into their electronic properties

Sharp, Emma Louise

Award date:
2007

Awarding institution:
University of Bath

Synthesis of Transition Metal Acetylide Complexes and Studies into their Electronic Properties.

Volume 1 of 1
Emma Louise Sharp
A thesis submitted for the degree of Doctor of Philosophy
University of Bath
Department of Chemistry
January 2007

COPYRIGHT

[*Signature*] 

ProQuest LLC
789 East Eisenhower Parkway
P.O. Box 1346
Ann Arbor, MI 48106-1346

Abstract

The research presented herein is concerned with the synthesis of gold(I) and platinum(II) acetylide complexes and studies into their structural, electronic and optical properties.

Chapter 1 introduces the area of molecular electronics and the application of poly-yne polymers as molecular wires. The advantages of incorporating transition metals into the backbone of these polymers and their effect on the electronic and optical properties of these materials are discussed.

Chapter 2 discusses the aurophilic interactions observed in gold(I) alkynyl phosphine complexes previously reported in the literature and provides an overview of their effect on the optical properties of these materials. The chemistry of a series of new gold(I) alkynyl triethylphosphines is described which were synthesised and characterised by spectroscopic and single crystal X-ray diffraction methods to assess the effect of the electronic properties of alkynyl substituents on the architecture of the resulting solid state structure.

Chapter 3 describes the synthesis of new alkynyl chalcogenophene ligands and their use in the preparation of a series of alkynyl chalcogenophene platinum(II) complexes by a novel dehydrohalogenation method involving the *in situ* deprotection of the ligands. Characterisation of the platinum(II) complexes by multinuclear NMR and UV-visible absorption spectroscopies is described along with the preparation and characterisation of a number of alkynyl chalcogenophene gold(I) complexes.

Chapter 4 discusses a series of novel heteroaromatic ligands and the synthetic steps undertaken to develop the chromophore of these compounds for potential use in conjugated organometallic polymers. The ligands and a set of corresponding model dialkynyl metal complexes have been characterised by NMR spectroscopy and their optical properties studied by electronic absorption/emission spectroscopies.

Chapter 5 describes the synthesis and characterisation for the compounds discussed in the previous chapters.

Chapter 6 details the preparation and characterisation of a series of polymer-supported organometallic fragments $[Ru(CO)_4]$ and $[Mo(CO)_5]$ completed at King's College London (2002–2003).

For My Parents
and T.F.Reay

Acknowledgments

I would like to say a huge thank you to my supervisors, Prof. Paul Raithby and Dr. Paul Wilson, not only for taking me in after the closure of King's College but also for their guidance, patience and support throughout my time at Bath.

Special thanks go to Marek Jura and David Bandy for a fun working environment, music compilations and all those cups of coffee and bacon rolls. The lab wouldn't have been the same without certain project students, Stephen, Russell, Olly, Mike and Emma.

Thanks go to Dr. Mary Mahon and Dr. Gabriele Kociok-Köhn for X-ray structures.

I'd like to also thank Dr. Nicholas Leadbeater and the group, Maria Marco, Hanna Torenius, Riina Arvela and Emilie Jolibois, for my time in London.

Thank you to my family for their support.

Finally I'd like to thank the EPSRC for funding.

List of Abbreviations

Å	angstrom
^{n}Bu	*n*-butyl
Cy	cyclohexyl
d	doublet
D	daltons
dbbp	1,4-bis(diphenylphosphino)benzene
DMSO	dimethyl sulphoxide
dppe	1,2-bis(diphenylphosphino)ethane
dppf	1,1'-bis(diphenylphosphino)ferrocene
dppm	bis(diphenylphosphino)methane
ε	molar extinction coefficient
esu	electrostatic unit
Et	ethyl
eV	electron volts
h	hour(s)
HMQC	heteronuclear multiple quantum coherence (NMR experiment)
HOMO	highest occupied molecular orbital
IR	infra red
L	ligand
LUMO	lowest unoccupied molecular orbital
m	multiplet
MLCT	metal to ligand charge transfer
Me	methyl
NLO	nonlinear optics
NMR	nuclear magnetic resonance
Ph	phenyl
^{i}Pr	*iso*-propyl
Py	pyridine
R	alkyl group
ROP	ring-opening polymerisation
s	singlet
S	solvent
t	triplet
tbbp	1,2,4,5-tetrakis(diphenylphosphino)benzene
TLC	thin layer chromatography
Tol	tolyl
UV/vis	ultra violet/visible
Xy	xylene

Chapter 1 Introduction

1.1 Molecular Electronics

The growing demand for ever more powerful computational devices has been the driving force behind the miniaturisation of electronic components. The production of devices which are continually reduced in size has considerable financial implications, however, such miniaturisation has physical limiting factors, for example, the silicon oxide layers used within silicon chips become poorly insulating when reduced to a "three-atom-thick level" resulting in charge leakage.[1]

Molecular electronics involves the replacement of electronic components, the simplest being wires, with one or several discrete molecules, and has allowed miniaturisation down to the nanometre scale with molecular-scale wires ranging from 1 – 100 nm in length and widths of approximately 0.3 nm.[2] A molecular wire generally consists of a molecule with a donor group and an acceptor group bridged by a conductive spacer group (Figure 1.1).

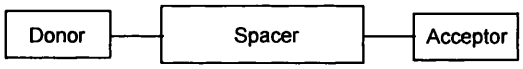

Figure 1.1: General requirements for a molecular wire

The first notion of using molecules as alternatives to silicon chips was made by Aviram and Ratner in 1974[3] who discussed the theoretical construction of a molecular rectifier comprising a single molecule with a donor π-system, such as thiofulvalene, and an acceptor π-system, tetracyanoquinodimethane, separated by a sigma-bonded unsaturated aliphatic ($-CH_2-$) bridge (Figure 1.2).

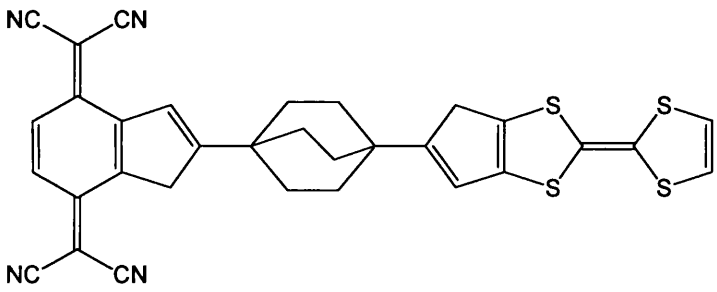

Figure 1.2: Example of a molecular rectifier

The starting point of many wires is a conjugated molecule consisting alternate carbon-carbon single and double or triple bonds which allows for the conduction of electrons through a π-system.[4] There are many examples of 'molecular wires' in the literature, all displaying the same desirable features, electrical conductivity, linearity and well defined length. Although a large extent of research has produced organic molecular wires there is an increasing amount of work on organometallic molecular wires.[5]

1.1.1 Organic Poly-ynes

Organic poly-ynes have received much attention due to their extended π-conjugation, rigid structure and linear geometry, all of which contribute to the novel optical properties of these materials, which show potential applications to molecular electronics and are good candidates for molecular wires.[1,6,7] Poly-ynes are materials which consist of alternating single and triple bonds, for example buta-1,3-diyne (Figure 1.3).

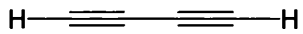

Figure 1.3: Example of a poly-yne

The structural and optical properties of a series of aryl end capped poly-ynes have been explored (Figure 1.4).[8] The structure of C_6H_5–$(C{\equiv}C)_6$–C_6H_5 is approximately linear with all C–C≡C bond angles in the range 177 – 180°. The electronic absorption spectra of these poly-ynes show red shifts in absorption maxima as the conjugation length is increased through n = 2 → n = 8 and on increasing the electron density, C_6H_5–$(C{\equiv}C)_6$–C_6H_5 → $MeOC_6H_4$–$(C{\equiv}C)_6$–C_6H_4OMe.

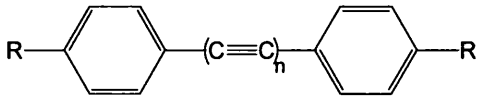

n = 2,4,8; R = H
n = 6; R = H, ^{t}Bu, MeO

Figure 1.4: Series of diarylpoly-ynes

1.2 Transition Metal-Containing Conjugated Polymers

The introduction of heavy transition metals into the backbone of organic polymers enhances the properties of the material by extending π-electron conjugation along the length of the polymer chain through mixing of the metal and ligand orbitals.[9] The presence of a heavy metal centre also increases spin-orbit coupling which relaxes the selection rules and allows intersystem crossing and light emission from the triplet excited state (phosphorescence) to occur[10] (Figure 1.5). In addition, the introduction of transition metal phosphines with long alkyl chains can improve the solubility of the polymers in organic solvents.[11]

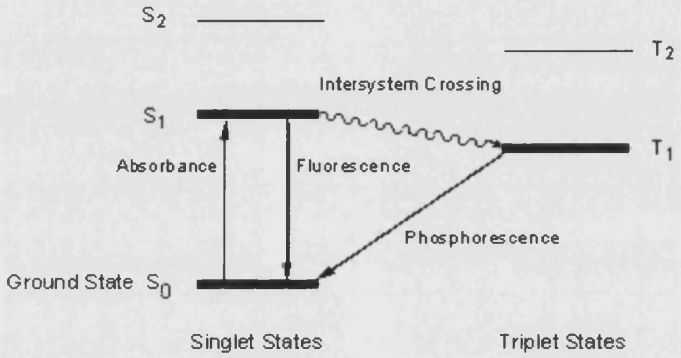

Figure 1.5: Intersystem crossing between triplet and singlet states

Considering the inherent luminescent properties of transition metal complexes, it is not surprising that alkynyl groups have been integrated into these materials producing systems with novel optical and electronic properties such as nonlinear optical effects,[12-14] luminescence,[15,16] electronic communication[5] and liquid crystallinity.[17] Transition metal alkynyl complexes have been the subject of several extensive reviews in the literature.[18-20]

1.2.1 Types of Transition Metal-Containing Conjugated Polymers

Transition metal-containing conjugated polymers may be divided into three groups identified as Types I, II and III and described as tethered, coupled and incorporated, respectively. Type I polymers are those with the metal group tethered to the backbone of the polymer by a linker group as shown by the example in Figure 1.6a where Ni^{2+} cyclam is incorporated into poly(3-methylthiophene).[21] In these materials the electronic and optical properties are generally very similar to those of the untethered complex. Materials with the metal directly coupled to the polymer backbone generally show properties that are a modification of both the properties of

the polymer and of the metal units, are classified as Type II. An example of this class is illustrated in Figure 1.6b in which a rhenium-containing fragment is integrated into a 5,5'-(2-thienyl)-2,2'-bithiazole polymer.[22] Since conducting polymer backbones and many metal ions are redox active it is possible to electrochemically tune the properties of these materials.[23] Finally, and pertinent to the work described in the following Chapters, are Type III materials where the metal is placed into the backbone of the polymer and has a greater influence over the electronic properties of the material (Figure 1.6c).[24]

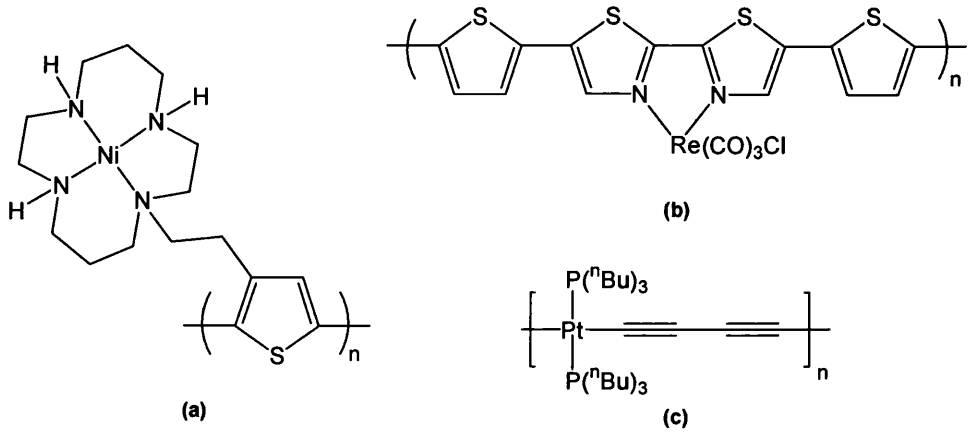

Figure 1.6: (a) Type I, (b) Type II and (c) Type III metal containing conjugated polymers

Type I and II polymers are most commonly formed by electropolymerisation methods, which were first used to prepare organic polymers such as polythiophene.[25] In the case of Type III materials, preparation is achieved by condensation routes, particularly for platinum 'rigid-rod' polymers (Figure 1.6c) or by ring-opening methods to obtain ferrocene-containing polymers. Ring-opening polymerisation (ROP) provides access to high molecular weight poly(ferrocenyl silanes) from silaferrocenophanes (Figure 1.7) and has been used extensively by Manners and co-workers to prepare ferrocene-containing polymeric species.[26-30]

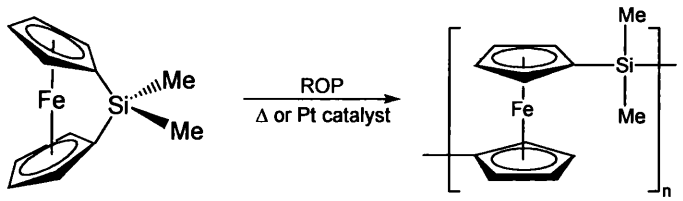

Figure 1.7: Ring-opening polymerisation of silaferrocenophane to poly(ferrocenylsilane)

The name 'rigid-rod', in reference to metal-acetylide polymers, is derived from the rigidity of the metal-alkyne unit due to its linear geometry. The rigid structure of these polymers facilitates the formation of $d\pi$-$p\pi$ interactions between the metal and acetylide, effectively increasing the conjugation length, along the polymer, through the metal centres.

1.3 Preparation of Transition Metal Alkynyl Polymers

1.3.1 Group 10 metals

In 1970 Hagihara and co-workers[31] developed a synthetic route to mono- and di-alkynyl transition metal compounds by a copper(I)-catalysed dehydrohalogenation reaction between a metal halide and an alkyne in the presence of an amine, under an inert atmosphere, as illustrated in Scheme 1.1.

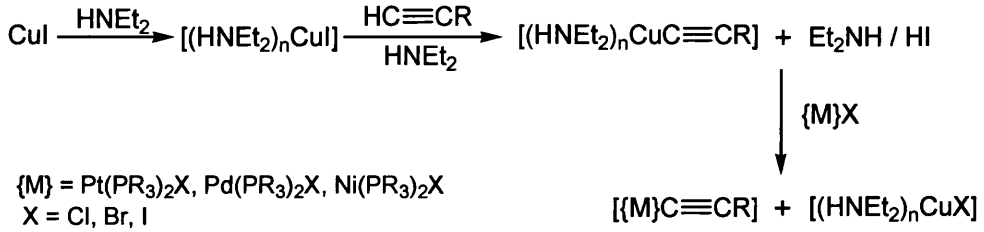

Scheme 1.1: Synthetic route to alkynyl transition metal compounds

This method was first used to prepare polymers of $Pd(P^nBu_3)_2$ and $Pt(P^nBu_3)_2$ groups bridged by butadiyne and diethynylbenzene units in 1975 (Scheme 1.2(i)).[32] The polymers were determined to have low molecular weights (M_w = 5700 – 7300 D). The tributylphosphine groups bound to the metal aid the solubility of the polymers; the solubility is seen to decrease in the order P^nBu_3> PEt_3 > PMe_3. Subsequent work by Hagihara has led to reports of Group 10 metal alkyne polymers with much higher molecular weights ($M_w > 10^5$ D) prepared by one of three general copper-catalysed routes: (i) dehydrohalogenation, (ii) oxidative coupling and (iii) alkynyl-ligand exchange.

(i) Dehydrohalogenation

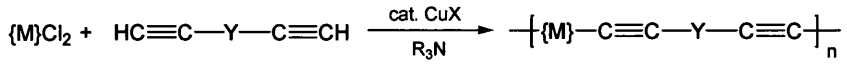

(ii) Oxidative Coupling

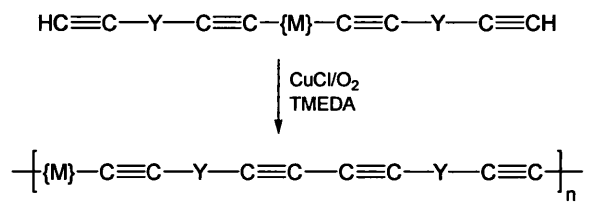

(iii) Alkynyl Ligand Exchange

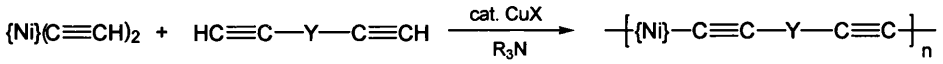

M = trans-Pt(PR_3)$_2$, trans-Pd(PR_3)$_2$; Ni = trans-Ni(PR_3)$_2$

Y = none, -C_6H_4-, 2,5-$C_6H_2Me_2$-, -C_6H_4-C_6H_4-

Scheme 1.2: Copper-catalysed synthetic methods

The first of the synthetic routes is dehydrohalogenation involving the copper-catalysed polycondensation reaction between transition metal halides and diterminal alkynes (Scheme 1.2) in an amine solvent, usually diethylamine, which also acts as an acid acceptor in the reaction. Polymerisation can occur at room temperature or under reflux conditions.[33] The oxidative coupling method extends the utility of the catalytic system used in Hay's Coupling reaction,[34] namely a copper halide and oxygen, to organometallic synthesis by coupling bis(terminalalkynyl) metal complexes. Unlike with dehydrohalogenation, progress of the reaction is dependent only on the availability of the monomer and allows high degrees of polymerisation to occur, thus, the degree of polymerisation achieved is invariably high. Generally, both of the above methods work well for platinum and palladium poly-ynes, but do not proceed for nickel due in part to the decomposition of nickel halide complexes in amine solvent and also to the reactivity of nickel centres in an oxidising environment. Thus, use of the copper-catalysed alkynyl ligand exchange reaction is necessary to prepare nickel-containing polymers.

Alternatively, Lewis *et al.* used bis-trimethylstannyl(acetylide) species, $Me_3SnC{\equiv}C–R–C{\equiv}CSnMe_3$ (R = none; C≡C; *p*-C_6H_4; *p*-C_6H_4-C_6H_4),[35-38] to prepare a number of nickel, palladium and platinum-containing poly-ynes in yields comparable to those of Hagihara

(Scheme 1.3). Transition metal halides, *trans*-[$M(PBu_3)_2Cl_2$], are treated with one equivalent of $Me_3SnC{\equiv}C–R–C{\equiv}CSnMe_3$ in the presence of a catalytic amount of copper iodide, in toluene, rather than amine thus eliminating the problems with instability of the metal halides. However, care has to be taken due to the toxicity of the tin-containing reagents.

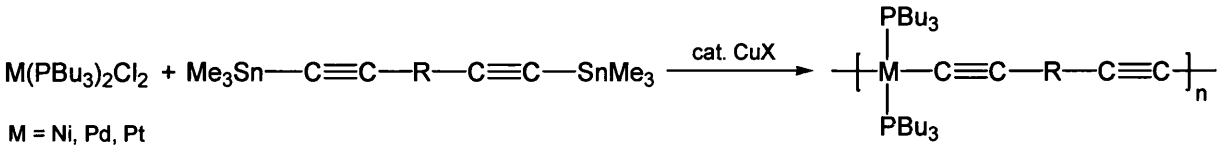

Scheme 1.3: Preparation of Group 10 poly-ynes using trimethylstannyl reagents

In order to assess whether this methodology was applicable to other transition metals [$Rh(PMe_3)_4Cl$] was treated with one equivalent of $Me_3SnC{\equiv}C–p\text{-}C_6H_4\text{-}C_6H_4\text{-}p–C{\equiv}CSnMe_3$ forming the oligomer, $[Rh(PMe_3)_3(SnMe_3)(–C{\equiv}C\text{-}p\text{-}C_6H_4\text{-}C_6H_4\text{-}p\text{-}C{\equiv}C–)]_n$, which was isolated as an insoluble white powder.[37]

The use of bis-trimethylstannyl(acetylides) has also provided access to Group 8 metal-containing monomeric and polymeric complexes (Figure 1.8).[39]

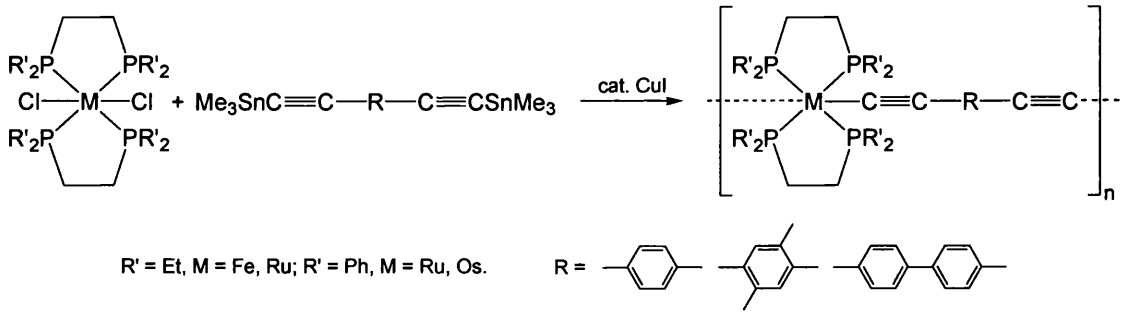

Figure 1.8: Fe, Ru and Os-containing polymers

The dehydrohalogenation process has been extended by Dixneuf to access heterobimetallic poly-yne systems by reaction of metal halides with organometallic tetra-ynes. By incorporating ferrocene or $Ru(dppe)_2$ into the tetra-ynes, Fe/Pd-, Fe/Ni-, and Ru/Pd-containing oligomers were prepared (Figure 1.9) with molecular weights of 21,400 D and 26,100 D for the ferrocene systems, respectively, and 14,800 for the ruthenium oligomer.[40]

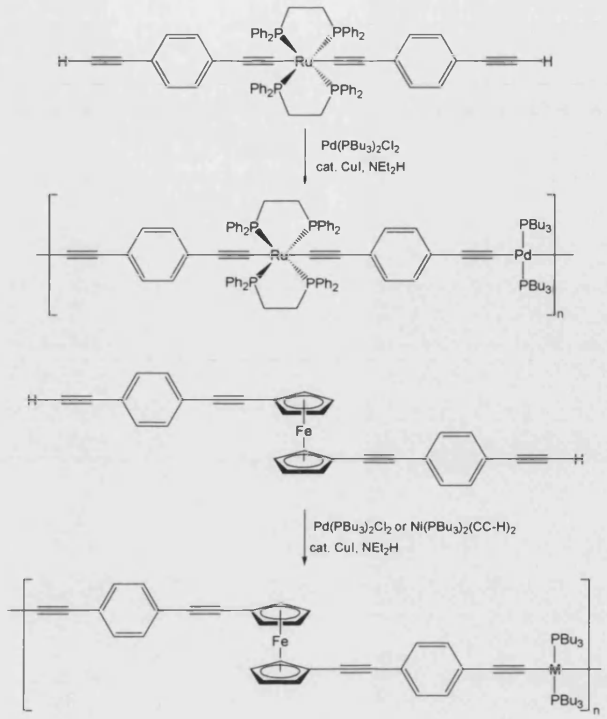

Figure 1.9: Preparation of Fe/Pd-, Fe/Ni-, and Ru/Pd-containing oligomers

1.3.2 Group 11 metals

Group 11 transition metal alkynyl complexes often have complex structures, for example polymeric structures displaying alkyne units which are σ-bonded to one metal centre and π-bound to others.[41] An example of such a complex is $\{[Ag(PMe_3)_2]^+[Ag(C{\equiv}CPh)_2]^-\}$ illustrated in Figure 1.10.[42]

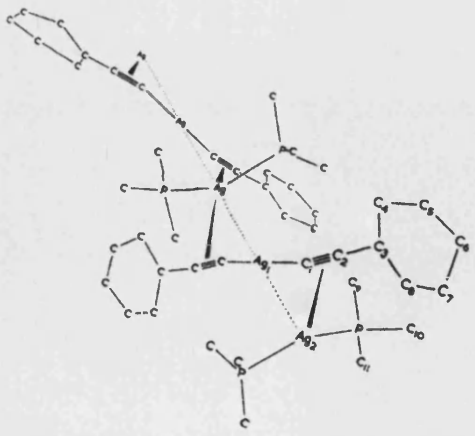

Figure 1.10: Polymeric structure of $\{[Ag(PMe_3)_2]^+[Ag(C{\equiv}CPh)_2]^-\}$[42]

Such materials are often relatively insoluble and, therefore, difficult to characterise beyond their solid state structures. In some systems, copper-copper and silver-silver interactions have been observed, for example, copper and silver complexes can adopt a triangular geometry with μ_3-η^1 bonding motif as seen in the structure of $[Ag_3(\mu\text{-dppm})_3(\mu_3\text{-}\eta^1\text{-}C{\equiv}C\text{-}C_6H_4\text{-}NO_2\text{-}p)]$ (Figure 1.11).[43]

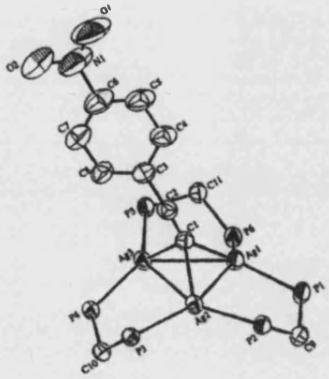

Figure 1.11: Structure of $[Ag_3(\mu\text{-dppm})_3(\mu_3\text{-}\eta^1\text{-}C{\equiv}C\text{-}C_6H_4\text{-}NO_2\text{-}p)]$[43]

The structures of gold(I) alkynyl complexes tend to be quite different to their copper and silver analogues due to the fact that gold(I) species generally exhibit linear coordination geometry. Puddephatt and co-workers reported a range of organometallic polymers of the general formula $[(AuC{\equiv}C\text{–}Ar\text{–}C{\equiv}CAuPR_2(C_6H_4)_nPR_2)_x]$ where Ar = 4,4'–C_6H_4–C_6H_4; 1,4–C_6H_4; 1,4–C_6H_4–2,5–Me_2 and R = Ph; ^{i}Pr (Figure 1.12).[44] These polymers were prepared by reaction of the gold(1) diacetylide complex, $[(AuC{\equiv}C\text{–}Ar\text{–}C{\equiv}CAu)_x]$, with a diphosphine, $PR_2(C_6H_4)_nPR_2$ in dichloromethane, at room temperature, or by the reaction of diethynylarene with the dinuclear gold(I) diphosphine complex, $[(ClAuR_2P\text{–}Ar\text{–}PR_2AuCl]$, in the presence of a base.

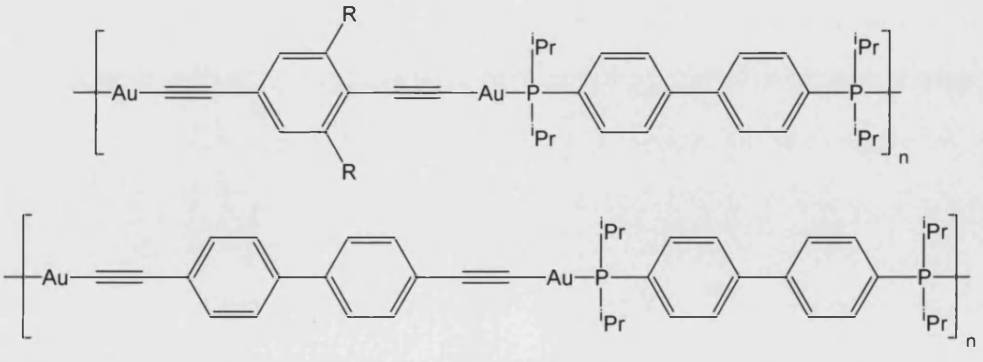

Figure 1.12: Gold(I) alkynyl polymers prepared by Puddephatt; R = H, Me.

The polymers are air stable, pale yellow powders with a molecular weight in the order of 15,000; they are insoluble in most organic solvents but have limited solubility in halogenated solvents such as dichloromethane.

Gold(I) alkynyl polymers incorporating diisocyanide and diacetylide bridging ligands have been formed by reaction of linear digold complexes, AuC≡CRC≡CAu, with diisocyanoarenes, C≡N-R'-N≡C, in dichloromethane (Figure 1.13).[45] As with the diphosphine bridged materials described previously, these polymers are insoluble in organic solvents making characterisation and study awkward; synthesis of more alkynyl isocyanide complexes has allowed characterisation of their general properties.

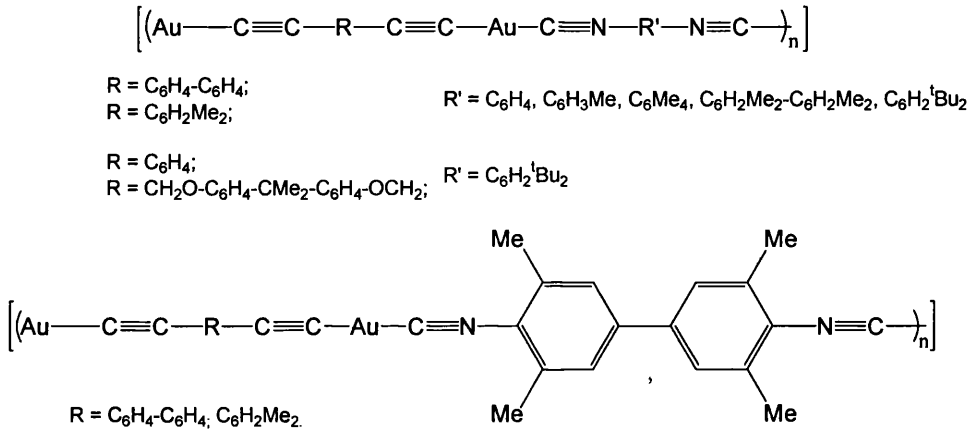

Figure 1.13: Gold(I) alkynyl polymers incorporating diisocyanide and diacetylide bridging ligands

In order to extend their research beyond one-dimensional polymers, a number of trigold(I) triacetylide complexes, $[C_6H_3(C{\equiv}C{-}Au{-}L)_3]$ (L = isocyanide, phosphite, phosphine), have been synthesised by Puddephatt *et al.*[46] These complexes form weakly bound polymers by intermolecular aurophilic interactions as well as covalently linked polymers of the type, $[\{C_6H_3(C{\equiv}C{-}Au)_3\}_2(L{-}L)_3]$, *via* bidentate ligands (L–L) (Figure 1.14). The polymers with bridging bidentate ligands precipitate as pale yellow solids which are insoluble in organic solvents. Comparison of their IR and X-ray photoelectron spectroscopy (XPS) spectral data with that of the corresponding model compounds corroborated the proposed structures.

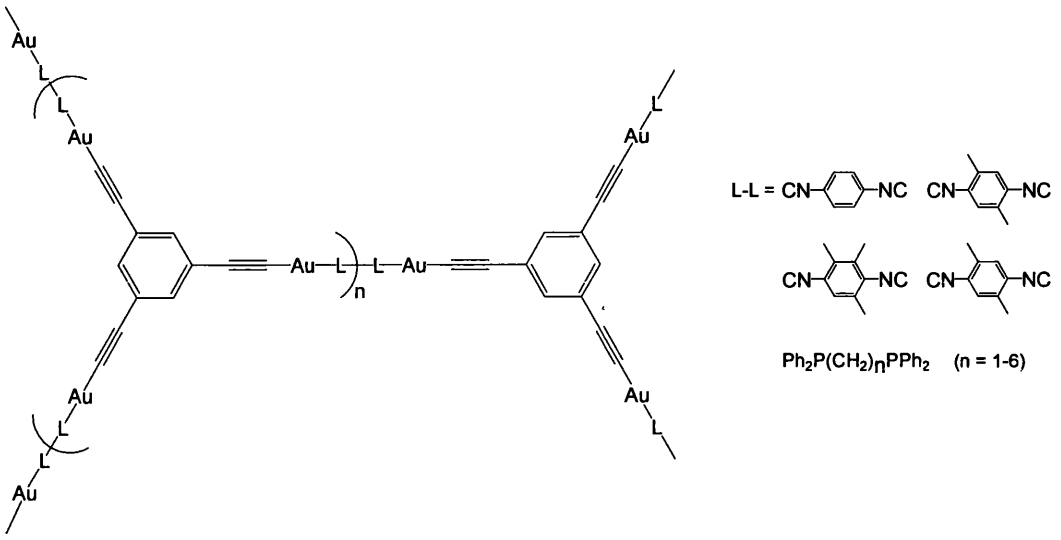

Figure 1.14: Trigold(I) triacetylide polymers bridged by bidentate ligands

The 3,5-diethynylpyridine-containing gold polymer shown in Figure 1.15a was prepared by reaction of [AuCl(SMe_2)] with 3,5-diethynylpyridine and triethylamine in a dichloromethane solution affording a bright yellow powder.[47] The polymer was found to be insoluble in all common solvents impeding further purification and NMR spectroscopic characterisation. Model dinuclear complexes (Figure 1.15b) with the general formula [$(AuL)_2\{\mu$-$(C\equiv C)_2Py\}$] (L = CN^tBu, PMe_3, PPh_3, P(*p*-Tol)$_3$ were obtained by reacting the polymer with monodentate ligands in a 1:2 molar ratio.

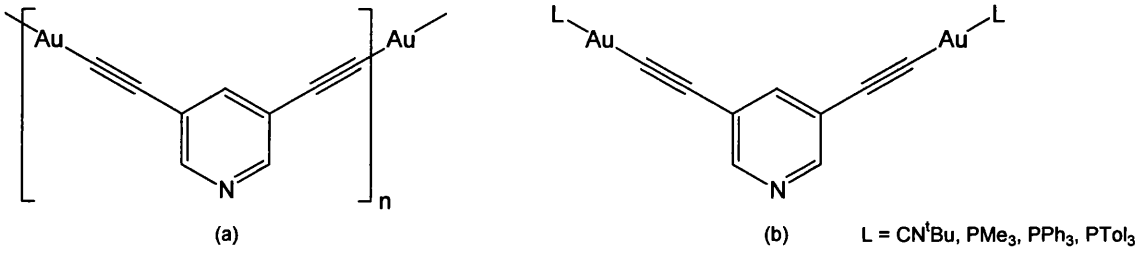

Figure 1.15: (a) 3,5-Diethynyl pyridine-containing gold polymer and (b) model compounds

The crystal structure of [$(AuP(p\text{-}Tol)_3)_2\{\mu$-$(C\equiv C)_2Py\}$] revealed the presence of intermolecular Au····Au interactions giving rise to infinite polymer chains of the digold molecules similar to that found in the crystal lattice of the digold complex, [$(Me_3P)Au$–C≡C–$(C_6H_2Me_2)$–C≡C–$Au(PMe_3)$], reported by Puddephatt *et al.*[48]

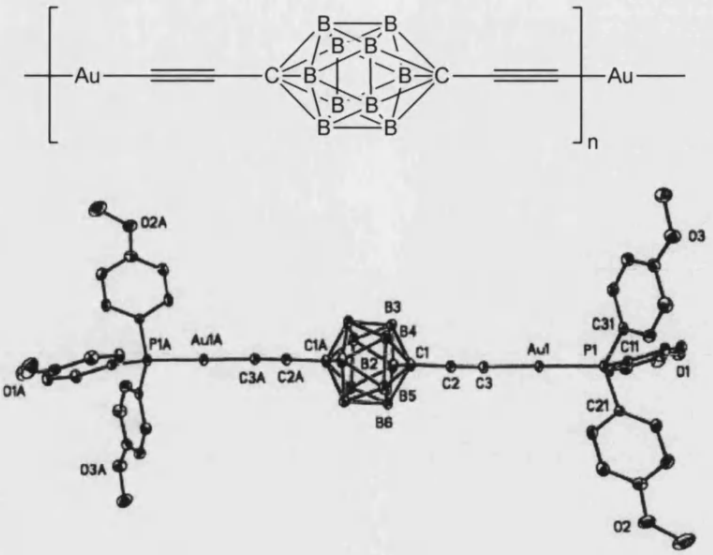

Figure 1.16: Gold-decH_2 polymer and crystal structure of model complex [{AuP(4-$C_6H_4OMe)_3$}$_2$(μ-dec)]

Using the same synthetic method Vicente *et al* have also prepared a rigid-rod gold(I) alkynyl polymer incorporating 1,12-bis(ethynyl)-1,12-dicarba-*closo*-dodecacarborane(12) (referred to as decH_2) and the crystal structure of model compound [{AuP(4-$C_6H_4OMe)_3$}$_2$(μ-dec)] determined to compare with the proposed structure (Figure 1.16).[49] The polymer was found to darken in colour and show signs of decomposition to metallic gold after washing with water and drying in air, for this reason, rather than characterising the material it was suspended in dichloromethane and treated with an excess of ^{t}BuNC to afford [(AuCN^tBu)$_2$(μ-dec)] which is more stable.

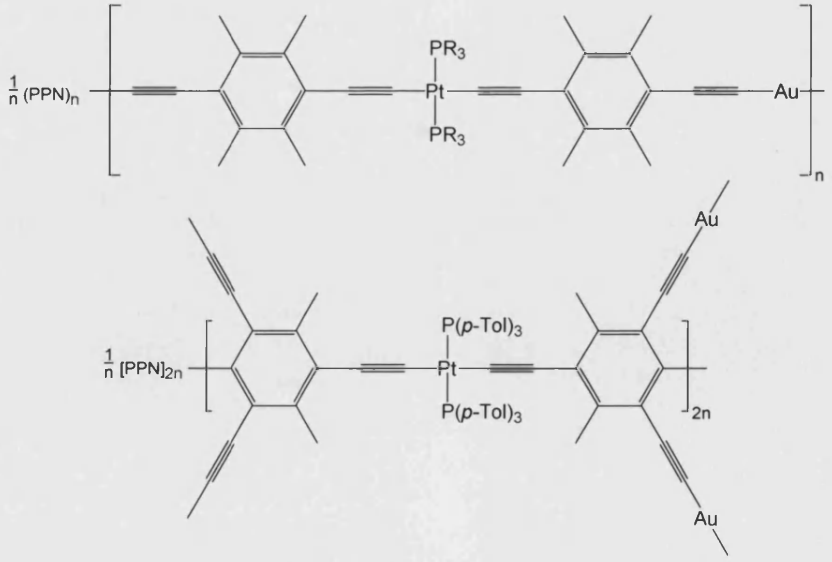

Figure 1.17: Pt(II)–Au(I) alkynyl polymers, R = Me, Bu, Ph.

Synthesising gold(I) alkynyls led these researchers to prepare novel anionic heteronuclear Pt(II)–Au(I) alkynyl polymers (Figure 1.17).[50] This was achieved by reacting *trans*-[Pt(C≡CC$_6$Me$_4$C≡CH-4)$_2$(PR$_3$)$_2$] (R = Me, Bu, Ph) or *trans*-[Pt{C≡CC$_6$Me$_2$(C≡CH)$_2$-3,5}$_2$(P(*p*-Tol)$_3$)$_2$] with PPN[Au(acac)$_2$] (PPN = Ph$_3$P=N=PPh$_3$; acac = acetylacetonate) in dichloromethane to form linear polymers (PPN)$_n$-[*trans*-Pt{(C≡CC$_6$Me$_4$C≡C-4)$_2$Au}(PR$_3$)$_2$]$_n$ or branched species, (PPN)$_{2n}$-[*trans*-Pt{C≡CC$_6$Me$_2$(C≡C)$_2$-3,5}$_2$Au$_2$(P(*p*-Tol)$_3$)$_2$]$_n$, respectively.

These polymers were found to be insoluble in common solvents hindering purification and full characterisation making the preparation of model compounds essential to obtain structural information, a recurring feature of gold poly-yne chemistry.

An important factor that relates to the formation of gold polymeric materials is the ability of gold(I) centres to form intermolecular Au····Au contacts and thus form chain structures in this way. This process has already been mentioned when discussing the crystal structure of [(AuP(p-Tol)$_3$)$_2${μ-(C≡C)$_2$Py}],[47] and this is a common feature in many gold-containing systems. The phenomenon is known as "aurophilicity" and is discussed in detail in the next section.

1.4 Aurophilicity

In particular, when comparing gold alkynyls to platinum alkynyls the presence of Au····Au aurophilic interactions represents a marked difference that can be exploited synthetically. The term 'aurophilicity' was first coined by Schmidbaur to describe the phenomenon in the structural chemistry of gold of low-coordinate gold(I) compounds associating into dimers, oligomers or polymers *via* Au····Au contacts following a growth of crystallographic evidence.[51,52]

Gold(I) is generally two-coordinate in its complexes with linear coordination geometry. The neutral gold complexes, L–Au–X, are formed by coordination of an anionic ligand (X) and a neutral ligand (L) while cationic and ionic species such as [AuL$_2$]$^+$ and [AuX$_2$]$^-$, are afforded by 2L or 2X, respectively. If the ligands X and L are small the individual molecules may

associate into dimer pairs or extended polymers depending on the nature of the ligands (Figure 1.18).[53]

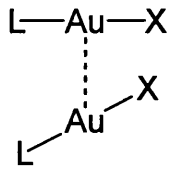

Figure 1.18: Intermolecular Au····Au interaction of linear gold(I) complexes (Aurophilicity)

This weak Au····Au bonding occurs between closed shell metal centres such as Au^+ ([Xe] $4f^{14}$ $5d^{10}$) and with an energy of ~ 5 – 10 kcal mol^{-1} (~ 4 – 40 kJ mol^{-1}) comparable with hydrogen bonds. Typical inter- and intramolecular Au····Au distances have been observed in the range of 2.75 – 3.40 Å[54] which is approaching the sum of their van der Waals radii (3.4 Å). These interactions are more commonly found than in the structural chemistry of copper and silver analogues.

Aurophilic interactions have the following characteristics[52]:

- They occur at two-coordinate gold centres perpendicular to the molecular axis.
- Metal-metal distances are shorter than the sum of two van der Waals radii (3.4 Å).
- Several gold atoms may associate at a given gold centre in a polynuclear species.
- Interaction has small bond energy.
- In solution, the solvation of molecules dominates over intermolecular interactions

The phenomenon of aurophilicity has undergone theoretical studies using *ab initio* and density functional methods by Pyykkö and co-workers[55,56] who conclude that "metallophilic attraction" is an electronic correlation effect which is strengthened by relativistic effects and has a maximum for gold.[57]

A systematic study of the geometrical properties of gold-gold interactions using the Cambridge Structural Database was reported by Desiraju and Pathaneni.[58] Their preliminary finding showed a large number of gold-gold distances with a range of 2.5 – 4.0 Å which included Au–Au bonds within clusters (2.55 – 3.10 Å) and longer bonds assigned to Au····Au non-bonded interactions in the region of 2.9 – 3.3 Å. Intermolecular Au····Au contacts between molecules containing a single gold atom were found to have gold-gold distances of 2.8 – 3.4 Å.

1.4.1 Aurophilic Interactions in Gold(I) Alkynyl Phosphine Complexes

Among the first structures determined in which a Au····Au interaction was observed was $[\{Au(C{\equiv}CPh)\}_2(\mu\text{-}Ph_2PCH_2CH_2PPh_2)]$.[59] The asymmetric unit of the cell consists of two molecules positioned *anti* to each other. The Au····Au distances are 3.153 Å [Au(1)····Au(2)] and 5.308 Å [Au(2)····Au(2')].

The electronic absorption spectrum of $[\{Au(C{\equiv}CPh)\}_2(\mu\text{-}Ph_2PCH_2CH_2PPh_2)]$, in dichloromethane, displays an intense band from 260 – 310 nm which was assigned to the intraligand $\pi - \pi^*$ transition of the C≡CPh groups by Che.[60] This was compared with the electronic absorption spectra of $[Au(PPh_3)(C{\equiv}CPh)]$ and $[N(PPh_3)_2][Au(C{\equiv}CPh)_2]$. All three spectra are similar which suggests that $[\{Au(C{\equiv}CPh)\}_2(\mu\text{-dppe})]$ may be thought of as two non-interacting Au(C≡CPh) units which are bridged by the dppe ligand. The emission spectrum of $[\{Au(C{\equiv}CPh)\}_2(\mu\text{-dppe})]$ in dichloromethane has a maximum at 420 nm but in the solid state this maximum is considerably red-shifted to 550 nm. This shift is attributed to Au····Au interactions present in the solid state structure increasing the contribution from MLCT. In solution the two $[\{Au(C{\equiv}CPh)\}_2(\mu\text{-dppe})]$ molecules are thought to separate allowing the intraligand phosphorescence to dominate.

While Che[61] and co-workers have done much further work in this area, the Puddephatt[62] and Yam[63] groups have also contributed significantly. Humphrey *et al*[64] have prepared a variety of gold(I) alkynyl complexes as part of their ongoing investigations into the use of organometallic complexes for non-linear optics.

Turning their attention away from covalently bonded gold containing rigid rod polymers to somewhat smaller complexes of gold(I) acetylides which associate in the solid state to form non-covalently bonded polymers through Au····Au interactions, a range of model compounds were synthesised and their photophysical properties investigated.[48,65,62] The structures of model compounds $[(Me_3P)Au{-}C{\equiv}C{-}(C_6H_2Me_2){-}C{\equiv}C{-}Au(PMe_3)]$ and $[XyNC{-}Au{-}C{\equiv}C{-}(C_6H_4NO_2)]$ were determined to gain structural and characterisation data.[48]

The asymmetric unit of the gold(I) diacetylide complex, [(Me_3P)Au–C≡C–($C_6H_2Me_2$)–C≡C–Au(PMe_3)] consists of two molecules (Figure 1.19). Each molecule is almost linear [C(1)–Au(1)–P(1), 177.9°; C(2)–C(1)–Au(1), 177.0°; C(1)–C(2)–C(3), 176.0°] with little deviation in bond lengths as compared with previous complexes and gold(I) phosphines. However, in the crystal lattice these molecules are packed in zigzag chains held together by short Au····Au interactions (3.136 Å), in effect producing a weakly bound polymer. The shortest distance between ring centroids is 9.18 Å which is too long for π-stacking interactions to be present.

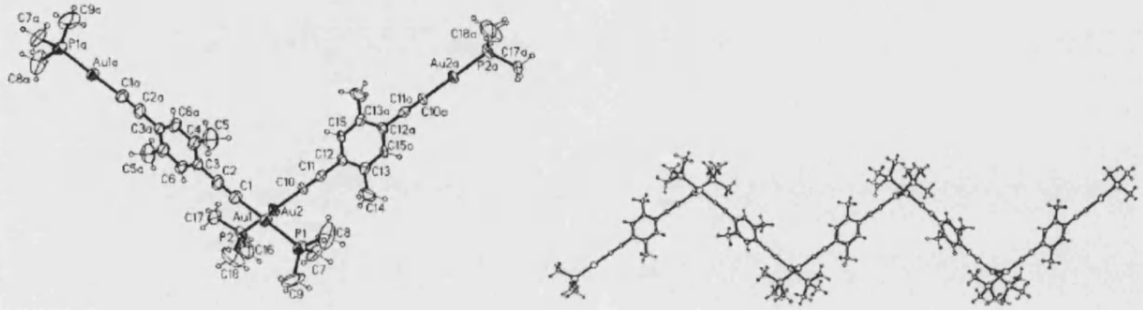

Figure 1.19: Structure of [(Me_3P)Au–C≡C–C_6H_2-Me_2–C≡C–Au(PMe_3)] and zigzag chains in crystal lattice

In contrast, the asymmetric unit of [XyNC–Au–C≡C–($C_6H_4NO_2$)] contains only one molecule. Although there are no short Au····Au interactions between neighbouring molecules, there is evidence of π-stacking with a distance of 3.722 Å between the ring centroids of the 4-nitrophenylacetylide and xylyl isocyanide on adjacent molecules. Despite the difference between these two complexes, both display a large red shift in emission on going from solution to the solid state.

Although Yam and co-workers have synthesised a variety of monogold(I) alkynyl phosphine complexes they have also made many polynuclear copper(I), silver(I) and gold(I) alkynyl phosphine complexes which exhibit luminescent properties.[63]

The structures of [Au_2(dbbp)($C{\equiv}CPh)_2$] and [Au_4(tbbp)($C{\equiv}CPh)_4$], where dbbp is 1,4-bis(diphenylphosphino)benzene and tbbp is 1,2,4,5-tetrakis(diphenylphosphino)benzene, have been determined.[66]

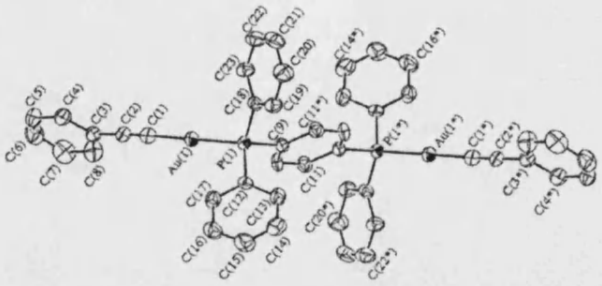

Figure 1.20: Structure of $[Au_2(dbbp)(C{\equiv}CPh)_2]$

$[Au_2(dbbp)(C{\equiv}CPh)_2]$ was prepared by the reaction of $[Au(C{\equiv}CPh)_2]_\infty$ with dbbp. The geometry about the gold centre is close to linear [P(1)–Au(1)–C(1), 175.5°; Au(1)–C(1)–C(2), 175.8°] and there are no short Au····Au intermolecular contacts present (Figure 1.20). The shortest distance between adjacent gold atoms is 4.62Å due to the phenyl rings on the phosphine blocking a close approach. However, on going from the dbbp ligand to the tbbp ligand the solid state structure is remarkably different (Figure 1.21).

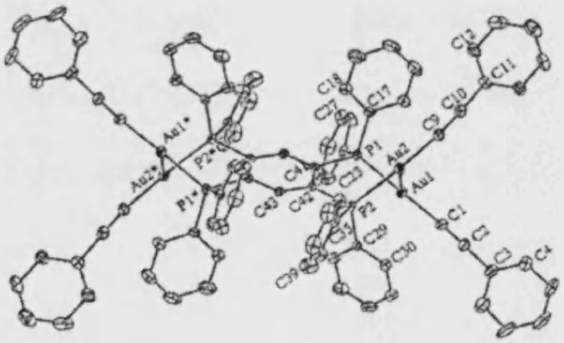

Figure 1.21: Structure of $[Au_4(tbbp)(C{\equiv}CPh)_4]$

The bond lengths are similar with other gold(I)alkynyl phosphine complexes in the literature and the bond angles of the gold alkyne units are approximately linear [P(1)–Au(1)–C(1), 174.3°; Au(1)–C(1)–C(2), 175.6° and 171.9°].

There are short intramolecular Au····Au contacts of 3.154 Å between adjacent gold atoms. The two adjacent Au(C≡CPh) groups are arranged in a crossed geometry with a torsion angle [P(1)–Au(1)–Au(2)–P(2)] of 75.31°. As a consequence, the shape of the molecule appears to be that of a distorted anthracene-like structure made up of a central benzene ring with two fused Au_2PC_2P six membered rings on either side arising from the presence of weak Au····Au interactions (Figure 1.22).

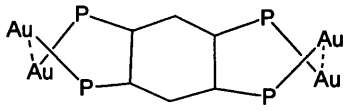

Figure 1.22: Schematic drawing of central distorted anthracene in $[Au_4(tbbp)(C{\equiv}CPh)_4]$

Yam *et al* have also reported an interesting structure for a trinuclear gold(I) alkynyl phosphine complex.[67] Figure 1.23 shows a schematic drawing of the complex where R is $C(=CH_2)Me$. The cation is made up of three gold(I) atoms in a triangular arrangement held by short Au····Au contacts of 3.115, 3.154 and 3.149 Å which are in the range for these aurophilic interactions. Two of the three gold centres are coordinated to an alkynyl ligand and a phosphorus atom of one of the (diphenylphosphino)methane ligands. The remaining gold atom is coordinated to two phosphorus atoms from two different dppm ligands. The counter anion consists of a gold centre with two alkynyl ligands.

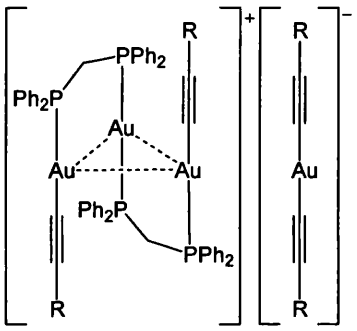

Figure 1.23: Schematic drawing of $[(dppm)_2Au_3\{C{\equiv}CC(=CH_2)Me\}_2][Au\{C{\equiv}CC(=CH_2)Me\}_2]$

As the chemistry and luminescent properties of gold(III) alkynyl species is relatively unexplored, Yam's group has recently turned its attention towards the synthesis and study of luminescent cyclometallated gold(III) alkynyl complexes (Figure 1.24).[68,69]

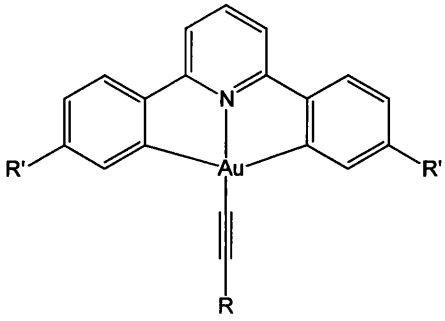

Figure 1.24: Cyclometallated gold(III) alkynes (R' = H; R = C_6H_5; C_6H_4-Cl-*p*; C_6H_4-OCH_3-*p*; C_6H_4-NH_2-*p*. R' = ^{t}Bu; R = C_6H_5)

Humphrey *et al* have synthesised ranges of gold alkynyl complexes as part of their investigations into the nonlinear optical properties of these materials. They have looked at the effect of varying the phosphine group on the NLO response by preparing gold(I) alkynyl complexes of the type LAu–C≡C–($C_6H_4NO_2$) and LAu–C≡C–R–C≡CAuL (R = 4-C_6H_4; 4,4'-$C_6H_4C_6H_4$; L = PCy_3; PPh_3; PMe_3).[70]

The introduction of a nitro group on the phenylacetylide ring causes a red-shift in λ_{max} and an increase in NLO response. They found that replacing the triarylphosphine with trialkylphosphine (in going from PPh_3 to PCy_3 to PMe_3) produced an increase in nonlinearity[71] which is in contrast to results observed with ligand replacements in nitropyridylalkynyl complexes where the reverse is true.[72]

Recent work by Puddephatt has moved in the direction of supramolecular systems.[62] Linear two-coordinate gold(I) units are useful for self assembly of organometallic macrocycles through aurophilic attractions. Using a flexible diacetylide and choosing a suitable bridging diphosphine allows the formation of ring complexes. Increasing the ring size in turn increases the cavity size and it becomes large enough to allow catenation.

In the case of $[Me_2C(C_6H_4OCH_2CCAu)_2\{\mu\text{-}Ph_2P(CH_2)_nPPh_2\}]_2$ the length of the phosphine bridge affects the structure of the catenane. When n = 2, a simple ring is formed; when n = 3, there is an equilibrium between ring and catenane (short Au···Au contacts are observed) and when n = 4 only the catenane is present (Figure 1.25).

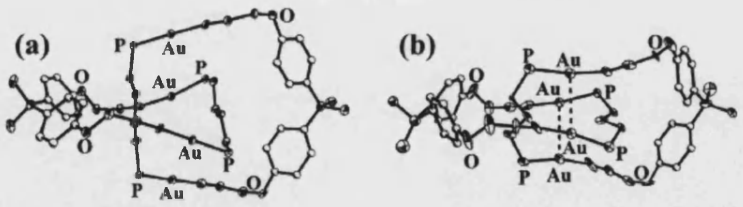

Figure 1.25: Structures of [2]-catenanes $[Me_2C(C_6H_4OCH_2CCAu)_2\{\mu\text{-}Ph_2P(CH_2)_nPPh_2\}]_2$. (a) n = 4 and (b) n = 3. Phenyl groups omitted for clarity.

Digold(I) diacetylide macrocycles incorporating a flexible polyether chain which forms a "gilded" crown ether have been synthesised in the hope that the large cavity would allow

catenation or the polyether chain would make encapsulation of cations possible (Figure 1.26).[73]

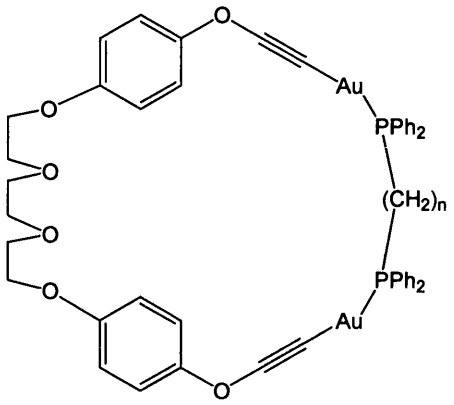

Figure 1.26: Gold(I) macrocycle (n = 1 – 5)

Although there are many solid state structures of alkynyl gold(I) phosphines reported in the literature it is noteworthy that there are no linear gold chains formed and that in the non-covalently bonded polymers observed the molecules are arranged in zigzag arrays.

In summary, the reported studies on gold(I) alkynyl phosphines to date suggest that the variety of observed structural forms is governed by the following factors:

i) The bulk of the phosphine group
ii) The electronic properties of the phosphine
iii) The length of the alkyne chain
iv) The electronic properties of the alkyne substituent

In addition, optical studies have shown that the profiles of electronic absorption and emission spectra of these complexes are similar to that of the uncoordinated ligands with the exception of a small red shift associated with mixing of the ligand π-orbitals with those of the Au 6p orbitals. In the cases where the presence of aurophilic d^{10}–d^{10} interactions is indicated by their crystal structures, the corresponding solid state spectra show additional absorption bands.

Aurophilic interactions are thought to contribute to the interesting luminescent properties of gold(I) acetylides.[45,46,48,74] The effect of aurophilic interactions observed in gold(I) alkynyl

phosphine complexes on the optical properties of these materials are discussed in the next section.

1.5 Luminescent Properties of Group 10 & 11 Transition Metal Alkynyl Polymers

Luminescence differs from incandescence in that it is the emission of light whose energy is not derived from the temperature of the emitting material. Luminescence usually occurs as fluorescence or phosphorescence. The processes involved in fluorescence and phosphorescence are illustrated in Figure 1.27. Fluorescence involves rapid conversion of absorbed radiation into re-emitted energy by radiative decay from an excited state with the same multiplicity as the ground state (e.g. $S_1 \rightarrow S_0$). In accordance with the Franck-Condon principle, all of the transitions are vertical. Fluorescence occurs very rapidly and at a lower frequency than that of the incident radiation due to the loss of some vibrational energy to the surroundings. In organometallic materials fluorescent lifetimes are generally in the nanosecond range.

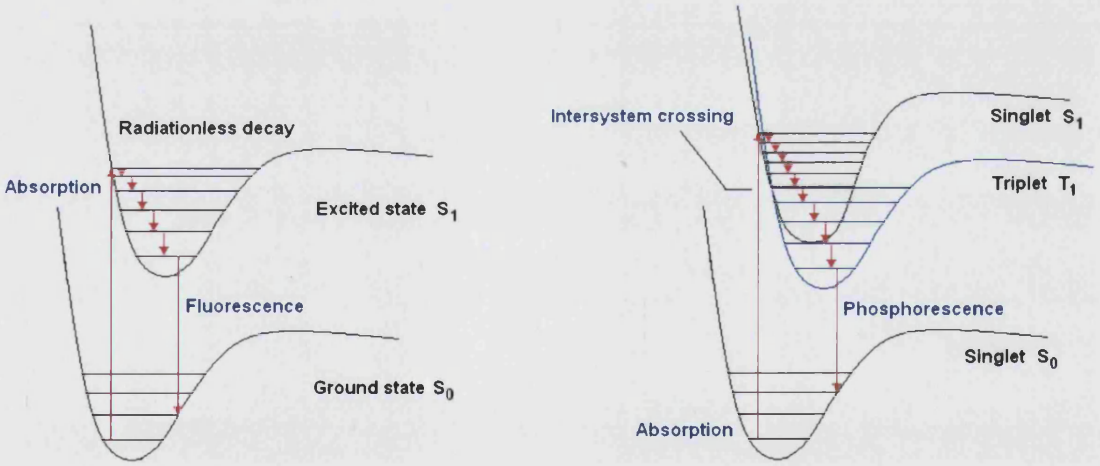

Figure 1.27: Fluorescence and phosphorescence processes

Phosphorescence involves intersystem crossing to an excited state with a different multiplicity to that of the ground state (e.g. $S_1 \rightarrow T_1$) followed by radiative decay. As return to the ground state ($T_1 \rightarrow S_0$) is spin-forbidden, the triplet excited state acts as an energy reservoir but the presence of spin-orbit coupling relaxes the selection rule and allows slow decay to the ground state. Thus, phosphorescence may continue minutes or hours after excitation. When a

molecule contains a heavy atom, such as a transition metal, the spin-orbit coupling is large and therefore intersystem crossing may be expected to occur.

Site-selective luminescence studies of the square planar platinum(II) complexes *trans*-$[Pt(PEt_3)_2(C{\equiv}CH)_2]$ and *trans*-$[Pt(PEt_3)_2(C{\equiv}CPh)_2]$ revealed an intense structured emission both in the solid state and in glass solutions (isopentane, ether/isopentane, 1:1, and methanol/water, 4:1) at 77 K.[75] The emissive state is assigned as Pt $\rightarrow \pi^*$ (C≡C) MLCT in character through excitation into the low-energy MLCT absorption bands. The luminescent properties of platinum(II) alkynyl polymers of the type *trans*-$[Pt(PR_3)_2(C{\equiv}C{-}L{-}C{\equiv}C)_2]_n$ (where R = alkyl group and L = none or aromatic spacer) have been studied extensively.[76-83] In these cases, the origin of the luminescence is thought to be derived from a metal perturbed intra-ligand $\pi - \pi^*$ (C≡C) excited state.

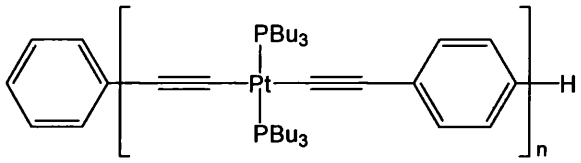

Figure 1.28: Platinum-acetylide oligomers, n = 1 – 5, 7.

Schanze and co-workers reported the systematic synthesis and photophysical characterisation of a series of linear platinum-acetylide oligomers in order to look at the effect of oligomers length on luminescence (Figure 1.28).[84] These oligomers were prepared by an iterative-convergent approach where the terminal acetylenes of the platinum-acetylide building blocks are protected by trimethylsilyl groups to allow selective deprotection.[85] The maxima of the absorption and emission bands in the spectra of these complexes shift to longer wavelength through the series n = 1 → 5 → 7 with only a small difference observed in going from n = 5 to n = 7 suggesting that the effective conjugation is approximately six repeat units.

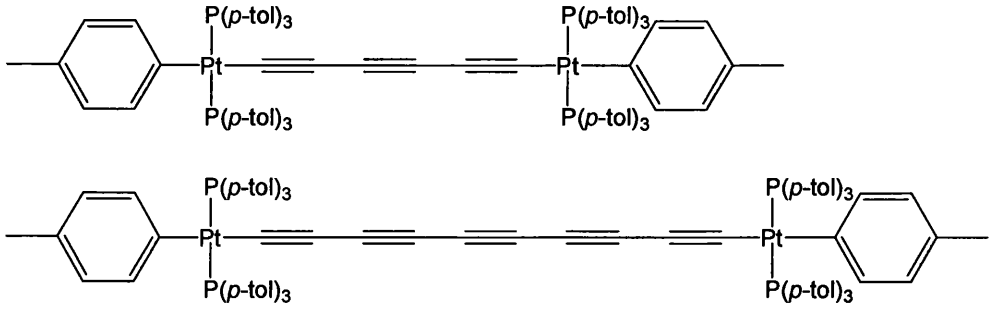

Figure 1.29: Diplatinum poly-ynediyl complexes

Recently Gladysz has reported the synthesis of diplatinum complexes, **PtC_xPt**, bridged by poly-ynediyl chains, C_x, where x = 6, 8, 10, 12, 16, 20, 24 and 28; those with an odd number of carbon–carbon triple bonds are shown in Figure 1.29.[86] The UV/visible electronic absorption spectra of these materials exhibit distinct shifts to longer wavelengths on increasing the conjugation length, reflected in their colours, which become progressively stronger through the series **PtC_6Pt** (yellow) > **$PtC_{10}Pt$** (orange) > **$PtC_{16}Pt$** (red) > **$PtC_{24}Pt$** (deep red) (Figure 1.30).

The red shifts suggest that the energy of the HOMO-LUMO gap is decreasing with increasing conjugation length. The shape of the absorption curves are found to follow that of related compounds, PhC_xPh, (where x = 4, 8, 12, 16)[8] which is consistent with an assignment of intra-ligand $\pi - \pi^*$ transitions but the maxima for the platinum systems are shifted to longer wavelength (lower energy) compared to the organic systems, consistent with conjugation extending along the length of the molecule through the metal centres.

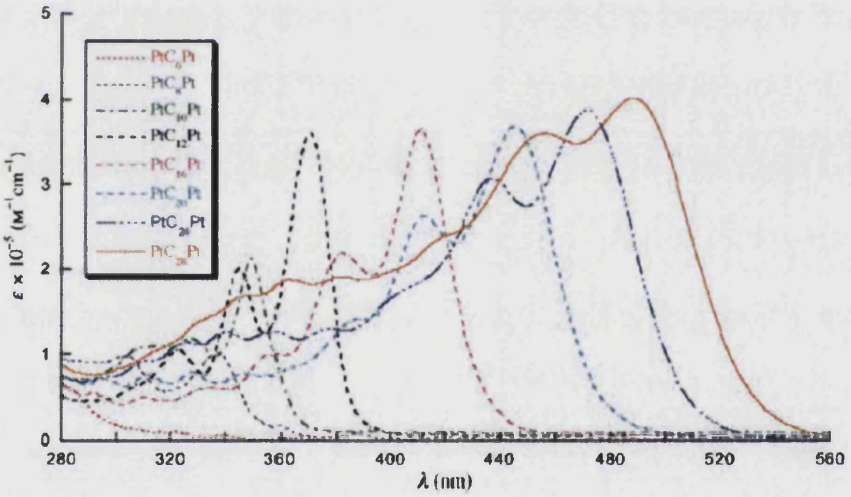

Figure 1.30: Absorption spectra of PtC_xPt (1.25 x 10^{-6} M in CH_2Cl_2)

Luminescence studies of the trinuclear copper(I) alkynyl complexes $[Cu_3(\mu\text{-dppm})_3(\mu_3\text{-}\eta^1\text{-}C{\equiv}C\text{-}C_6H_5)]^{2+}$ and $[Cu_3(\mu\text{-dppm})_3(\mu_3\text{-}\eta^1\text{-}C{\equiv}C\text{-}C_6H_5)_2]^{+}$ (Figure 1.31), first reported by Gimeno and co-workers,[87,88] have been carried out by Yam and co-workers.[89,90] The electronic absorption spectra of these materials in acetonitrile exhibit intense bands in the 300–330 nm region and solid state emission, at room temperature, occurs in the 490–500 nm range. The emission is thought to arise either from a MLCT [$Cu \rightarrow \pi^*$ ($RC{\equiv}C^-$)] transition or a ligand-centred $\pi \rightarrow \pi^*$ (acetylide) transition.

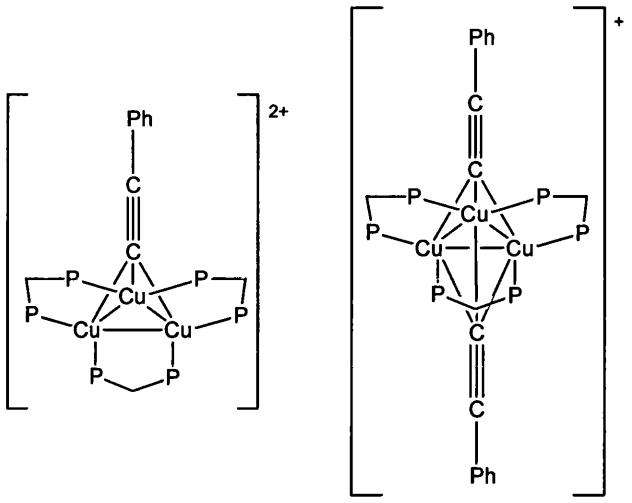

Figure 1.31: Trinuclear copper(I) alkynyl complexes $[Cu_3(\mu\text{-dppm})_3(\mu_3\text{-}\eta^1\text{-}C{\equiv}C\text{-}C_6H_5)]^{2+}$ and $[Cu_3(\mu\text{-dppm})_3(\mu_3\text{-}\eta^1\text{-}C{\equiv}C\text{-}C_6H_5)_2]^{+}$

A series of related analogues with different acetylide ligands, of the type $[Cu_3(\mu\text{-dppm})_3(\mu_3\text{-}\eta^1\text{-}C{\equiv}C\text{-}R)_2]^{+}$ and $[Cu_3(\mu\text{-dppm})_3(\mu_3\text{-}\eta^1\text{-}C{\equiv}C\text{-}R)]^{2+}$ (R = ^{t}Bu, 4-C_6H_4-NO_2, 4-C_6H_4-Ph, 4-C_6H_4-OMe, 4-C_6H_4-NH_2 and $^n C_6H_{13}$) were prepared by Yam and co-workers in order to gain an understanding of the nature of the excited state of these complexes.[15] The electronic absorption spectra of $[Cu_3(\mu\text{-dppm})_3(\mu_3\text{-}\eta^1\text{-}C{\equiv}C\text{-}R)]^{2+}$ exhibit bands at 252 – 268 nm and 292 – 328 nm which are assigned to ligand-centred π – π^* (dppm) and ligand-centred π – π^* (acetylide) transitions, respectively, due to the similar absorption energies of the free ligands.

The complexes all display intense, long-lived luminescence upon excitation. In general, it was found that complexes containing electron rich acetylide ligands emit at a lower energy. The emission energies of $[Cu_3(\mu\text{-dppm})_3(\mu_3\text{-}\eta^1\text{-}C{\equiv}C\text{-}R)]^{2+}$, in acetone solution, are ordered: 4-C_6H_4-OMe (483 nm) $\approx$ 4-C_6H_4-Ph (499 nm) > 4-C_6H_4-NH_2 (504, 564 nm) > ^{t}Bu (640 nm) > $^n C_6H_{13}$ (650 nm). The origin of the emission is proposed to involve substantial ligand-to-metal charge transfer (acetylide → Cu). However, for complexes incorporating an acetylide with a strong electron withdrawing group, such as $[Cu_3(\mu\text{-dppm})_3(\mu_3\text{-}\eta^1\text{-}C{\equiv}C\text{-}4\text{-}C_6H_4\text{-}NO_2)]^{2+}$, the emission bands are very similar to those of free acetylide ligands indicating ligand-centred π – π^* character of the emissive state.

The optical properties of the analogous silver(I) complexes $[Ag_3(\mu\text{-dppm})_3(\mu_3\text{-}\eta^1\text{-}C{\equiv}C\text{-}R)]^{2+}$ (R =, 4-C_6H_4-OMe, 4-C_6H_4-NO_2) have also been studied.[74] The silver(I) complexes $[Ag_3(\mu$-

dppm)$_3$(μ_3-η^1-C≡C-Ph)]$^{2+}$ and [Ag$_3$(μ-dppm)$_3$(μ_3-η^1-C≡C-4-C$_6$H$_4$-OMe)]$^{2+}$ were found to exhibit higher energy emission than the copper counterparts.

The first report of luminescent properties of gold(I) alkynyl complexes was made by Che *et al*,[59] describing the emissive behaviour of [{Au(C≡CPh)}$_2$(μ-Ph$_2$PCH$_2$CH$_2$PPh$_2$)], which contains a chelating phosphine bridging the gold(I) centres as illustrated in Figure 1.32. The intense band from 260–310 nm in the UV/visible electronic absorption spectrum of [{Au(C≡CPh)}$_2$(μ-dppe)], in dichloromethane solution, is assigned to the intraligand $\pi - \pi^*$ transition of the C≡CPh groups.

The emission spectrum of [{Au(C≡CPh)}$_2$(μ-dppe)], in dichloromethane solution, exhibits a maximum at 420 nm which is considerably red-shifted to 550 nm in the solid state. The shift is attributed to the presence of Au····Au interactions in the solid state structure increasing the contribution from MLCT.

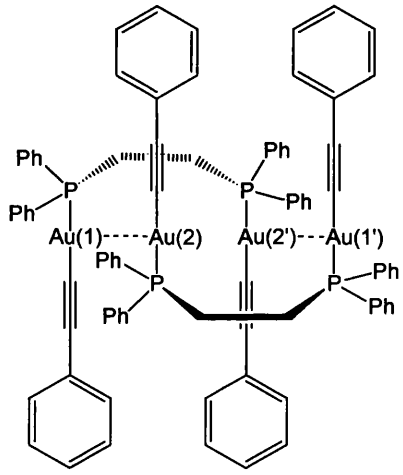

Figure 1.32: Schematic drawing of [{Au(C≡CPh)}$_2$(μ-Ph$_2$PCH$_2$CH$_2$PPh$_2$)]

Puddephatt *et al* carried out the first study of the emission behaviour of rigid-rod gold polymers[48] of the type [–Au–C≡C–Ar–C≡C–Au–L–L–]$_x$, where Ar represents an aromatic group and L–L = diphosphine or bis(isocyanide) ligands (described in Section 1.3.2). The insolubility of the polymers meant that they could only be studied in the solid state and all exhibited weak, broad, featureless emission bands around 585–600 nm when excited at 350 or 380 nm. Comparing the spectra with those of model compounds, corresponding monomers and binuclear complexes, there is a general red shift in the order: monomer > dimer > polymer

reflecting the increase in conjugation length. The emission bands observed for the polymeric materials are thought to arise from a metal-centred d_σ^* – p_σ excited state and indicate the presence of intermolecular Au····Au interactions as revealed by X-ray analysis.

1.5.1 Aromatic Spacer Groups

The optical gap, lowest energy transition from the HOMO to the LUMO, varies dependent on the nature of the metal, alkyne or ligands forming the poly-yne. Control of this optical gap allows tuning of the opto-electronic properties of the material. This tuning can be achieved by altering the metal, the auxiliary ligands and, most effectively, by altering the aromatic or heteroaromatic spacer group in the rigid rod platinum poly-ynes.

A common feature in the electronic spectra of poly-yne polymers is MLCT transitions and they tend to have a much smaller optical gap, usually taken from the position of the onset of absorption, than the corresponding dialkynyl monomers which indicates an increase in conjugation along the polymer. Polymers with optical gaps of ~3 eV are described as 'wide-band gap' semiconductors or insulators and compare unfavourably with organic polymers such as polyacetylene, which has an optical gap of 1.48 eV[91] and those with optical gaps of <1 eV are known.[92] By an appropriate choice of aromatic spacer group it is possible to reduce the optical gap in the metal-containing poly-yne polymers below 2 eV.

Using the dehydrohalogenation reaction, detailed in Section 1.3.1, a wide range of platinum poly-ynes have been prepared by Raithby, Khan and co-workers, with a variety of aromatic spacer groups in order to study the effect on changing the spacer on the properties of the material; some examples are shown in Figure 1.33.[11]

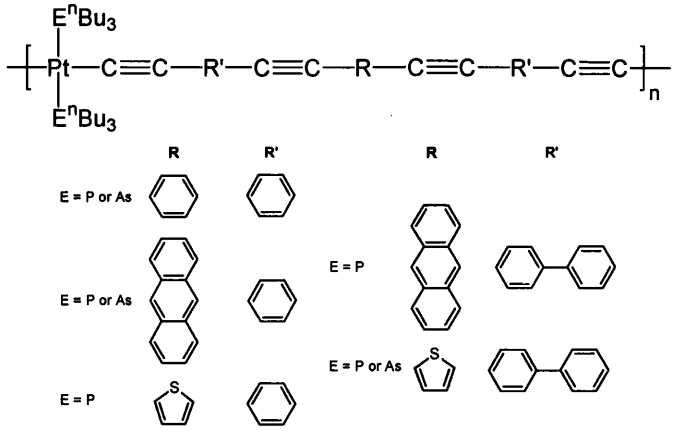

Figure 1.33: Examples of Platinum poly-ynes with different aromatic spacers

The optical properties of platinum-containing polymers of the type $[-Pt(PBu_3)_2-C\equiv C-Ar-C\equiv C-]_n$ where the alkynyl units are separated by either pyridine, phenylene or thiophene have been investigated.[80] The energy of the HOMO-LUMO transition decreases in the order: $[-Pt(PBu_3)_2-C\equiv C-C_5H_4N-C\equiv C-]_n$ > $[-Pt(PBu_3)_2-C\equiv C-C_6H_4-C\equiv C-]_n$ > $[-Pt(PBu_3)_2-C\equiv C-C_4H_2S-C\equiv C-]_n$ which suggests that the electron rich thiophene ring is enhancing the conjugation while the pyridine unit, which is electron deficient, reduces the conjugation.

The use of naphthalene and anthracene as bridging units in conjugated platinum di- and poly-ynes and studies into their effect on the luminescent properties of these materials (Figure 1.34) has also been reported by these researchers.[93] The first absorption band in the spectra of these materials was assigned to transitions between the mixed ligand π and platinum 5d orbitals and the ligand π^* and platinum 6p orbitals.

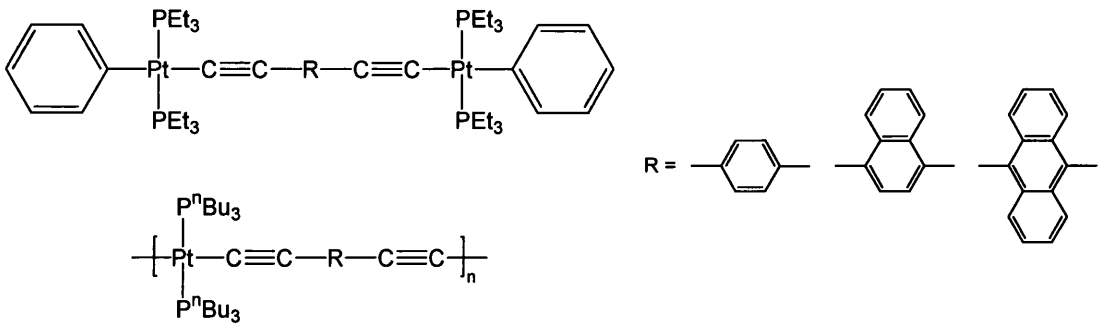

Figure 1.34: Platinum(II) di-ynes and poly-ynes incorporating aromatic spacer groups

The absorption shifts to longer wavelength through the series benzene → naphthalene → anthracene suggesting an increase in the donor-acceptor interaction between the metal centre

and the conjugated spacer. The optical gap is shown to decrease as the electron delocalisation increases through progressively larger aromatic units with the di-yne with a benzene linker having an optical gap of 3.4 eV and that of the di-yne with the anthracene linker being 2.45 eV. For the analogous polymers the observed optical gaps were 2.9 eV and 2.35 eV, respectively.

While these values are within the range seen for platinum poly-ynes, values of less than 2 eV have been reported for polymers containing electron withdrawing heteroaromatic rings.[81] With the optical gaps of their platinum complexes observed in the range of 2.4 – 3.4 eV, Raithby and co-workers aimed to prepare a metal poly-yne with an optical gap of less than 2 eV by synthesising a poly-yne polymer designed using the concept of alternating donor (electron rich thiophene) and acceptor (electron deficient thieno[3,4-b]pyrazine) units (Figure 1.35).[94] The *n*-butyl phosphine substituted platinum(II) acetylene group acts as a donor and the thieno[3,4-b]pyrazine as an acceptor in this case and the polymer has an optical gap of 1.77 eV.

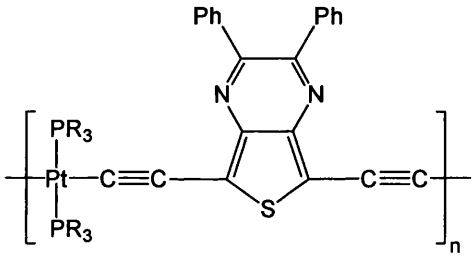

Figure 1.35: Donor-acceptor platinum poly-yne

Since this work there have been a number of metal poly-ynes with donor/acceptor systems published in the literature[95-99] but most notable of these is that incorporating a 9-dicyanomethylenefluorene-2,7-diyl unit[100] (Figure 1.36) with an optical gap of 1.58 eV which, half a decade later, remains the lowest reported for a metal poly-yne system.

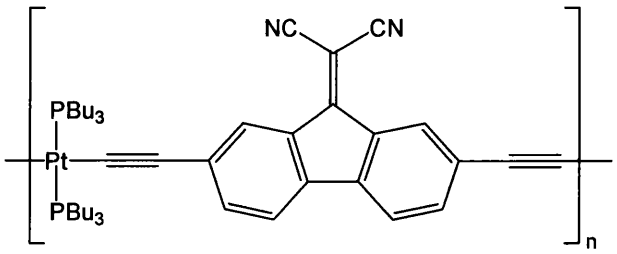

Figure 1.36: Platinum(II) poly-yne incorporating 9-dicyanomethylenefluorene-2,7-diyl

1.6 Aims for this work

The enhancement and the ability to 'fine tune' the properties of organic conjugated polymers by incorporation of transition metals into the backbone has led to a rapid growth of research in this area and investigations into applications relating to material science. With many of the polymeric materials, insolubility is a problem and, therefore, to better understand structural effects on their optical properties it is necessary to prepare model compounds which may be fully characterised and studied. While the chemistry of platinum alkynyl complexes and investigations into their properties are well established, gold alkynyls present an interesting alternative for use in transition metal-containing polymers due to the presence of aurophilic interactions in these materials. This work describes the preparation of gold(I) alkynyl complexes and the effect of Au····Au interactions on the structural conformations and optical properties in Chapter 2. In the search for new aromatic spacer groups for transition metal alkynyl complexes, a series of new ethynyl chalcogenophenes are prepared and the optical studies of their gold(I) and platinum(II) complexes presented in Chapter 3 followed by the preparation of a range of fused and non-fused thiophene and selenophene based systems in Chapter 4.

1.7 References

1. Tour, J. M., *Acc. Chem. Res.,* 2000, **33**, 791-804.
2. James, D. K.; Tour, J. M., *Top. Curr. Chem.,* 2005, **257**, 33-62.
3. Aviram, A.; Ratner, M. A., *Chem. Phys. Lett.,* 1974, **29**, 277-283.
4. Robertson, N.; McGowan, C. A., *Chem. Soc. Rev.,* 2002, **32**, 96-103.
5. Paul, F.; Lapinte, C., *Coord. Chem. Rev.,* 1998, **180**, 431-509.
6. Martin, R. E.; Diederich, F., *Angew. Chem. Int. Ed. Engl.,* 1999, **38**, 1350-1377.
7. Morales, R. G. E.; Gonzalez-Rojas, C., *J. Phys. Org. Chem.,* 2005, **18**, 941-944.
8. Luu, T.; Elliott, E.; Slepkov, A. D.; Eisler, S.; McDonald, R.; Hegmann, F. A.; Tywinski, R. R., *Org. Lett.,* 2005, **7**, 51-54.
9. Beljonne, D.; Wittmann, H. F.; Kohler, A.; Graham, S.; Younus, M.; Lewis, J.; Raithby, P. R.; Khan, M. S.; Friend, R. H.; Bredas, J. L., *J. Chem. Phys.,* 1996, **105**, 3868-3877.
10. Chawdhury, N.; Kohler, A.; Friend, R. H.; Wong, W. Y.; Lewis, J.; Younus, M.; Raithby, P. R.; Corcoran, T. C.; Al-Mandhary, M. R. A.; Khan, M. S., *J. Chem. Phys.,* 1999, **110**, 4963-4970.
11. Khan, M. S.; Kakkar, A. K.; Long, N. J.; Lewis, J.; Raithby, P.; Nguyen, P.; Marder, T. B.; Wittmann, F.; Friend, R. H., *J. Mater. Chem.,* 1994, **4**, 1227-1232.
12. Long, N. J., *Angew. Chem. Int. Ed. Engl.,* 1995, **34**, 21-38.
13. Barlow, S.; O'Hare, D., *Chem. Rev.,* 1997, **97**, 637-669.
14. Wong, W.-Y.; Ho, C.-L., *Coord. Chem. Rev.,* 2006, **250**, 2627-2690.
15. Yam, V. W.-W.; Lo, K. K.-W.; Wong, K. M.-C., *J. Organomet. Chem.,* 1999, **578**, 3-30.
16. Yam, V. W.-W., *Acc. Chem. Res.,* 2002, **35**, 555-563.
17. Takahashi, S.; Takai, Y.; Morimoto, H.; Sonagashira, K., *J. Chem. Soc. Chem. Commun.,* 1984, 3-5.
18. Long, N. J.; Williams, C. K., *Angew. Chem. Int. Ed.,* 2003, **42**, 2586-2617.
19. Yam, V. W.-W.; Wong, K. M.-C., *Top. Curr. Chem.,* 2005, **257**, 1-32.
20. Nguyen, P.; Gomez-Elipe, P.; Manners, I., *Chem. Rev.,* 1999, **99**, 1515-1548.
21. Christensen, P. A.; Hamnett, A.; Higgins, S. J., *J. Chem. Soc. Faraday Trans.,* 1996, **92**, 773-781.
22. Wolf, M. O.; Wrighton, M. S., *Chem. Mater.,* 1994, **6**, 1526-1533.

23. King, G.; Higgins, S. J.; Price, N., *Analyst,* 1992, **117**, 1243-1246.
24. Sonagashira, K.; Takahashi, S.; Hagihara, N., *Macromolecules,* 1977, **10**, 879-880.
25. Tourillon, G.; Garnier, F., *J. Electroanal. Chem.,* 1982, **135**, 173-178.
26. Foucher, D. A.; Tang, B. Z.; Manners, I., *J. Am. Chem. Soc.,* 1992, **114**, 6246-6248.
27. Honeyman, C. H.; Foucher, D. A.; Dahmen, F. Y.; Rulkens, R.; Lough, A. J.; Manners, I., *Organometallics,* 1995, **14**, 5503-5512.
28. Sheridan, J. B.; Temple, K.; Lough, A. J.; Manners, I., *J. Chem. Soc. Dalton Trans.,* 1997, 711-713.
29. Ni, Y. Z.; Manners, I.; Sheridan, J. B.; Oakley, R. T., *J. Chem. Educ.,* 1998, **75**, 766-768.
30. Abd-El-Aziz, A. S.; Manners, I., *J. Inorg. Organomet. Polym. Mater.,* 2005, **15**, 157-195.
31. Sonogashira, K.; Yatake, T.; Tohda, Y.; Takahashi, S.; Hagihara, N., *J.C.S. Chem. Comm.,* 1977, 291 - 292.
32. Fujikura, Y.; Sonogashira, K.; Hagihara, N., *Chem. Lett.,* 1975, 1067-1070.
33. Sonogashira, K.; Kataoka, S.; Takahashi, S.; Hagihara, N., *J. Organomet. Chem.,* 1978, **160**, 319-327.
34. Hay, A. S., *J. Org. Chem.,* 1962, **27**, 3320-3321.
35. Davies, S. J.; Johnson, B. F. G.; Khan, M. S.; Lewis, J., *J. Chem. Soc. Chem. Commun.,* 1991, 187-188.
36. Johnson, B. F. G.; Kakkar, A. K.; Khan, M. S.; Lewis, J.; Dray, A. E.; Friend, R. H.; Wittmann, F., *J. Mater. Chem.,* 1991, **1**, 485-486.
37. Khan, M. S.; Davies, S. J.; Kakkar, A. K.; Schwartz, D.; Lin, B.; Johnson, B. F. G.; Lewis, J., *J. Organomet. Chem.,* 1992, **424**, 87-97.
38. Lewis, J.; Khan, M. S.; Kakkar, A. K.; Johnson, B. F. G.; Marder, T. B.; Fyfe, H. B.; Wittmann, F.; Friend, R. H.; Dray, A. E., *J. Organomet. Chem.,* 1992, **425**, 165-176.
39. Atherton, Z.; Faulkner, C. W.; Ingham, S. L.; Kakkar, A. K.; Khan, M. S.; Lewis, J.; Long, N. J.; Raithby, P. R., *J. Organomet. Chem.,* 1993, **462**, 265-270.
40. Lavastre, O.; Even, M.; Dixneuf, P. H., *Organometallics,* 1996, **15**, 1530-1531.
41. Puddephatt, R. J., *Chem. Commun.,* 1998, 1055-1062.
42. Corfield, P. W. R.; Shearer, H. M. M., *Acta Cryst.,* 1966, **20**, 502-508.
43. Yam, V. W.-W.; Fung, W. K.-M.; Cheung, K.-K., *Organometallics,* 1997, **16**, 2032-2037.

44. Jia, G. C.; Puddephatt, R. J.; Scott, J. D.; Vittal, J. J., *Organometallics,* 1993, **12**, 3565-3574.
45. Irwin, M. J.; Jia, G. C.; Payne, N. C.; Puddephatt, R. J., *Organometallics,* 1996, **15**, 51-57.
46. Irwin, M. J.; Manojlovic-Muir, L.; Muir, K. W.; Puddephatt, R. J.; Yufit, D. S., *Chem. Commun.,* 1997, 219-220.
47. Vicente, J.; Chicote, M. T.; Alvarez-Falcon, M. M.; Bautista, D., *Organometallics,* 2004, **23**, 5707-5712.
48. Irwin, M. J.; Vittal, J. J.; Puddephatt, R. J., *Organometallics,* 1997, **16**, 3541-3547.
49. Vicente, J.; Chicote, M. T.; Alvarez-Falon, M. M.; Fox, M. A.; Bautista, D., *Organometallics,* 2003, **22**, 4792-4797.
50. Vicente, J.; Chicote, M. T.; Alvarez-Falcon, M. M.; Jones, P. G., *Organometallics,* 2005, **24**, 2764-2772.
51. Jones, P. G., *Gold Bull.,* 1981, **14**, 102-118.
52. Schmidbaur, H., *Gold Bull.,* 1990, **23**, 11-21.
53. Schmidbaur, H., *Chem. Soc. Rev.,* 1995, **24**, 391-400.
54. Li, J.; Pyykko, P., *Chem. Phys. Lett.,* 1992, **197**, 586-590.
55. Pyykko, P.; Zhao, Y. F., *Angew. Chem. Int. Edit. Engl.,* 1991, **30**, 604-605.
56. Pyykko, P.; Li, J.; Runeberg, N., *Chem. Phys. Lett.,* 1994, **218**, 133-138.
57. Pyykko, P., *Chem. Rev.,* 1997, **97**, 597-636.
58. Pathaneni, S. S.; Desiraju, G. R., *J. Chem. Soc. Dalton Trans.,* 1993, 319-322.
59. Li, D.; Hong, X.; Che, C. M.; Lo, W. C.; Peng, S. M., *J. Chem. Soc. Dalton Trans.,* 1993, 2929-2932.
60. Li, D.; Hong, X.; Che, C. M.; Lo, W. C.; Peng, S. M., *J. Chem. Soc. Dalton Trans.,* 1993, 2929-2932.
61. Che, C. M.; Lai, S. W., *Coord. Chem. Rev.,* 2005, **249**, 1296-1309.
62. Puddephatt, R. J., *Coord. Chem. Rev.,* 2001, **216**, 313-332.
63. Yam, V. W. W.; Lo, K. K. W., *Chem. Soc. Rev.,* 1999, **28**, 323-334.
64. Cifuentes, M. P.; Humphrey, M. G., *J. Organomet. Chem.,* 2004, **689**, 3968-3981.
65. MacDonald, M. A.; Puddephatt, R. J.; Yap, G. P. A., *Organometallics,* 2000, **19**, 2194-2199.
66. Yam, V. W. W.; Choi, S. W. K.; Cheung, K. K., *Organometallics,* 1996, **15**, 1734-1739.

67. Yam, V. W. W.; Cheung, K. L.; Yip, S. K.; Cheung, K. K., *J. Organomet. Chem.,* 2003, **681**, 196-209.

68. Yam, V. W. W.; Wong, K. M. C.; Hung, L. L.; Zhu, N. Y., *Angew. Chem. Int. Edit.,* 2005, **44**, 3107-3110.

69. Wong, K. M. C.; Zhu, X. L.; Hung, L. L.; Zhu, N. Y.; Yam, V. W. W.; Kwok, H. S., *Chem. Commun.,* 2005, 2906-2908.

70. Vicente, J.; Chicote, M. T.; Abrisqueta, M. D.; de Arellano, M. C. R.; Jones, P. G.; Humphrey, M. G.; Cifuentes, M. P.; Samoc, M.; Luther-Davies, B., *Organometallics,* 2000, **19**, 2968-2974.

71. Hurst, S. K.; Cifuentes, M. P.; McDonagh, A. M.; Humphrey, M. G.; Samoc, M.; Luther-Davies, B.; Asselberghs, I.; Persoons, A., *J. Organomet. Chem.,* 2002, **642**, 259-267.

72. Naulty, R. H.; Cifuentes, M. P.; Humphrey, M. G.; Houbrechts, S.; Boutton, C.; Persoons, A.; Heath, G. A.; Hockless, D. C. R.; Luther-Davies, B.; Samoc, M., *J. Chem. Soc. Dalton Trans.,* 1997, 4167-4174.

73. Mohr, F.; Puddephatt, R. J., *J. Organomet. Chem.,* 2004, **689**, 374-379.

74. Yam, V. W. W.; Fung, W. K. M.; Cheung, K. K., *Organometallics,* 1997, **16**, 2032-2037.

75. Sacksteder, L.-A.; Baralt, E.; DeGraff, B. A.; Lukehart, C. M.; Demas, J. N., *Inorg. Chem.,* 1991, **30**, 2468-2476.

76. Lewis, J.; Raithby, P. R.; Wong, W. Y., *J. Organomet. Chem.,* 1998, **556**, 219-228.

77. Wong, W. Y.; Wong, W. K.; Raithby, P. R., *J. Chem. Soc. Dalton Trans.,* 1998, 2761-2766.

78. Lewis, J.; Khan, M. S.; Kakkar, A. K.; Johnson, B. F. G.; Marder, T. B.; Fyfe, H. B.; Wittmann, F.; Friend, R. H.; Dray, A. E., *J. Organomet. Chem.,* 1992, **425**, 165-176.

79. Wittmann, H. F.; Friend, R. H.; Khan, M. S.; Lewis, J., *J. Chem. Phys.,* 1994, **101**, 2693-2698.

80. Chawdhury, N.; Kohler, A.; Friend, R. H.; Younus, M.; Long, N. J.; Raithby, P. R.; Lewis, J., *Macromolecules,* 1998, **31**, 722-727.

81. Younus, M.; Kohler, A.; Cron, S.; Chawdhury, N.; Al-Mandhary, M. R. A.; Khan, M. S.; Lewis, J.; Long, N. J.; Friend, R. H.; Raithby, P. R., *Angew. Chem. Int. Edit.,* 1998, **37**, 3036-3039.

82. Wilson, J. S.; Kohler, A.; Friend, R. H.; Al-Suti, M. K.; Al-Mandhary, M. R. A.; Khan, M. S.; Raithby, P. R., *J. Chem. Phys.,* 2000, **113**, 7627-7634.

83. Kohler, A.; Wilson, J. S.; Friend, R. H.; Al-Suti, M. K.; Khan, M. S.; Gerhard, A.; Bassler, H., *J. Chem. Phys.,* 2002, **116**, 9457-9463.

84. Liu, Y.; Jiang, S. J.; Glusac, K.; Powell, D. H.; Anderson, D. F.; Schanze, K. S., *J. Am. Chem. Soc.,* 2002, **124**, 12412-12413.

85. Diederich, F.; Martin, R. E., *Angew. Chem. Int. Ed.,* 1999, **38**, 1350-1377.

86. Zheng, Q. L.; Bohling, J. C.; Peters, T. B.; Frisch, A. C.; Hampel, F.; Gladysz, J. A., *Chem. Eur. J.,* 2006, **12**, 6486-6505.

87. Gamasa, M. P.; Gimeno, J.; Lastra, E.; Aguirre, A.; Garciagranda, S., *J. Organomet. Chem.,* 1989, **378**, C11-C14.

88. Diez, J.; Pilar Gamasa, M.; Gimeno, J.; Aguirre, A.; Garcia-Granda, S., *Organometallics,* 1991, **10**, 380-382.

89. Yam, V. W. W.; Lee, W. K.; Lai, T. F., *Organometallics,* 1993, **12**, 2383-2387.

90. Yam, V. W.-W.; Lee, W.-K.; Cheung, K.-K.; Crystall, B.; Phillips, D., *J. Chem. Soc. Dalton Trans.,* 1996, 3283-3287.

91. Lee, Y.-S.; Kertesz, M., *J. Chem. Phys.,* 1988, **88**, 2609-2617.

92. Karikomi, M.; Kitamura, C.; Tanaka, S.; Yamashita, Y., *J. Am. Chem. Soc.,* 1995, **117**, 6791-6792.

93. Khan, M. S.; Al-Mandhary, M. R. A.; Al-Suti, M. K.; Al-Battashi, F. R.; Al-Saadi, S.; Ahrens, B.; Bjernemose, J. K.; Mahon, M. F.; Raithby, P. R.; Younus, M.; Chawdhury, N.; Kohler, A.; Marseglia, E. A.; Tedesco, E.; Feeder, N.; Teat, S. J., *Dalton Trans.,* 2004, 2377-2385.

94. Havinga, E. E.; Tenhoeve, W.; Wynberg, H., *Synth. Met.,* 1993, **55**, 299-306.

95. Khan, M. S.; Al-Mandhary, M. R. A.; Al-Suti, M. K.; Feeder, N.; Nahar, S.; Kohler, A.; Friend, R. H.; Wilson, P. J.; Raithby, P. R., *J. Chem. Soc. Dalton Trans.,* 2002, 2441-2448.

96. Wong, W. Y.; Wong, C. K.; Poon, S. Y.; Lee, A. W. M.; Mo, T.; Wei, X., *Macromol. Rapid Commun.,* 2005, **26**, 376-380.

97. Naka, K.; Uemura, T.; Chujo, Y., *J. Polym. Sci. Pol. Chem.,* 2001, **39**, 4083-4090.

98. Wong, W. Y.; Chan, S. M.; Choi, K. H.; Cheah, K. W.; Chan, W. K., *Macromol. Rapid Commun.,* 2000, **21**, 453-457.

99. Wong, W. Y.; Choi, K. H.; Cheah, K. W., *J. Chem. Soc. Dalton Trans.,* 2000, 113-115.

100. Wong, W. Y.; Choi, K. H.; Lu, G. L.; Shi, J. X., *Macromol. Rapid Commun.*, 2001, **22**, 461-465.

Chapter 2 Gold(I) Alkynyl Phosphine Complexes

2.1 Introduction

The tendency of gold(I) to have a coordination number of two and to form complexes with a linear geometry suggests its suitability for use in forming linear rigid rod polymers of gold centres.[1,2] However, these polymeric materials are generally insoluble and difficult to characterise, therefore the majority of the polymers reported in the literature retain display a zigzag, rather than linear, conformation. While these materials tend to be molecular in solution it is found that they aggregate in the solid state by way of ligand π-stacking, or intermolecular Au····Au interactions (Figure 2.1). The latter weak 'aurophilic' interactions arise from relativistic London forces and have a similar strength to hydrogen bonds (~ 5 – 10 kcal mol^{-1}) with Au····Au distances generally falling in the range 2.75 – 3.40 Å.[3]

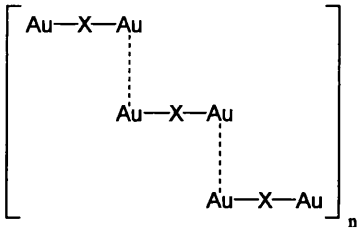

Figure 2.1: Aggregation of gold complexes in solid state (X is an aromatic spacer group)

Gold(I) alkynyls and their coordination complexes with phosphine ligands were first studied in 1962 by Coates and Parkin[4] but it was a study of the photoluminescent properties of these complexes almost a decade later which initially sparked interest in phosphine complexes of d^{10} metals.[5] Since then a plethora of gold(I) alkynyl phosphine complexes have been reported [6-17] along with accordant spectroscopic and photochemical studies.[18-24]

The first reported X-ray structure of a gold(I)alkynyl phosphine complex was that of phenylethynyl (isopropyl)aminegold(I) where the gold atoms are aligned in an infinite zigzag chain.[25] The Au····Au distances along the chains are 3.722 Å with an intergold angle [Au····Au····Au] of 153°. The chains are grouped together in pairs with intermolecular Au····Au separations of 3.274 Å as illustrated in Figure 2.2.

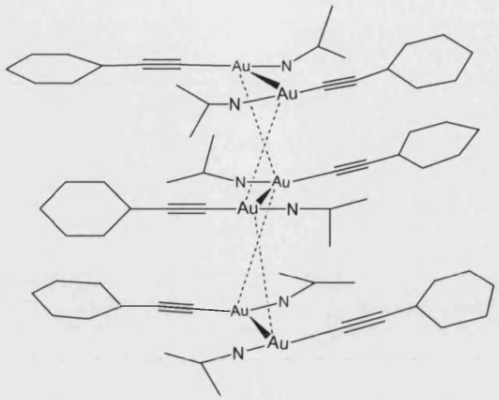

Figure 2.2: Structure of phenylethynyl(isopropylamine)gold(I)

The distances between gold atoms and ethynyl carbons on neighbouring chains are all in excess of 4.2 Å which implies that there is no possibility for Au–C π-bonding to occur and it is the Au····Au contacts which hold the structure together.

Bruce and co-workers reported the solid state structure of $[(PPh_3)AuC{\equiv}C\text{-}C_6F_5]$ in 1984.[26] The complex is approximately linear at the gold centre (P–Au–C, 177.9°; Au–C≡C, 175.4°; C≡C–C, 178.4°). The Au–P distance is 2.274 Å which is similar to that found in $Au(PPh_3)Cl$ (2.235 Å),[27] $Au(PPh_3)(CN)$ (2.270 Å) [28] and $Au(PPh_3)Me$ (2.279 Å).[29] As noted by Corfield[25] there is no association between molecules; the Au····Au separation is greater than 5 Å. The solid state structure is very different from those of copper(I)[30] and silver(I)[31] analogues which adopt a zwitterionic structure of the type $\{[M(PR_3)_2][M(C{\equiv}CR')_2]\}_n$. However, when Bruce published the structure of $[(PPh_3)AuC{\equiv}C\text{-}C_6H_5]$ it proved different again (Figure 2.3).[32]

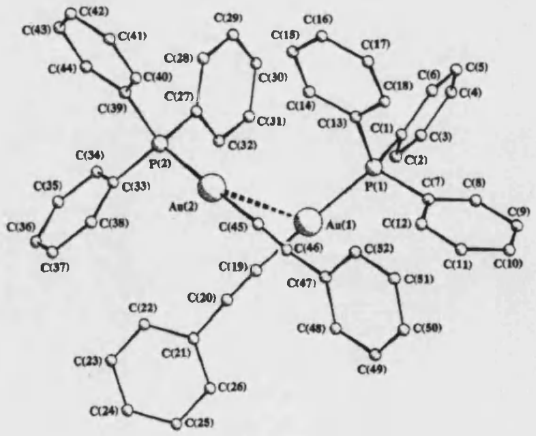

Figure 2.3: Structure of $Au(PPh_3)(C{\equiv}C\text{-}C_6H_5)$

In this case, two molecules make up the asymmetric unit each consisting of a gold atom with one alkyne ligand and one triphenylphosphine ligand in an approximately linear geometry. The Au····Au separation of 3.379 Å is considered to be a bonding interaction between the two molecules, forming a weakly bound dimer, with the phosphine groups approximately orthogonal (torsion angle P(1)-Au(1)-Au(2)-P(2) 103.6°). It is thought that the bulkier C_6F_5 group hinders the approach of a second molecule preventing Au····Au interactions.

Since then a wide variety of $R_3PAu–C\equiv C–X$ species, where R = a range of alkyl and aryl groups and X spans a range of aromatic and heteroaromatic groups, have been reported. The aim of these studies has been to investigate both the steric and electronic effects of changing R and X on the structural and electronic properties of these molecules and to establish what factors favour the formation of intermolecular Au····Au interactions between gold(I) centres.[21,33-36] A general trend is that bulky phosphine groups such as tricyclohexyl phosphine, through their steric bulk, limit the presence of Au····Au interactions.[21] It has also been found that not only variation in the ligand group X but even the way that the molecules pack in the solid state can alter the emissive properties of the material.[33] Of particular interest are the ethynylpyridine derivatives due to the inherent properties of the pyridine and the variety of positions (e.g. 2-, 3-, 4-) that can be taken up by the pyridine nitrogen atom. The next section summarises these studies.

2.1.1 Previous Work on 3-Ethynylpyridine Gold(I) Phosphine Complexes

The gold complexes of 2-ethynylpyridine derivatives, $[(Me_3P)AuC\equiv CC_5H_3N\text{-}NO_2\text{-}5]$, $[(Ph_3P)AuC\equiv CC_5H_3N\text{-}NO_2\text{-}5]$ and $[(Ph_3P)AuC\equiv CC_5H_4N]$,[9] along with the 4-ethynylpyridine gold complex $[(Cy_3P)AuC\equiv C\text{-}4\text{-}C_5H_4N]$[21] may be found in the literature, while gold complexes of 3-ethynylpyridine have previously been studied in the Raithby Group.[37] Reaction of triphenylphosphine gold chloride with 3-ethynylpyridine in the presence of sodium methoxide and methanol gave $[(Ph_3P)AuC\equiv C\text{-}3\text{-}C_5H_4N]$ as a pale cream solid. The crystal structure exhibited an intermolecular Au····Au interaction between gold atoms of 3.336 Å which is in line with previously reported Au····Au interactions in the literature (Figure 2.4). The result of these interactions is the formation of a loosely bound dimer in the solid state. As the steric bulk of the triphenyl phosphine group prevents more than two molecules aligning it

was thought that substituting the phenyl rings for ethyl groups may allow the formation of polymer chains held in place by Au····Au interactions.

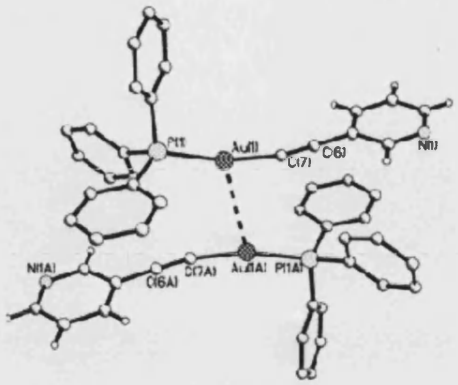

Figure 2.4: Dimer pairs in [$(Ph_3P)AuC{\equiv}C\text{-}3\text{-}C_5H_4N$] held together by Au····Au interactions

Conversely, reaction of triethylphosphine gold chloride with 3-ethynylpyridine resulted in a completely different product, a complex whose solid state structure exhibits a polymer chain, bound together by Au····Au interactions. What was unexpected about the structure was the exchange of ligands so that alternate gold atoms have two alkynes or two phosphine groups attached (Figure 2.5a).

If both gold centres are considered to be gold(I), each gold centre with two alkyne ligands bound would carry a single negative charge and each gold atom with two phosphine ligands, a single positive charge. The compound may then be thought of as$\{[Au(PEt_3)_2]^+[Au(C{\equiv}CPy)_2]^-\}$[37] similar to the observed structure of phenylethynyl(trimethylphosphine)silver(I)[31] (Figure 2.5b).

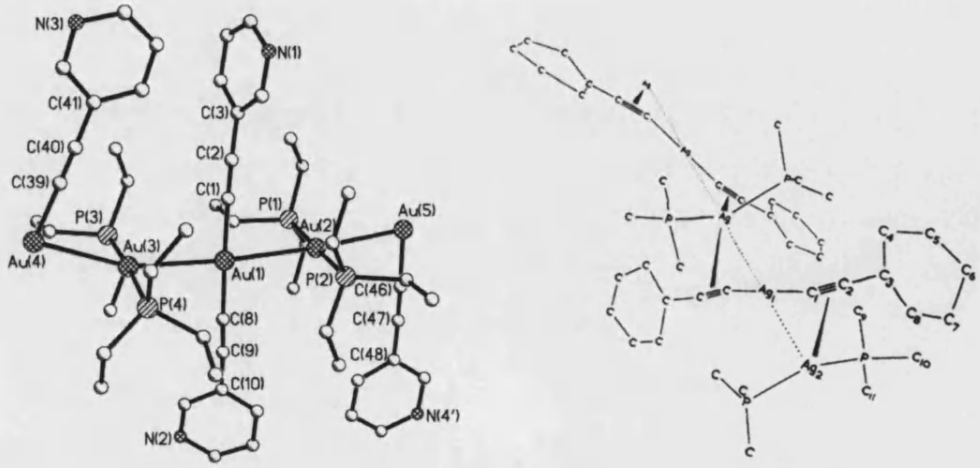

Figure 2.5: a) Unit cell of $\{[Au(PEt_3)_2]^+[Au(C{\equiv}CPy)_2]^-\}$[37]; b) Structure of $\{[Ag(PMe_3)_2]^+[Ag(C{\equiv}CPh)_2]^-\}$[31]

$\{[Au(PEt_3)_2]^+[Au(C{\equiv}CPy)_2]^-\}_n$		$\{[Ag(PMe_3)_2]^+[Ag(C{\equiv}CPh)_2]^-\}_n$	
Contact	Bond Angle (°)	Contact	Bond Angle (°)
Au(3)-Au(1)-Au(2)	176.172(13)	Ag(3)-Ag(1)-Ag(2)	175.0
C(1)-Au(1)-C(8)	175.9(3)	C(1)-Ag-C(1')	107.4
P(1)-Au(2)-P(2)	178.05(8)	P(1)-Ag(2)-P(1')	118.4
C(2)-C(1)-Au(1) C(9)-C(8)-Au(1)	175.4(8) 175.7(8)	C(2)-C(1)-Ag(1)	172.9
C(1)-C(2)-C(3) C(8)-C(9)-C(10)	177.6(9) 178.2(10)	C(1)-C(2)-C(3)	175.5

Table 2.1: Comparison of bond angles in $\{[Au(PEt_3)_2]^+[Au(C{\equiv}CPy)_2]^-\}$ and $\{[Ag(PMe_3)_2]^+[Ag(C{\equiv}CPh)_2]^-\}$

Table 2.1 lists selected bond angles observed for $\{[Au(PEt_3)_2]^+[Au(C{\equiv}CPy)_2]^-\}$ and $\{[Ag(PMe_3)_2]^+[Ag(C{\equiv}CPh)_2]^-\}$. As can be seen, although the Au–Au–Au and Ag–Ag–Ag angles are both approximately linear at 176.172(13)° and 175.0°, respectively, the position of the ligands provides considerable differences between the two chains. While the alkyne and phosphine units are arranged approximately linearly in $\{[Au(PEt_3)_2]^+[Au(C{\equiv}CPy)_2]^-\}$ [C(1)-Au(1)-C(8), 175.9(3)°; P(1)-Au(2)-P(2), 178.05(8)°] these angles are much smaller in the silver analogue and are much closer to an orthogonal arrangement [C(1)-Ag-C(1'), 107.4°; P(1)-Ag(2)-P(1'), 118.4°] to allow for the side on interaction between the silver atoms and alkynes on neighbouring molecules.

Although structures of this kind have been reported for copper and silver σ-acetylide complexes[30,31] this was the first occurrence of such a phenomenon in a gold complex. Recently, Elsegood *et al* have reported a series of (isocyanide)gold(I) halides, $[(Me)_3NB(H_2)NCAuX]$ where X = Cl, Br, those solid state structures show zigzag chains of monomers held together by aurophilic interactions (Figure 2.6).[38]

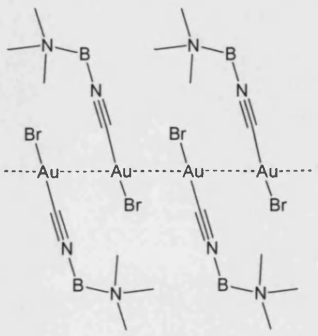

Figure 2.6: Schematic drawing of $[(CH_3)_3NB(H_2)NCAuBr]$

The asymmetric unit of $[(CH_3)_3NB(H_2)NCAuBr]$ consists of a dimeric unit with the molecules aligned antiparallel to each other and a Au····Au distance of 3.233 Å which is within the range for aurophilic interactions. Each molecule is approximately linear [C–Au–Br, 178.1°; N–C–Au, 176.8°; B–N–C 179.4°]. In the extended solid state structure these dimers aggregate to form non-covalently bound polymeric chains with Au····Au distances of 3.221 Å between dimers.

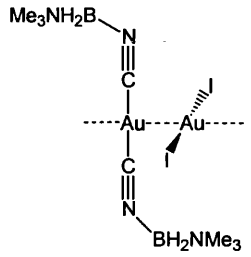

Figure 2.7: Schematic drawing of $[((Me)_3NB(H_2)NC)_2Au][AuI_2]$

The crystal structure of the iodo-analogue, $[(CH_3)_3NB(H_2)NCAuI]$, displays a rearrangement of ligands as seen in the structure of $[(Et_3P)AuC{\equiv}C\text{-}3\text{-}C_5H_4N]$ (Figure 2.5a), with the formula $[((CH_3)_3NB(H_2)NC)_2Au][AuI_2]$ shown in Figure 2.7. This structure is thought to occur due to the presence of a mixture of products in the solution from which the crystals were obtained and represents the most stable isomeric arrangement.[38]

2.1.2 Objectives for this Chapter

As the effect of substitution of the phosphine group (L) had previously been studied (L = Ph, Cy, Et, Me)[37] and only triethylphosphine shows the ligand rearrangement and Au····Au chain formation it was of interest to examine how different ring substitution patterns on the alkyne ligand effect the alignment of molecules and possible rearrangement of the resultant gold complexes. Using triethylphosphine gold chloride each time, with various RC≡CR' ligands, shown in Figure 2.8, a range of gold complexes will be synthesised and characterised.

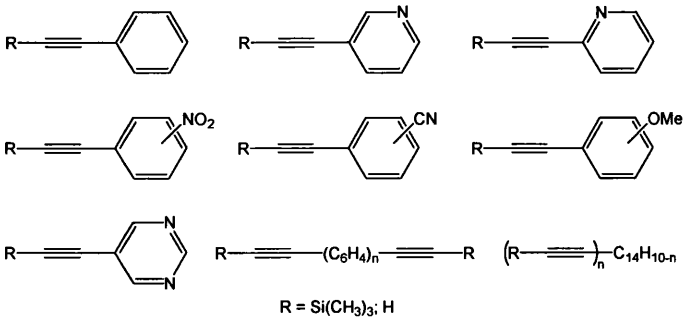

Figure 2.8: Range of alkyne ligands

2.2 Results and discussion

2.2.1 Synthesis of Gold(I) Alkynyl Phosphine Complexes

Gold(I) alkynyl phosphine complexes, $[(L_3P)AuC{\equiv}C\text{-}R]$, were prepared by the general reaction shown in eq. 1. The trimethylsilyl protected alkyne ligand was reacted with phosphine gold(I) chloride (L = Et, Ph) in methanol in the presence of sodium methoxide for between 12–18h in a variation of the method reported by Humphrey *et al.*[9]

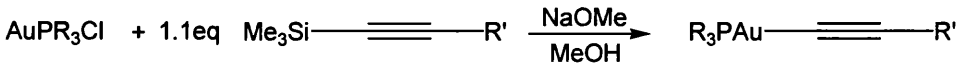

(1)

Table 2.2 lists synthetic data for complexes **2.01-2.03**. Characterisation of **2.01** was achieved by spectroscopic methods and X-ray structure determination which was in agreement with the previous structure (Figure 2.5a).[37] The 2-pyridine derivative **2.02** and phenyl derivative **2.03** were also prepared by this method allowing comparisons with the analogous triphenylphosphine complexes reported in the literature.

	Compound	Nature of Product	Yield/%
2.01	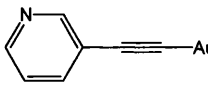	yellow crystals	14
2.02	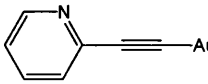	pale brown crystals	50
2.03	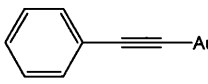	pale yellow crystals	39

Table 2.2: Synthetic data for complexes 2.01 – 2.03

In the interest of investigating the effect of ring substitutions within the alkyne ligand and the consequent alignment of molecules or rearrangement of ligands, the nitrophenyl gold(I) complexes **2.04–2.07** and benzonitriles gold(I) complexes **2.08–2.11** were prepared (Table 2.3). Following on from electron withdrawing ring substituents, it was of interest to study the effect of an electron donating substituent. Therefore, the methoxyphenylacetylene gold(I) phosphine complexes **2.12–2.16** were synthesised (Table 2.3). While the structures of **2.12** and **2.15** have been determined, the remaining complexes were characterised by spectroscopic methods and elemental analysis only.

	Compound	Nature of Product	Yield/%
2.04	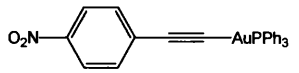	orange crystals	43
2.05	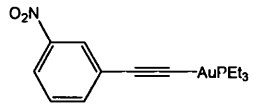	pale orange needles	44
2.06	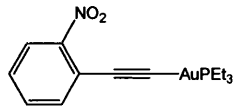	yellow crystals	7
2.07	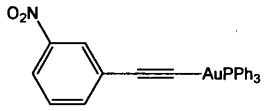	yellow crystals	30
2.08	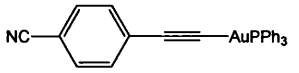	yellow crystals	30
2.09	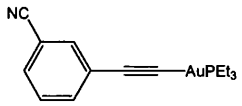	yellow solid	11
2.10	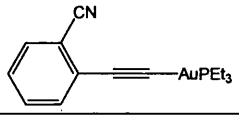	pale yellow crystals	48
2.11	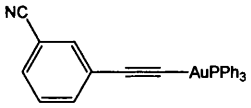	pale brown crystals	28
2.12	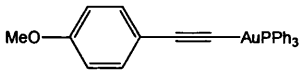	white crystals	48
2.13	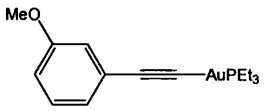	dark yellow solid	24
2.14	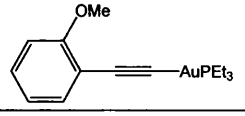	pale yellow solid	14
2.15	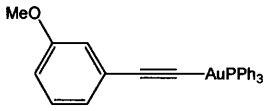	white crystals	75
2.16	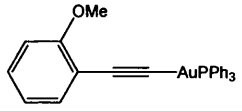	cream solid	69

Table 2.3: Synthetic data for complexes 2.04 – 2.16

Although ethynyl pyrimidine has previously been used as a ligand in a platinum(II) alkynyl complex,[39] the preparation and studies of the properties of gold alkynyl phosphine complexes

incorporating pyrimidines are so far unexplored. The study of ethynyl pyrimidine complexes of gold(I), **2.17** and **2.18**, was undertaken to establish the effect of increasing the electron withdrawing properties of the alkyne substituent without introducing additional steric features resulting from the presence of substituent groups on the aromatic ring (Table 2.4).

	Compound	Nature of Product	Yield/%
2.17	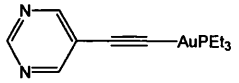	yellow needle crystals	82
2.18	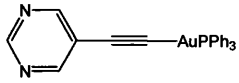	pale yellow crystals	50

Table 2.4: Synthetic data for 2.17 and 2.18

To further develop the study of triethylphosphine gold(I) alkynyl systems a series of digold phenyl and biphenyl complexes were also synthesised by the same synthetic route. While $[(R_3P)AuC{\equiv}C\text{-}C_6H_4\text{-}C{\equiv}CAu(PR_3)]$ (where R = Ph, Cy;[14] R = *p*-Tol;[19] R = Me[40]) and $[(R_3P)AuC{\equiv}C\text{-}(C_6H_4)_2\text{-}C{\equiv}CAu(PR_3)]$ (where R = Ph, Cy;[14] R = Me[40]) are reported, their triethylphosphine analogues **2.19** and **2.20** are not found in the literature (Table 2.5).

	Compound	Nature of Product	Yield/%
2.19		yellow crystals	49
2.20	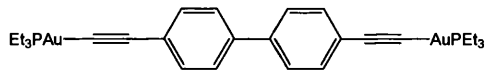	yellow crystals	52
2.21 (R = Et) **2.23 (R = Ph)**	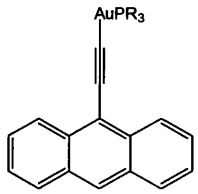	dark yellow solid yellow solid	32 81
2.22 (R = Et) **2.24 (R = Ph)**	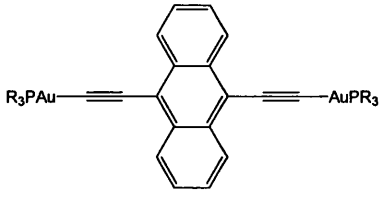	pale orange solid red crystals	12 4

Table 2.5: Synthetic data for complexes 2.19–2.24

Finally, in the development of the chemistry of triethylphosphine gold(I) alkynes the use of ethynyl substituted anthracene was explored. Incorporation of these extended chromophores

with their inherent luminescent properties would allow examination of the influence they have on the absorption and emission properties of the gold complexes.

The use of naphthalene and anthracene as a bridging unit in conjugated platinum di- and poly-ynes and studies into their effect on the luminescent properties of these complexes have been reported in the literature.[41] Yam and co-workers have prepared [(*p*-$C_6H_4Me)_3PAuC{\equiv}C\text{-}C_{14}H_8\text{-}C{\equiv}CAuP(C_6H_4Me\text{-}p)_3$] and reported its photophysical properties[19] but no other gold phosphine complexes containing ethynyl anthracene or diethynyl anthracene appear in the literature.

It was of interest to prepare and characterise the complexes **2.21–2.24** by reaction of $Me_3SiC{\equiv}C\text{-}C_{14}H_9$ or $Me_3SiC{\equiv}C\text{-}C_{14}H_8\text{-}C{\equiv}CSiMe_3$ with the corresponding gold phosphine, in order to study their structural and optical properties (Table 2.5).

2.2.2 NMR and IR Spectroscopic Characterisation

Complexes **2.01 – 2.24** have been fully characterised by multinuclear NMR spectroscopies. The ^1H NMR spectra for these complexes are relatively simple showing protons on the alkyne ligand along with those of the phosphine groups in each case. In the $^{13}C\{^1H\}$ NMR spectra of these complexes all of the expected carbon resonances are observed except for the quaternary alkyne carbon bonded to the gold atom. This is a common occurrence both in the complexes reported herein and for similar complexes in the literature and may be due to quadrupolar line broadening caused by the ^{197}Au nuclei, which is 100% abundant.[7]

Table 2.6 summarises selected spectral data for mono-gold complexes **2.01 – 2.18, 2.21 and 2.23**. The singlet resonances observed in the $^{31}P\{^1H\}$ NMR spectra are shifted downfield by 6-7 ppm from 31.60 ppm for $Au(PEt_3)Cl$, which is in a similar region to that of other gold(I) alkynyl triethylphosphine complexes,[37] or by ~9 ppm from the ^{31}P NMR signal observed at 33.35 ppm for $Au(PPh_3)Cl$.[37] The position of the ^{31}P NMR signal in the complexes shows little or no dependence on the nature of the ethynyl ligand.

Compound	PR_3	δ ^{31}P / ppm	IR / cm^{-1}
2.01	PEt_3	38.07	2105 ν(C≡C)
2.02	PEt_3	38.18	2106 ν(C≡C)
2.03	PEt_3	38.21	2102 ν(C≡C)
2.04	PEt_3	38.13	2108 ν(C≡C); 1589, 1343 ν(N=O)
2.05	PEt_3	38.14	2104 ν(C≡C); 1521, 1350 ν(N=O)
2.06	PEt_3	37.46	2108 ν(C≡C); 1522, 1348 ν(N=O)
2.07	PPh_3	42.19	2108 ν(C≡C); 1521, 1346 ν(N=O)
2.08	PEt_3	38.09	2097 ν(C≡C); 2226 ν(C≡N)
2.09	PEt_3	38.12	2106 ν(C≡C); 2228 ν(C≡N)
2.10	PEt_3	37.62	2109 ν(C≡C); 2222 ν(C≡N)
2.11	PPh_3	42.21	2113 ν(C≡C); 2226 ν(C≡N)
2.12	PEt_3	38.21	2094 ν(C≡C)
2.13	PEt_3	38.10	2105 ν(C≡C)
2.14	PEt_3	37.75	2114 ν(C≡C)
2.15	PPh_3	42.45	2115 ν(C≡C)
2.16	PPh_3	42.44	2110ν(C≡C)
2.17	PEt_3	38.08	2112 ν(C≡C)
2.18	PPh_3	42.03	2117 ν(C≡C)
2.21	PEt_3	37.81	2088 ν(C≡C)
2.23	PPh_3	42.48	2100 ν(C≡C)

Table 2.6: Selected spectral data for complexes 2.01 – 2.18, 2.21 and 2.23

The ν(C≡C) vibrational stretches show little variation through the series and are at lower frequencies than exhibited by the corresponding ligands, $Me_3SiC{\equiv}C\text{-}R$, due to the mass effect of the gold phosphine unit in the complexes.

Table 2.7 summarises spectral data for **2.19, 2.20, 2.22** and **2.24** which contain two gold phosphine units. In each case a singlet resonance is observed in the $^{31}P\{^1H\}$ NMR spectrum which is consistent with the two phosphorus nuclei being equivalent. Again there is little variation in the position of the ^{31}P NMR signal with varying the nature of the ethynyl ligand.

	PR_3	δ ^{31}P / ppm	IR / cm^{-1}
2.19	PEt_3	38.09	2106 ν(C≡C)
2.20	PEt_3	38.14	2107 ν(C≡C)
2.22	PEt_3	37.80	2091 ν(C≡C)
2.24	PPh_3	42.44	-

Table 2.7: Selected spectral data for 2.19, 2.20, 2.22 and 2.24

In the $^{31}P\{^1H\}$ NMR spectrum of **2.22**, as well as the singlet at 37.80 ppm, there is a lower intensity signal at 31.60 ppm corresponding to $Au(PEt_3)Cl$. This signal increases in intensity as the product signal decreases with prolonged exposure to $CDCl_3$ which suggests that the complex is reacting with the solvent. Similarly, the $^{31}P\{^1H\}$ NMR spectrum of **2.24** exhibits a small signal at 33.35 ppm, corresponding to $Au(PPh_3)Cl$, which increases in intensity with time. However, the $^{31}P\{^1H\}$ NMR spectrum of **2.24**, in benzene, exhibits only the signal for the product at 42.39 ppm suggesting that the complex is not stable in chlorinated solvent, and decomposes to reform the gold starting material.

2.2.3 Molecular Structures

The structure of **2.02** was determined from a single crystal grown from ethyl acetate at -25 °C. The asymmetric unit consists of a two coordinate gold centre with an alkyne ligand and a phosphine ligand (Figure 2.9). There is a molecule of water present in the asymmetric unit (which is omitted in the figure below). Selected bond lengths and angles are listed in Table 2.8. The C–C, Au–C and Au–P bonds are all within the range of similar species in the literature.[9] As can be seen there is a bend in the molecule away from the expected linearity about the Au–C≡C linkage [Au(1)–C(7)–C(8), 168.1(3)°]. This may be explained by the presence of Au····Au interactions in the solid state structure.

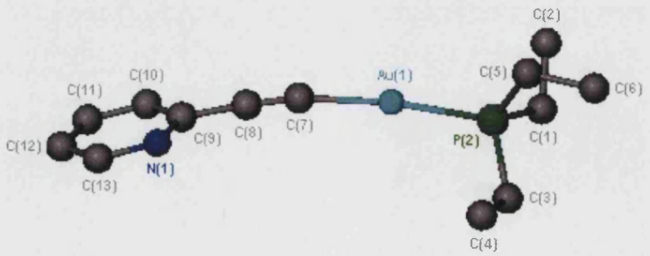

Figure 2.9: Structure of [Et_3PAuCC-2-C_5H_4N] 2.02 (hydrogen atoms omitted for clarity)

Contact	Bond Length (Å)	Contact	Bond Angle (°)
C(7)–C(8)	1.169(6)	C(7)–C(8)–C(9)	176.8(5)
Au(1)–C(7)	2.047(4)	Au(1)–C(7)–C(8)	168.1(3)
P(1)–Au(1)	2.2816(11)	P(1)–Au(1)–C(7)	172.03(10)

Table 2.8: Selected bond lengths and angles for 2.02

The shortest intermolecular Au····Au distance of 3.403 Å is towards the longer end of the range of Au····Au distances in which there is thought to be an interaction between the metal centres. Figure 2.10 illustrates how these interactions result in a continuous weakly bound polymer in the solid state with a triangular central channel, the side of each triangle is made up of the P(1)–Au(1)–C(7) unit of each molecule. From this arrangement it appears that the bend in the molecule is necessary to reduce steric interactions between the pyridine ring of one molecule and the phosphine group of a neighbouring molecule.

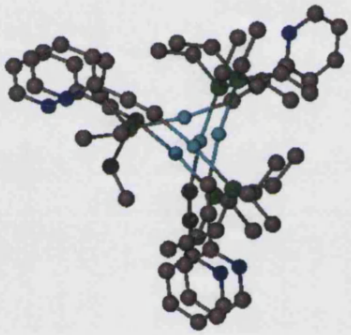

Figure 2.10: Continuous chains in 2.02 held together by weak Au····Au contacts

The solid state structure of $[(Et_3P)AuC{\equiv}C\text{-}C_6H_5]$, **2.03**, (Figure 2.11) was determined allowing comparisons to be made with the pyridine analogues. In the crystal structure, the molecule is approximately linear at the gold centre [P(1)–Au(1)–C(1), 178.75(11)°; Au(1)–C(1)–C(2), 177.0(3)°; C(1)–C(2)–C(3), 177.2(4)°]. There are no Au····Au contacts present in the solid state structure with the shortest Au····Au distance, 4.321 Å, outside the expected range defined for Au····Au interactions.

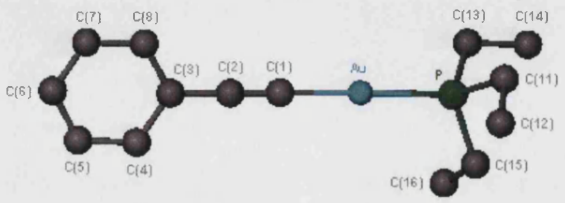

Figure 2.11: Structure of 2.03 (hydrogen atoms omitted for clarity)

	R_3PAu-C≡C-3-C_5H_4N		R_3PAu-C≡C-2-C_5H_4N		R_3PAu-C≡C-C_6H_5	
R =	PEt_3 (**2.01**)	PPh_3	PEt_3 (**2.02**)	PPh_3	PEt_3 (**2.03**)	PPh_3
C(1)-C(2) (Å)	1.185(12)–1.208(12)	1.194(8)	1.169(6)	1.21(1)	1.217(5)	1.18(2)
Au(1)-C(1) (Å)	1.989(9)–2.004(9)	2.015(5)	2.047(4)	1.95(1)	1.994(4)	1.97(2)
Au(1)-P(1) (Å)	2.303(2)–2.311(2)	2.2812(13)	2.2816(11)	2.263(3)	2.2806(9)	2.276(5)
C(1)-C(2)-C(3) (°)	176.9(10)–178.4(10)	178.3(6)	176.8(5)	177(1)	177.2(4)	176.5(18)
Au(1)-C(1)-C(2)(°)	175.4(8)–179.4(9)	169.2(5)	168.1(3)	177(1)	177.0(3)	175.7(16)
P(1)-Au(1)-C(1)(°)	n/a	167.94(17)	172.03(10)	177.3(3)	178.75(11)	173.8(5)
Au····Au (Å)	3.0960(3)–3.1823(3)	3.3364(4)	3.40297(11)	–	4.321	3.379(1)

Table 2.9: Selected bond lengths and angles for 2.01, 2.02, 2.03, [(Ph_3P)Au-C≡C-3-C_5H_4N],[37] [(Ph_3P)Au-C≡C-2-C_5H_4N][9] and [(Ph_3P)Au-C≡C-C_6H_5][32]

In Table 2.9 selected bond lengths and angles of **2.01**, **2.02** and **2.03** are listed along with their triphenylphosphine analogues in the literature. The rearrangement observed in the structure of **2.01** means that it is not strictly comparable with the other five compounds as, although the C(1)–C(2)–C(3) and Au(1)–C(1)–C(2) angles are approximately linear, there are either two alkyne ligands or two phosphine ligands coordinated to each gold atom.

As can be seen from the data, there is little variation in C≡C, Au–C and Au–P bond lengths between triethylphosphine to triphenylphosphine analogues. The notable difference is in the Au–C≡C and P–Au–C bond angles and the bend away from linearity. This bend is due to the proximity of molecules in the solid state and is enforced to reduce steric interactions between phosphine groups on neighbouring molecules. The bending of the molecules may also be attributed, in part, to the formation of the Au····Au bonding interactions, as the gold centres are "directed" towards each other showing a deviation towards three-coordination. This distortion from linearity at the gold centre has been observed in the majority of structural examples where aurophilic interactions are proposed[1,2] and is further evidenced by the fact that in **2.03** and [(PPh_3)Au–C≡C-2-C_5H_4N], where there are no Au····Au contacts present, the bond angles about the gold centre are approximately linear.

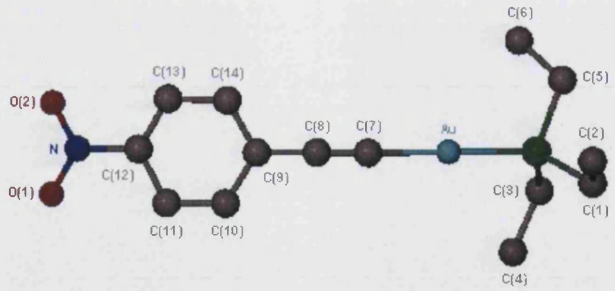

Figure 2.12: Structure of [(Et_3P)AuC≡C-4-C_6H_4-NO_2] 2.04 (hydrogen atoms omitted for clarity)

Figure 2.12 illustrates the asymmetric unit of the cell in the crystal structure of **2.04** which comprises an independent molecule. Selected bond lengths and angles are listed in Table 2.10. Although the P(1)–Au(1)–C(7) bond angle is approximately linear at 176.1(3)°, the Au(1)–C(7)–C(8) unit bends away from linearity to 169.4(10)° which is similar to the bend in the alkyne unit of **2.02** and again is clearly a consequence of minimising the steric interactions between the nitrophenyl ring on one molecule and the phosphine group on a neighbouring molecule. There is an absence of intermolecular association in the solid state with the shortest Au····Au distance between adjacent molecules being 8.250 Å (Figure 2.13).

Contact	Bond Length (Å)	Contact	Bond Angle (°)
C(7)–C(8)	1.214(15)	C(7)–C(8)–C(9)	172.9(10)
Au(1)–C(7)	2.002(13)	Au(1)–C(7)–C(8)	169.4(10)
P(1)–Au(1)	2.280(3)	P(1)–Au(1)–C(7)	176.1(3)

Table 2.10: Selected bond lengths and angles for 2.04

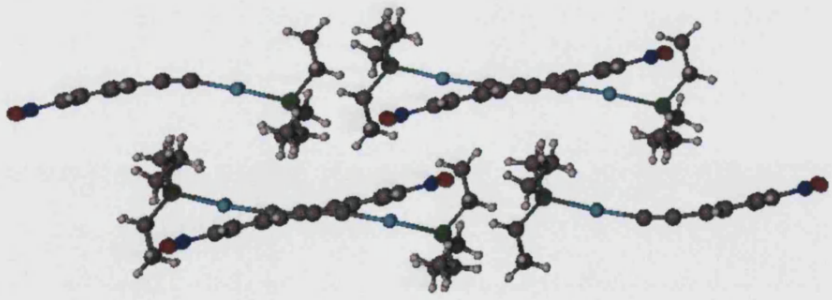

Figure 2.13: Alignment of [(Et_3P)AuCC-4-C_6H_4-NO_2] 2.04 molecules

The asymmetric unit within the unit cell of **2.05** comprises two independent molecules of [(Et_3P)AuC≡C-3-$C_6H_4NO_2$] arranged as illustrated in Figure 2.14a. Table 2.11 lists a selection of bond lengths and angles for the gold alkyne unit of the two molecules which show the molecules to possess an approximately linear geometry in each case. However, in the

extended solid state structure each of these molecules form half of a dimeric pair held together by an Au····Au interaction, with an Au····Au distance of 3.1695(6) Å and torsion angle [P(1)–Au(1)–Au(2)–P(3)] of 118.5° (Figure 2.14b).

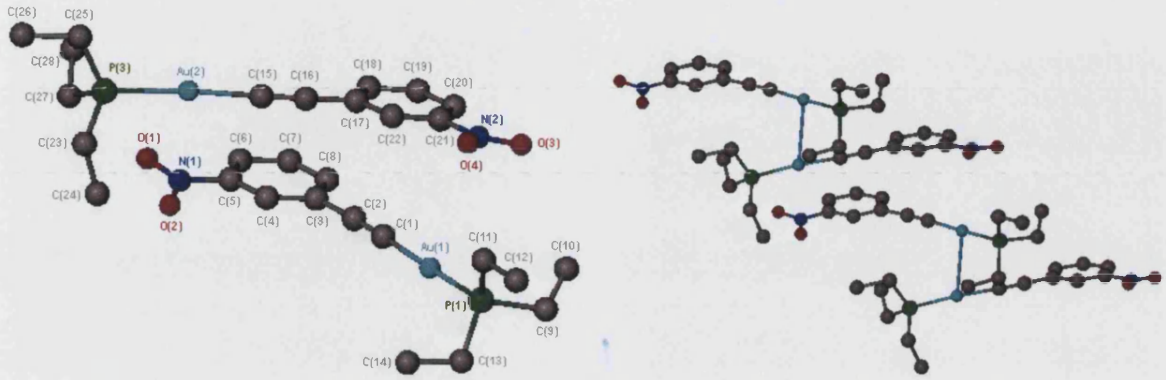

Figure 2.14: a) Asymmetric unit of 2.05; b) Dimer pairs in solid state structure

Contact	Bond Length (Å)	Contact	Bond Angle (°)
C(1)–C(2)	1.218(14)	C(1)–C(2)–C(3)	175.1(12)
C(15)–C(16)	1.218(15)	C(15)–C(16)–C(17)	174.3(12)
Au(1)–C(1)	2.005(10)	Au(1)–C(1)–C(2)	178.1(10)
Au(2)–C(15)	2.018(11)	Au(2)–C(15)–C(16)	178.4(4)
P(1)–Au(1)	2.281(3)	P(1)–Au(1)–C(1)	176.1(3)
P(3)–Au(2)	2.287(3)	P(3)–Au(2)–C(15)	174.7(3)

Table 2.11: Selected bond lengths and angles in 2.05

The asymmetric unit of **2.06** consists of two molecules held together by an Au····Au interaction (3.1865(3) Å) effectively forming a loosely bound dimer (Figure 2.25). The gold alkyne unit of each molecule is approximately linear [P(1)–Au(1)–C(1), 175.05(19)°; Au(1)–C(1)–C(2), 177.2(6)°; C(1)–C(2)–C(3), 177.8(7)°] with little deviation in bond lengths as compared with previously discussed complexes and gold(I) phosphines. The torsion angle, P(1)–Au(1)–Au(2)–P(2), of 123.1° is similar to that in **2.05**. As can be seen from the data in Table 2.12, there no significant variation in bond lengths or angles between the two molecules.

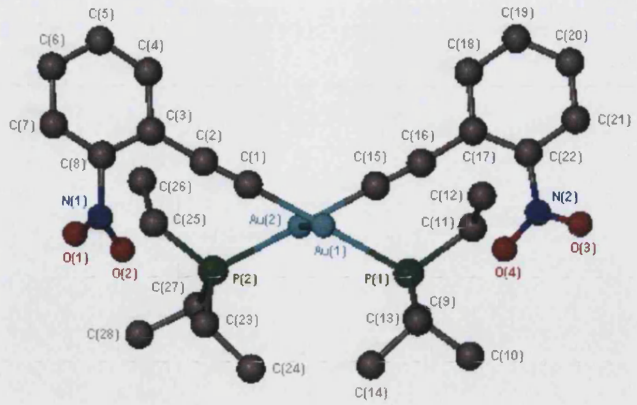

Figure 2.15: Structure of $[(Et_3P)AuC{\equiv}C\text{-}2\text{-}C_6H_4\text{-}NO_2]$ 2.06 (hydrogens omitted for clarity)

Bond Length (Å)	Molecule 1	Molecule 2	Bond Angle (°)	Molecule 1	Molecule 2
C(1) – C(2)	1.188(9)	1.188(9)	C(1)–C(2)–C(3)	177.8(7)	174.8(7)
Au(1) – C(1)	2.025(7)	2.027(7)	Au(1)–C(1)– C(2)	177.2(6)	177.2(6)
P(1) – Au(1)	2.2905(15)	2.2891(16)	P(1)–Au(1)– C(1)	175.05(19)	175.85(18)

Table 2.12: Selected bond lengths and angles of the two molecules in asymmetric unit of 2.06

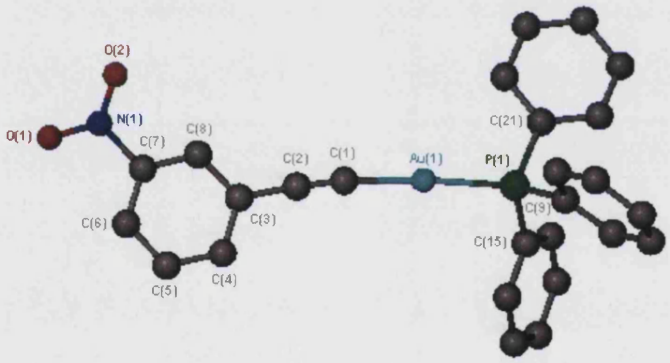

Figure 2.16: Structure of $[(Ph_3P)AuC{\equiv}C\text{-}3\text{-}C_6H_4NO_2]$, 2.07 (hydrogen atoms omitted for clarity)

In the solid state structure of **2.07**, the asymmetric unit consists of an independent molecule which has an approximately linear geometry about the gold centre [Au(1)–C(1)–C(2), 173.6(2)°; P(1)–Au(1)–C(1), 175.93(7)°] (Figure 2.16). The C(1)–C(2), Au(1)–C(1) and Au(1)–P(1) bond lengths are all within range of other alkynyl gold(I) phosphine complexes previously quoted herein. There are no Au····Au interactions observed in the solid state structure with the shortest distance between gold atoms being 6.560 Å.

Contact	**2.05**	**2.07**
C(1)–C(2) (Å)	1.218(14)	1.206(3)
Au(1)–C(1) (Å)	2.005(10)	2.000(2)
Au(1)–P(1) (Å)	2.281(3)	2.2784(6)
C(1)–C(2)–C(3) (°)	175.1(12)	174.8(3)
Au(1)–C(1)–C(2) (°)	178.1(10)	173.6(2)
P(1)–Au(1)–C(1) (°)	176.1(3)	175.93(7)
Au····Au (Å)	3.1695(6)	-

Table 2.13: Selected bond lengths and angles for 2.05 and 2.07

From the data in Table 2.13 it is clear that there is little variation in bond length between the two complexes **2.05** and **2.07**. The absence of Au····Au interactions in **2.07**, present in **2.05**, is a steric consequence of the steric size of the phenyl rings on the phosphine preventing the close approach of neighbouring molecules. The slight bend away from linearity in **2.07** [Au(1)–C(1)–C(2), 173.6(2)°], as compared with **2.05**, may also be necessary to prevent steric interactions between the phenyl rings of the phosphine group with the nitrophenyl ring of a neighbouring molecule as they align in an anti-parallel arrangement in the solid state structure.

The structure of **2.08** (Figure 2.17) was determined crystallographically with the Au(I) centre being two coordinate with linear geometry as seen in the previously discussed systems. The asymmetric unit of the cell consists of two molecules held together by a Au····Au contact of 3.1656(2) Å which forms a non-covalently bonded dimer with a torsion angle P(1)–Au(1)–Au(2)–P(2) of 118.1°. Again this angle is similar to those found in the previously described dimer pairs and is a consequence of reducing steric interactions between the phosphine groups and alkynyl ligands.

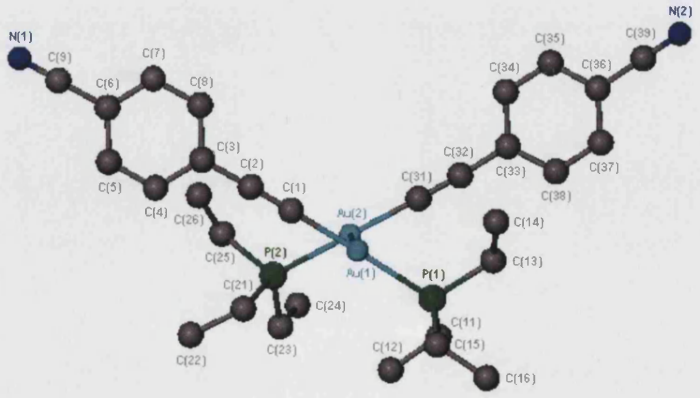

Figure 2.17: Asymmetric cell unit of 2.08 (hydrogen atoms omitted for clarity)

Selected bond lengths and angles for both molecules in the asymmetric unit are listed in Table 2.14. There is little variation in bond length between the molecules which have an approximately linear P–Au–C≡C backbone.

Bond Length (Å)	Molecule 1	Molecule 2	Bond Angle (°)	Molecule 1	Molecule 2
C(1) – C(2)	1.214(6)	1.224(6)	C(1)–C(2)–C(3)	178.1(4)	176.5(4)
Au(1) – C(1)	2.005(4)	1.994(4)	Au(1)–C(1)– C(2)	178.9(4)	178.1(4)
P(1) – Au(1)	2.2913(10)	2.2890(10)	P(1)–Au(1)– C(1)	176.24(12)	174.79(12)

Table 2.14: Selected bond lengths and angles of the two molecules in asymmetric unit of 2.08

The complex $[(Et_3P)AuC{\equiv}C\text{-}3\text{-}C_6H_4CN]$ **2.09** was prepared but attempts to grow single crystals were unsuccessful therefore characterisation was achieved by spectroscopic methods and by microanalysis.

The somewhat unexpected structure of **2.10** is illustrated in Figure 2.18 and bond lengths and angles of interest are listed in Table 2.15. The structure is effectively composed of a gold trimer and a gold monomer with interesting rearrangement of ligands coordinated to the gold centres and may be compared with that of $[Au_3(Ph_2PCH_2PPh_2)_2(C{\equiv}CR)_2][Au(C{\equiv}CR)_2]$.[23] The main difference between the structure of **2.10** and the structures reported by Yam *et al* is that while **2.10** has a linear geometry the latter has a triangular architecture, which is most likely due to the presence of the chelating phosphine.

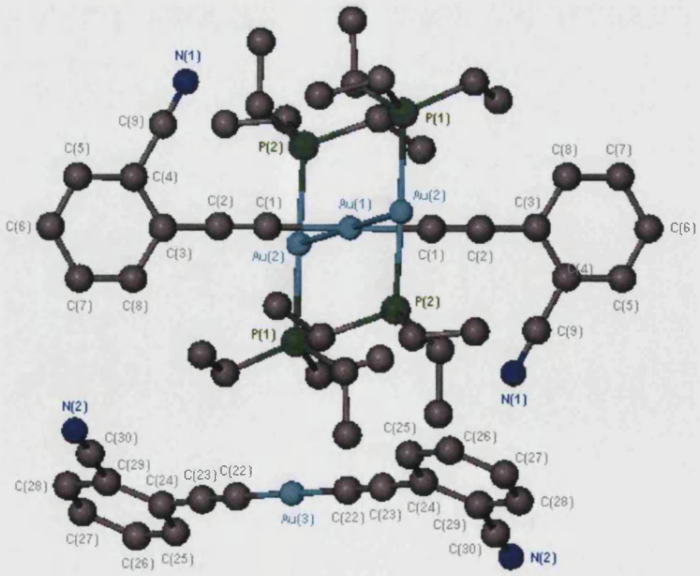

Figure 2.18: Rearrangement of 2.10 molecules in solid state (hydrogen atoms omitted for clarity)

In the trimeric unit, the two outside gold centres, Au(2), have two triethylphosphine groups coordinated in a linear geometry and the central gold atom, Au(1), has two alkyne ligands also coordinated linearly. The monomer consists of a gold atom with two alkyne ligands coordinated which maintains the overall neutral charge.

Contact	Bond Length (Å)	Contact	Bond Angle (°)
C(1)–C(2)	1.199(16)	Au(2)–Au(1)–Au(2)	180
Au(1)–C(1)	2.017(12)	C(1)–C(2)–C(3)	178.0(12)
Au(2)–Au(1)	2.9773(4)	P(1)–Au(2)–P(2)	174.98(11)
Au(2)–P(1)	2.314(3)	C(1)–Au(1)–C(1)	180
Au(2)–P(2)	2.321(3)	C(22)–C(23)–C(24)	178.2(10)
Au(3)–C(22)	1.984(10)	C(22)–Au(3)–C(22)	180
C(22)–C(23)	1.220(13)		

Table 2.15: Selected bond lengths and angles for 2.10

The trimer is crystallographically linear at the Au(1) centre with Au(2)–Au(1)–Au(2) bond angle 180.0° and Au····Au distance 2.9773(4) Å which is the shortest reported herein. The bond lengths are within the range observed in other alkynyl gold(I) phosphine complexes.[7] The alkyne ligands are arranged linearly about the central gold atom [C(1)–Au(1)–C(1), 180°; C(1)–C(2)–C(3) 178.0(12)°] while the phosphine ligands on the outside gold atoms exhibit a slight bend away from linearity which may reduce steric interactions between the ethyl groups on neighbouring molecules. The gold monomer is also approximately linear [C(22)–Au(3)–C(22), 180°; C(22)–C(23)–C(24), 178.2(10)°] and forms a sandwich layer between gold trimer layers as shown in Figure 2.19.

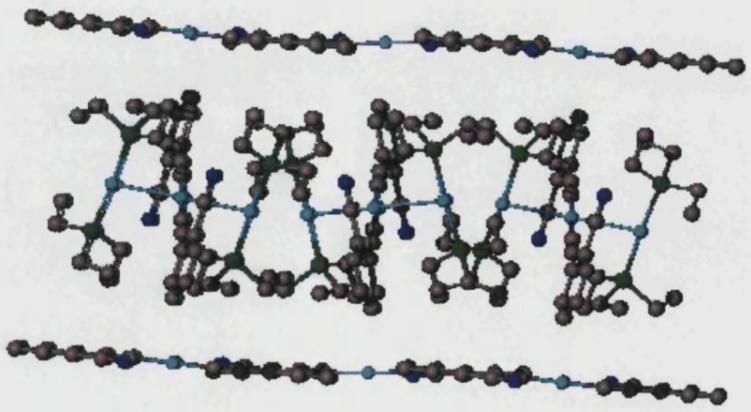

Figure 2.19: Association of 2.10 molecules in solid state

As with **2.07**, the asymmetric unit of **2.11** consists of a single molecule (Figure 2.20). Selected bond angles and lengths are listed in Table 2.16. The molecule has an approximately linear backbone [P(1)–Au(1)–C(1), 175.86(16)°; Au(1)–C(1)–C(2), 175.4(5)°; C(1)–C(2)–C(3), 177.8(6)°]. There are no Au····Au contacts observed in the solid state structure as the shortest distance between gold centres is 6.935 Å, a consequence of the steric bulk of the triphenylphosphine ligand preventing close approach of molecules.

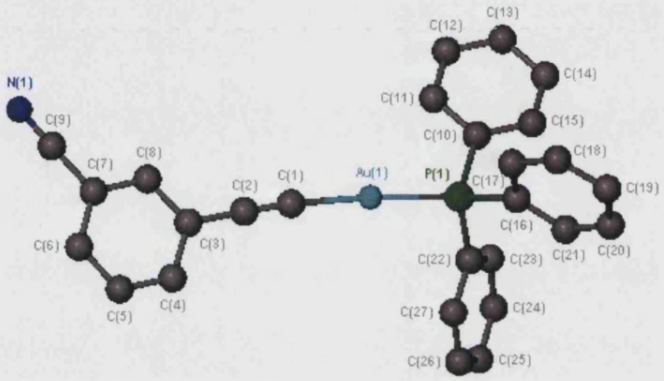

Figure 2.20: Asymmetric unit of 2.11 (hydrogen atoms omitted for clarity)

Contact	Bond Length (Å)	Contact	Bond Angle (°)
C(1)–C(2)	1.201(8)	C(1)–C(2)–C(3)	177.8(6)
Au(1)–C(1)	1.995(6)	Au(1)–C(1)–C(2)	175.4(5)
P(1)–Au(1)	2.2746(15)	P(1)–Au(1)–C(1)	175.86(16)

Table 2.16: Selected bond lengths and bond angles for 2.11

In the crystal structure of **2.12**, the asymmetric unit consists of a single molecule (Figure 2.21). While the molecule has an approximately linear backbone [C(1)–C(2)–C(3), 177.4(3)°; P(1)–Au(1)–C(1), 177.10(8)°], the gold alkyne unit displays a slight bend [Au(1)–C(1)–C(2), 175.6(2)°]. Selected bond lengths and angles for **2.12** are listed in Table 2.17. The bond lengths are within the range observed for other alkynyl gold(I) phosphine complexes herein. The shortest distance between gold atoms is 4.685 Å which is outside the range for Au····Au interactions between the molecules to be present.

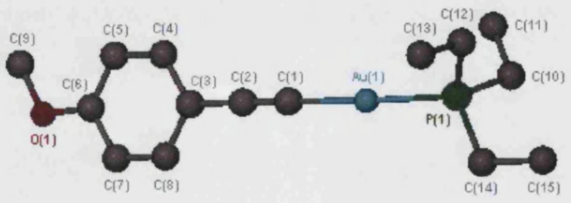

Figure 2.21: Asymmetric unit of 2.12 (hydrogen atoms omitted for clarity)

Contact	Bond Length (Å)	Contact	Bond Angle (°)
C(1)–C(2)	1.203(4)	C(1)–C(2)–C(3)	177.4(3)
Au(1)–C(1)	2.004(3)	Au(1)–C(1)–C(2)	175.6(2)
P(1)–Au(1)	2.2818(6)	P(1)–Au(1)–C(1)	177.10(8)

Table 2.17: Selected bond lengths and angles for 2.12

Figure 2.22 illustrates how the molecules of **2.21** pack in the solid state. The bend in the molecule reduces steric interaction between the aromatic ring on one molecule and the triethylphosphine groups on neighbouring molecules.

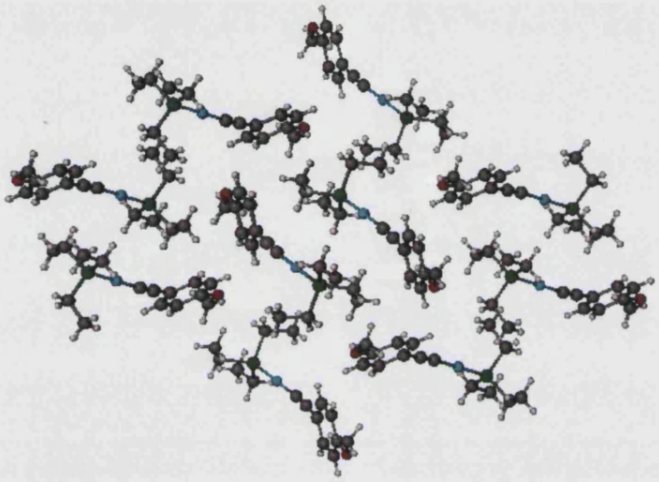

Figure 2.22: Association of molecules in sold state structure of 2.12

The structure of [$(Ph_3P)AuC{\equiv}C\text{-}3\text{-}C_6H_4OMe$] **2.15** is illustrated in Figure 2.23. The asymmetric unit of the cell consists of an independent molecule. The shortest distance between gold centres is 7.231 Å which is too long for any Au···Au interaction to be present between them. The backbone of the molecule is approximately linear about the P–Au–C unit [P(1)–Au(1)–C(1), 177.91(7)°] and alkyne [C(1)–C(2)–C(3), 176.3(3)°] but there is a slight bend of the ring away from linearity [Au(1)–C(1)–C(2), 174.5(2)°]. The bond lengths and angles, listed in Table 2.18, are in the range of those observed in other alkynyl gold(I) phosphines.

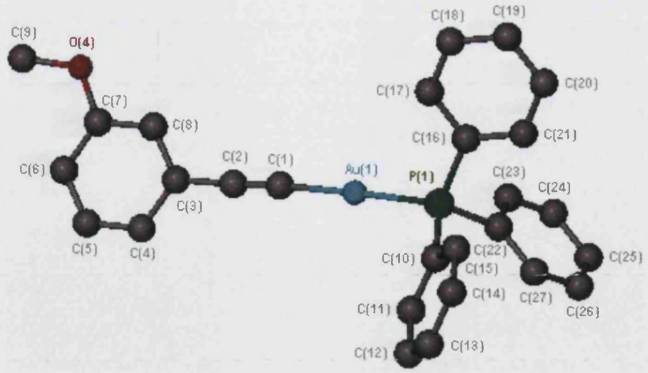

Figure 2.23: Asymmetric unit of 2.15 (hydrogen atoms omitted for clarity)

Contact	Bond Length	Contact	Bond Angle (°)
C(1)–C(2)	1.203(3)	C(1)–C(2)–C(3)	176.3(3)
Au(1)–C(1)	2.001(2)	Au(1)–C(1)–C(2)	174.5(2)
P(1)–Au(1)	2.2756(6)	P(1)–Au(1)–C(1)	177.91(7)

Table 2.18: Selected bond lengths and angles for 2.15

While the structure of **2.17** is twinned it was possible to determine the key features. The structure consists of a polymeric chain of gold atoms. Figure 2.24a illustrates the asymmetric unit, with disorder in the pyrimidine ring and phosphine group omitted for clarity. The ligands are arranged perpendicular to the Au····Au contact [C(1)–Au(1)–Au(2), 89.1(5)–90.9(5)°; P(1)–Au(2)–Au(1), 89.8(3)–90.2(3)°]. The Au····Au contacts extend through the structure by links to symmetry related gold atoms and the second phosphine or alkyne is generated by a two fold rotation.

Figure 2.24b shows the view along the gold chain axis and, as with **2.01**, the ligands have rearranged so that alternating gold atoms have either two alkyne ligands or two phosphine ligands and form linear gold chains [Au(1)–Au(2)–Au(1), 180.0°] with Au····Au separations of 3.114 – 3.118 Å. Selected bond length and bond angle ranges are listed in Table 2.19.

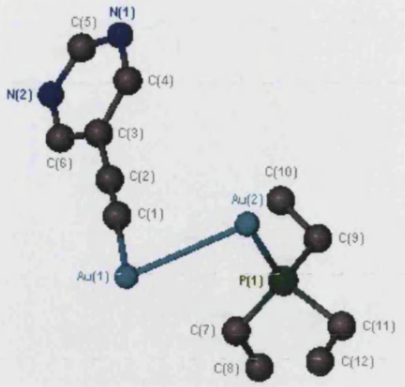

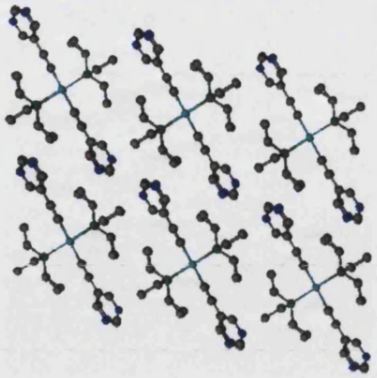

Figure 2.24: a) Asymmetric unit of 2.17; b) view along gold chain axis

Contact	Bond length (Å)	Contact	Bond Angle (°)
Au(2)–P(1)	2.3077(12)	C(1)–C(2)–C(3)	165.0(2) – 173.5(18)
Au(1)–C(1)	1.990(4)	Au(1)–C(1)–C(2)	176.7(16)
C(1)–C(2)	1.211(5)	C(1)–Au(1)–C(1)#	178.2(10)
C(2)–C(3)	1.443(8) – 1.448(9)	C(1)–Au(1)–Au(2)	89.1(5) – 90.9(5)
C(3)–C(4)	1.377(8) – 1.405(9)	C(7)–P(1)–Au(2)	110.8(6) – 117.8(7)
C(4)–N(1)	1.333(8) – 1.342(10)	P(1)–Au(2)–P(1)#	179.6(6)
N(1)–C(5)	1.320(8) – 1.340(9)	P(1)–Au(2)–Au(1)	89.8(3) – 90.2(3)
Au····Au	3.1140(10) – 3.1180(10)	Au(2)–Au(1)–Au(2)	180.0

Table 2.19: Selected bond lengths and angles for 2.17

Selected bond angles for $[(Et_3P)AuC{\equiv}C\text{-}3\text{-}C_5H_4N]$ **2.01**, **2.17** and $[((Me)_3NB(H_2)NC)_2Au][AuI_2]$ along with Au····Au contacts present in the structures are listed in Table 2.20. The structures have a similar linear arrangement of ligands about each gold centre. The Au(2)–Au(1)–Au(2) bond angles in **2.17** and $[((Me)_3NB(H_2)NC)_2Au][AuI_2]$ are fixed by crystallographic symmetry due to the nature of the asymmetric unit, in each case comprising of a C≡CR ligand and a phosphine or iodide coordinated to a distinct gold atom unlike that of **2.01** (Figure 2.5a).

Contact	**2.01**	**2.17**	**$[((Me)_3NB(H_2)NC)_2Au][AuI_2]$**
C(1)–Au(1)–C(1)#	175.9(3)	178.2(10)	180.0
P(1)–Au(2)–P(1)#	178.05(8)	179.6(6)	n/a
Au(2)–Au(1)–Au(2)	176.172(13)	180.0	180.0
Au····Au	3.0960(3) – 3.1823(3)	3.1140(10) – 3.1180(10)	3.0438(7)

Table 2.20: Selected bond lengths and angles for 2.01, 2.17 and $[((Me)_3NB(H_2)NC)_2Au][AuI_2]$[42]

In the crystal structure of **2.18**, the asymmetric unit consists of one independent molecule (Figure 2.25a), however, in the extended solid state structure there are Au····Au interactions between two molecules [Au(1)–Au(2), 3.2784(2) Å] forming weakly bound dimers. The bond lengths and angles for **2.18** are similar to those observed in **2.17** and are listed in Table 2.21.

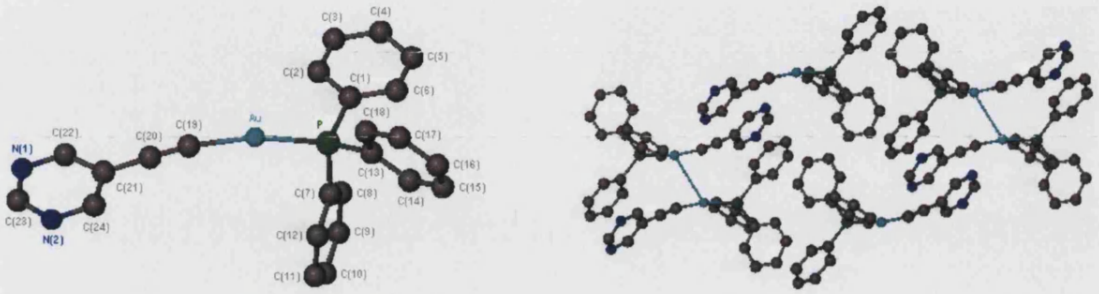

Fig 2.25: a) Structure of $[(Ph_3P)AuC{\equiv}C\text{-}5\text{-}C_4H_3N_2]$; b) association of molecules in solid state

Contact	Bond length (Å)	Contact	Bond Angle (°)
C(1)–C(2)	1.196(5)	C(1)–C(2)–C(3)	178.5(4)
Au(1)–C(1)	2.001(4)	Au(1)–C(1)–C(2)	171.5(3)
P(1)–Au(1)	2.2801(8)	P(1)–Au(1)–C(1)	167.21(11)

Table 2.21: Selected bond lengths and bond angles for 2.18

The two molecules comprising each dimer adopt an anti-parallel arrangement, relative to each other, which forces a bend in the P–Au–C unit [P(1)–Au(1)–C(1), 167.21(11)°] to reduce steric interactions between the pyrimidine ring of one molecule and the phenyl rings on the other molecule (Figure 2.25b), and assists with the Au····Au interaction.

Attempts to grow single crystals of **2.21** and **2.22** were unsuccessful. Recrystallisation of **2.21** and **2.22** afforded a dark yellow solid and a pale orange solid, respectively. Single crystals of **2.23** were grown from methanol/dichloromethane (1:1). As can be seen in Figure 2.26, the asymmetric unit consists of an independent molecule which has an approximately linear backbone [C(19)–C(20)–C(21), 177.7(4)°; Au(1)–C(19)–C(20), 175.1(3)°; P(1)–Au(1)–C(19), 175.63(11)°]. The shortest distance between gold centres is 8.694 Å which is too long for there to be Au····Au interactions present. A selection of bond lengths and angles are listed in Table 2.22.

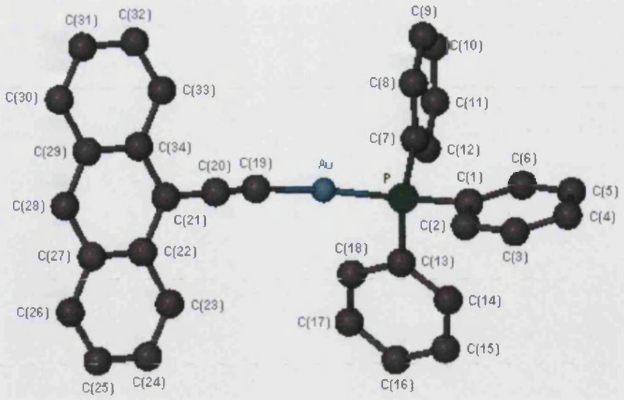

Figure 2.26: Structure of 2.23 (hydrogen atoms omitted for clarity)

Contact	Bond Length (Å)	Contact	Bond Angle (°)
C(19)–C(20)	1.200(5)	C(19)–C(20)–C(21)	177.7(4)
Au(1)–C(19)	2.002(3)	Au(1)–C(19)–C(20)	175.1(3)
P(1)–Au(1)	2.2723(8)	P(1)–Au(1)–C(19)	175.63(11)

Table 2.22: Selected bond lengths and bond angles for 2.23

Although Yam and co-workers reported that the triphenylphosphine analogue of [(*p*-$C_6H_4Me)_3PAuC{\equiv}C\text{-}C_{14}H_8\text{-}C{\equiv}CAuP(C_6H_4Me\text{-}p)_3$] was insoluble in most organic solvents,[19] single crystals of [$(Ph_3PAuC{\equiv}C\text{-}C_{14}H_8\text{-}C{\equiv}CAuPPh_3)$] **2.24** were grown from dichloromethane/ methanol (1:1). While it was possible to determine the solid state structure (Figure 2.27) there was insufficient material to allow full characterisation.

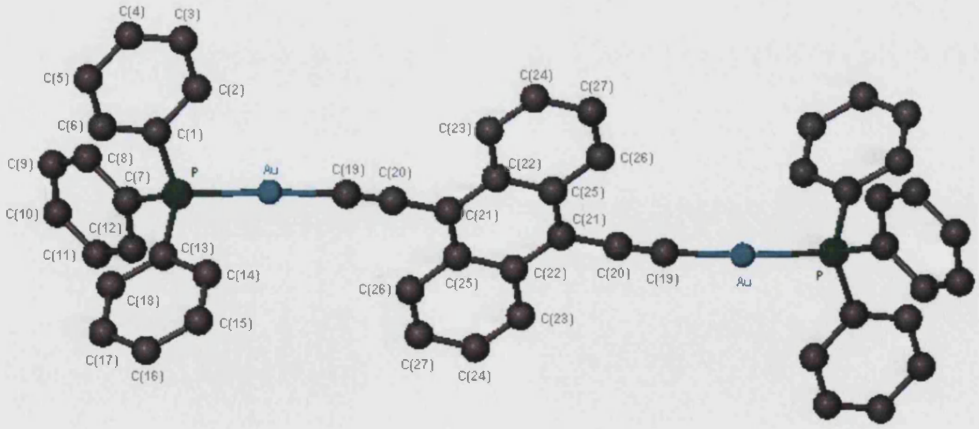

Figure 2.27: Structure of 2.24 (hydrogen atoms omitted for clarity)

Table 2.23 lists selected bond lengths and angles for the gold alkyne units of **2.24**. The gold phosphine units are slightly bent in opposite directions away from the anthracene unit to

reduce steric interactions with neighbouring molecules. The shortest distance between gold centres is 9.221 Å which is outside the range for Au····Au contacts to be present. The steric bulk of the phenyl rings on the phosphine prevent the close approach of molecules preventing the possibility of Au····Au interactions.

Contact	Bond Length (Å)	Contact	Bond Angle (°)
C(19)–C(20)	1.200(5)	C(19)–C(20)–C(21)	176.3(4)
Au(1)–C(19)	2.002(4)	Au(1)–C(19)–C(20)	174.7(4)
P(1)–Au(1)	2.2794(10)	P(1)–Au(1)–C(19)	174.91(12)

Table 2.23: Selected bond lengths and bond angles for 2.24

Table 2.24 lists bond angle and bond length data about the gold centre for the complexes whose solid state structures were crystallographically determined. There is little variation throughout the series which suggests a relative insensitivity of the gold centre to different ring substituents on the alkyne ligands.

	P–Au (Å)	Au–C (Å)	P–Au–C (°)
2.01*	2.303(2)– 2.311(2)	1.989(9)–2.004(9)	n/a
2.02	2.2816(11)	2.047(4)	172.03(10)
2.03	2.2806(9)	1.994(4)	178.75(11)
2.04	2.280(3)	2.002(13)	176.1(3)
2.05	2.281(3)–2.287(3)	2.005(10)–2.018(11)	174.7(3)–176.1(3)
2.06	2.2891(16)–2.2905(15)	2.025(7)–2.027(7)	175.05(19)–175.85(18)
2.07	2.2784(6)	2.000(2)	175.93(7)
2.08	2.2890(10)–2.2913(10)	1.994(4)–2.005(4)	174.79(12)–176.24(12)
2.10*	2.314(3)–2.321(3)	1.984(10)–2.017(12)	n/a
2.11	2.2746(15)	1.995(6)	175.86(16)
2.12	2.2818(6)	2.004(3)	177.10(8)
2.15	2.2756(6)	2.001(2)	177.91(7)
2.17*	2.3077(12)	1.990(4)	n/a
2.18	2.2801(8)	2.001(4)	167.21(11)
2.23	2.2723(8)	2.002(3)	175.63(11)
2.24	2.2794(10)	2.002(4)	174.91(12)

Table 2.24: Bond lengths and angles about the gold centre of each complex (* complexes with rearrangement of ligands)

2.2.4 UV/visible Spectroscopic Studies

The electronic absorption spectra of gold complexes **2.01–2.23** were obtained for 0.05 mM solutions in dichloromethane at room temperature. Table 2.25 lists the electronic absorption spectral data along with the optical gap for each complex taken as the onset of absorption. In each case the spectra have a similar profile to that of the corresponding trimethylsilyl-protected ligand. This similarity suggests a strong dependence on the alkyne and that the absorptions arise from ligand centred π–π^* C≡C transitions. There is a red shift on complexation of the gold phosphine unit to the alkyne which is consistent with a small but significant increase in conjugation length along the molecule through the metal centre or reflects the presence of a heavy metal unit on the dipole of the C≡C–R groups.[20] As expected, the emission spectra exhibit an approximate mirror image of the lowest energy bands observed in the electronic absorption spectrum.

	Absorption λ (nm) (ε = 10^4 $mol^{-1}dm^3$ cm^{-1}) *	Optical gap (eV)
[$(Et_3P)AuC{\equiv}C\text{-}3\text{-}C_5H_4N$] **2.01**	255 (0.9), 268 (1.4), 280 (1.3), 288 (1.1)	3.75
[$(Et_3P)AuC{\equiv}C\text{-}2\text{-}C_5H_4N$] **2.02**	255 (1.2), 265 (1.6), 289 (1.7), 297 (1.6)	4.00
[$(Et_3P)AuC{\equiv}C\text{-}C_6H_5$] **2.03**	255 (1.3), 267 (2.5), 281 (2.6)	4.08
[$(Et_3P)AuC{\equiv}C\text{-}4\text{-}C_6H_4NO_2$] **2.04**	337 (2.1)	2.99
[$(Et_3P)AuC{\equiv}C\text{-}3\text{-}C_6H_4NO_2$] **2.05**	255 (1.9), 266 (2.8), 281 (2.8)	3.10
[$(Et_3P)AuC{\equiv}C\text{-}2\text{-}C_6H_4NO_2$] **2.06**	259 (1.5), 279 (1.2), 348 (0.4)	2.76
[$(Ph_3P)AuC{\equiv}C\text{-}3\text{-}C_6H_4NO_2$] **2.07**	255 (4.9), 268 (4.6), 283 (4.4)	3.08
[$(Et_3P)AuC{\equiv}C\text{-}4\text{-}C_6H_4CN$] **2.08**	269 (1.3), 285 (3.0), 302 (4.1), 325 (0.6)	3.57
[$(Et_3P)AuC{\equiv}C\text{-}3\text{-}C_6H_4CN$] **2.09**	268 (1.2), 281 (1.6), 310 (0.1)	3.86
[$(Et_3P)AuC{\equiv}C\text{-}2\text{-}C_6H_4CN$] **2.10**	265 (1.5), 279 (2.4), 306 (0.9), 316 (1.0), 335 (0.2)	3.59
[$(Ph_3P)AuC{\equiv}C\text{-}3\text{-}C_6H_4CN$] **2.11**	269 (4.6), 283 (4.4), 311 (4.0)	3.87
[$(Et_3P)AuC{\equiv}C\text{-}4\text{-}C_6H_4OMe$] **2.12**	258 (1.2), 270 (2.2), 281 (2.9), 295 (2.2)	3.89
[$(Et_3P)AuC{\equiv}C\text{-}3\text{-}C_6H_4OMe$] **2.13**	268 (1.0), 277 (1.2), 294 (0.6), 303 (0.5)	3.99
[$(Et_3P)AuC{\equiv}C\text{-}2\text{-}C_6H_4OMe$] **2.14**	260 (0.9), 273 (1.4), 300 (1.0), 310 (1.3)	3.86
[$(Ph_3P)AuC{\equiv}C\text{-}3\text{-}C_6H_4OMe$] **2.15**	269 (2.4), 279 (2.5), 295 (1.5), 303 (1.4)	3.92
[$(Ph_3P)AuC{\equiv}C\text{-}2\text{-}C_6H_4OMe$] **2.16**	261 (1.2), 275 (1.7), 300 (1.2), 311 (1.6)	3.75
[$(Et_3P)AuC{\equiv}C\text{-}5\text{-}C_4H_3N_2$] **2.17**	256 (1.2), 269 (1.8), 283 (2.0), 302 (1.0)	3.65
[$(Ph_3P)AuC{\equiv}C\text{-}5\text{-}C_4H_3N_2$] **2.18**	256 (5.8), 270 (8.0), 285 (7.0)	3.77

Table 2.25: Electronic absorption spectra data for 2.01–2.18 (*CH_2Cl_2, room temperature)

The optical gap for 3-ethynylpyridine derivative **2.01** is 3.75 eV as compared with 4.08 eV for phenyl derivative **2.03** which is most likely due to the presence of the electron withdrawing heteroatom in the phenyl ring.

The electronic absorption spectrum of **2.04** illustrates the red shift from that of the trimethylsilyl protected ligand and the resemblance of the absorption spectrum to that of the uncoordinated ligand (Figure 2.28). The optical gap for **2.04** is 2.99 eV which is lower than that of **2.03** (4.08 eV) due to the presence of the electron withdrawing nitro substituent on the phenyl ring. In the series of nitrophenylacetylene gold(I) complexes **2.04–2.07**, the smallest optical gap is observed for **2.06** at 2.76 eV.

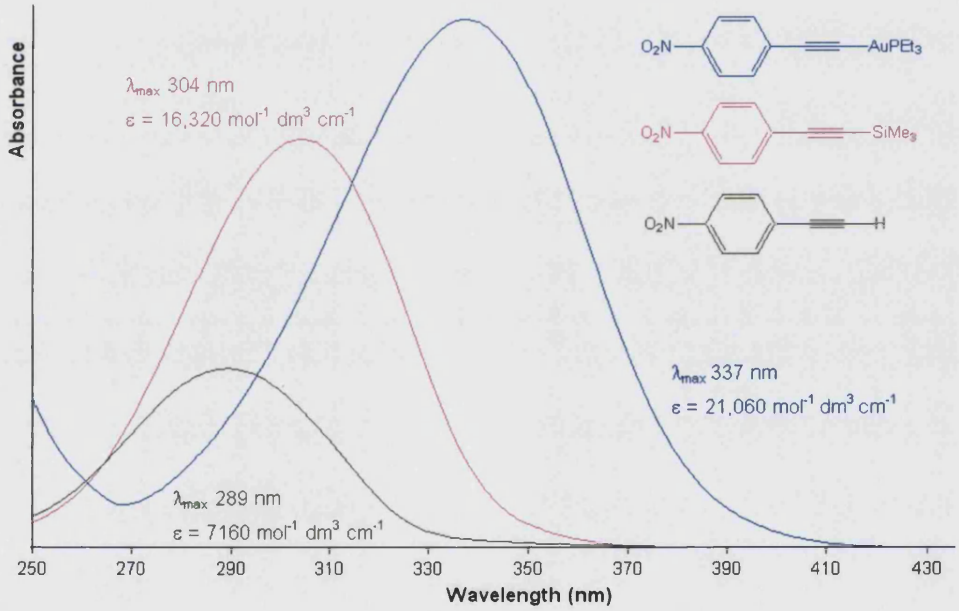

Figure 2.28: Electronic absorption spectra of 2.04, $Me_3SiC{\equiv}C\text{-}4\text{-}C_6H_4NO_2$ and $HC{\equiv}C\text{-}4\text{-}C_6H_4NO_2$

The similarity between the absorption spectra of $[(Et_3P)AuC{\equiv}C\text{-}3\text{-}C_6H_4NO_2]$ **2.05** and $[(Ph_3P)AuC{\equiv}C\text{-}3\text{-}C_6H_4NO_2]$ **2.07** indicate the relative insensitivity of the absorption bands to differences in the nature of the phosphine ligands.

The electronic absorption spectrum of the 4-benzonitrile complex **2.08** resembles the general profile of that of the trimethylsilyl protected ligand suggesting that, as with the previous examples, the absorption is dominated by ligand centred π–π^* transitions, with the exception of a small additional band at 325 nm (ε = 5,700). This low energy absorption may contain

some metal-to-ligand charge-transfer (MLCT) Au → π* character as identified by Yam *et al.*[19] The emission spectrum shows the expected mirror image of the lowest energy absorption bands observed in the electronic absorption spectrum. A similar low energy transition is observed in the electronic absorption spectrum of **2.10** at 335 nm (ε = 1840 mol^{-1} dm^3 cm^{-1}) which may also have MLCT Au → π* character.

The optical gaps for the benzonitrile complexes **2.08**, **2.09** and **2.10** are 3.57 eV, 3.86 eV and 3.59 eV, respectively, with the energies for the *ortho*- and *para*-substituted complexes lower than that of the *meta* complex. These values are larger than those of the nitrobenzene analogues due to the more electron withdrawing nature of the NO_2 group over the C≡N group.

	Absorption λ (nm)* (Energy, eV)
2.05	255 (4.9), 266 (4.7), 281 (4.4)
2.07	255 (4.9), 268 (4.6), 283 (4.4)
2.09	268 (4.6), 281 (4.4), 310 (4.0)
2.11	269 (4.6), 283 (4.4), 311 (4.0)

Table 2.26: Absorption spectra data for 2.05, 2.07, 2.09 and 2.11 (*CH_2Cl_2, room temperature)

As with the *meta*-substituted nitrophenyl complexes **2.05** and **2.07**, the profiles of the absorption spectra and band energies of **2.09** and **2.11** are very similar (Table 2.26) suggesting once again that the absorption bands are relatively insensitive to changes in the phosphine substituent and are dominated by intraligand π–π* transitions.

The electronic absorption spectra of the methoxyphenylacetylene complexes **2.14** and **2.16** exhibit bands at 310 and 311 nm, respectively, with shoulders at 300 nm. The presence of these low energy bands ≥ 300 nm may suggest a rearrangement of ligands but the structures would need to be determined to test this theory. The optical gaps for **2.12**, **2.13** and **2.14** are greater than those of the nitrophenyl and benzonitrile analogues due to the presence of the electron donating methoxy group. The profile of the absorption spectrum of **2.15** is again comparable with that of its triethylphosphine analogue **2.12** which is consistent with the absorption arising from intraligand π–π* transitions and is not affected by changes to the phosphine unit.

The energy of the electronic absorption bands and overall shape of the spectra for ethynyl pyrimidine complexes **2.17** and **2.18** show little variation on changing the phosphine unit as previously observed for the gold(I) alkyne complexes in this Chapter. The additional band at 302 nm in the spectrum of **2.17**, due to MLCT, is not observed in the spectrum of **2.18** which may reflect the separation of the weakly bound dimers in solution. The optical gap of 3.65 eV for **2.17** is smaller than that of **2.01** due to the presence of a second nitrogen atom in the ring.

2.2.4.1 Gold Ethynyl Phenyls

The electronic absorption spectrum of **2.19** has a similar profile to that of $Me_3SiC{\equiv}C\text{-}C_6H_4\text{-}C{\equiv}CSiMe_3$ (λ_{max} 293 nm) with two bands at 303 nm (ε = 62,600 mol^{-1} dm^3 cm^{-1}) and 323 nm (ε = 98,200 mol^{-1} dm^3 cm^{-1}) and two small shoulders at 286 nm and 294 nm. The red shift upon complexation is again consistent with a small increase in conjugation along the length of the molecule through the gold centres. The electronic absorption spectrum of **2.20** is also similar to that of the ligand, $Me_3SiC{\equiv}C\text{-}(C_6H_4)_2\text{-}C{\equiv}CSiMe_3$, suggesting the absorption is due to ligand centred π–π^* transitions. On going from **2.19** → **2.20** the optical gap is decreased (3.68 eV → 3.42 eV) due to the presence of the extra arene ring increasing the conjugation length of the molecule.

	Absorption λ (nm)* ($\varepsilon = 10^4$ $mol^{-1}dm^3$ cm^{-1})
$[(Cy_3P)AuC{\equiv}C\text{-}C_6H_4\text{-}C{\equiv}CAu(Cy_3)]$[21] $[((p\text{-}Tol)_3P)AuC{\equiv}C\text{-}C_6H_4\text{-}C{\equiv}CAu(P(p\text{-}Tol)_3))]$[19] **2.19**	288sh (3.2), 304 (8.1), 323 (13.1) 242 (7.1), 294 (3.0), 308 (6.2), 328 (8.6) 286 (2.6), 294 (3.0), 303 (6.3), 323 (9.8)
$[(Cy_3P)AuC{\equiv}C\text{-}(C_6H_4)_2\text{-}C{\equiv}CAu(PCy_3)]$[21] **2.20**	323 (7.3) 322 (7.5)

Table 2.27: Absorption data for 2.19, 2.20 and similar complexes in the literature (*CH_2Cl_2, room temperature)

The absorption data for **2.19** and **2.20** are compared with that of similar complexes reported in the literature, all obtained in dichloromethane solutions at room temperature, in Table 2.27. Again, the spectra are very similar with regard to the energy of the bands indicating the strong dependence of the absorption on intra-ligand π–π^* transitions and the relative insensitivity of the spectra to changes in the nature of the phosphine ligand. Thus, we assume that changing the nature of the phosphine has little effect on the solution chemistry of these systems.

2.2.4.2 Gold Ethynyl Anthracenes

The electronic absorption spectra of **2.21** and **2.22** were recorded in dichloromethane at room temperature. These materials are highly fluorescent as can be seen in Figure 2.29. The electronic absorption spectrum of **2.21** exhibits a series of low energy bands and follows a similar profile to that of the trimethylsilyl protected ligand $Me_3SiC{\equiv}C\text{-}C_{14}H_9$ suggesting that the absorption is predominately due to ligand centred transitions (Figure 2.30).

Figure 2.29: Dichloromethane solutions of 2.21 and 2.22 in the absence (left) and the presence (right) of UV light

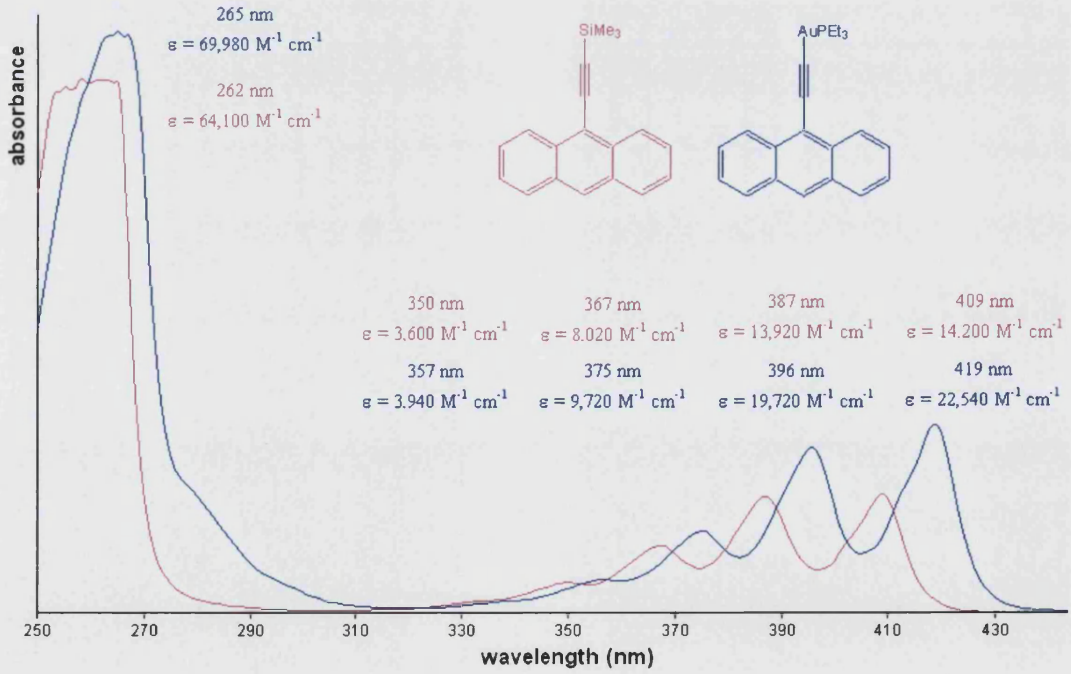

Figure 2.30: Absorption spectrum of $Me_3SiC{\equiv}C\text{-}C_{14}H_9$ and 2.21

There is a shift to longer wavelength on complexation of the gold phosphine unit which is consistent with an extension of conjugation across the molecule through the gold centres. The

emission spectrum displays an approximate mirror image of the lowest energy bands observed in the absorption spectrum. The electronic absorption spectrum of **2.23** is very similar to that of **2.21** with a red shift observed on coordination to the gold phosphine.

The electronic absorption spectrum of **2.22** again closely resembles the spectrum of the trimethylsilyl protected ligand $Me_3SiC{\equiv}C\text{-}C_{14}H_8\text{-}C{\equiv}CSiMe_3$. It is interesting to note that the absorption coefficients of the lowest energy bands are approximately double those of the bands in **2.21** possibly reflecting the presence of the two gold centres on the chromophore unit in **2.22** (Table 2.28) and have vibrational spacings of ~1400 cm^{-1} typical of ν(C≡C) stretches.

	λ_{max} [nm] (ε, 10^4 mol^{-1} dm^3 cm^{-1}) *	Optical gap (eV)
$Me_3SiC{\equiv}C\text{-}C_{14}H_9$	367 (0.8), 387 (1.3), 409 (1.4)	2.92
$[(Et_3P)AuC{\equiv}C\text{-}C_{14}H_9]$ **2.21**	375 (0.9), 396 (1.9), 419 (2.3)	2.86
$Me_3SiC{\equiv}C\text{-}C_{14}H_8\text{-}C{\equiv}CSiMe_3$	391 (1.3), 414 (3.2), 439 (4.4)	2.65
$[(Et_3P)AuC{\equiv}C\text{-}C_{14}H_8\text{-}C{\equiv}CAu(PEt_3)]$ **2.22**	409 (1.4), 434 (3.3), 461 (4.5)	2.54

Table 2.28: Comparison of absorption coefficients for 2.21 and 2.22 (*CH_2Cl_2, room temperature)

The optical gaps observed for **2.21** and **2.22** are much smaller than that of $[(Et_3P)AuCC\text{-}C_6H_5]$ **2.03** (4.09 eV) indicating that delocalisation is increased on going to a larger aromatic spacer group.[41]

Table 2.29 lists the absorption data for **2.22** along with that of reported complex $[(p\text{-}C_6H_4Me)_3PAuC{\equiv}C\text{-}C_{14}H_8\text{-}C{\equiv}CAuP(C_6H_4Me\text{-}p)_3]$.[19] As expected the general shape and band energies of both spectra are very similar indicating that the absorption has a strong dependence on intraligand π–π* transitions and there is little variation on changing the phosphine unit.

	λ_{max} [nm] (ε, 10^4 mol^{-1} dm^3 cm^{-1})
$[(Et_3P)AuC{\equiv}C\text{-}C_{14}H_8\text{-}C{\equiv}CAu(PEt_3)]$ **2.22**	277(7.1), 294(2.1), 316(0.6), 387(0.5), 409(1.3), 434(3.2), 461(4.4)
$[(p\text{-Tol})_3PAuC{\equiv}C\text{-}C_{14}H_8\text{-}C{\equiv}CAuP(p\text{-Tol})_3]$[19]	242(10.7), 276(10.9), 300(2.6), 324(0.7), 410(2.0), 436(4.8), 464(6.6)

Table 2.29: Absorption data for 2.22 and $[(p\text{-}C_6H_4Me)_3PAuC{\equiv}C\text{-}C_{14}H_8\text{-}C{\equiv}CAuP(C_6H_4Me\text{-}p)_3]$

2.3 Conclusions

In this Chapter investigation into how changes to the alkyne ligand affect the solid state structure of a series of triethylphosphine gold(I) alkynyl complexes and some triphenylphosphine analogues has been described. Building upon previous work in the Raithby group,[37] the ethynylpyridine complexes **2.01** and **2.02** were prepared. While **2.01** rearranges to form a linear gold chain, **2.02** consists of a basic monomeric unit but associates in the solid state via Au····Au interactions to form a weakly bound polymer.

To study the effect of substituents on the phenylacetylene ring a series of complexes with electron withdrawing or donating groups were prepared. The structure determination of nitrobenzene complexes, **2.04**, **2.05** and **2.06**, benzonitrile complexes **2.08** and **2.10** and methoxyphenylacetylene complex **2.12** allowed examination as to whether position of the group on the ring had an effect on the solid state structure.

The structures of the gold(I) alkynyl phosphine complexes discussed in this Chapter are summarised in Table 2.22 with the categories *ortho*, *meta* and *para* corresponding to 2-, 3- and 4-positions in the ring for the ring substituent, or placement of the heteroatom in the case of pyridine and pyrimidine, with respect to the alkyne group.

R	X	Ortho	Meta	Para
PEt_3	Pyridine	Polymer	Rearranged Chain	
	$Ph\text{-}NO_2$	Dimer	Dimer	Monomer
	Ph-CN	Trimer		Dimer
	Ph-OMe			Monomer
	Pyrimidine		Rearranged Chain	
PPh_3	$Ph\text{-}NO_2$		Monomer	
	Ph-CN		Monomer	
	Ph-OMe		Monomer	
	Pyrimidine		Dimer	

Table 2.22: Summary of $R_3PAuC{\equiv}C\text{–}X$ architectures

For the triethylphosphine complexes, while the *para* substituted complexes are monomeric with the exception of the benzonitrile derivative **2.08**, substituents in *ortho* positions all produce structures with Au····Au interactions present. The presence of a heteroatom in the *meta* position of the ring induces a rearrangement resulting in a highly unusual structure with a

chain of gold atoms with alternate gold atoms coordinated to two alkyne ligands or two phosphine ligands.

It is clear that the rearranged polymer chain structure is observed in the complexes which contain a combination of both a heteroatom in the phenylacetylene ring and a triethylphosphine group. In the case of **2.18**, where there is a pyrimidine ring and a triphenyl phosphine group, although there is an Au····Au contact present it is holding two molecules together in a loosely bound dimer rather than rearranging into a chain suggesting that the steric bulk of the phosphine is a consideration in the final structure of these complexes. The difference in the structures of $[(Et_3P)AuC{\equiv}C\text{-}2\text{-}C_5H_4N]$ and $[(Et_3P)AuC{\equiv}C\text{-}3\text{-}C_5H_4N]$ between a loosely bound polymeric chain in the solid state structure and a rearranged chain must be a consequence of the electronic properties of the substituted alkyne.

Only small variations are observed in the NMR and IR spectroscopic data for these complexes, however, which would seem to suggest that the $R_3PAuC{\equiv}C$ unit is relatively insensitive to changes in the ring substituent of the alkyne ligand. The electronic absorption spectra are dominated by ligand centred π–π^* transitions as seen in related gold(I) ethynyl phosphine systems.[21,33]

Previous studies into the effect of the size of R group on the phosphine on the association of molecules in the solid state by aurophilic interactions[37] were also further confirmed by this work. Triphenylphosphine gold(I) alkynyl complexes **2.07**, **2.11** and **2.15** are all monomeric with no intermolecular Au····Au interactions present and no association in the solid state. This is due to the steric bulk of the triphenylphosphine group preventing a close approach of neighbouring molecules.

In conclusion, this work has introduced the idea of studying how the electronic properties of ring substituents and their ring position affect the association of molecules in the solid state and the presence of aurophilic interactions. UV/visible absorption spectroscopy has shown that changes to the nature of the phosphine group are inconsequential to the general profile of the spectra and band energies of the complexes. The importance of the steric size of the phosphine group on the overall architecture of the molecule has also been confirmed.

2.4 References

1. Puddephatt, R. J., *Chem. Commun.,* 1998, 1055-1062.
2. Puddephatt, R. J., *Coord. Chem. Rev.,* 2001, **216**, 313-332.
3. Li, J.; Pyykko, P., *Chem. Phys. Lett.,* 1992, **197**, 586-590.
4. Coates, G. E.; Parkin, C., *J. Chem. Soc.,* 1962, 3220 - 3226.
5. Ziolo, R. F. L., S.; Dori, Z., *Chem. Commun.,* 1970, 1124 - 1125.
6. Shieh, S. J.; Hong, X.; Peng, S. M.; Che, C. M., *J. Chem. Soc. Dalton Trans.,* 1994, 3067-3068.
7. Whittall, I. R.; Humphrey, M. G.; Houbrechts, S.; Persoons, A.; Hockless, D. C. R., *Organometallics,* 1996, **15**, 5738-5745.
8. Irwin, M. J.; Jia, G. C.; Payne, N. C.; Puddephatt, R. J., *Organometallics,* 1996, **15**, 51-57.
9. Naulty, R. H.; Cifuentes, M. P.; Humphrey, M. G.; Houbrechts, S.; Boutton, C.; Persoons, A.; Heath, G. A.; Hockless, D. C. R.; Luther-Davies, B.; Samoc, M., *J. Chem. Soc. Dalton Trans.,* 1997, 4167-4174.
10. Irwin, M. J.; Manojlovic-Muir, L.; Muir, K. W.; Puddephatt, R. J.; Yufit, D. S., *Chem. Commun.,* 1997, 219-220.
11. Muller, T. E.; Green, J. C.; Mingos, D. M. P.; McPartlin, C. M.; Whittingham, C.; Williams, D. J.; Woodroffe, T. M., *J. Organomet. Chem.,* 1998, **551**, 313-330.
12. Vicente, J.; Chicote, M. T.; Abrisqueta, M. D.; de Arellano, M. C. R.; Jones, P. G.; Humphrey, M. G.; Cifuentes, M. P.; Samoc, M.; Luther-Davies, B., *Organometallics,* 2000, **19**, 2968-2974.
13. Li, P. Y.; Ahrens, B.; Choi, K. H.; Khan, M. S.; Raithby, P. R.; Wilson, P. J.; Wong, W. Y., *Cryst. Eng. Comm.,* 2002, 405-412.
14. Hurst, S. K.; Cifuentes, M. P.; McDonagh, A. M.; Humphrey, M. G.; Samoc, M.; Luther-Davies, B.; Asselberghs, I.; Persoons, A., *J. Organomet. Chem.,* 2002, **642**, 259-267.
15. Vicente, J.; Singhal, A. R.; Jones, P. G., *Organometallics,* 2002, **21**, 5887-5900.
16. Vicente, J.; Chicote, M. T.; Alvarez-Falcon, M. M.; Abrisqueta, M. D.; Hernandez, F. J.; Jones, P. G., *Inorg. Chim. Acta,* 2003, **347**, 67-74.
17. Liau, R. Y.; Schier, A.; Schmidbaur, H., *Organometallics,* 2003, **22**, 3199-3204.

18. Li, D.; Hong, X.; Che, C. M.; Lo, W. C.; Peng, S. M., *J. Chem. Soc.-Dalton Trans.*, 1993, 2929-2932.
19. Yam, V. W. W.; Choi, S. W. K., *J. Chem. Soc.-Dalton Trans.*, 1996, 4227-4232.
20. Irwin, M. J.; Vittal, J. J.; Puddephatt, R. J., *Organometallics*, 1997, **16**, 3541-3547.
21. Chao, H. Y.; Lu, W.; Li, Y. Q.; Chan, M. C. W.; Che, C. M.; Cheung, K. K.; Zhu, N. Y., *J. Am. Chem. Soc.*, 2002, **124**, 14696-14706.
22. Lu, W.; Zhu, N. Y.; Che, C. M., *J. Organomet. Chem.*, 2003, **670**, 11-16.
23. Yam, V. W. W.; Cheung, K. L.; Yip, S. K.; Cheung, K. K., *J. Organomet. Chem.*, 2003, **681**, 196-209.
24. Yam, V. W. W.; Wong, K. M. C.; Hung, L. L.; Zhu, N. Y., *Angew. Chem.-Int. Edit.*, 2005, **44**, 3107-3110.
25. Corfield, P. W. R.; Shearer, H. M. M., *Acta Cryst.*, 1967, **23**, 156 - 162.
26. Bruce, M. I.; Horn, E.; Matisons, J. G.; Snow, M. R., *Aust. J. Chem.*, 1984, **37**, 1163-1170.
27. Baenziger, N. C.; Bennett, W. E.; Soboroff, D. M., *Acta Crystallogr. Sect. B-Struct. Commun.*, 1976, **32**, 962-963.
28. Bellon, P. L. M., M.; Sansoni, M., *Ric. Sci.*, 1969, **39**, 173.
29. Gavens, P. D.; Guy, J. J.; Mays, M. J.; Sheldrick, G. M., *Acta Crystallogr. Sect. B-Struct. Commun.*, 1977, **33**, 137-139.
30. Corfield, P. W. R.; Shearer, H. M. M., *Acta Cryst.*, 1966, **21**, 957 - 965.
31. Corfield, P. W. R.; Shearer, H. M. M., *Acta Cryst.*, 1966, **20**, 502-508.
32. Bruce, M. I.; Duffy, D. N., *Aust. J. Chem.*, 1986, **39**, 1697-1701.
33. Lu, W.; Zhu, N. Y.; Che, C. M., *J. Am. Chem. Soc.*, 2003, **125**, 16081-16088.
34. Hogarth, G.; Alvarez-Falcon, M. M., *Inorg. Chim. Acta*, 2005, **358**, 1386-1392.
35. Schuster, O.; Liau, R. Y.; Schier, A.; Schmidbaur, H., *Inorg. Chim. Acta*, 2005, **358**, 1429-1441.
36. Khairul, W. M.; Porres, L.; Albesa-Jove, D.; Senn, M. S.; Jones, M.; Lydon, D. P.; Howard, J. A. K.; Beeby, A.; Marder, T. B.; Low, P. J., *J. Clust. Sci.*, 2006, **17**, 65-85.
37. Griffiths, C. *PhD Thesis*, Cambridge 2003.
38. Humphrey, S. M.; Mack, H. G.; Redshaw, C.; Elsegood, M. R. J.; Young, K. J. H.; Mayer, H. A.; Kaska, W. C., *Dalton Trans.*, 2005, 439-446.
39. Yam, V. W. W.; Hui, C. K.; Yu, S. Y.; Zhu, N. Y., *Inorg. Chem.*, 2004, **43**, 812-821.

40. Jia, G. C.; Puddephatt, R. J.; Scott, J. D.; Vittal, J. J., *Organometallics,* 1993, **12**, 3565-3574.

41. Khan, M. S.; Al-Mandhary, M. R. A.; Al-Suti, M. K.; Al-Battashi, F. R.; Al-Saadi, S.; Ahrens, B.; Bjernemose, J. K.; Mahon, M. F.; Raithby, P. R.; Younus, M.; Chawdhury, N.; Kohler, A.; Marseglia, E. A.; Tedesco, E.; Feeder, N.; Teat, S. J., *Dalton Trans.,* 2004, 2377-2385.

42. Kaska, W. C.; Mayer, H. A.; Elsegood, M. R. J.; Horton, P. N.; Hursthouse, M. B.; Redshaw, C.; Humphrey, S. M., *Acta Crystallogr. Sect. E.-Struct Rep. Online,* 2004, **60**, M563-M565.

Chapter 3 Gold and Platinum Complexes of Group 16 Heterocyclic Alkynes

3.1 Introduction

3.1.1 Conjugated polymers incorporating heterocycles

Conjugated polymers are a class of materials whose electronic properties suggest the potential for use in many different applications such as light emitting diodes (LEDs)[1-4] and organic transistors.[5] A conjugated polymer consists of a backbone of alternating single and multiple bonds which results in π-conjugation along the polymer by overlap of p-orbitals (Figure 3.1).

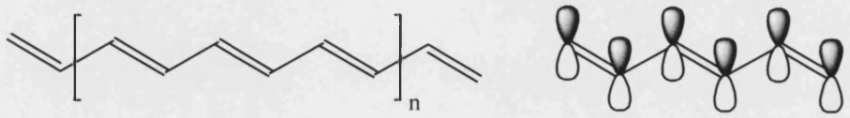

(a) (b)

Figure 3.1: Schematic drawing of (a) polyacetylene and (b) conjugated p-orbitals

Of the various types of conjugated polymers, polyarylene ethynylenes (PAEs), those consisting of alternate aryl and alkyne units,[6] have been the centre of much research with a view to materials science applications, in particular LEDs.[7]

The chemical stabilities and nonlinear optical properties of polythiophene and polypyrrole (Figure 3.2) have led to these materials being amongst the most studied of organic conjugated polymers.[8-12] The optical gaps for polypyrrole and polythiophene, of 2.85 eV and 2.0 eV, respectively, result in the neutral forms of these polymers acting as insulators whereas oxidative doping of polythiophene and polypyrrole produces conductors by the introduction of 'holes'. Research into these materials has largely concentrated on lowering the optical gaps by chemical modification of the backbone of the polymers.[9]

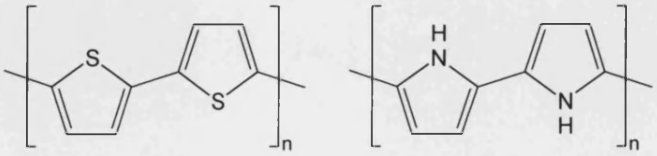

Figure 3.2: Polythiophene and polypyrrole

There has been little published in the literature concerning polyfuran and the higher period analogues polyselenophene and polytellurophene. In the case of polyfuran this is due to difficulties in synthesising the material. High quality films of polyfuran have been prepared by electrochemical oxidation using terfuran as the monomer for polymerisation rather than furan, followed by reduction of the doped material to its neutral form, with an optical gap of 2.35 eV (Scheme 3.1).[13]

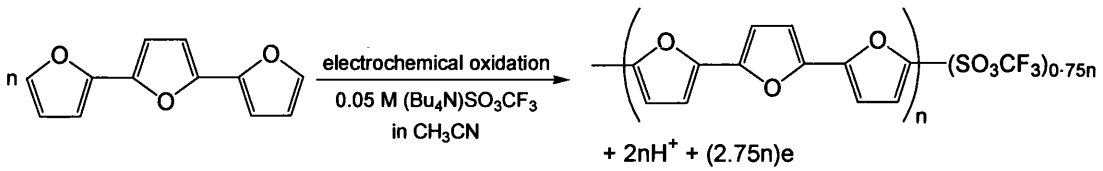

Scheme 3.1: Electrochemical synthesis of polyfuran from terfuran

Polyselenophene films have been prepared by electropolymerisation of selenophene on the surface of platinum electrodes and were found to have an optical gap of 2.0 eV as observed for polythiophene but exhibits a low conductivity of 3.7×10^{-2} Scm^{-1}.[14] Polytellurophene has been prepared by both galvanostatic polymerisation of tellurophene in nitrobenzene or benzonitriles and the electropolymerisation of 2,2'-bitellurophene, as a black powder or black film with conductivities of 10^{-7}–10^{-11} Scm^{-1} and 10^{-6}–10^{-9} Scm^{-1}, respectively.[15]

Theoretical studies of the polychalcogenophenes have been reported and their electronic properties compared with experimental observations and those of polyacetylene (PA) and polypyrrole (PPy).[16] Table 3.1 lists the theoretical and experimental optical gap energies. The theoretical optical gap for polyfuran is 0.37 eV larger than that of polythiophene which is in excellent agreement with the experimentally observed values of 2.35 eV and 2.0 eV.

	E_g theor. (eV)	E_g expt. (eV)
Polyacetylene	1.57	1.48 [17]
Polypyrrole	3.16	2.85 [18]
Polyfuran	2.67	2.35 [13]
Polythiophene	2.30	2.0 [19]
Polyselenophene	2.06	2.0 [14]
Polytellurophene	1.87	-

Table 3.1: Theoretical and experimental optical gaps for polychalcogenophenes, PA and PPy.[16]

Otsubo and co-workers have reported a series of oligoselenophenes and their spectroscopic properties (Figure 3.3).[20] These oligomers were found to absorb at wavelengths 0.2–0.3 eV longer than their analogous thiophene oligomers leading to the expectation of a smaller optical gap for polyselenophene over polythiophene though this is clearly not observed experimentally.[14,19]

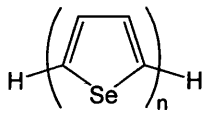

Figure 3.3: Oligoselenophenes, n = 1 – 5.

Although the optical gap for polytellurophene has not been reported, Otsubo and co-workers have looked at the electronic absorption spectra of tellurophene, bitellurophene and tertellurophene.[21] The absorption maxima for the tellurophenes and their sulphur and selenium analogues are listed in Table 3.2.

	λ_{max} / nm	λ_{max} / eV
Thiophene	230	5.39
Selenophene	250	4.96
Tellurophene	281	4.41
Bithiophene	304	4.08
Biselenophene	328	3.78
Bitellurophene	362	3.42
Terthiophene	353	3.51
Terselenophene	386	3.21
Tertellurophene	423	2.93

Table 3.2: Absorption maxima for series of chalcogenophenes[21]

The data clearly show that as Group 16 is descended the absorption maxima are shifted to longer wavelength, lower energy, indicating a decrease in the HOMO-LUMO gap. In the bi- and terchalcogenophenes series the tellurophenes again exhibit the longest wavelengths. A number of tellurophene-containing hybrid chalcogenophenes have also been synthesised and are illustrated in Figure 3.4. The absorption maxima for sulphur-containing **A** and **C** are similar at 391 and 388 nm, respectively, while those of selenium-containing **B** and **D** are both observed at 402 nm. This suggests that replacing the tellurium in the inner heterocyclic ring has more effect over the red shift than replacing the heteroatoms in the outer rings.

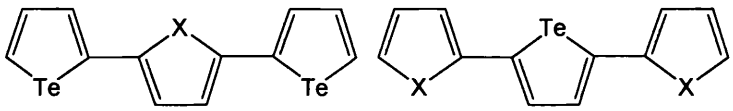

A) X = S; B) X = Se C) X = S; D) X = Se

Figure 3.4: Series of tellurophene-containing hybrid chalcogenophenes

In general the higher chalcogenophene systems have so far been largely overlooked and present interesting possibilities for the preparation and fine tuning of low optical gap materials, based on thiophene systems.

3.1.2 Transition Metal Containing Polymers

Interest in transition metal poly-ynes has grown due to their electronic and optical properties which show potential for materials science applications such as molecular wires,[22] liquid crystals[23] and nonlinear optical materials.[24]

Polymeric alkynyl platinum(II) phosphine compounds with a *trans*-configuration, in which the alkyne ligands have a linear geometry about the metal centre, are abundant in the literature and their electronic properties have been studied extensively (Figure 3.5).[25-34]

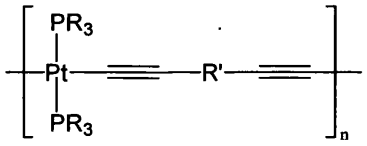

Figure 3.5: Platinum(II) alkynyl polymers, R = alkyl; R' = aromatic spacer

Studying the structural and electronic properties of such polymers can be problematic due to reduced solubility and polydispersity – the variation of chain lengths in a given polymeric sample. For this reason, model compounds have generally been prepared in order to gain characterisation data and investigate the effect of structural changes, such as increase in conjugation length, on the optical properties of the material.[35]

Thiophene oligomers and polymers, in particular, have been shown to be good electrical conductors in their own right.[36-38] With so much interest in the properties of conjugated systems incorporating thiophenes it is not surprising that the platinum-acetylide complexes of these species have been explored.[28] Raithby and co-workers reported a range of acetylide

functionalised oligothiophenes and their corresponding platinum compounds (Figure 3.6). The electronic absorption spectra of the alkynyl oligothiophenes exhibit a strong low energy absorption, the position of which shifts to longer wavelength on increasing number of thiophene rings, from m = 1 (331 nm) → m = 2 (371 nm) → m = 3 (410 nm). The absorption spectra of the platinum complexes are found to be dominated by ligand centred π–π* transitions and show that the addition of the platinum unit lowers the energy of the transitions equivalent to lowering the band gap in the polymers.

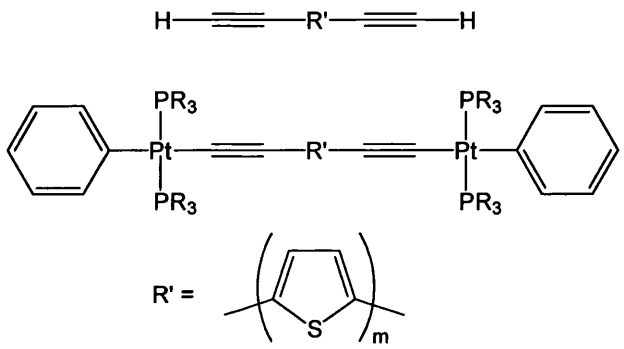

Figure 3.6: Series of alkynyl oligothiophenes and corresponding dinuclear platinum complexes (m = 1 – 3)

Although thiophene-based linker groups have been examined, metal alkynyl complexes of other ethynyl chalcogenophenes have not been reported. In fact, the terminal alkynes 2-ethynylselenophene and 2-ethynyltellurophene have not been described in the literature, with only studies into the optimisation of palladium catalysed cross-coupling of 2-haloselenophene with a variety of terminal alkynes[39] and the preparation of one alkynyl tellurophene compound detailed.[21]

The single report of an alkynyl selenophene in the formation of a metal complex has been reported by Humphrey and coworkers who have prepared mixed metal clusters linked by thiophene or selenophene.[40] The reaction of 2,5-di(oct-1-ynyl)selenophene with $M_2Ir_2(CO)_{10}(\eta^5\text{-}C_5H_4Me)_2$ (where M = Mo, W) in dichloromethane under reflux affords $[M_2Ir_2(CO)_8(\eta^5\text{-}C_5H_4Me)_2]_2\{\mu_8\text{-}\eta^4\text{-}Me(CH_2)_5C_2\text{-}2\text{-}C_4H_2Se\text{-}5\text{-}C_2(CH_2)_5Me\}$ where the alkynyl carbons form part of the $Ir_2M_2C_2$ cage (Scheme 3.2).

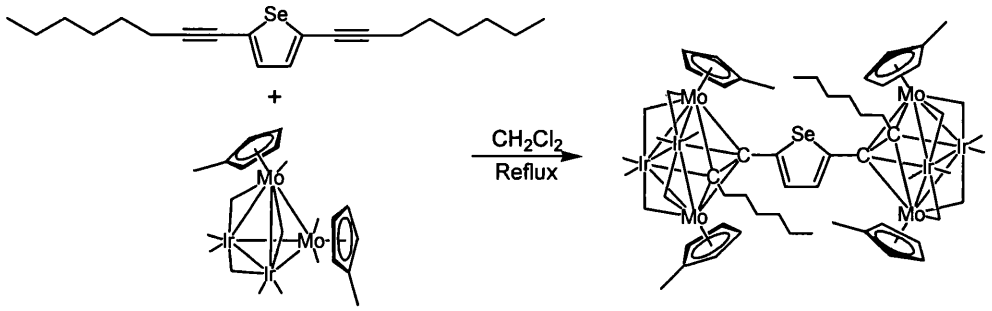

Scheme 3.2: Synthesis of $[Mo_2Ir_2(CO)_8(\eta^5\text{-}C_5H_4Me)_2]_2\{\mu_8\text{-}\eta^4\text{-}Me(CH_2)_5C_2\text{-}2\text{-}C_4H_2Se\text{-}5\text{-}C_2(CH_2)_5Me\}$ cluster

3.1.3 Objectives for this Chapter

It is clear from the literature that a systematic study of the effect of substituting the chalcogen on the electronic and optical properties of alkynyl chalcogenophene species has not previously been reported. Furthermore, the metal complexes of Group 16 heterocycles remain a relatively unexplored area of chemistry.

In order to study the platinum-acetylide complexes of Group 16 heterocycles it will first be necessary to prepare and characterise the ethynyl chalcogenophenes from their corresponding bromo-derivatives. Figure 3.7 shows a schematic drawing of ethynyl chalcogenophenes and the corresponding platinum(II) and gold(I) complexes to be prepared.

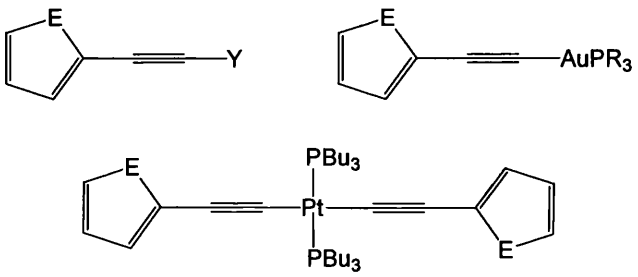

Figure 3.7: Schematic drawing of ethynyl chalcogenophenes, Y = $SiMe_3$, H; R = Et, Ph; E = O, S, Se, Te

Following the work of Hagihara in the 1970s,[41] the synthesis of alkynyl platinum complexes of the type $[Pt(C{\equiv}CR)_2L_2]$ (L = phosphine) has been achieved by copper catalysed dehydrohalogenation reaction between the acetylene and metal halide in the presence of an amine and under an inert atmosphere as shown in Scheme 3.3.

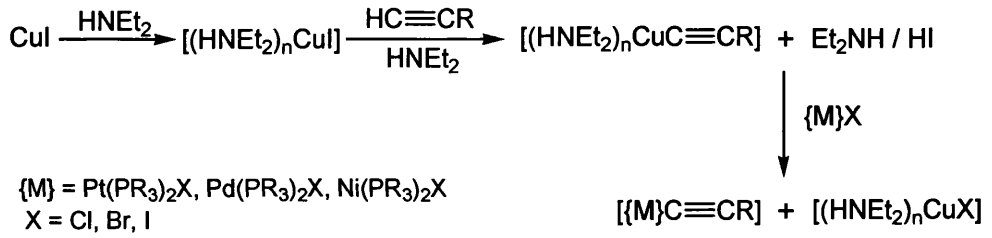

Scheme 3.3

The use of a terminal alkyne can cause problems when employing this synthetic route as they tend to be light sensitive and highly volatile. To this end, silylated alkynes are usually deprotected just prior to use by treatment with potassium hydroxide in methanol.

3.2 Results and Discussion

3.2.1 Synthesis and Characterisation of Alkynyl chalcogenophene ligands

The silylated ethynyl chalogenophenes 2-(trimethylsilylethynyl)furan[42] **3.01** and 2-(trimethylsilylethynyl)thiophene[43] **3.02** have been reported previously, although no NMR spectroscopic characterisation existed for **3.01**. In contrast selenophene and tellurophene species have not been described.

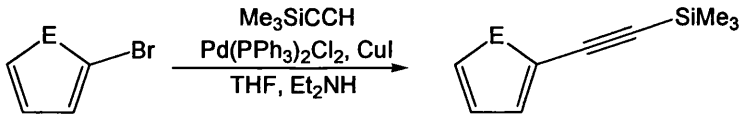

Scheme 3.4: Sonogashira coupling reaction, E = O, S, Se, Te

The silylated ethynyl chalcogenophenes 2-C_4H_3O-C≡CSiMe$_3$ **3.01**, 2-C_4H_3S-C≡CSiMe$_3$ **3.02**, 2-C_4H_3Se-C≡CSiMe$_3$ **3.03** and 2-C_4H_3Te-C≡CSiMe$_3$ **3.04** were prepared by the palladium(II) /copper(I) catalysed cross-coupling reaction of trimethylsilylacetylene with the respective bromochalcogenophene in diethylamine and tetrahydrofuran solvent (Scheme 3.4).[44,45] After purification by elution through a short plug of alumina (hexane) **3.01 – 3.04** were obtained as oils in 70 – 98% yield. Each of the species **3.01 – 3.04** were fully characterised by multinuclear NMR experiments. The ^{1}H NMR spectral data for 2-C_4H_3E-C≡CSiMe$_3$ is listed in Table 3.3.

E	δ ^{1}H / ppm		
	3-	4-	5-
O	6.60	6.36	7.35
S	7.23	6.95	7.23
Se	7.42	7.18	7.96
Te	8.82	7.66	8.95

Table 3.3: ^{1}H NMR spectral data for 2-C_4H_3E-C≡CSiMe$_3$, E = O, S, Se, Te.

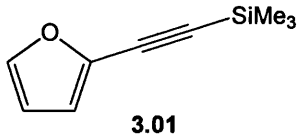

3.01

In the proton-decoupled ^{13}C NMR spectrum of **3.01**, the methine carbons of the furan ring are observed at 143.5, 115.7 and 110.8 ppm with the *ipso* carbon in the 2-position of the ring resonating at 137.1 ppm. The alkyne carbons and the methyls of the trimethylsilyl group are observed at 99.5, 94.2 and -0.30 ppm, respectively.

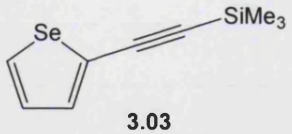

3.03

Figure 3.8 shows the ^{77}Se (I = ½, 7.58% abundant) NMR spectrum for **3.03** and an expansion of the multiplet at 7.96 ppm in the ^{1}H spectrum which shows selenium-proton coupling with a coupling constant of 46 Hz consistent with other observed $^{2}J_{SeH}$ values.[46] This coupling is clearly mirrored in the ^{77}Se NMR spectrum, where the multiplet is centred at 692.7 ppm, along with coupling from the selenium nuclei to the protons in the 3- and 4-positions of the ring, $^{3}J_{SeH}$ 13 Hz, which manifests itself as a *pseudo*-triplet.

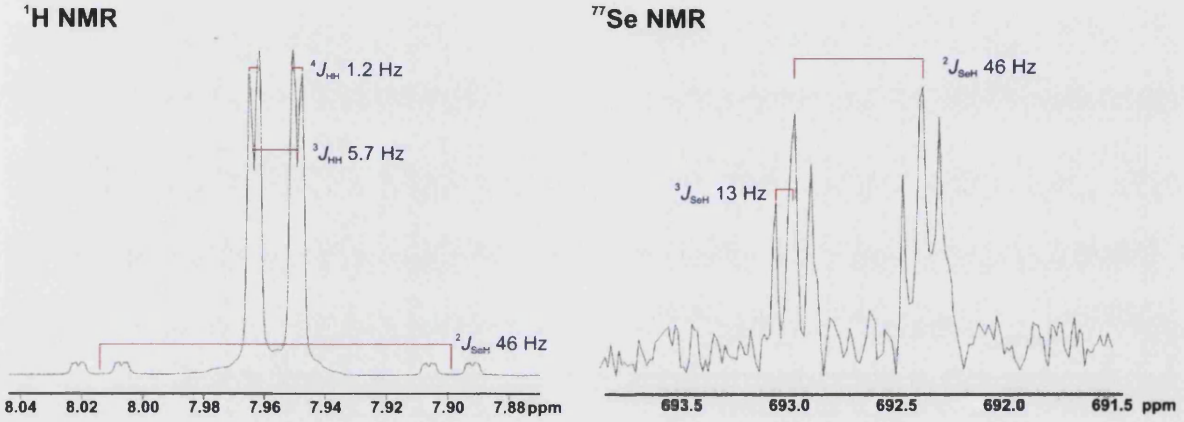

Figure 3.8: 400.13 MHz ^{1}H and 76.311 MHz ^{77}Se NMR spectra for 3.03

3.04

There is evidence of tellurium-proton coupling about the multiplet at 8.95 ppm in the ^{1}H NMR spectrum of **3.04**, through two bonds with coupling constant, $^{2}J_{TeH}$, of 96 Hz. The ^{125}Te NMR spectrum shows a doublet of doublet of doublets centred at 959.9 ppm with tellurium-proton coupling constants of $^{2}J_{TeH}$ 96 Hz, $^{3}J_{TeH}$ 16 Hz and $^{3}J_{TeH}$ 11 Hz. There are seven signals in the ^{13}C{^{1}H} NMR spectrum of **3.04** corresponding to the symmetry independent carbons of the tellurophene ring, alkyne and methyl groups. The absorption at 2132 cm^{-1} is assigned to the ν(C≡C) stretch and is similar to that of 2138 cm^{-1} observed for the selenophene analogue.

The electronic absorption and emission data for 2-C_4H_3E-C≡CSiMe$_3$ **3.02 – 3.04**, recorded as 0.01 mM dichloromethane solutions, at room temperature, are listed in Table 3.5. As can be seen, there is a red shift of *ca* 10 nm in each spectrum from E = S → Se → Te indicating a decrease in HOMO-LUMO gap as shown. As expected the difference between band maxima in the absorption and emission spectra, the Stokes shift, is similar in each case as changing the heteroatom does not change the basic geometry in either the ground state or expected excited state of the molecule. The general shapes of the bands in the absorption spectrum are similar due to the dominance of π-π* transitions.

	Absorption (nm) ($\varepsilon = 10^3$ mol^{-1} dm^3 cm^{-1})	Emission (nm)	Optical Gap (eV)
3.02	259 sh (9.26), 277 (12.6), 289 sh (9.28)	-	4.09
3.03	271 (13.0), 286 (11.7), 301 sh (9.06)	369	3.86
3.04	288 (8.96), 295 (9.02), 320 sh (5.46)	375	3.46

Table 3.5: Absorption/emission data for C_4H_3E–C≡CSiMe$_3$, E = S, Se or Te (CH_2Cl_2, room temperature)

The terminal alkynes 2-C_4H_3SeC≡CH **3.05** and 2-C_4H_3TeC≡CH **3.06** were obtained by desilylation of **3.03** and **3.04**, respectively, with potassium hydroxide in dichloromethane/ methanol (1:1) (Scheme 3.5). Although both compounds were characterised by multinuclear NMR experiments, they are highly volatile and sensitive to light which prevented further characterisation.

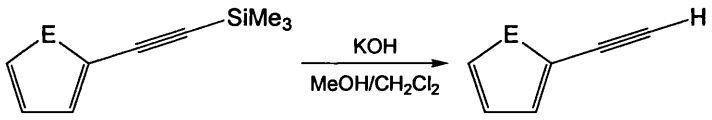

Scheme 3.5: Preparation of terminal alkynes, E = Se, Te

The chemical shift data for the proton and ^{77}Se/^{125}Te NMR spectra of **3.05** and **3.06** are shown in Table 3.6 including observed chalcogen-proton coupling which is similar to that of their trimethylsilyl-protected analogues. The $^{13}C\{^1H\}$ NMR spectra in each case show six resonances with the alkyne carbons seen at 82.9 (C_{quat}) and 79.1(CH) for **3.05** and 84.2 (C_{quat}) and 83.6 (CH) for **3.06**.

	δ^1H (ppm)	δ^{77}Se/^{125}Te (ppm)
3.05	7.99 ($^2J_{SeH}$ 47 Hz), 7.48, 7.21, 3.51($^4J_{SeH}$ 4.1 Hz)	693.2
3.06	8.98 ($^2J_{TeH}$ 97 Hz), 7.90, 7.69, 3.70 ($^4J_{TeH}$ 8.6 Hz)	961.5

Table 3.6: Selected NMR data for 3.05 and 3.06

The ^{125}Te (I = ½, 6.99% abundant) NMR spectrum of **3.06** is shown in Figure 3.9 where the coupling observed in the proton spectrum is clearly mirrored along with a $^3J_{TeH}$ coupling constant of 15.4 Hz. The multiplet appears as a doublet of doublets of triplets (ddt) due to the tellurium nuclei coupling to the alkyne proton and proton in the 4-position of the tellurophene ring.

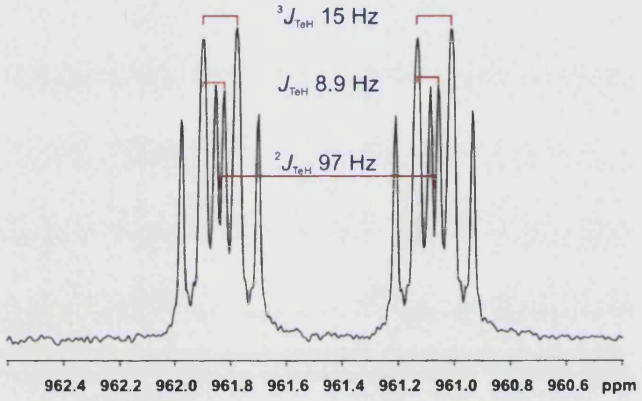

Figure 3.9: 126.26 MHz ^{125}Te NMR spectrum of 3.06

3.2.2 Ethynyl chalcogenophene platinum(II) complexes

3.2.2.1 Development of *in situ* deprotection-dehydrohalogenation method

In order to prepare the di-substituted platinum(II) complexes, **3.07 – 3.10**, the proposed method involved the reaction of *trans*-bis(tributyl phosphine)platinum(II) chloride[47] with the corresponding ethynyl chalcogenophene in the presence of a catalytic amount of copper iodide, diethylamine and dichloromethane solvent at room temperature (Scheme 3.6).

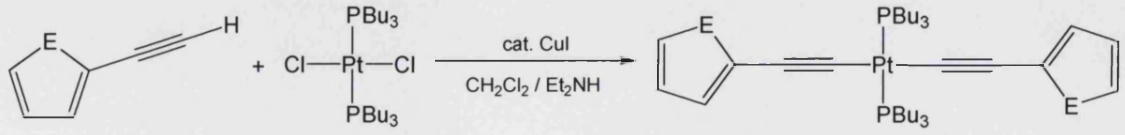

Scheme 3.6: Proposed preparation of platinum(II) complexes E = O, S, Se, Te

The synthesis was carried out using 2-ethynylthiophene due to its relative stability over the remaining Group 16 analogues. After 24 h, TLC of the reaction mixture showed only platinum starting material present with no ethynylthiophene remaining. This was most likely a result of the volatile nature of the ligand and method of addition to the reaction mixture.

The next step was to try deprotection of the 2-(trimethylsilylethynyl)thiophene followed by immediate transfer, *via* cannula, into the dehydrohalogenation reaction mixture (Scheme 3.7). The reaction resulted in a mixture of complexes which where separated by column chromatography (alumina, 4:1, hexane/dichloromethane) and identified as *trans*-$[PtCl(PBu_3)_2(C{\equiv}C\text{-}C_4H_3S)]$ and *trans*-$[Pt(PBu_3)_2(C{\equiv}C\text{-}C_4H_3S)_2]$ by ^1H and $^{31}P\{^1H\}$ NMR spectroscopy. The generation of mono- and di-substituted products indicates that this method does not provide a stoichiometric amount of ethynylthiophene.

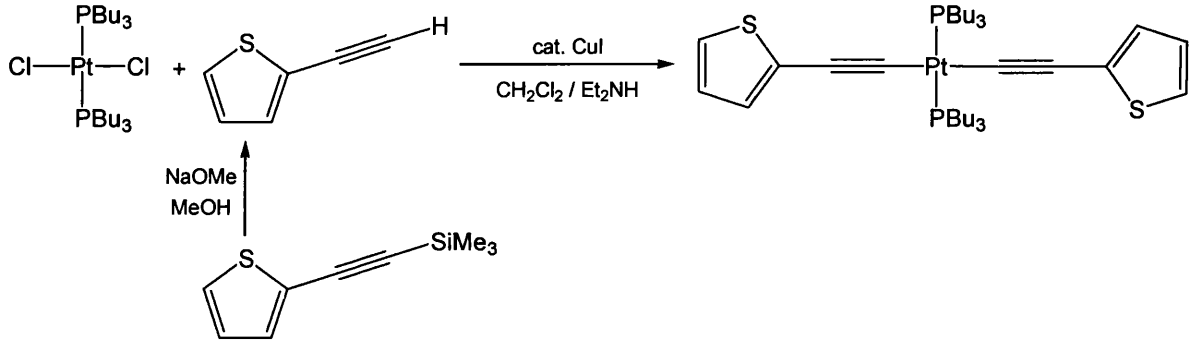

Scheme 3.7: Next step in development of route to di-substituted platinum complexes

In Chapter Two, the gold(I) alkynes are prepared by reaction of a gold phosphine with a trimethylsilyl-protected alkyne in the presence of sodium methoxide, in methanolic solution. Bearing this in mind, 2-(trimethylsilylethynyl)thiophene and sodium methoxide were added to the dehydrohalogenation reaction mixture [*trans*-bis(tributylphosphine)platinum(II) chloride, copper iodide, diethylamine and dichloromethane solvent]. Omission of methanol in the reaction mixture shut down the progress of the reaction, clearly indicating the need for a proton source for the reaction to proceed to completion. Thus, an *in situ* deprotection-dehydrohalogenation method was developed (Scheme 3.8).

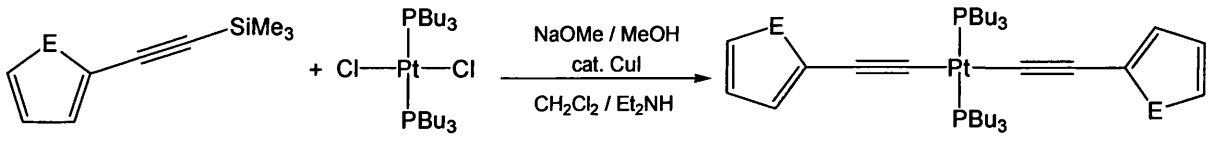

Scheme 3.8: Preparation of 3.07 – 3.10, by *in situ* deprotection-dehydrohalogenation method

The di-substituted platinum complexes *trans*-$[Pt(PBu_3)_2(C{\equiv}C\text{-}C_4H_3O)_2]$, **3.07**, *trans*-$[Pt(PBu_3)_2(C{\equiv}C\text{-}C_4H_3S)_2]$, **3.08**, *trans*-$[Pt(PBu_3)_2(C{\equiv}C\text{-}C_4H_3Se)_2]$, **3.09** and *trans*-$[Pt(PBu_3)_2(C{\equiv}C\text{-}C_4H_3Te)_2]$ **3.10** were prepared using the *in situ* deprotection-dehydrohalogenation method described above and were isolated as yellow solids in 72 – 80% yields.

3.2.2.2 NMR Spectrocopic Characterisation of Platinum(II) Ethynyl Chalcogenophenes

Complexes **3.07 – 3.10** have been fully characterised by multinuclear NMR spectroscopy. In each case, three separate resonances for each of the protons on the chalcogenophene ring and multiplets corresponding to the tributylphosphine groups are observed in the ^1H NMR spectrum. Table 3.7 summarises selected multinuclear NMR spectral data for **3.07 – 3.10**. The observed $^1J_{PtP}$ coupling constants are in a similar range to that of other *trans*-platinum(II) tributylphosphine dialkynyl complexes reported in the literature.[48]

	$\delta\ ^{31}P$	$^1J_{PtP}$ / Hz	$\delta\ ^{195}Pt$	$\delta\ ^{77}Se/\ ^{125}Te$	$^4J_{PtE}$ / Hz	$^5J_{EP}$ / Hz
3.07	5.42	2327	-4713	-	-	-
3.08	5.73	2339	-4702	-	-	-
3.09	5.91	2338	-4688	665.7	27	4.0
3.10	6.29	2343	-4671	890.6	57	9.0

Table 3.7: Selected NMR spectroscopic data for 3.07–3.10

As can be seen, although there is a small downfield shift in $\delta\ ^{31}P$ as the series progresses from E = O → Te, the platinum-phosphorus coupling shows little variation suggesting that the Pt–P bond is relatively insensitive to changes in the nature of the alkyne ligand.

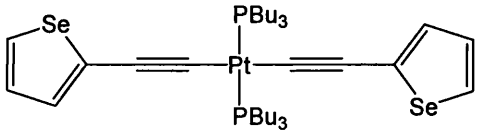

3.09

Proton-selenium coupling is observed in the ^1H NMR spectrum of **3.09** with a coupling constant of 44 Hz ($^2J_{SeH}$). It is possible to distinguish between the two alkyne carbons, observed at 116.8 and 103.7 ppm, in the $^{13}C\{^1H\}$ NMR spectrum of **3.09**, due to the presence of platinum-carbon coupling about the resonance at 103.7 ppm with a coupling constant of

275 Hz which is consistent with $^{2}J_{PtC}$ whereas observed $^{1}J_{PtC}$ coupling constants for platinum alkynyl species have a magnitude of 800 – 1000 Hz.[49]

The $^{77}Se\{^{1}H\}$ and ^{77}Se NMR spectra for **3.09** are shown in Figure 3.10. Although the ^{77}Se NMR spectrum appears complicated with multiplets centred at 665.7 ppm, the selenium-proton coupling mirrored in the ^{1}H NMR spectrum is clearly evident. The coupling between the selenium nuclei and the protons in the 3- and 4-positions of the selenophene rings manifests itself in the observation of a *pseudo* triplet with a $^{3}J_{SeH}$ coupling constant of 7 Hz.

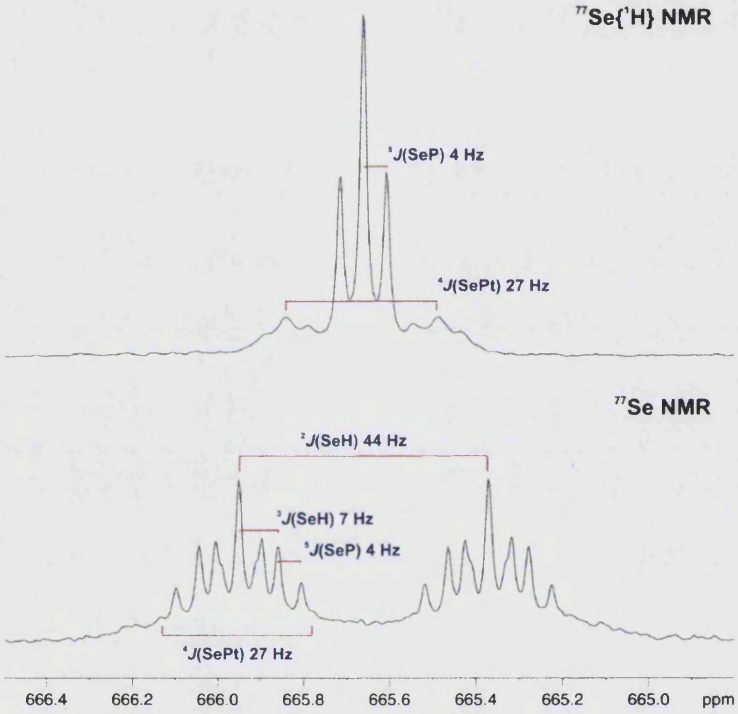

Figure 3.10: 76.311 MHz $^{77}Se\{^{1}H\}$ and ^{77}Se NMR spectra for 3.09

Coupling between the selenium nuclei and platinum through four bonds with $^{4}J_{PtSe}$ coupling constant of 27 Hz and between the selenium and phosphorus nuclei, $^{5}J_{SeP}$ 4 Hz, is also observed. To our knowledge this is the first reported occurrence of coupling between ^{77}Se and ^{31}P or ^{195}Pt nuclei across more than two bonds.[50-55] The long range coupling is more clearly evident in the $^{77}Se\{^{1}H\}$ spectrum of **3.09** (Figure 3.10, top).

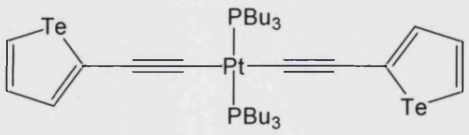

3.10

In the ^{1}H NMR spectrum of *trans*-[Pt(PBu$_3$)$_2$(C≡C-C$_4$H$_3$Te)$_2$], **3.10**, three resonances for the protons in the 3-, 4- and 5- positions on the tellurophene ring are observed at 7.32, 5.51 and 8.59 ppm, respectively, the latter clearly showing tellurium-proton coupling with a coupling constant of 93 Hz which is consistent with reported $^{2}J_{TeH}$ values.[56]

The tellurium chemical shift is centred at 890.6 ppm in the ^{125}Te NMR spectrum for **3.10** (Figure 3.11). The tellurium-proton coupling observed in the ^{1}H NMR spectrum is clearly observed along with coupling arising from the protons in the 3- and 4-positions of the tellurophene manifesting as a *pseudo*-triplet as seen in the analogous case of **3.09**.

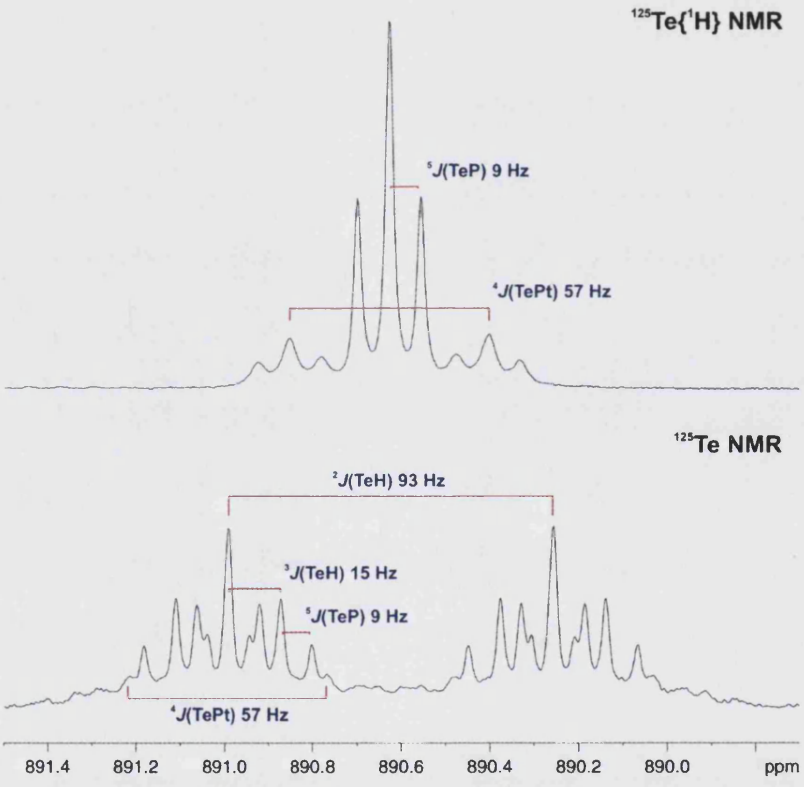

Figure 3.11: 126.26 MHz ^{125}Te and ^{125}Te{^{1}H} NMR spectra of 3.10

Along with coupling to the protons, the tellurium nuclei also couple through five bonds to the phosphorus nuclei with $^{5}J_{TeP}$ of 9 Hz. Long range tellurium-platinum coupling is observed through four bonds with a large $^{4}J_{PtTe}$ of 57 Hz as indicated by the ^{125}Te proton-decoupled spectrum and mirrored in the ^{195}Pt{^{1}H} NMR spectrum (Figure 3.12).

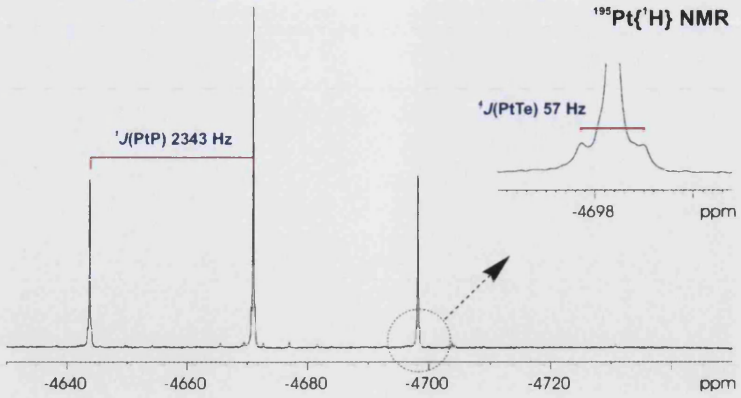

Figure 3.12: ^{195}Pt{^{1}H} NMR spectra of 3.10 in $CDCl_3$ solution (collected at 86.015 MHz).

3.2.2.3 Molecular Structure

The structure of **3.08** was determined from a single crystal grown from heptane at -25 °C. The molecule has a square planar geometry with the ligands around the platinum centre in a *trans*-arrangement (Figure 3.13). Within the crystal lattice the platinum atom sits on a crystallographic centre of symmetry, thus the C–Pt–C and P–Pt–P units are precisely linear by symmetry. Selected bond lengths and bond angles are listed in Table 3.8. All bond parameters within the complex lie in the ranges found in related platinum alkynyl species.[28,57-59]

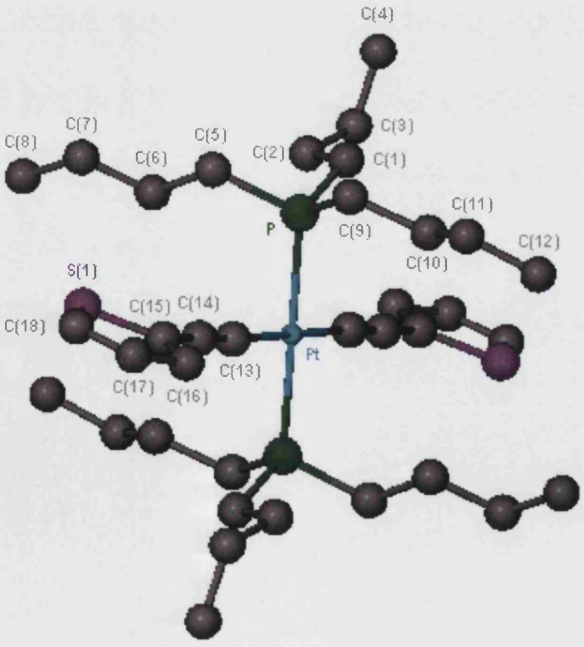

Figure 3.13: Structure of 3.08 (hydrogens omitted for clarity)

Contact	Bond length (Å)	Contact	Bond Angle (°)
Pt–P	2.2973(8)	C(13)–Pt–C(13)#	180
Pt–C(13)	2.002(3)	P–Pt–P#(1)	180
C(13)–C(14)	1.211(4)	C(13)–Pt–P	94.25(9)
C(14)–C(15)	1.418(4)	C(13)#–Pt–P	85.75(9)
C(15)–S(1)	1.632(6)	C(14)–C(13)–Pt	176.0(3)
C(16)–C(17)	1.43(2)	C(15)–C(14)–C(13)	177.0(4)
C(17)–C(18)	1.331(12)	C(15)–C(14)–S(1)	123.3(4)
C(18)–S(1)	1.583(9)	C(16)–C(15)–C(14)	131.0(8)

Table 3.8: Selected bond lengths and bond angles for 3.08

3.2.2.4 UV/visible Spectroscopic Studies

The absorption spectra for **3.07 – 3.10** are shown in Figure 3.14 and spectral data is listed in Table 3.9. There is a clear red shift of the lowest energy absorption through the series from E = O → Te. The spectra follow the general shape of the corresponding ligands indicating that the absorption is dominated by intraligand π – π* transitions. The Stokes shift in each case is approximately the same as changing the heteroatom has little effect on the basic geometry in either the ground state or expected excited state of the molecule.

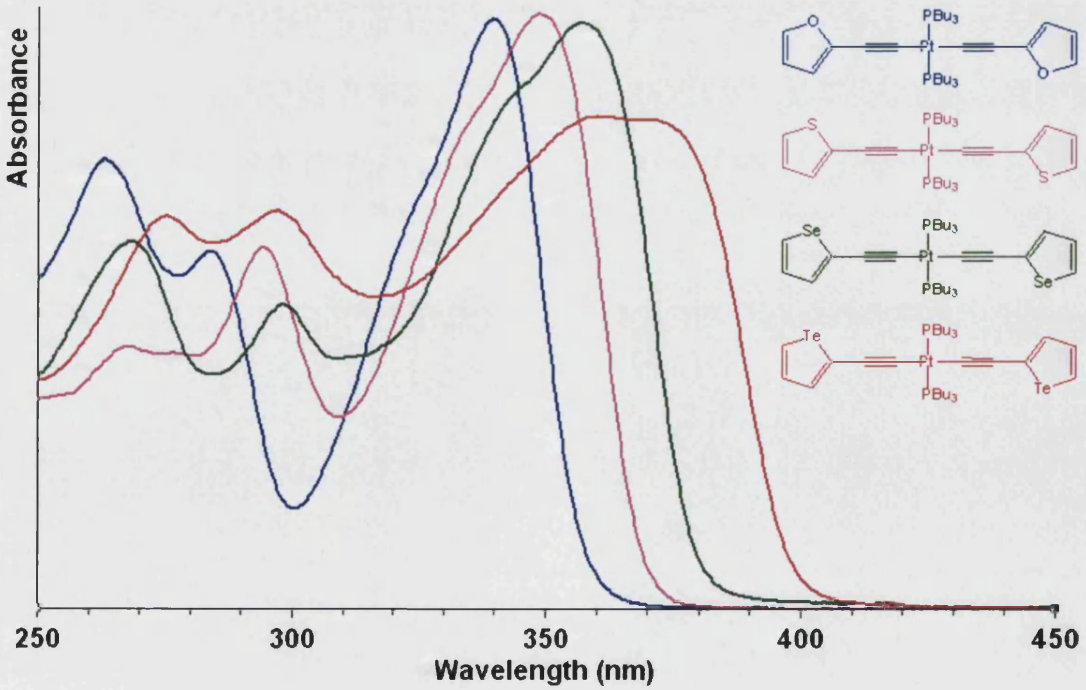

Figure 3.14: Absorption spectra of 3.07 – 3.10

	Absorption λ_{max} (nm)	Emission (nm)	Optical gap (eV)
3.07	340	-	3.36
3.08	349	371	3.26
3.09	357	379	3.17
3.10	360, 371	403	3.05

Table 3.9: Absorption and emission data for 3.07 – 3.10 (CH_2Cl_2, room temperature).

3.2.2.5 Density Functional Theory (DFT) calculations

In order to investigate the electronic structures of **3.07** – **3.10** density functional theory calculations have been carried out on the model compounds *trans*-$PtL_2(PMe_3)_2$, **3.07'** – **3.10'** (Figure 3.15) and their geometries optimised under C_i symmetry using the Gaussian 03 program using the B3LYP functional[60-62] along with the in-built 6-31G* basis set for H, C, O, P and S and the SDD energy consistent pseudo-potential basis sets for Se, Te and Pt.[63,64] Surprisingly, although a PH_3 model of **3.08** has previously been reported,[65] there are few examples of theoretical studies of platinum alkyne systems.[66-68]

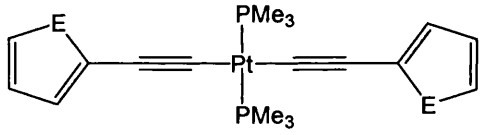

Figure 3.15: Model compounds *trans*-$PtL_2(PMe_3)_2$, 3.07' – 3.10', E = O – Te, respectively.

The frontier molecular orbitals for **3.07'** are illustrated in Figure 3.18. In general the HOMO of the molecule comprises the ethynyl chalcogenophene π orbitals in an out-of-phase combination with the $5d_{xz}$ orbital on the platinum. There is little contribution to the HOMO from the chalcogen np_z orbitals. The π^* orbitals based on the ethynyl chalcogenophene ligands and phosphorus centres along with the empty platinum $6p_z$ orbital form the LUMO.

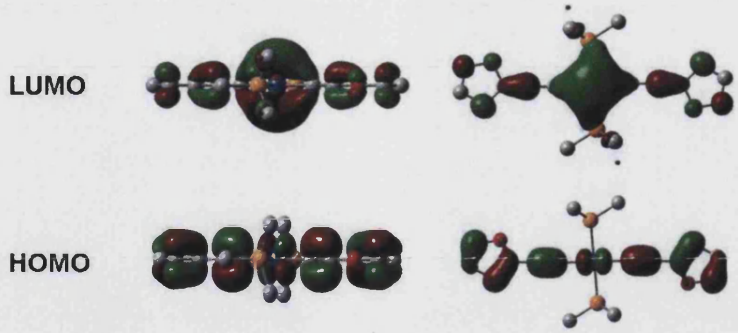

Figure 3.16: Molecular orbital plots for the frontier molecular orbitals of 3.07' (Hydrogen atoms have been omitted for clarity).

The calculations for **3.08' – 3.10'** show the frontier molecular orbitals to be similar to those shown in Figure 3.16. There is a decrease in the energy of the LUMO from E = O → Te observed as a result of decreased antibonding interactions between the carbon $2p_z$ and chalcogen np_z orbitals. As the chalcogen orbitals contribute little to the make up of the HOMO it is less affected; combined, this in turn leads to a decrease in the HOMO–LUMO gap from E = O → Te as evidenced from the UV/visible absorption spectra of **3.07 – 3.10**.

	Observed λ_{max} / nm	Observed energy/eV	Observed ε/ M^{-1} cm^{-1}		Calc. excitation wavelength/ nm	Calc. excitation energy/eV	Calc. oscillator strength (f)
3.07	340	3.65	32,600	**3.07'**	365	3.40	0.697
3.08	349	3.55	32,900	**3.08'**	376	3.30	0.774
3.09	357	3.47	32,400	**3.09'**	385	3.22	0.783
3.10	360, 371	3.44, 3.34	27200, 27000	**3.10'**	397	3.13	0.731

Table 3.10: Observed electronic absorption data for 3.07 – 3.10 and calculated data for 3.07' – 3.10'

Table 3.10 summarises the observed electronic absorption data for **3.07 – 3.10** and the calculated electronic absorption data and oscillator strength, a measure of the transition probabilities, for the model compounds **3.07' – 3.10'**. The calculated excitation wavelengths correlate well with the experimentally observed onsets of absorption.

3.2.2.6 Summary

Herein is the first time that a full series of chalcogenophene containing transition metal acetylide complexes have been prepared and fully characterised. Multinuclear NMR experiments have allowed observation of the unique coupling present. Solution UV/vis studies, supported by DFT calculations, show that clear variations occur along the series and suggest these systems may provide interesting new conjugated polymers those electronic properties may be 'tuned' by altering the chalcogen.

3.2.3 Gold(I) complexes incorporating ethynyl chalcogenophenes

Very few examples of alkynyl chalcogenophene complexes of gold are to be found in the literature. Yam *et al.*[69] have reported di- and trinuclear gold(I) phosphine alkynyl complexes incorporating ethynylthiophene, as illustrated in Figure 3.17, where the bridging phosphine $R_2P^{\frown}PR_2$ is dppe or dppf for the dinuclear species and R' = Me, Cy, Ph, *p*-Tol for the trinuclear species. The trinuclear cation comprises three gold(I) atoms held in a triangular arrangement due to the presence of short Au····Au contacts. The counter anion consists of a gold centre with two ethynylthiophene ligands.

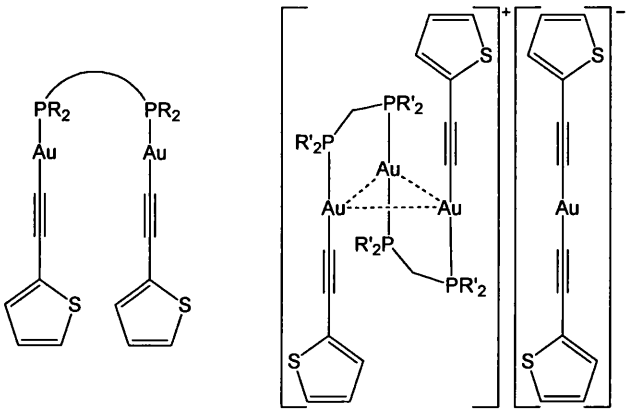

Figure 3.17: Schematic drawings of di-and trinuclear gold(I) phosphine alkynes

The electronic absorption and emission spectra for these compounds are found to be similar to that of the alkynyl ligand. The emission energies are generally lower in the trinuclear complexes, thought to be a consequence of the presence of Au····Au interactions. To date, independent mononuclear gold complexes incorporating this ligand have not been reported in the literature.

3.2.3.1 Synthesis and Characterisation of Gold(I) Alkynyl Chalcogenophene Complexes

In order to further develop this area of gold chemistry and to obtain experimental data that may be compared the results with those obtained for the platinum systems, the gold(I) alkynyl chalcogenophene phosphine complexes [(Ph_3P)AuC≡C–C_4H_3S], **3.11**, [(Ph_3P)AuC≡C–C_4H_3Se], **3.12**, and [(Et_3P)AuC≡C–C_4H_3S], **3.13**, were prepared from their respective trimethylsilyl-protected alkynes by a similar method to that described in Chapter Two (Scheme 3.9) and their structures determined. Preparation of the furan analogues was unsuccessful due to their low stability in solution.

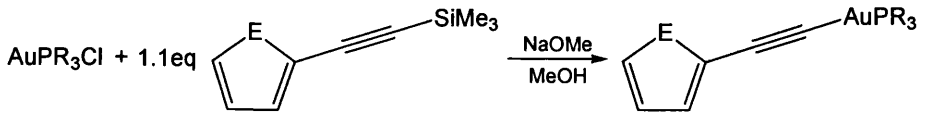

Scheme 3.9: Preparation gold(I) alkynyl chalcogenophene complexes, R = Et, Ph; E = S, Se.

The thiophene-containing gold(I) alkynyl complexes [(Ph_3P)AuC≡C-C_4H_3S], **3.11**, and [(Et_3P)AuC≡C–C_4H_3S], **3.13**, were obtained as pale yellow solids in 72% and 39% yield, respectively. Complex **3.13** is much less stable to light than its triphenylphosphine analogue and the corresponding selenium and tellurium analogues decompose readily, therefore it was not possible to isolate these materials. The ethynyl chalcogenophene gold(I) complex [(Ph_3P)AuC≡C-C_4H_3Se] **3.12** was obtained as orange crystals in 40% yield.

The complexes **3.11 – 3.13** were characterised by multinuclear NMR spectroscopy. In all three cases, the ^1H NMR spectrum shows the expected resonances for the ethynylthiophene ligand along with multiplets corresponding to the ethyl groups on the phosphine. Table 3.11 summarises selected NMR spectral data and lists the ν(C≡C) stretch for each complex.

	δ ^1H			δ ^{31}P	δ ^{77}Se	ν(C≡C) cm^{-1}
	3-	4-	5-			
3.11	7.09	6.89	7.16	42.28	-	2104
3.12	7.34	7.12	7.80	42.38	689.0	2090
3.13	7.07	6.87	7.13	38.19	-	2093

Table 3.11: Selected spectral data for 3.11 – 3.13

The $^{13}C\{^1H\}$ NMR spectra show the expected signals for all of the symmetry independent carbons in the molecule except that of the acetylide carbon bonded to the gold atom which is a consequence of quadrupolar line broadening caused by the ^{197}Au nuclei,[70] which is 100% abundant. The singlet observed in the $^{31}P\{^1H\}$ NMR spectra of **3.11** and **3.12** are shifted from that of 33.35 ppm for $Au(PPh_3)Cl$, while that of **3.13** is shifted from 31.60 ppm for $Au(PEt_3)Cl$. Selenium-proton coupling through two bonds with $^2J_{SeH}$ coupling constant of 45.2 Hz is clearly observed around the multiplet observed at 7.80 ppm in the ^1H NMR spectrum of **3.12**.

The absorptions at 2104 cm^{-1} in the IR spectrum of **3.11** and at 2093 cm^{-1} in the IR spectrum of **3.13** are assigned to the ν(C≡C) stretch and are at a lower frequency than that of 2144 cm^{-1} for C_4H_3S-C≡C$SiMe_3$[71] due to the mass effect of adding the gold phosphine unit. Similarly, the frequency of the ν(C≡C) stretch in the IR spectrum of **3.12** is lowered from that of 2138 cm^{-1} observed for 2-(trimethylsilylethynyl)selenophene, **3.03**, as a result of metal to ligand backbonding.

3.2.3.2 Molecular Structures

The structure of **3.11** was determined from a single crystal grown from a methanol solution at -25 °C. The crystallographic asymmetric unit of **3.11** consists of an independent molecule where the two coordinate gold atom has approximately linear geometry [P–Au–C(19), 176.00(9)°] (Figure 3.18). Table 3.12 lists selected bond lengths and bond angles for **3.11**. The Au–P bond length is within the range (2.2723(8) – 2.2784(6) Å) observed in the discrete triphenylphosphine gold complexes discussed in Chapter Two.

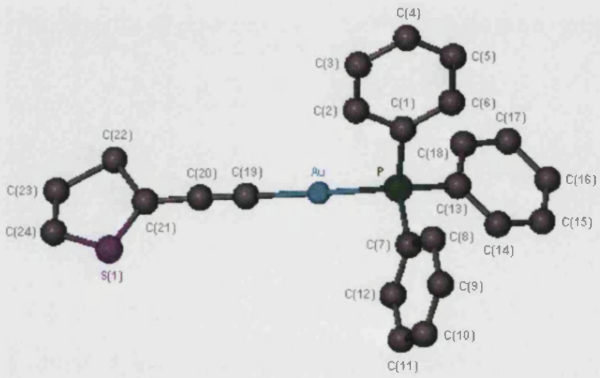

Figure 3.18: Asymmetric unit of 3.11 (hydrogen atoms omitted for clarity).

Contact	Bond length (Å)	Contact	Bond Angle (°)
P–Au	2.2737(7)	P–Au–C(19)	176.00(9)
Au–C(1)	1.985(3)	Au–C(19)–C(20)	173.0(3)
C(19)–C(20)	1.214(4)	C(19)–C(20)–C(21)	175.0(4)
C(20)–C(21)	1.425(4)	C(20)–C(21)–C(22)	123.5(6)
C(21)–C(22)	1.691(17)	C(21)–C(22)–C(23)	90.9(8)
C(21)–S	1.639(7)	C(21)–S–C(24)	98.0(5)

Table 3.12: Selected bond lengths and angles for 3.11

Molecules of **3.11** align in anti-parallel pairs in the solid state to minimise steric interaction between the bulky phosphine groups as shown in Figure 3.19. As a consequence of this, the shortest distance between gold atoms is 6.837 Å which is too long for there to be any Au····Au interactions in existence between neighbouring molecules.

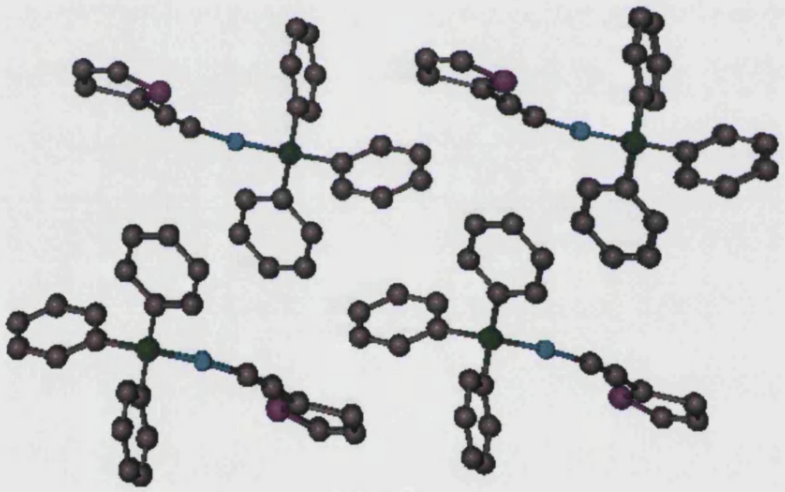

Figure 3.19: Expanded solid state structure of 3.11

Single crystals of **3.12** were obtained from a methanol/chloroform solution (1:1) at -25 °C. The asymmetric unit of the cell contains an approximately linear two coordinate gold centre with one ethynylselenophene ligand and one triphenylphosphine ligand as shown in Figure 3.20 with selected bond lengths and bond angles listed in Table 3.13. The bond lengths and bond angles observed in the selenophene ring are comparable with those quoted for the selenophene ring in the mixed metal cluster $[W_2Ir_2(CO)_8(\eta^5\text{-}C_5H_4Me)_2]_2\{\mu_8\text{-}\eta^4\text{-}Me(CH_2)_5C{\equiv}C\text{-}2\text{-}C_4H_2Se\text{-}5\text{-}C{\equiv}C(CH_2)_5Me\}$[40] [C(24)–Se, 1.82(2)Å; C(24)–C(23), 1.38(3)Å; C(23)–C(22), 1.40(5) Å, C(22)–C(21), 1.330(3) Å and C(21)–Se, 1.820(8) Å *cf.* 1.899(10) Å,

1.376(14) Å, 1.374(15) Å, 1.362(14) Å and 1.865(10) Å respectively; C(23)–C(24)–Se 110.6(10)°; C(24)–C(23)–C(22) 115.0(17)° *cf.* 108.7(8)° and 117.7(9)°, respectively].

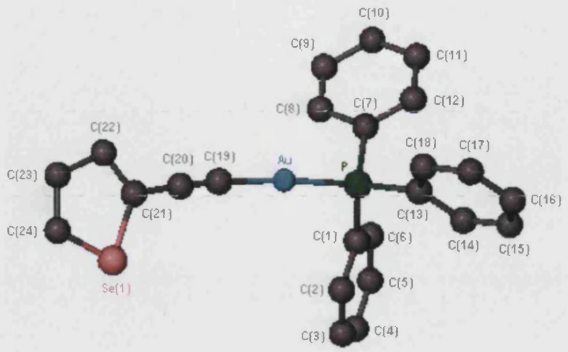

Figure 3.20: The asymmetric unit of 3.12 (hydrogen atoms omitted for clarity)

Contact	Bond length (Å)	Contact	Bond Angle (°)
P–Au	2.2742(16)	P–Au–C(19)	177.0(2)
Au–C(1)	2.005(7)	Au–C(19)–C(20)	175.0(7)
C(19)–C(20)	1.185(10)	C(19)–C(20)–C(21)	177.9(9)
C(20)–C(21)	1.429(10)	C(20)–C(21)–C(22)	122.2(15)
C(21)–C(22)	1.330(3)	C(21)–C(22)–C(23)	109.0(2)
C(21)–Se	1.820(8)	C(21)–Se–C(24)	89.0(8)

Table 3.13: Selected bond lengths and bond angles for 3.12

Figure 3.21 shows how the molecules align in the solid state with pairs of molecules in an anti-parallel arrangement forming a herring bone pattern. The distance between gold atoms is 8.353 Å which is more than double the upper distance limit of the commonly reported range in which Au····Au interactions occur (2.75 – 3.40 Å[72]), indicating that there are no such interactions present.

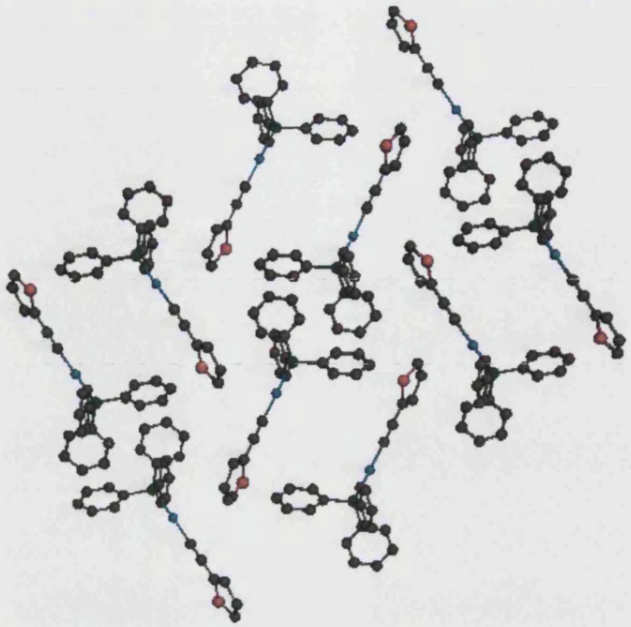

Figure 3.21: Association of molecules of 3.12 in solid state.

Single crystals of **3.13** were grown from a methanol solution at -25 °C. Figure 3.22 shows the asymmetric unit of the cell which consists of an independent molecule with a bend away from linearity [P–Au–C(1), 170.68(13)°; Au–C(1)–C(2), 169.7(4)°; C(1)–C(2)–C(3), 175.9(5)°] and Table 3.14 lists selected bond lengths and angles. The metric data observed for the ethynylthiophene unit are similar to those of **3.11** and the Au–P bond length of 2.2839(11) Å is similar to the range observed for the discrete triethylphosphine gold(I) alkynes (2.2800(3) – 2.2818(6) Å) discussed in Chapter Two.

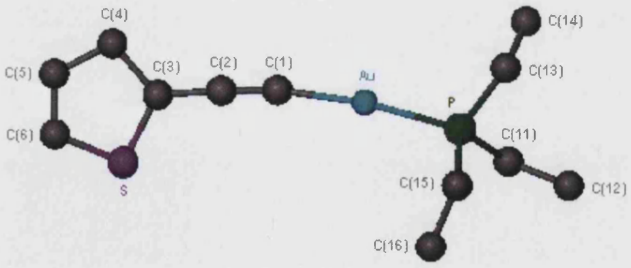

Figure 3.22: Asymmetric unit of 3.13 (hydrogens omitted for clarity)

Contact	Bond length (Å)	Contact	Bond Angle (°)
Au–P	2.2839(11)	P–Au–C(1)	170.68(13)
Au–C(1)	1.993(4)	Au–C(1)–C(2)	169.7(4)
C(1)–C(2)	1.225(6)	C(1)–C(2)–C(3)	175.9(5)
C(2)–C(3)	1.422(6)	C(1)– Au–Au#1	89.99(12)
C(3)–C(4)	1.529(6)	C(1)– Au–Au#2	87.98(12)
C(3)–S	1.679(5)	P–Au–Au#1	94.67(3)
Au–Au#1	3.3276	P–Au–Au#2	92.84(3)
Au–Au# 2	3.3277	Au#1–Au–Au#2	144.642(7)

Table 3.14: Selected bond lengths and angles for 3.13

Unlike the triphenylphosphine complexes described above which have a discrete structure, the solid state structure of **3.13** shows a continuous chain of molecules held together by Au····Au interactions (Figure 3.23) with Au····Au distances of 3.3276 Å, an Au–Au–Au bond angle of 144.642(7)° and P–Au–Au–P torsion angle of 117.3°.

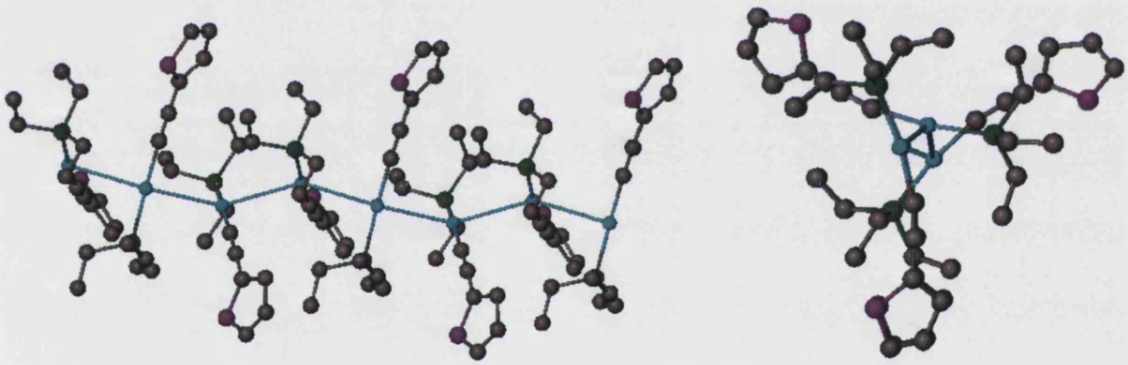

Figure 3.23: Two views of gold chain structure of 3.13

Unlike the gold chain structures of the heterocycle-containing gold(I) alkynyl complexes observed in Chapter Two, there is no rearrangement of ligands about the gold centre and each gold atom has one phosphine group and one ethynylthiophene group coordinated. The bend in the P–Au–C≡C unit of the molecules [P–Au–C(1), 170.68(13); Au–C(1)–C(2), 169.7(4)] reduces steric interaction between the phosphine groups and thiophene rings on neighbouring molecules.

3.2.3.3 UV/visible Spectroscopic Studies

The absorption spectra for **3.11** – **3.13** are shown in Figure 3.24 and spectral data is summarised in Table 3.15. For the thiophene-containing materials, the optical gap decreases in the order C_4H_3S-C≡CSiMe$_3$ (4.09 eV) > [(Et_3P)AuC≡C–C_4H_3S] (4.00 eV) > [(Ph_3P)AuC≡C–C_4H_3S] (3.71 eV). This is in agreement with the clearly observed red shift of the lowest energy absorption in the spectra of **3.11** and **3.13** from that of the trimethylsilyl-protected ligand. This is consistent with coordination of the gold phosphine unit increasing the conjugation length in the molecule through the metal centre. The ordering of the gold phosphine complexes is due to the greater π-acceptor ability of the triphenylphosphine groups of **3.11** over the triethylphosphine groups of **3.13**.

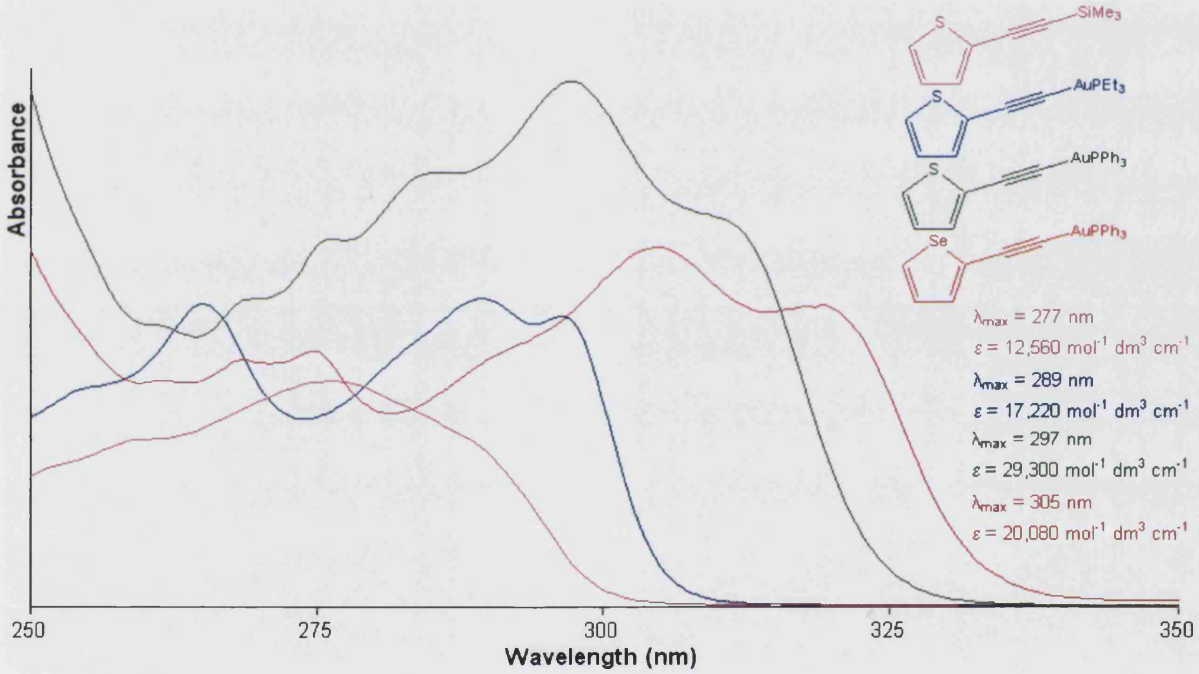

Figure 3.24: Absorption spectra for 3.02 and 3.11 – 3.13 (CH_2Cl_2, room temperature)

	Absorption λ_{max} (nm)	Emission (nm)	Optical gap (eV)
3.11	297	368	3.71
3.12	305	361	3.64
3.13	289	446	4.00

Table 3.15: Absorption and emission data for 3.11 – 3.13 (CH_2Cl_2, room temperature)

The spectrum of **3.13** follows the general shape of that of **3.02**, indicating a dependence on ligand centred $\pi - \pi^*$ transitions, with an additional absorption band at 265 nm. Although absorption bands in the 250–270 nm region of the electronic absorption spectra of mononuclear triphenylphosphine gold(I) complexes are assigned as phosphine-centered intraligand transitions by Yam *et al.*[69] the corresponding absorptions for $Au(PEt_3)Cl$ in dichloromethane at room temperature are observed >250 nm at 223 and 235 nm. The profile of the emission spectrum of **3.13** is a mirror image of the lowest energy absorption bands.

The electronic absorption spectrum of **3.12** has a λ_{max} at 305 nm (ε = 20,080 mol^{-1} dm^3 cm^{-1}) with a shoulder at 319 nm (ε = 16,820 mol^{-1} dm^3 cm^{-1}). As would be expected, the spectrum displays a red shift from that of **3.03** which is consistent with an increase in conjugation length when the trimethylsilyl groups are replaced with the gold triphenylphosphine unit. This is in agreement with the observed decrease in the energy of the optical gap of 3.64 eV for **3.12** which is lowered from that of 3.90 eV for **3.03**.

Table 3.16 lists spectral data for **3.11** and **3.12** from which the effect of replacing the heteroatom in the chalcogenophene ring can be observed. As found in the electronic spectra of the platinum complexes described above, the optical gap decreases from **3.11** → **3.12** due to a lowering of the energy level of the LUMO while the HOMO is relatively unchanged and this decrease in HOMO – LUMO separation is reflected in the red shift in the absorption spectra.

	Onset of Absorption (nm)	Optical gap (eV)	$\delta^{31}P$ (ppm)	IR ν(C≡C) (cm^{-1})
3.11	334	3.71	42.28	2104
3.12	341	3.64	42.38	2090

Table 3.16: Spectral data for 3.11 and 3.12

There is little difference in chemical shift of the singlets observed in the $^{31}P\{^1H\}$ NMR spectra and the ν(C≡C) stretches are both at a lower frequency than their respective trimethylsilyl-protected ligands suggesting that the gold phosphine unit has a mass effect on the stretching frequency.

3.3 Conclusions

A series of ethynyl chalcogenophenes have been synthesised and characterised. The corresponding platinum complexes *trans*-[Pt(PBu_3)$_2$($C_4H_3EC{\equiv}C$)$_2$] (E = O, S, Se, Te) have been successfully prepared in a novel *in situ* deprotection-dehydrohalogenation reaction. The electronic absorption spectra of the complexes exhibit a clear red shift of the absorption maxima through the series from E = O → Te. The spectra follow the general shape of the corresponding free ligands indicating that the absorption is dominated by intraligand $\pi - \pi^*$ transitions. The solution UV/visible studies, in conjunction with DFT calculations, have given an insight into the optical properties and the electronic structures of these materials and the small variations which occur along the series, thus proving good systems for the fine tuning of electronic properties. Multinuclear NMR spectroscopy of the platinum complexes has allowed the observation of unprecedented long range coupling.

Several alkynyl gold(I) phosphine complexes incorporating the ethynyl chalcogenophenes have also been prepared and examined by X-ray crystallographic methods and solution UV/visible absorption studies.

While the asymmetric unit of the cell of $Et_3PAuC{\equiv}C\text{-}C_4H_3S$ (**3.13**) displays a discreet molecule, in the solid state the molecules align into a continuous chain held together by Au····Au interactions. These interactions are not observed in the structures of the triphenylphosphine analogue, $Ph_3PAuC{\equiv}C\text{-}C_4H_3S$ (**3.11**), nor $Ph_3PAuC{\equiv}C\text{-}C_4H_3Se$ (**3.12**) and may be a consequence of steric interactions caused by the presence of the bulky phenyl rings on the phosphine.

The electronic absorption spectra for the thiophene containing species exhibit a red shift in the lowest energy absorption in going from $C_4H_3S\text{-}C{\equiv}CSiMe_3$, **3.02**, → **3.13** → **3.11**. This trend is consistent with an increase in the conjugation length of the molecule through the metal centre on coordination of the gold phosphine unit and reflects the stronger π-acceptor properties provided by phenyl groups on the phosphine rather than ethyl groups. In keeping with the observations for the platinum systems, the electronic absorption spectra for **3.11** and **3.12** show a red shift and therefore a decrease in optical gap from E = S → Se.

3.4 References

1. Yin, S. G.; Li, C. X.; Huang, W. Q.; He, B. L., *Acta Polym. Sin.,* 1998, 248-251.
2. Yin, S. G.; Peng, J. B.; Li, C. X.; Huang, W. Q.; Liu, X. Y.; Li, W. L.; He, B. L., *Synth. Met.,* 1998, **93**, 193-195.
3. Song, S. Y.; Jang, M. S.; Shim, H. K.; Song, I. S.; Kim, W. H., *Synth. Met.,* 1999, **102**, 1116-1117.
4. Ahn, T.; Shim, H. K., *Synth. Met.,* 2001, **121**, 1663-1664.
5. Takimiya, K.; Otsubo, T., *Phosphorus Sulfur Silicon Relat. Elem.,* 2005, **180**, 873-881.
6. Bunz, U. H. F. In *Poly(Arylene Ethynylene)s: From Synthesis to Application*; Springer-Verlag: Berlin, 2005; Vol. 177; pp. 1-52.
7. Kraft, A.; Grimsdale, A. C.; Holmes, A. B., *Angew. Chem. Int. Ed.,* 1998, **37**, 402-428.
8. Skotheim, T. A. In *Handbook of Conducting Polymers;* Skotheim, T. A.; Reynolds, J. R. Eds.; CRC Press, 2006.
9. Roncali, J., *Chem. Rev.,* 1997, **97**, 173 - 205.
10. McCullough, R. D., *Adv. Mater.,* 1998, **10**, 93 - 116.
11. Krinichnyi, V. I., *Synth. Met.,* 2000, **108**, 173-222.
12. Njuguna, J.; Pielichowski, K., *J. Mater. Sci.,* 2004, **39**, 4081-4094.
13. Glenis, S.; Benz, M.; LeGoff, E.; Schindler, J. L.; Kannewurf, C. R.; Kanatzidis, M. G., *J. Am. Chem. Soc.,* 1993, **115**, 12519-12525.
14. Glenis, S.; Ginley, D. S.; Frank, A. J., *J. Appl. Phys.,* 1987, **62**, 190-194.
15. Otsubo, T.; Inoue, S.; Nozoe, H.; Jigami, T.; Ogura, F., *Synth. Met.,* 1995, **69**, 537-538.
16. Salzner, U.; Lagowski, J. B.; Pickup, P. G.; Poirier, R. A., *Synth. Met.,* 1998, **96**, 177-189.
17. Lee, Y.-S.; Kertesz, M., *J. Chem. Phys.,* 1988, **88**, 2609-2617.
18. Zotti, G.; Martina, S.; Wegner, G.; Schluter, A.-D., *Adv. Mater.,* 1992, **4**, 798-801.
19. Heeger, A. J. In *Conjugated Polymers and Related Materials;* Salanack, W. R.; Lundstrom, I.; Ranby, B. Eds.; Oxford University Press; pp. 28-62.
20. Inoue, S.; Nakanishi, H.; Takimiya, K.; Aso, Y.; Otsubo, T., *Synth. Met.,* 1997, **84**, 341-342.
21. Inoue, S.; Jigami, T.; Nozoe, H.; Aso, Y.; Ogura, F.; Otsubo, T., *Heterocycles,* 2000, **52**, 159-170.
22. Paul, F.; Lapinte, C., *Coord. Chem. Rev.,* 1998, **180**, 431-509.

23. Long, N. J.; Williams, C. K., *Angew. Chem.-Int. Edit.*, 2003, **42**, 2586-2617.
24. Powell, C. E.; Humphrey, M. G., *Coord. Chem. Rev.*, 2004, **248**, 725-756.
25. Lewis, J.; Khan, M. S.; Kakkar, A. K.; Johnson, B. F. G.; Marder, T. B.; Fyfe, H. B.; Wittmann, F.; Friend, R. H.; Dray, A. E., *J. Organomet. Chem.*, 1992, **425**, 165-176.
26. Wittmann, H. F.; Friend, R. H.; Khan, M. S.; Lewis, J., *J. Chem. Phys.*, 1994, **101**, 2693-2698.
27. Beljonne, D.; Wittmann, H. F.; Kohler, A.; Graham, S.; Younus, M.; Lewis, J.; Raithby, P. R.; Khan, M. S.; Friend, R. H.; Bredas, J. L., *J. Chem. Phys.*, 1996, **105**, 3868-3877.
28. Lewis, J.; Long, N. J.; Raithby, P. R.; Shields, G. P.; Wong, W. Y.; Younus, M., *J. Chem. Soc.-Dalton Trans.*, 1997, 4283-4288.
29. Chawdhury, N.; Kohler, A.; Friend, R. H.; Younus, M.; Long, N. J.; Raithby, P. R.; Lewis, J., *Macromolecules*, 1998, **31**, 722-727.
30. Younus, M.; Kohler, A.; Cron, S.; Chawdhury, N.; Al-Mandhary, M. R. A.; Khan, M. S.; Lewis, J.; Long, N. J.; Friend, R. H.; Raithby, P. R., *Angew. Chem.-Int. Edit.*, 1998, **37**, 3036-3039.
31. Chawdhury, N.; Kohler, A.; Friend, R. H.; Wong, W. Y.; Lewis, J.; Younus, M.; Raithby, P. R.; Corcoran, T. C.; Al-Mandhary, M. R. A.; Khan, M. S., *J. Chem. Phys.*, 1999, **110**, 4963-4970.
32. Wilson, J. S.; Kohler, A.; Friend, R. H.; Al-Suti, M. K.; Al-Mandhary, M. R. A.; Khan, M. S.; Raithby, P. R., *J. Chem. Phys.*, 2000, **113**, 7627-7634.
33. Wilson, J. S.; Chawdhury, N.; Al-Mandhary, M. R. A.; Younus, M.; Khan, M. S.; Raithby, P. R.; Kohler, A.; Friend, R. H., *J. Am. Chem. Soc.*, 2001, **123**, 9412-9417.
34. Kohler, A.; Wilson, J. S.; Friend, R. H.; Al-Suti, M. K.; Khan, M. S.; Gerhard, A.; Bassler, H., *J. Chem. Phys.*, 2002, **116**, 9457-9463.
35. Silverman, E. E.; Cardolaccia, T.; Zhao, X. M.; Kim, K. Y.; Haskins-Glusac, K.; Schanze, K. S., *Coord. Chem. Rev.*, 2005, **249**, 1491-1500.
36. Chan, H. S. O.; Ng, S. C., *Prog. Polym. Sci.*, 1998, **23**, 1167-1231.
37. Perepichka, I. F.; Perepichka, D. F.; Meng, H.; Wudl, F., *Adv. Mater.*, 2005, **17**, 2281-2305.
38. Guernion, N. J. L.; Hayes, W., *Curr. Org. Chem.*, 2004, **8**, 637-651.
39. Barros, O. S. D.; Favero, A.; Nogueira, C. W.; Menezes, P. H.; Zeni, G., *Tetrahedron Lett.*, 2006, **47**, 2179-2182.

40. Notaras, E. G. A.; Lucas, N. T.; Humphrey, M. G.; Willis, A. C.; Rae, A. D., *Organometallics,* 2003, **22**, 3659-3670.
41. Sonogashira, K.; Yatake, T.; Tohda, Y.; Takahashi, S.; Hagihara, N., *J.C.S. Chem. Comm.,* 1977, 291 - 292.
42. Zeni, G.; Ludtke, D. S.; Nogueira, C. W.; Panatieri, R. B.; Braga, A. L.; Silveira, C. C.; Stefani, H. A.; Rocha, J. B. T., *Tetrahedron Lett.,* 2001, **42**, 8927-8930.
43. Wang, F.; Kaafarani, B. R.; Neckers, D. C., *Macromolecules,* 2003, **36**, 8225 - 8230.
44. Takahashi, S.; Kuroyama, Y.; Sonogashira, K.; Hagihara, N., *Synthesis,* 1980, **8**, 627-630.
45. Astruc, D., *Inorg. Chem.,* 2007, **46**, 1884-1894.
46. Bucci, P.; Chidichimo, G.; Lelj, F.; Longeri, M.; Russo, N., *J.C.S. Perkin Trans. II,* 1979, 109-111.
47. Younus, M. *PhD Thesis*, Cambridge 1999.
48. Liu, Y.; Jiang, S. J.; Glusac, K.; Powell, D. H.; Anderson, D. F.; Schanze, K. S., *J. Am. Chem. Soc.,* 2002, **124**, 12412-12413.
49. Falvello, L. R.; Fornies, J.; Gomez, J.; Lalinde, E.; Martín, A.; Moreno, M. T.; Sacristan, J., *Chem. Eur. J.,* 1999, **5**, 474-491.
50. Otto, S.; Ionescu, A.; Roodt, A., *J. Organomet. Chem.,* 2005, **690**, 4337-4342.
51. Herberhold, M.; Schmalz, T.; Milius, W.; Wrackmeyer, B., *Z.Naturforsch.(B),* 2002, **57**, 53-60.
52. Grossmann, G.; Ohms, G.; Kruger, K.; Karaghiosoff, K.; Eckstein, K.; Hahn, J.; Hopp, A.; Malkina, O. L.; Hrobarik, P., *Z. Anorg. Allg. Chem.,* 2001, **627**, 1269-1278.
53. Tattershall, B. W.; Sandham, E. L., *J. Chem. Soc. Dalton Trans.,* 2001, 1834-1840.
54. Grossmann, G.; Potrzebowski, M. J.; Fleischer, U.; Kruger, K.; Malkina, O. L.; Ciesielski, W., *Solid State Nucl. Magn. Reson.,* 1998, **13**, 71-85.
55. Tattershall, B. W.; Blachnik, R.; Baldus, H. P., *J. Chem. Soc.-Dalton Trans.,* 1989, 977-984.
56. Catalano, D.; Caporusso, A. M.; Dasettimo, F.; Forte, C.; Veracini, C. A., *Gazz. Chim. Ital.,* 1988, **118**, 529-532.
57. Saha, R.; Qaium, M. A.; Debnath, D.; Younus, M.; Chawdhury, N.; Sultana, N.; Kociok-Kohn, G.; Ooi, L. L.; Raithby, P. R.; Kijima, M., *Dalton Trans.,* 2005, 2760-2765.

58. Long, N. J.; White, A. J. P.; Williams, D. J.; Younus, M., *J. Organomet. Chem.,* 2002, **649**, 94-99.

59. Wong, W. Y.; Lu, G. L.; Ng, K. F.; Choi, K. H.; Lin, Z. Y., *J. Chem. Soc. Dalton Trans.,* 2001, 3250-3260.

60. Lee, C. T.; Yang, W. T.; Parr, R. G., *Phys. Rev. B,* 1988, **37**, 785-789.

61. Becke, A. D., *Phys. Rev. A,* 1988, **38**, 3098-3100.

62. Becke, A. D., *J. Chem. Phys.,* 1993, **98**, 5648-5652.

63. Hehre, W. J.; Radom, L.; Schleyer, P. V.; Pople, J. A. *Ab initio Molecular Orbital Theory*; Wiley-Interscience: New York, 1986.

64. Dolg, M.; Wedig, U.; Stoll, H.; Preuss, H., *J. Chem. Phys.,* 1987, **86**, 866-872.

65. Norman, P.; Cronstrand, P.; Ericsson, J., *Chem. Phys.,* 2002, **285**, 207-220.

66. Cooper, T. M.; Blaudeau, J. P.; Hall, B. C.; Rogers, J. E.; McLean, D. G.; Liu, Y. L.; Toscano, J. P., *Chemical Physics Letters,* 2004, **400**, 239-244.

67. Cooper, T. M.; Krein, D. M.; Burke, A. R.; McLean, D. G.; Rogers, J. E.; Slagle, J. E., *J. Phys. Chem. A,* 2006, **110**, 13370-13378.

68. Glusac, K.; Kose, M. E.; Jiang, H.; Schanze, K. S., *J. Phys. Chem. B,* 2007, **111**, 929-940.

69. Yam, V. W. W.; Cheung, K. L.; Yip, S. K.; Cheung, K. K., *J. Organomet. Chem.,* 2003, **681**, 196-209.

70. Whittall, I. R.; Humphrey, M. G.; Houbrechts, S.; Persoons, A.; Hockless, D. C. R., *Organometallics,* 1996, **15**, 5738-5745.

71. Van Overmeire, I.; Boldin, S. A.; Venkataraman, K.; Zisling, R.; De Jonghe, S.; Van Calenbergh, S.; De Keukeleire, D.; Futerman, A. H.; Herdewijn, P., *J. Med. Chem.,* 2000, **43**, 4189-4199.

72. Li, J.; Pyykko, P., *Chem. Phys. Lett.,* 1992, **197**, 586-590.

Chapter 4 New aromatic ligands for conjugated polymers

4.1 Introduction

4.1.1 Thiophene-containing Polymers

Since the preparation of polythiophene, first reported in 1980,[1,2] there has been great interest in thiophene-containing oligomers and polymers and the potential use of these materials in molecular devices. Due to the ease of synthesis and stability of polythiophene there are many examples of derivatives in the literature and the area has been reviewed extensively.[3,4]

A series of oligo-[thiophene-2,5-diyl]vinylenes with extended conjugated π-systems, of the type shown in Figure 4.1, have been reported by Nakayama and Fujimori.[5] In these oligomers all of the vinyl double bonds have a *trans* geometry which is necessary to maintain optimal overlap of orbitals and therefore effective conjugation over the length of the molecule.

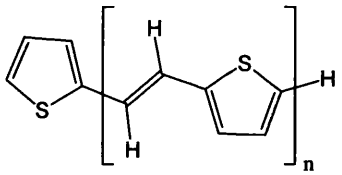

Figure 4.1: Oligo-[thiophene-2,5-diyl]vinylenes, n = 1 – 6.

Compounds containing an even number of thiophene rings can be synthesised by McMurry coupling[6] of thiophene-carboxaldehydes in the presence of a low valent titanium reagent and those with an odd number of thiophene rings are prepared by Horner-Wadsworth-Emmons[7,8] reaction (Scheme 4.1).

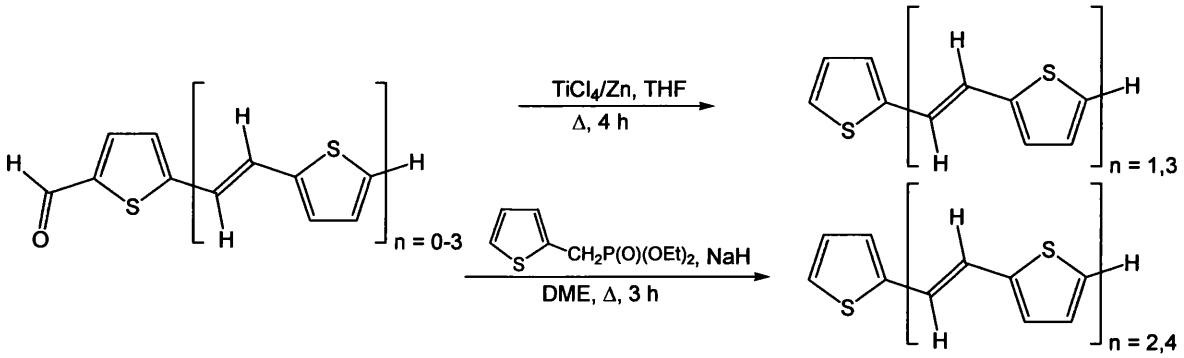

Scheme 4.1: Synthetic steps to oligo-[thiophene-2,5-diyl]vinylenes containing even or odd numbers of thiophene rings

The electronic absorption spectra of these materials all show a similar profile with a red shift in absorption maxima concurrent with the increasing number of thiophene rings and double bonds. The magnitude of the molar absorptivities is also found to increase as the number of thiophene rings is increased. These observations reflect the conjugation of the π-system along the molecule and suggest the potential of these materials for use as spacers in organometallic polymers.

Among the many thiophene derivatives in the literature, fused thiophene ring systems, such as thienothiophenes illustrated in Figure 4.2, have recently received a surge in interest due to their interesting electrochemical and optical properties attributed to their rigid structures and extended π-conjugated systems.[9,10]

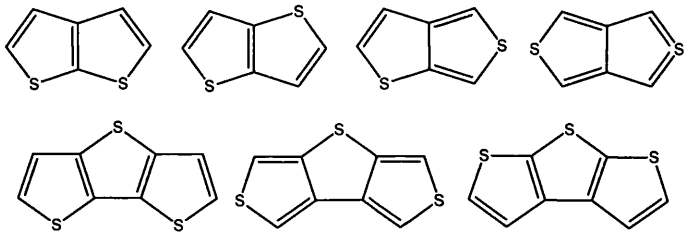

Figure 4.2: Isomeric thienothiophenes and selected dithienothiophenes

Methods of preparation of thieno- and dithienothiophenes are tailored to particular isomers as some are more synthetically accessible than others. Generally, these materials are obtained by formylation of a bromine derivative of thiophene *via* a lithiated derivative, followed by further metallation and treatment with elemental sulphur and methylbromoacetate. Ring closure occurs in the presence of sodium alkoxide and the resulting carboxylic acid is decarboxylated to afford the bromothienothiophene (Scheme 4.2).[10]

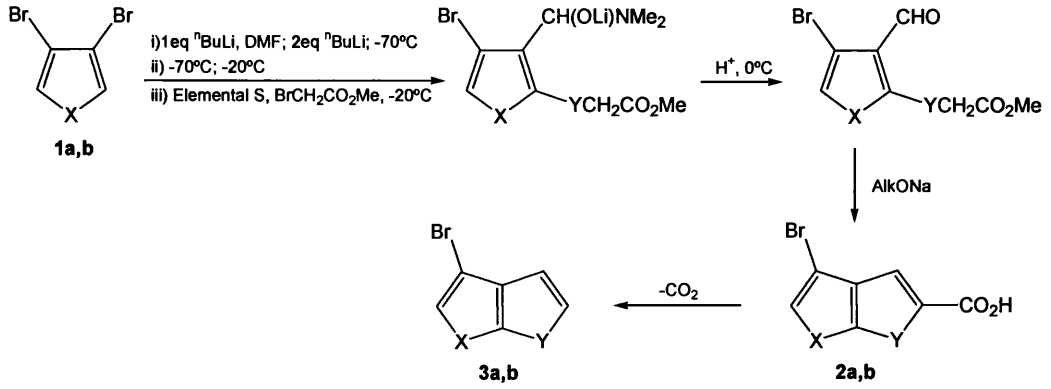

Scheme 4.2: Example of synthetic route to thienothiophenes, (a) X = Y = S; (b) X = Se, Y = S.

In contrast to this rather complicated route to fused heteroaromatic systems, di-(chalcogenophene)ethylenes have been converted into their corresponding fused systems by photochemical cyclisation in the presence of an oxidising agent (Figure 4.3).[11]

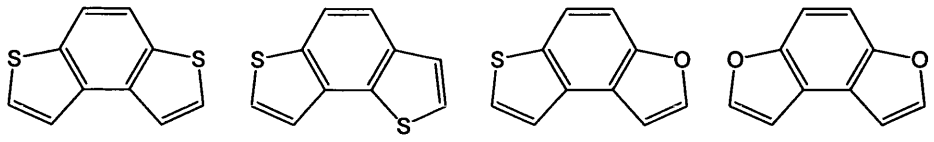

Figure 4.3: Fused heteroaromatic systems synthesised from di-(chalcogenophene)ethylenes[11]

4.1.2 Photochemical Synthesis of Heteroaromatic Fused Systems

Mechanistic studies of the high yielding photochemical cyclisation of *cis*-stilbene to phenanthrene have been reported by Mallory *et al*[12-14] in the early 1960s. The cyclisation proceeds *via* a dihydrophenanthrene intermediate which may ring open to reform the starting *cis*-stilbene or, in the presence of oxygen or other suitable oxidant lose two hydrogens to give phenanthrene as illustrated in Figure 4.4.

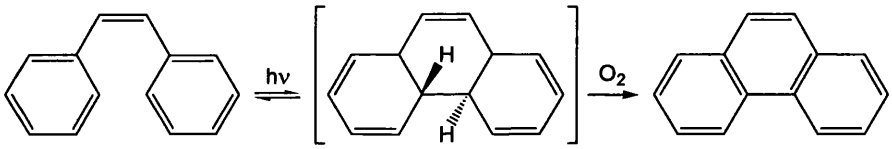

Figure 4.4 Photochemical conversion of *cis*-stilbene to phenanthrene

The mechanism was further confirmed by irradiation of stilbene under an inert atmosphere where only *cis–trans* isomerisation occurs with no net loss of stilbene or detection of fused product.

Following this work, Wynberg and co-workers studied an analogous system of thienyl- and furylethenes[11] in an attempt to produce condensed ring systems which were difficult to prepare by non-photochemical synthesis.

The modified Wittig reaction[15,16] reported by Wadsworth and Emmons[8] for the synthesis of *trans*-stilbene has been used to prepare a range of *trans*-thienylethenes. Benzene solutions of these thienylethenes (8 mM) irradiated in the presence of 0.2 equivalents of iodine gave the corresponding cyclised products in yields of 70 – 90% depending on the wavelength range of

the UV source used. As observed in the phenanthrene system, the cyclisation proceeds via a dihydrobenzodithiophene intermediate (Figure 4.5).

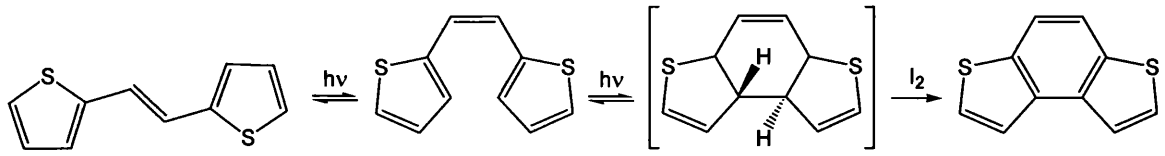

Figure 4.5: Photochemical conversion of 1,2-di(2-thienyl)ethene to 3,6-dithia-*as*-indacene

This discovery led Wynberg to attempt the synthesis of higher heterohelicenes, of interest due to their optical activity, incorporating thiophene rings (Figure 4.6) and furan rings.[17] In this context, 'helicene' refers to *ortho* fused aromatic hydrocarbons in which all of the rings are angularly arranged to form helically shaped molecules.

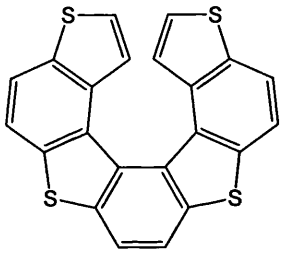

Figure 4.6: Example of a thiaheterohelicene

The heterohelicenes were prepared by the conversion of cyclised benzothiophenes to aldehydes or phosphonium salts for use in a Wittig reaction to form the alkene and then photocyclisation to give the helicene (Scheme 4.3).

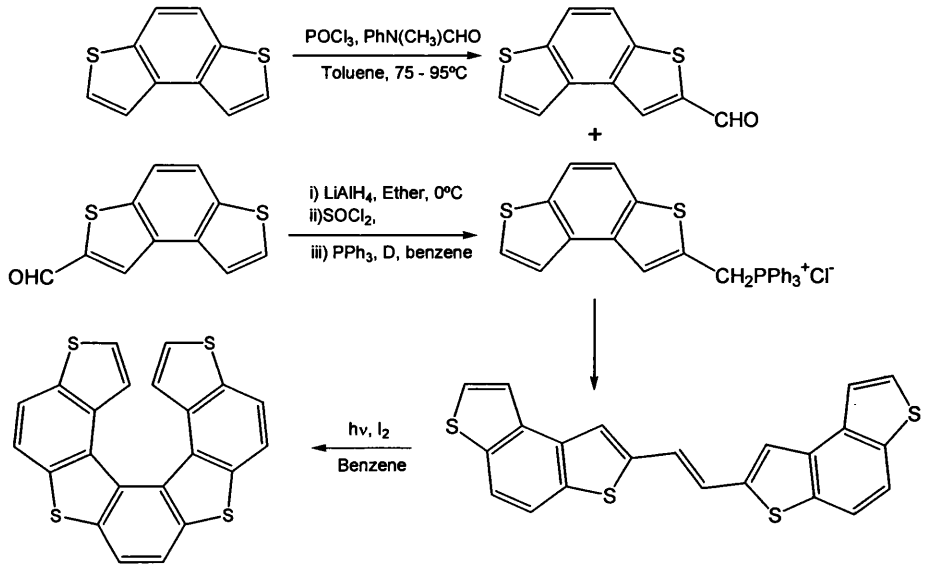

Scheme 4.3: Synthesis of thiaheterohelicene[17]

There has been renewed interest in synthetic routes to heterohelicenes,[18-21] (including the formation of molecular springs[22]) and their optical properties[23-26] along with those of benzodithiophene dimers bound by either a single bond[27] or alkene functionality.[28] Reports of the precursor benzodithiophenes however, are limited to investigations into their substitution[29] and NMR studies.[30]

4.1.3 Previous Work on Gold Alkynyls Containing Polythiophene Linker Groups

Oligomers of fused aromatic systems can have limited solubility in organic solvents which may be overcome by the introduction of transition metal phosphines which contain long alkyl chains.[31]

The incorporation of heavy transition metal atoms into the backbone of organic polymers connected by conjugated alkynyl ligands is of great interest due to:

i) Mixing of the metal and ligand orbitals allowing π-electron conjugation along the length of the polymer chain.[32,33]

ii) Spin-orbit coupling enhancement which allows light emission from the triplet excited state (phosphorescence) to be detected.[34]

In order to further studies of metal-containing polymers and oligomers current attention is paid to developing new chromophores.

Raithby and Khan[35] have reported a series of gold complexes incorporating alkynyl thienothiophene and dithienothiophene and described their optical properties as compared with related gold alkynyl dithiophene and terthiophene complexes (Figure 4.7).[36] These complexes were prepared from the corresponding trimethylsilyl-protected dialkynyl thiophene derivatives by treatment with two equivalents of triphenylphosphine gold(I) chloride in the presence of a methanol solution of potassium hydroxide similar to the methods discussed in Chapter Two.

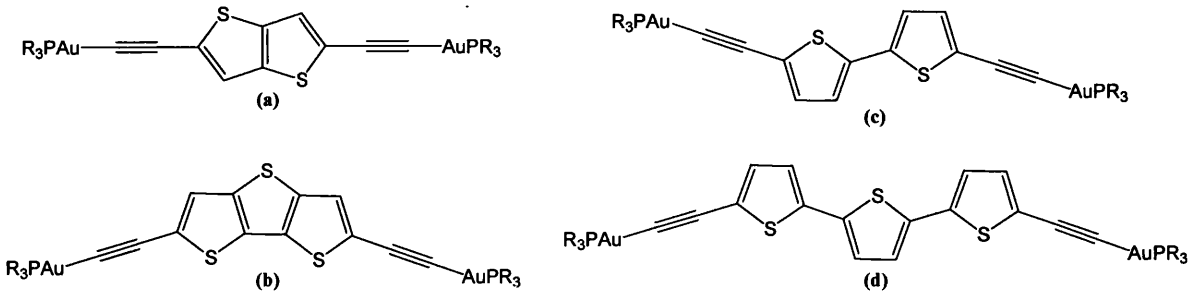

Figure 4.7: Gold alkynyl thiophene and thienothiophene complexes

The electronic absorption spectra of these compounds show a strong dependence on intraligand π–π^* transitions and a red shift in absorption maxima on coordination to the gold phosphine unit as compared with that of the free ligands, consistent with an increase in conjugation length across the molecule through the metal centres. A blue shift was also observed on going from dithiophene complex (c) to fused dithienothiophene complex (b) reflecting the higher energy transitions in the fused ring.

4.1.4 Objectives for this Chapter

Thienylethene and benzodithiophene (also known as thia-indacene) compounds show potential for use as ligands in metal containing diynes and polymers of the type previously prepared[31,35] (Figure 4.8) due to their stability and potential optical properties.

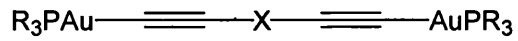

Figure 4.8: Gold containing diyne, X = aromatic or heteroaromatic spacer group

Figure 4.9 illustrates the proposed ligands **1-3d** and **1-3i**, along with their corresponding precursors, and gold complexes **1-3e** and **1-3j** to be prepared. The structural characterisation and optical properties of these materials will be studied by spectroscopic methods.

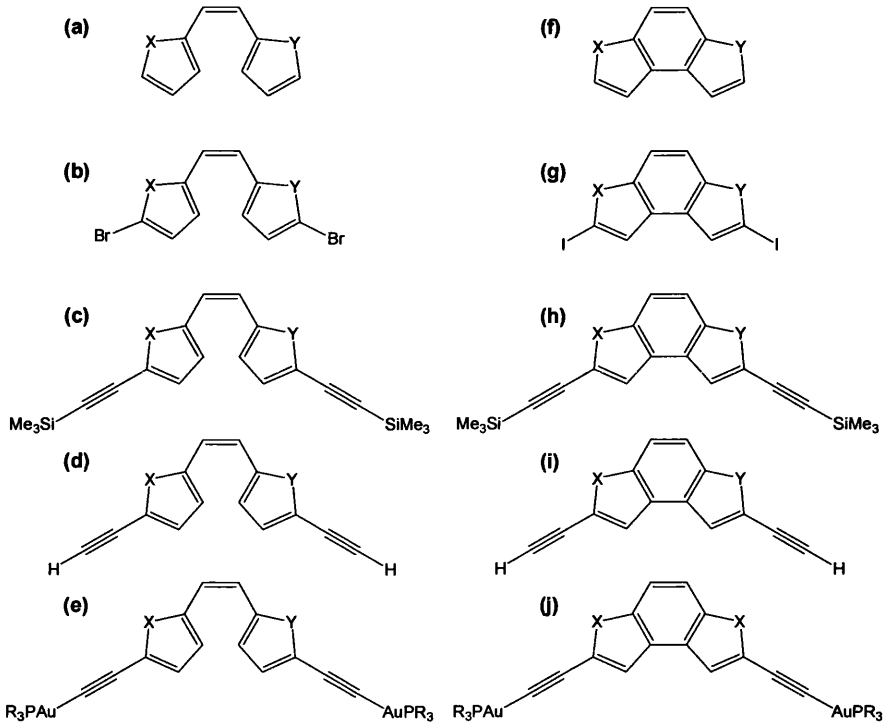

Figure 4.9: Proposed range of ligands, 1a-j X = S, Y = S; 2a-j X = S, Y = Se; 3a-j X = Se, Y = Se.

4.2 Results and discussion

4.2.1 Symmetric non-cyclised ligands

1,2-Bis(5'-Bromo-2'-thienyl)ethene, **4.01**, was synthesised by a McMurry coupling of 5-bromo-thiophene-2-carboxaldehyde in the presence of bis(tetrahydrofuran)titanium(IV) chloride and zinc powder following the literature method reported for the preparation of dithienylethene.[37] Although **4.01** has previously been reported,[38] full characterisation has not been detailed.

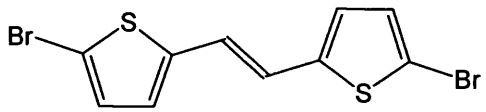

4.01

The doublets at 6.94 ppm (^3J = 3.7 Hz) and 6.77 ppm (^3J = 3.7 Hz) in the ^{1}H NMR spectrum of **4.01** correspond to the thiophene protons and a singlet at 6.80 ppm is assigned to the alkene protons. All five of the symmetry independent carbons are seen in the $^{13}C\{^1H\}$NMR spectrum confirming the proposed structure.

The electronic absorption spectrum for **4.01**, recorded in dichloromethane at room temperature, exhibits a band at 359 nm (ε = 39,180 mol^{-1} dm^3 cm^{-1}), with shoulders at 343 (31,620 mol^{-1} dm^3 cm^{-1}) and 377 nm (27,580 mol^{-1} dm^3 cm^{-1}), assigned as $\pi \rightarrow \pi^*$ (C=C) transitions, which is confirmed by the observed vibrational spacings of ~1400 cm^{-1} typical of ν(C=C) stretches. The optical gap, taken from the position of the onset of absorption, is 3.05 eV. The emission spectrum exhibits a mirror image of the lowest energy absorption bands. A strong absorption at 1442 cm^{-1} is observed in the IR spectrum of **4.01** which is assigned to a ν(C=C) stretch.

The palladium/copper catalysed cross coupling reaction of **4.01** with trimethylsilylacetylene, in the presence of triethylamine and tetrahydrofuran, afforded $Me_3SiC{\equiv}C\text{-}C_4H_2S\text{-}CH{=}CH\text{-}C_4H_2S\text{-}C{\equiv}CSiMe_3$, **4.02**, as gold flakes on purification in 63% yield (Scheme 4.4). The protected alkyne was found to be light and air stable at room temperature and was fully characterised by spectroscopic methods and elemental analysis.

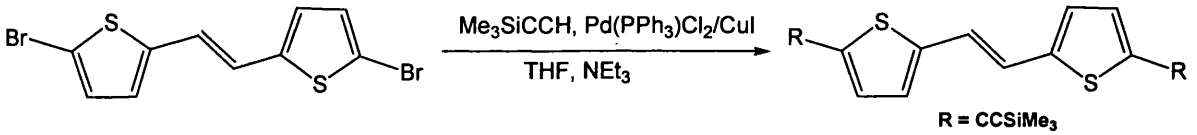

Scheme 4.4: Preparation of 1,2-Bis(5'-Trimethylsilylethynyl-2'-thienyl)ethene

The ^1H NMR spectrum exhibits a similar arrangement of doublets and singlet as observed in the spectrum of **4.01**, with an additional singlet at δ 0.25 corresponding to the protons of the $SiMe_3$ groups. The utilised numbering of carbons in the symmetric molecule is illustrated in Figure 4.10. Resonances for all eight symmetry independent carbons are observed in the $^{13}C\{^1H\}$NMR spectrum of **4.02** and were assigned as follows: 143.5 (C2), 133.4 (C1), 126.4 (C4), 122.1 (C5), 121.8 (C3), 100.5 (C6), 97.71 (C7) and -0.167 ppm (C8).

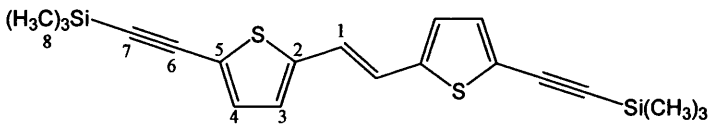

Figure 4.10: Numbering of carbons in 4.02

The electronic absorption spectrum of **4.02** exhibits a similar profile to that of **4.01** with a shift to longer wavelength and λ_{max} at 395 nm which is consistent with an increase in conjugation along the length of the molecule, as would be expected, by addition of the alkyne groups. This

increase in conjugation length is also reflected in the lowering of the optical gap to 2.79 eV by the addition of acetylide groups. There are strong absorptions at 1457 cm^{-1} and 2141 cm^{-1} in the IR spectrum of **4.02** corresponding to ν(C=C) and ν(C≡C) stretches, respectively.

Scheme 4.5 depicts the general deprotection method used to form the corresponding terminal alkynes. This is achieved by reaction of the protected alkyne with methanolic potassium hydroxide. Using this method **4.03** [HC≡C-C_4H_2S-CH=CH-C_4H_2S-C≡CH] was prepared as an orange solid.

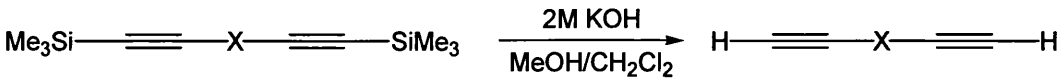

Scheme 4.5: General method for desilylation of protected alkynes (X = aromatic spacer)

The ^1H NMR spectrum of **4.03** shows the doublet, singlet, doublet arrangement of the dithienyl ethene spacer along with a singlet at 3.36 ppm corresponding to the terminal alkyne protons. The resonances for the seven symmetry independent carbons are observed in the $^{13}C\{^1H\}$ NMR spectrum. It was found that the orange solid (**4.03**) was unstable to prolonged exposure to light and air and formed a purple insoluble material, most likely a result of polymerisation.

5-Bromoselenophene-2-carboxaldehyde, **4.04**, has previously been prepared by treatment of selenophene-2-carboxaldehyde with bromine in the presence of aluminium trichloride.[39] The reaction predominantly forms 4-bromoselenophene-2-carboxaldehyde along with the 5-substituted mono bromide and the 4,5-dibromo derivative.

Efforts to prepare 5-bromo selenophene-2-carboxaldehyde by treatment of selenophene-2-carboxaldehyde with N-Bromosuccinimide resulted in a similar mixture of products. Therefore, a different synthetic strategy was attempted. A tetrahydrofuran solution of 2,5-dibromoselenophene was treated with one equivalent of ^{n}butyllithium (2.6M in hexanes) followed by addition of *N,N*-dimethylformamide which afforded **4.04** as a yellow oil in 34% yield (Scheme 4.6).

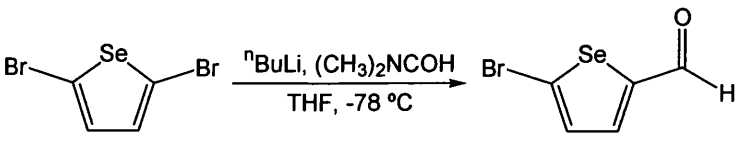

Scheme 4.6: Preparation of selenophene-2-carboxaldehyde

The ^{1}H NMR spectrum exhibits a *pseudo* triplet at 9.71 ppm, with proton-selenium coupling $^{3}J_{SeH}$ of 8.4 Hz, assigned to the aldehyde proton and doublets at 7.71 and 7.43 ppm (^{3}J = 4.3 Hz) for the protons on the selenophene ring.

The selenium analogue of **4.01** was prepared by McMurry coupling of **4.04** affording Br-C_4H_2Se-CH=CH-C_4H_2Se-Br **4.05** as a dark green solid after purification. The ^{1}H NMR spectrum exhibits a doublet at 7.12 ppm, with ^{77}Se satellites which have a coupling constant $^{2}J_{SeH}$ of 26 Hz, along with a doublet at 6.87 ppm and a singlet for the alkene protons at 6.75 ppm due to the symmetry of the molecule (Figure 4.11).

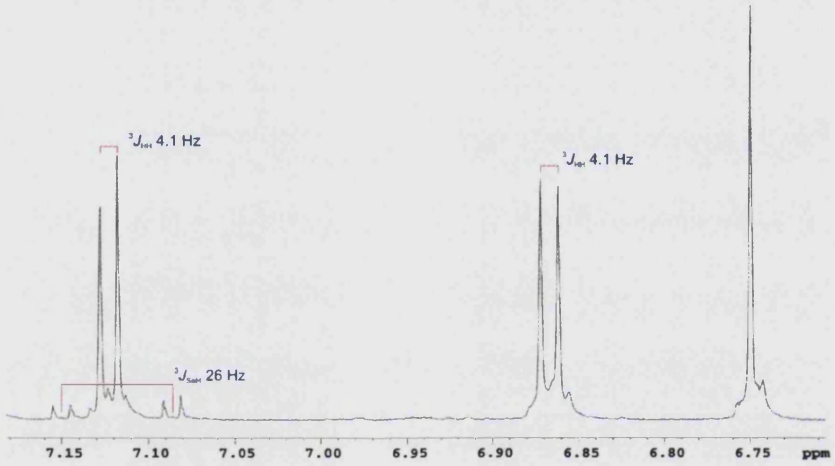

Figure 4.11: ^{1}H NMR spectrum of 4.05 (collected at 400.13 MHz)

The five symmetry independent carbons are observed in the ^{13}C{^{1}H}NMR spectrum and show little variation in chemical shift from those of **4.01**. The ^{77}Se{^{1}H}NMR spectrum shows a singlet at 648 ppm which suggests that the two nuclei are equivalent. The IR spectrum of **4.05** exhibits absorptions at 1452 cm^{-1} ν(C=C) and 802 cm^{-1} (C–Br). The absorption spectrum exhibits a maximum at 279 nm (ε = 3,420 mol^{-1} dm^{3} cm^{-1}).

Sonogashira coupling of **4.05** with trimethylsilylacetylene afforded $Me_3SiC{\equiv}C$-C_4H_2Se-CH=CH-C_4H_2Se-C≡C$SiMe_3$, **4.06**, as gold flakes on purification in 75% yield. Resonances for the diselenyl ethene spacer, with doublets corresponding to the protons on the selenophene ring shifted downfield (~0.2 ppm) from **4.05**, and a singlet at 0.25 ppm assigned to the methyl groups on the silicon are observed in the ^{1}H NMR spectrum of **4.06**.

The IR spectrum exhibits a strong absorption at 1463 cm^{-1} corresponding to a ν(C=C) stretch along with an absorption at 2134 cm^{-1} indicative of a ν(C≡C) stretch. The electronic absorption spectrum has a maximum at 307 nm (ε =17,260 mol^{-1} dm^3 cm^{-1}) which is shifted to longer wavelength on addition of the trimethylsilylacetylene groups consistent with an increase in conjugation across the molecule.

4.2.2 Asymmetric non-cyclised ligands

Due to the nature of the McMurry coupling reaction it is not used as a route to asymmetric alkenes as coupling RCHO with R'CHO would give a mixture of RCH=CHR, R'CH=CHR' and RCH=CHR'. The preparation of the asymmetric heterocyclic analogue of stilbene, 1-(2-furyl)-2-(2-thienyl)ethene, has been achieved using a Wittig reaction between 2-furaldehyde and triphenyl-thiophen-2-ylmethyl-phosphonium chloride in the presence of sodium methoxide (Scheme 4.7).[40]

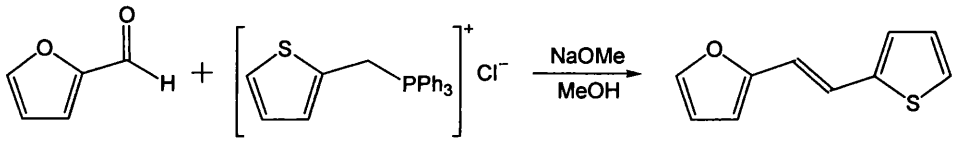

Scheme 4.7: Wittig reaction of furaldehyde to form 1-(2-furyl)-2-(2-thienyl)ethene

As the series of dithienylethene and diselenylethene-based ligands had been synthesised it was of interest to prepare 1-(2-thienyl)-2-(2-selenyl)ethene based ligands to complete the series and examine whether the properties of these ligands are affected by replacing one or both sulphur atoms with selenium.

1-(5-Bromo-2-thienyl)-2-(5-bromo-2-selenyl)ethene, **4.07**, was prepared by Wittig reaction of (5-Bromo-thiophen-2-ylmethyl)triphenyl phosphonium chloride with 5-bromoselenophene-2-carboxaldehyde in the presence of sodium methoxide and methanol affording a pale orange solid in a 63% yield.

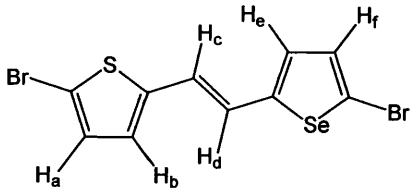

Figure 4.12: Utilised labelling of protons in 4.07

The ^{1}H NMR spectrum of **4.07** exhibits six doublets assigned following the labelling illustrated in Figure 4.12: 7.13 (H_f, *J* 4.1 Hz), 6.93 (H_a, *J* 3.9 Hz), 6.87 (H_d, *J* 15.9 Hz), 6.86 (H_e, *J* 4.1 Hz) 6.77 (H_b, *J* 3.9 Hz) and 6.68 ppm (H_c, *J* 15.9 Hz). Alkenes generally exhibit coupling constants in the range of 7 – 11 Hz ($^3J_{HH}$) for *cis* isomers and 12 – 18 Hz for *trans* isomers.[41] The observed coupling constant for the alkene protons in **4.07** is therefore indicative of a *trans* arrangement about the double bond. The ^{77}Se{^{1}H} NMR spectrum exhibits a singlet at 647 ppm.

The electronic absorption spectrum of **4.07** exhibits a λ_{max} at 365 nm (ε = 23,800 mol^{-1} dm^3 cm^{-1}) which follows a similar profile to that of **4.01** with a shift to longer wavelength. The emission spectrum is an approximate mirror image with a maximum at 429 nm. The absorptions observed at 1447 cm^{-1} ν(C=C) and 803 cm^{-1} (C–Br) in the IR spectrum of **4.07** show little variation from those of its symmetric analogues.

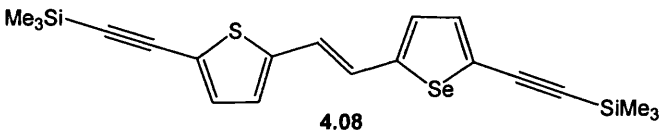

4.08

Sonogashira coupling of **4.07** with trimethylsilylacetylene afforded $Me_3SiC{\equiv}C\text{-}C_4H_2S\text{-}CH{=}CH\text{-}C_4H_2Se\text{-}C{\equiv}CSiMe_3$ **4.08** as a golden yellow solid in 96% yield. The expected resonances are observed in the ^{1}H NMR spectrum with six doublets for the central spacer and two singlets at δ0.24 and 0.25 ppm corresponding to the two non-equivalent trimethylsilyl groups. Fifteen carbon resonances are observed in the ^{13}C{^{1}H} NMR spectrum and there is a singlet at 654 ppm in the ^{77}Se{^{1}H} NMR spectrum.

The IR spectrum exhibits an absorption at 2142 cm^{-1} assigned to a ν(C≡C) stretch along with the ν(C=C) observed at 1454 cm^{-1}. The electronic absorption spectrum of **4.08**, obtained from a dichloromethane solution at room temperature, exhibits bands at 301 nm (ε = 8,460 mol^{-1} dm^3 cm^{-1}) and 402 nm (ε = 17,180 mol^{-1} dm^3 cm^{-1}) which has shoulders at 382 nm and 427 nm and vibrational spacings of 1300 – 1400 cm^{-1}, typical of a ν(C=C) stretch. The shape of the spectrum is similar to that of **4.07** suggesting that the bands arise from π–π* (C=C) transitions in the heterocyclic spacer. There is a shift to longer wavelength which is consistent with an increase in conjugation length in the molecule.

	Optical gap (eV)	
	R = Br	R = C≡CSiMe$_3$
R-C_4H_3S-CH=CH-C_4H_3S-R	3.05	2.79
R-C_4H_3S-CH=CH-C_4H_3Se-R	3.01	2.72
R-C_4H_3Se-CH=CH-C_4H_3Se-R	2.86	2.60

Table 4.1: Optical gaps from absorption spectra

Table 4.1 lists the optical gaps, taken as the position of the onset of absorption, for **4.02**, **4.06**, **4.08** and their dibromo precursors **4.01**, **4.05** and **4.07**, respectively. The optical gap is decreased by approximately 0.3 eV in each case on replacing the bromine with a trimethylsilylacetylene group and therefore increasing the conjugation along the molecule. Replacing one sulphur atom with selenium decreases the optical gap by 0.07 eV and replacing both decreases the optical gap by 0.19 eV.

4.2.3 Cyclised ligands

Attempts to cyclise 1,2-bis(5'-bromo-2'-thienyl)ethene to 2,7-dibromo-3,6-dithia-*as*-indacene gave solely the unsubstituted benzodithiophene product (Scheme 4.8). A similar result was obtained by Blackburn *et al* when attempting to prepare a cyclic 7-bromo derivative of dithia-*as*-indacene from 1-(5-Bromo-2-thienyl)-2-(2-thienyl)ethene.[30] This outcome is likely to be due to the C–Br bonds in bromothiophenes being more easily cleaved.

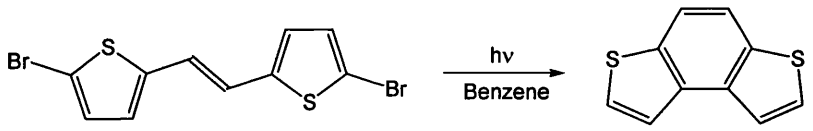

Scheme 4.8: Photochemical cyclisation of 1,2-bis(5'-bromo-2'-thienyl)ethene

Attempted bromination of 3,6-dithia-*as*-indacene with two equivalents of bromine in chloroform, at room temperature, gave two isomeric dibromo derivatives in a 2.5:1 ratio, thought to be 2,7-dibromo-3,6-dithia-*as*-indacene and 1,7-dibromo-3,6-dithia-*as*-indacene respectively, along with ~10% of mono substituted product.[42] Metallation of 3,6-dithia-*as*-indacene with two equivalents of ^{n}butyllithium followed by reaction with iodine has proven more selective giving 2,7-diiodo-3,6-dithia-*as*-indacene in an 83% yield.[43]

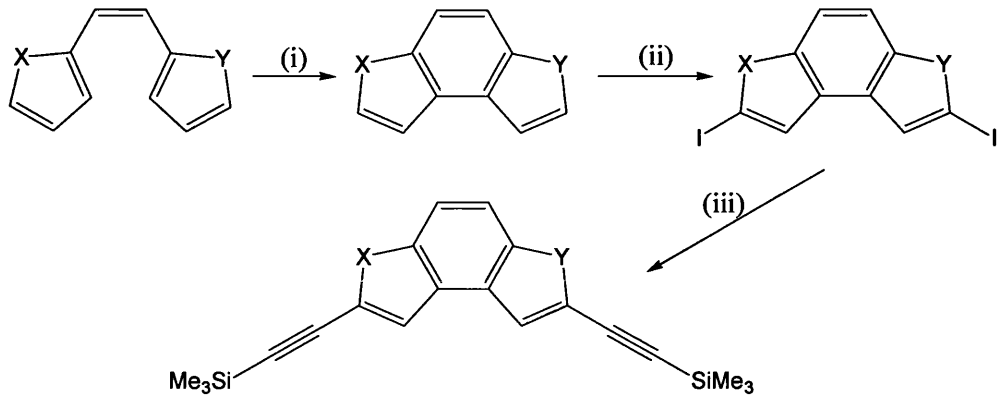

Scheme 4.9: (i) Benzene, hν, I_2; (ii) THF,TMEDA, ^{n}BuLi, I_2; (iii) Pd(II)/Cu(I), THF/ NEt_3, $Me_3SiC{\equiv}CH$

It was, therefore, necessary to prepare the heteroaromatic indacenes from their vinyl precursors and then iodinate to form the disubstituted halogen derivatives required for the next synthetic step (Scheme 4.9).

While 1,2-bis(2'-thienyl)ethene has previously been prepared by McMurry coupling,[37] the preparation of 1,2-bis(2'-selenyl)ethene has only been reported in a 44% yield by a Wittig reaction of selenophene-2-carboxaldehyde and triphenyl-(selen-2-ylmethyl)-phosphonium chloride in the presence of sodium methoxide.[40]

To prepare 1,2-bis(2'-selenyl)ethene by McMurry coupling it was necessary to synthesise selenophene-2-carboxaldehyde **4.09**. Selenophene was treated with ^{n}butyllithium in tetrahydrofuran followed by reaction with *N,N*-dimethylformamide to give **4.09** as a yellow oil in 91% yield. This subsequently underwent McMurry coupling to give 1,2-bis(2'-selenyl)ethene **4.10** in a 55% yield.

Figure 4.13 depicts the ^{1}H and ^{77}Se NMR spectra for **4.10**. There are three doublets of doublets observed in the ^{1}H NMR spectrum at 7.83, 7.21 and 7.18 ppm corresponding to the protons on the selenophene ring along with a singlet at 6.99 ppm with an integration of two for the alkene protons.

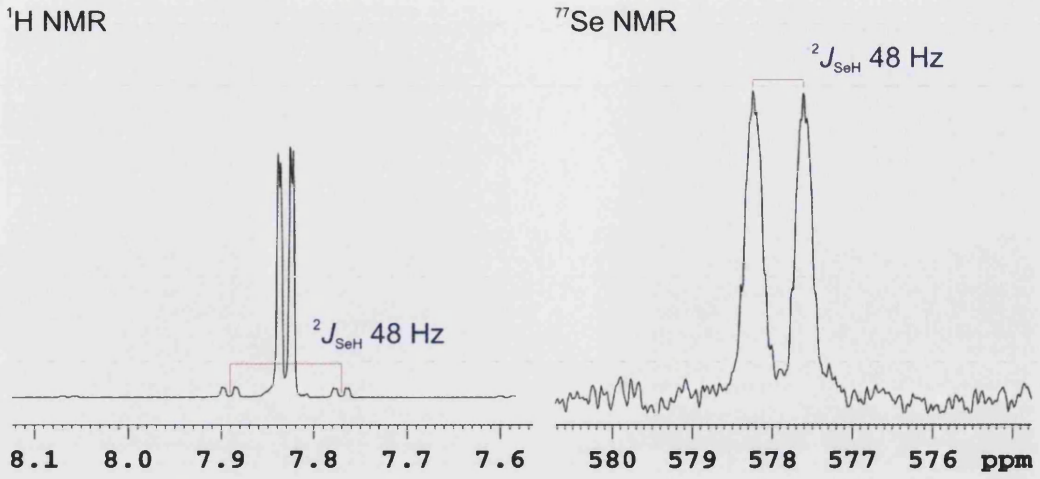

Figure 4.13: ^{1}H and ^{77}Se NMR spectra of 4.10 (collected at 400.13 and 76.311 MHz, respectively)

The doublet of doublets at 7.83 ppm is assigned to the proton in the 5-position of the selenophene ring due to the presence of satellites displaying a $^2J_{SeH}$ coupling constant of 48 Hz. The ^{77}Se NMR spectrum in turn exhibits a doublet with coupling constant of 48 Hz.

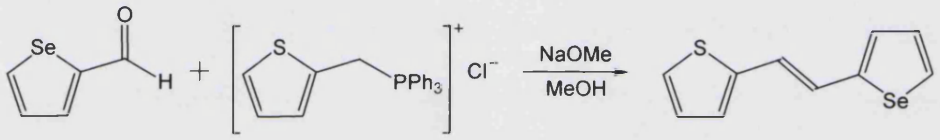

Scheme 4.10: Preparation of 1-(2-thienyl)-2-(2-selenyl)ethene (4.11)

As with **4.07**, 1-(2-thienyl)-2-(2-selenyl)ethene **4.11** was prepared by Wittig reaction of triphenyl-(thiophen-2-ylmethyl)-phosphonium chloride with selenophene-2-carboxaldehyde to form the asymmetric alkene as a pale yellow solid in 71% yield (Scheme 4.10). The labelling adopted for the protons present in **4.11** is shown in Figure 4.14.

The assignment of the ^{1}H NMR spectrum is as follows: 7.82 (d, ^3J 5.5 Hz, $^2J_{SeH}$ 48.1 Hz, H_h), 7.21 (dd, ^3J 5.5 Hz, ^3J 3.7 Hz, H_g), 7.19 – 7.18 (m, 2H, H_f and H_a), 7.09 (d, ^3J 15.7 Hz, H_e), 7.04 (d, ^3J 3.5 Hz, H_c), 6.99 (dd, ^3J 5.1 Hz, ^3J 3.5 Hz, H_b) and 6.95 (d, ^3J 15.7 Hz, H_d). The coupling constants for the alkene protons are in the range seen for *trans* arrangement.

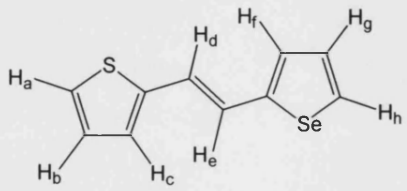

Figure 4.14: Utilised labelling of protons on 4.11

The electronic absorption/emission spectra of dithienylethene, **4.10** and **4.11** are illustrated in Figure 4.15 and corresponding data is listed in Table 4.2. There is a red shift on going from dithienylethene → **4.11** → **4.10**. The Stokes shifts are all approximately the same as is expected as changing the heteroatom has little effect on the basic geometry in either the ground state or expected excited state of the molecule. The lowest energy bands observed in the range of 300 – 400 nm arise due to π–π* (C=C) transitions in the molecules. The decrease in optical gap on replacing a sulphur atom with selenium is due to the lowering in energy of the LUMO level on changing the heteroatom while the energy level of the HOMO is less affected and relatively unchanged.

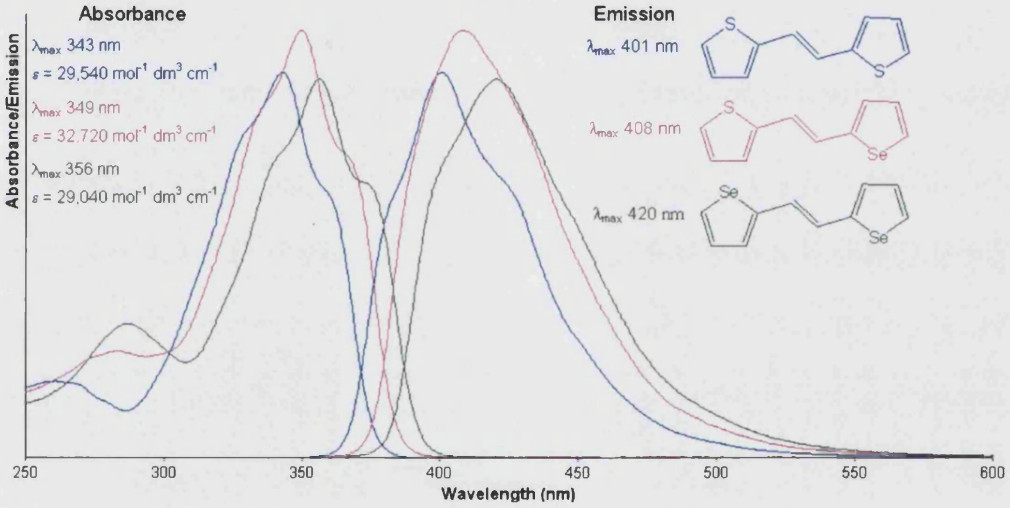

Figure 4.15: Electronic absorption/Emission spectra of dithienylethene, 4.10 and 4.11

	Absorption λ (nm)* ($\varepsilon/10^4$ mol^{-1} dm^3 cm^{-1})	Emission λ (nm)* (excited at λ_{max})	Optical gap (eV)
C_4H_3S-CH=CH-C_4H_3S	261 (0.6), 328 sh (2.1), 343 (3.0) 358 sh (2.4)	401, 426 sh	3.18
4.10	286 (1.0), 339 sh (2.3), 356 (2.9), 373 sh (2.1)	420	3.06
4.11	283 (0.8), 334 sh (2.6), 349 (3.3), 365 sh (2.3)	408	3.09

Table 4.2: Absorption and emission data for dithienyl ethene, 4.10 and 4.11 (*CH_2Cl_2, room temperature)

The hetero-indacenes 3,6-dithia-*as*-indacene (**4.12**), 3-thia-6-selena-*as*-indacene (**4.13**) and 3,6-diselena-*as*-indacene (**4.14**) were prepared by photocyclisation of dithienylethene, **4.11** and **4.10**, respectively. The alkene precursors were dissolved in benzene and irradiated with a broadband UV light source at room temperature for 22 hours in the presence of iodine (0.5 eq) and a flow of air (Scheme 4.11).

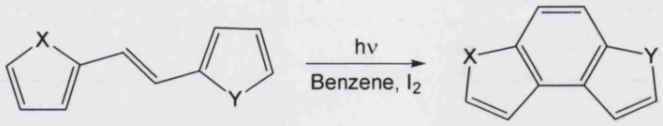

Scheme 4.11: Preparation of hetero-indacenes, X = Y = S, 4.12; X = S, Y = Se, 4.13; X = Y = Se, 4.14.

The ^{1}H and ^{13}C NMR spectra of **4.12** are consistent with those quoted in the literature and the yield of 77% higher than that previously reported.[19] The electronic absorption spectrum shows clear fine structure with λ_{max} at 289 nm and is consistent with that observed by Kellogg *et al.*[11] The emission spectrum shows a similar shape to that of the absorption suggesting the emission comes from the lowest energy absorption.

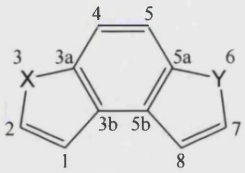

Figure 4.16: Utilised numbering of hetero-indacene ring

Hetero-indacenes **4.13** and **4.14** have not previously been reported in the literature. The ^{1}H NMR spectrum of **4.13** consists of six doublets and are assigned as follows: 8.15 (7-C*H*), 8.00 (8-C*H*), 7.88 (5-C*H*), 7.79 (4-C*H*), 7.72 (2-C*H*) and 7.55 ppm (1-C*H*) with the numbering of the hetero-indacene ring illustrated in Figure 4.16.

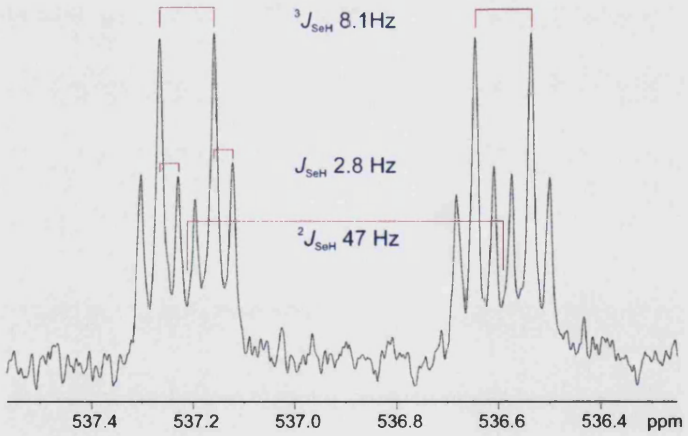

Figure 4.17: ^{77}Se NMR spectrum of 4.13 (collected at 76.311 MHz)

The $^{13}C\{^{1}H\}$ NMR spectrum exhibits resonances for nine of the ten symmetry independent carbons with an absent quaternary carbon which can often be difficult to observe due to relaxation properties. The signal centred at 537 ppm in the ^{77}Se NMR spectrum of **4.13**, illustrated in Figure 4.17, is observed as a multiplet due to the asymmetry of the molecule with

coupling constants $^2J_{SeH7}$ and $^3J_{SeH8}$ of 47 Hz and 8.1 Hz, respectively. The coupling between the selenium nucleus and H_4 and H_5 on the indacene ring manifests itself in the observation of a *pseudo* triplet with coupling constant of 2.8 Hz.

The ^{1}H NMR spectrum of **4.14** exhibits two doublets and a singlet as expected on symmetry grounds and are assigned as: 8.12 (d, $^2J_{SeH}$ 47 Hz, 2- & 7-C*H*), 8.01 (d, ^3J 5.9 Hz, 1- & 8-C*H*) and 7.84 (s, 4- & 5-C*H*).

The ^{77}Se NMR spectrum of **4.14** exhibits a doublet of doublets at 535 ppm with coupling constants $^2J_{SeH}$ of 47 Hz and $^3J_{SeH}$ of 8.4 Hz. Four resonances are observed in the ^{13}C NMR spectrum with the one of the quaternary carbons on the thiophene fused to the benzene ring absent.

The electronic absorption spectra of **4.13** and **4.14** both exhibit similar fine structure to that of **4.12**, each red shifted by 5 nm from the spectrum of the preceding molecule in the series. The optical gaps of these materials reflect this red shift as they decrease with increasing number of selenium atoms in going from **4.12** → **4.13** → **4.14** from 3.84 eV → 3.77 eV → 3.71 eV. The emission spectra of **4.13** and **4.14** both display a broad band centred at 372 nm and 350 nm, respectively.

When comparing absorption spectra for the uncyclised precursor and the hetero-indacene a blue shift in the absorption is observed on cyclisation. Figure 4.18 shows the absorption spectra of dithienyl ethene and 3,6-dithia-*as*-indacene which clearly displays the shift to lower wavelength affected by cyclisation of dithienyl ethene to **4.12**.

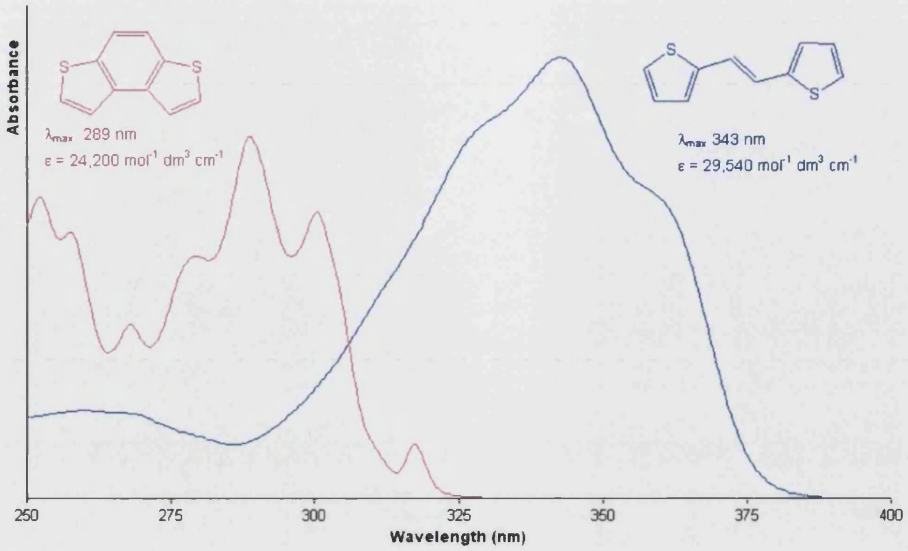

Figure 4.18: Absorption spectra of dithienylethene and 4.12 (CH_2Cl_2, room temperature)

This was initially unexpected as both dithienylethene and **4.12** contain the same number of "formal" conjugated double bonds. The shift can be explained by looking at the resonance structure of **4.12** shown in Figure 4.19. The resonance form on the right shows that the shortest path across the molecule has only three double bonds and not the five present in dithienylethene. This reduction in formal double bond path increases the energy separation between the HOMO and LUMO levels which moves the absorption to shorter wavelength (higher energy).

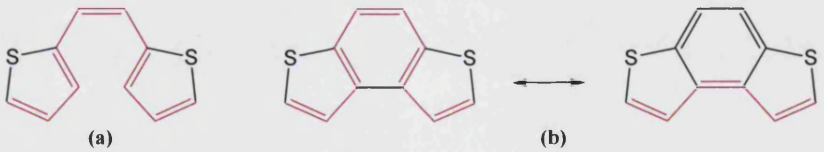

Figure 4.19: Shortest bond path of molecule is shown in red (a) Path across dithienylethene (b) Resonance forms of 4.12

2,7-Diiodo-3-thia-6-selena-*as*-indacene **4.15** and 2,7-diiodo-3,6-diselena-*as*-indacene **4.16** were prepared following the literature method used to prepare 2,7-diiodo-3,6-dithia-*as*-indacene.[43]

There are two doublets and two singlets observed in the ^{1}H NMR spectrum of **4.15** corresponding to the protons on the backbone of the benzene ring and those on the selenophene and thiophene rings, respectively. There are only two singlets observed in the ^{1}H NMR spectrum of **4.16** due to the symmetry of the molecule.

The ^{13}C NMR spectrum of **4.15** exhibits resonances for nine of the ten symmetry independent carbons as compared with that of **4.16** where there are five resonances observed due to the symmetry of the molecule.

There is a singlet observed at 659 ppm in the $^{77}Se\{^{1}H\}$ NMR spectrum of **4.15** though it was not possible to obtain a ^{77}Se spectrum to observe any selenium-proton coupling present, possibly due to the small percentage of selenium in the molecule. The ^{77}Se NMR spectrum of **4.16** on the other hand exhibits a doublet of doublets centred at 658 ppm with coupling constants 5.54 Hz ($^{3}J_{SeH}$) and 2.59 Hz ($^{3}J_{SeH}$).

The absorption and emission data for **4.15** and **4.16** are shown in Table 4.3. The absorption spectra have the same shape as their unsubstituted indacene precursors, showing that π–π^* (C=C) transitions dominate, and there is a clear red shift on addition of iodine.

	Absorption λ (nm)* ($\varepsilon/10^4$ mol^{-1} dm^3 cm^{-1})	Emission λ (nm)* (excited at λ_{max})
4.15	258 (1.1), 270 sh (0.9), 282 (0.8), 297 sh (0.9), 309 (1.0), 324 (0.8)	317 sh, 417, 433 sh
4.16	264 (2.3), 275 sh (2.3), 287 (2.1), 302 sh (2.4), 313 (2.8), 328 (2.4)	378

Table 4.3: Absorption and emission data for 4.15 and 4.16 (*CH_2Cl_2, room temperature)

The series of trimethylsilylethynyl substituted hetero-indacenes 2,7-bis(trimethylsilylethynyl)-3,6-dithia-*as*-indacene **4.17**, 2,7-bis(trimethylsilylethynyl)-3-thia-6-selena-*as*-indacene **4.18** and 2,7-bis(trimethylsilylethynyl)-3,6-diselena-*as*-indacene **4.19** were prepared by the Pd(II)/ Cu(I) cross coupling of trimethylsilylacetylene with 2,7-diiodo-3,6-dithia-*as*-indacene, **4.15** or **4.16** in tetrahydrofuran and diethylamine.

Table 4.4 lists the ^{1}H NMR spectral data for **4.17** – **4.19**, with the number of resonances observed corresponding to the change of symmetry in going through the series (X = Y, X ≠ Y, X = Y where X = S, Se and Y = S, Se), along with the IR ν(C≡C) stretches which shift to lower wavenumber.

	^{1}H NMR (ppm)	ν(C≡C) (cm^{-1})
4.17	7.75 (s), 7.70 (s), 0.30 (s)	2151
4.18	7.98 (s), 7.75 (s), 7.74 (d), 7.67 (d), 0.30 (s), 0.29 (s)	2142
4.19	7.99 (s), 7.71 (s), 0.29 (s)	2134

Table 4.4: ^{1}H NMR (400.14 MHz) and IR data for 4.17 – 4.19

The electronic absorption/emission spectral data are summarised in Table 4.5. The profiles of the spectra are similar to those of their dihalogenated precursors with an identical red shift of 33 nm in each case on coordination of the trimethylsilylacetylene groups suggesting an increase in conjugation length across the molecule. As expected from our previous results, in going from **4.17** → **4.18** → **4.19** the optical gap of the material decreases by 0.07 eV from **4.17** → **4.18** and by almost twice this amount in going from **4.17** → **4.19**. It is interesting to note that the Stokes shifts for **4.17**, **4.18** and **4.19** are smaller than those for their uncyclised analogues **4.02**, **4.08** and **4.06** respectively. This reflects the reduced degrees of freedom induced by ring fusion and therefore a decrease in the number of rearrangements in the excited state.

	Absorption λ (nm)* ($\varepsilon/10^4$ mol^{-1} dm^3 cm^{-1})	Emission λ (nm)* (excited at λ_{max})	Optical gap (eV)
4.17	277(1.7), 295(1.4), 307(2.2), 321(3.5), 336(5.2), 354(4.1)	363sh, 380, 399sh	3.34
4.18	274(1.6), 281(1.7), 312(1.4), 326(1.8), 342(2.3), 360(1.8)	375sh, 389, 411sh	3.27
4.19	272(0.7), 284(0.7), 318(0.8), 330(1.1), 346(1.6), 365(1.3)	379sh, 398, 416sh	3.23

Table 4.5: Absorption and emission data for 4.17 – 4.19 (*CH_2Cl_2, room temperature)

Desilylation of **4.17** with potassium hydroxide in methanol/dichloromethane afforded 2,7-diethynyl-3,6-dithia-*as*-indacene **4.20** as a pale yellow solid in 86%. The ^{1}H NMR spectrum exhibits resonances at 7.81 and 7.73 ppm corresponding to the protons on the hetero-indacene ring and a singlet at 3.51 ppm for the terminal alkyne protons. There is no signal observed in the region associated with the protons of the trimethylsilyl groups thus confirming that full deprotection of the material has occurred.

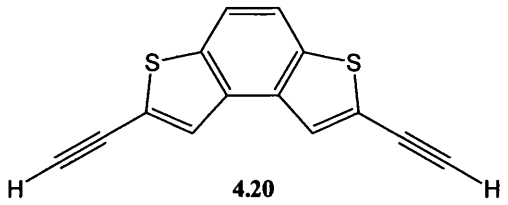

4.20

Seven resonances are observed in the $^{13}C\{^{1}H\}$ NMR spectrum with the following assignment: 137.4 (3a- & 5a-*C*), 133.6 (3b- & 5b-*C*), 127.7 (1- & 8-*C*H), 122.8 (C_{ipso}, *C*–C≡C–H), 119.6 (4- & 5-*C*H), 83.53 (C≡*C*–H) and 77.07 (*C*≡C–H). The diterminal alkyne solid material was found to be unstable to light and formed a dark insoluble material preventing further characterisation.

In an extension to this work, 2,5-bis(2-(5-bromothiophen-2-yl)-vinyl)selenophene **4.21** and 2,5-bis(2-(5-trimethylsilylethynylthiophen-2-yl)-vinyl)selenophene **4.22** were prepared and characterised by spectroscopic methods (Scheme 4.12).

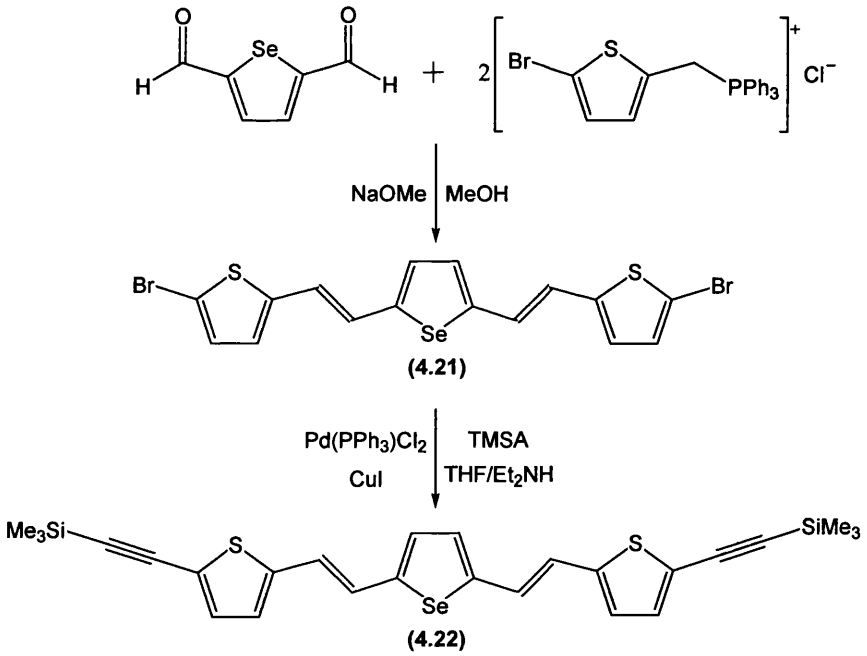

(4.21)

(4.22)

Scheme 4.12: Synthetic route to 4.21 and 4.22

An anhydrous methanolic solution of selenophene-2,5-carboxaldehyde and triphenyl-(5-bromo-2-thienyl)phosphonium chloride, refluxed in the presence of sodium methoxide for 17 hours, gave a bright yellow solid on cooling. The yellow solid was dissolved in hexane/

dichloromethane (4:1) and eluted through a short plug of silica to remove triphenylphosphine oxide formed during the reaction affording **4.21** in 77% yield.

The ^{1}H NMR spectrum of **4.21** shows a singlet at 7.04 ppm corresponding to the protons on the selenophene ring along with doublets at 6.94 and 6.78 ppm, with coupling constant ^{3}J 3.8 Hz, for the protons present on the thiophene rings. There are also two doublets observed at 6.90 ppm and 6.75 ppm assigned to the alkene protons next to the selenophene ring and those next to the thiophene rings, respectively. The coupling constant for these doublets is 15.5 Hz which is consistent with a *trans*-arrangement of the double bonds.

All eight of the symmetry independent carbons are observed in the $^{13}C\{^{1}H\}$ NMR spectrum of **4.21** with the following assignments: 146.3 (C_{ipso}, selenophene ring), 144.1 (C_{ipso}, thiophene ring), 133.0 (C–Br), 130.7 and 130.3 (alkene CH), 126.5 (selenophene CH), 124.3 and 122.2 (thiophene CH). It was not possible to obtain a ^{77}Se NMR spectrum of **4.21** due to the relatively small percentage of selenium present in the molecule. The IR spectrum shows a strong absorption at 1422 cm^{-1} assigned to ν(C=C) stretch.

The absorption spectrum of **4.21**, at room temperature in dichloromethane, has a λ_{max} at 429 nm (ε = 37,920 mol^{-1} dm^{3} cm^{-1}) with shoulders at 407 and 457 nm. The latter showing a vibrational spacing of 1430 cm^{-1} typical of a ν(C=C) stretch. The onset of absorption occurs at 502 nm which corresponds to an energy of 2.47 eV. The emission spectrum exhibits a mirror image of the lowest energy absorption bands.

The Pd(II)/Cu(I) catalysed cross coupling reaction of **4.21** with trimethylsilylacetylene gave **4.22** as a bright orange/red solid. The ^{1}H NMR spectrum of **4.22** is similar to that of **4.21** with a small downfield shift and the presence of a singlet at 0.06 ppm which corresponds to the 18 protons of the trimethylsilyl groups.

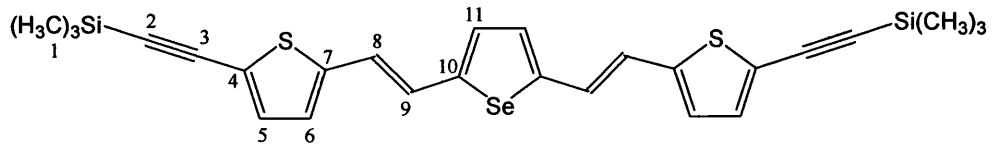

Figure 4.20: Numbering of carbon atoms in 4.22

The numbering of the carbon atoms of **4.22** is illustrated in Figure 4.20. Eleven resonances are observed in the $^{13}C\{^1H\}$ spectrum and are assigned as follows: 146.6 (C10), 143.9 (C7), 133.5 (C8), 130.5 (C9), 126.1 (C11), 124.8 (C5), 122.4 (C6), 121.9 (C4), 100.5 (C3), 97.80 (C2) and -0.16 (C1). The $^{77}Se\{^1H\}$ NMR shows a small singlet at 620.6 ppm. In the IR spectrum of **4.22** there are strong absorptions at 2140 cm^{-1} and 1251 cm^{-1} which arise from the ν(C≡C) stretch and the ν(C=C) stretch, respectively.

The electronic absorption spectrum follows the general shape of that of **4.21** with a λ_{max} at 455 nm and a red shift of *ca.* 30 nm which is consistent with the addition of the trimethylsilylacetylene groups leading to an increase in conjugation length across the molecule. This is also reflected in the decrease in optical gap to 2.26 eV. As is expected the optical gap is smaller than that of **4.08** due to the additional thiophene unit which increases the delocalisation of π-electrons along the backbone of the molecule.[34] The emission spectrum shows a broad band with a maximum at 547 nm.

4.2.4 Metal Complexes

Although dithienylethene has been used as a spacer group in ruthenium oligothienylacetylide complexes,[44-46] the heteroaromatic unit has only been functionalised with an alkyne at one end and an aldehyde[45,46], nitro group, vinylnitrobenzene or malonitrile group[44] at the opposite end of the molecule as illustrated in Figure 4.21.

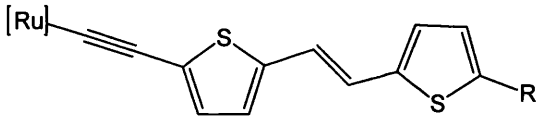

Figure 4.21: Ru-oligothienylacetylide complexes. R = COH, NO_2, CH=C-*p*-C_6H_4-NO_2 or $CH=C(CN)_2$.

Other than this small series of compounds there have been no reports of dithienylethene based metal acetylide complexes reported in the literature.

1,2-bis(5'-platinumphenyl(triethylphosphine)ethynyl-2'-thienyl)ethene **4.23** was prepared by copper(I) iodide-catalysed dehydrohalogenation[47] of **4.03** and platinum(II)(triethylphosphine) phenyl chloride in diisopropylamine and dichloromethane (Scheme 4.13).

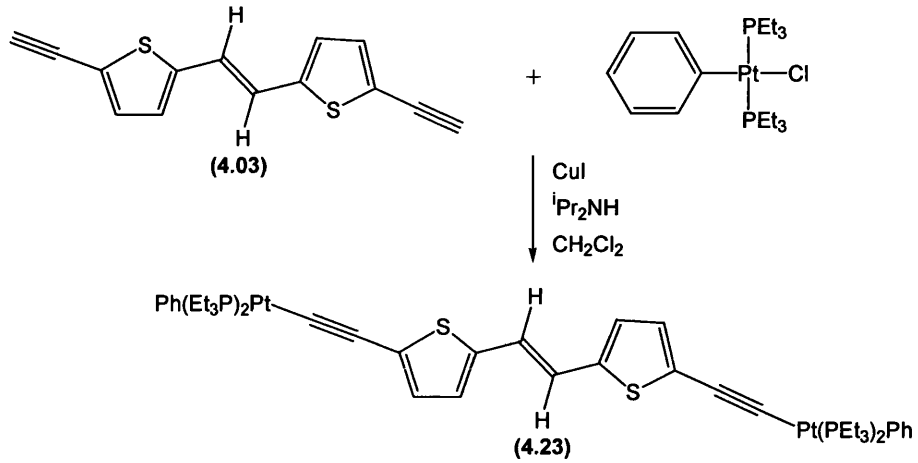

Scheme 4.13: Synthesis of 1,2-Bis(5'-platinumphenyl(triethylphosphine)ethynyl-2'-thienyl)ethene 4.23

The ^{1}H NMR spectrum of **4.23** exhibits the eight expected resonances. The assignments were assisted by running a ^{1}H-^{13}C HMQC spectrum of the material which determines direct carbon to proton connectivity. The peaks at 7.31 (d), 6.97 (t) and 6.80 ppm (t) correspond to the protons on the phenyl ring. The singlet at 6.79 ppm arises from the alkene protons due to the symmetry of the molecule and similarly the doublets at 6.74 and 6.70 ppm correspond to the protons on the thiophene ring. The presence of the triethylphosphine groups is confirmed by the two multiplets observed at 1.7 and 1.1 ppm in the spectrum.

Ten resonances are observed in the $^{13}C\{^{1}H\}$ NMR spectrum of **4.23**. The three absent signals are assigned to the quaternary carbons 1) in the phenyl ring, 2) bonded to the platinum atom and 3) in the thiophene ring bonded to the alkene. A singlet is observed in the ^{31}P NMR spectrum at δ 10.15 ppm which displays satellites arising due to Pt-P coupling with a coupling constant of 2629 Hz.

The ν(C≡C) stretch in the IR spectrum is observed at 2081 cm^{-1} which is lowered in frequency from 2141 cm^{-1} for **4.02** due to the effect of attaching the heavy platinum atom. The ν(C=C) stretch at 1457 cm^{-1} for the dithienylethene spacer group is also seen, with little variation from that of **4.02**.

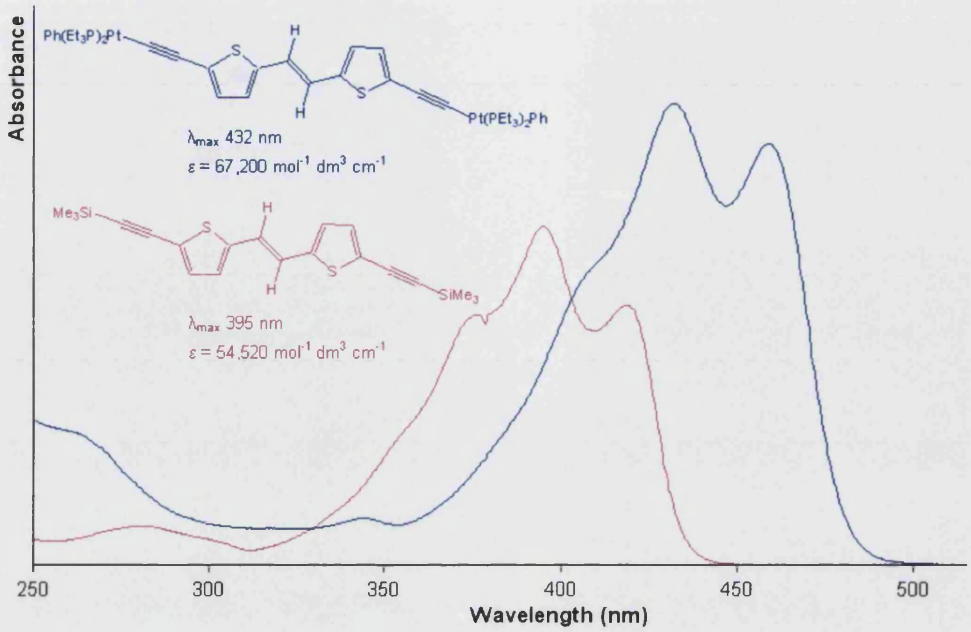

Figure 4.22: Absorption spectra of 4.02 and 4.23 (CH_2Cl_2, room temperature)

The electronic absorption spectrum of **4.23** exhibits three bands with a maximum at 432 nm (ε = 67,200 mol^{-1} dm^3 cm^{-1}). As expected, when the spectrum is compared with that of **4.02** (Figure 4.22), there is a red shift on addition of the platinum phosphine units consistent with an increase in conjugation across the length of the molecule through the metal centres. The emission spectrum of **4.23** is an approximate mirror image of the lowest energy absorption bands.

Attempts to grow single crystals of **4.23** for structure determination from a range of solvents were unsuccessful.

The gold(I) alkynyl complex, 1,2-bis(5'-goldtriethylphosphineethynyl-2'-thienyl)ethene **4.24** was prepared by the method previously described in Chapter 2 involving reaction of **4.02** with $Au(PPh_3)Cl$ in a methanol solution of sodium methoxide.

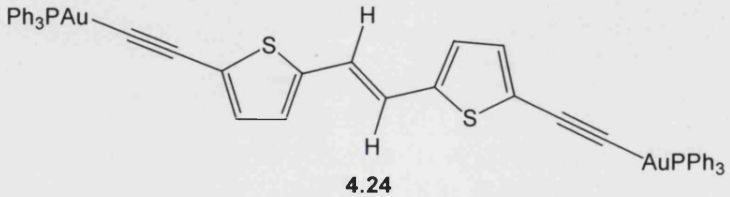

4.24

The ^{1}H NMR spectrum of **4.24** exhibits the expected doublet, singlet, doublet arrangement for the dithienylethene group within the ligand. There is also a set of multiplets centred at 7.5 ppm which corresponds to the thirty protons of the phosphine groups. Ten resonances are observed in the $^{13}C\{^{1}H\}$ NMR spectrum with the quaternary alkyne carbon bonded to the gold atom absent. A singlet is seen in the $^{31}P\{^{1}H\}$ NMR spectrum at 42.30 ppm which is shifted from 33.35 ppm for $Au(PPh_3)Cl$ and suggests that the two phosphorus nuclei are equivalent.

As with **4.23**, in the IR spectrum the $\nu(C{\equiv}C)$ stretching frequency is at a lower frequency, 2090 cm^{-1}, due to the addition of the heavy transition metal atom. The absorption spectrum of **4.24** has a similar profile to that of **4.02** suggesting that the bands arise from ligand $\pi - \pi^*$ transitions with vibrational spacings of ~1400 cm^{-1} typical of a $\nu(C{=}C)$ stretch. As expected there is a red shift on coordination to the gold fragment consistent with the conjugation length across the molecule being extended through the metal centre. This is also reflected in the position of the onset of absorption, which occurs at a longer wavelength and therefore is indicative of a smaller optical gap of 2.63 eV (*cf.* 2.79 eV for **4.02**).

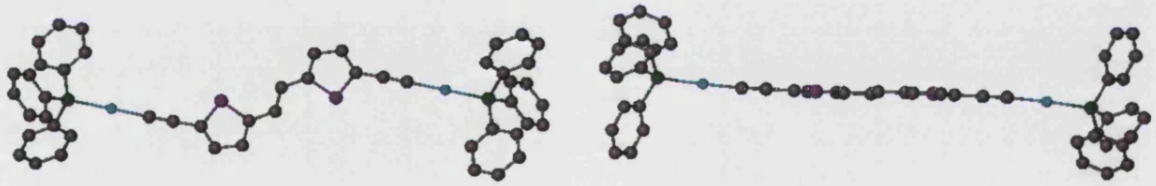

Figure 4.23: Structure of 4.24 (hydrogens omitted for clarity).

Two views of the structure of **4.24** are depicted in Figure 4.23, where the asymmetric unit of the cell consists of half of the molecule ($Ph_3PAuC{\equiv}C\text{-}C_4H_2S\text{-}CH\text{-}$); the two halves being related by a centre of symmetry. The structure has the thiophene rings in a planar arrangement [torsion angle C(24)–C(25)–C25#–C24#, 180°] with the phosphine phenyl rings in an eclipsed geometry. Table 4.6 lists selected bond lengths and angles for **4.24**.

Contact	Bond Length (Å)	Contact	Bond Angle (°)
Au–C(19)	1.978(8)	C(19)–Au–P	177.5(2)
Au–P	2.2770(17)	C(20)–C(19)–Au	176.4(7)
C(19)–C(20)	1.223(11)	C(21)–C(20)–C(19)	178.4(8)
C(20)–C(21)	1.425(10)	C(22)–C(21)–S	110.9(5)
C(21)–C(22)	1.341(11)	C(20)–C(21)–S	119.9(5)
C(22)–C(23)	1.425(10)	C(21)–C(22)–C(23)	113.5(7)
C(23)–C(24)	1.371(11)	C(23)–C(24)–C(25)	126.8(7)
C(24)–C(25)	1.455(9)	C(23)–C(24)–S	110.2(5)
C(25)–C(25)#	1.320(14)	C(25)–C(24)–S	123.0(6)
S–C(21)	1.735(6)	C(24)–S–C(21)	92.3(4)
S–C(24)	1.726(7)	C(25)#–C(25)–C(24)	125.6(9)

Table 4.6: Selected bond lengths and angles for 4.24

The bond lengths and angles found in the thiophene rings of **4.24** are consistent with those found in the literature[48] and those of the alkene unit linking them are in a similar range to the bond lengths and angles reported for the aforementioned ruthenium complexes.[44] The gold alkyne unit is approximately linear [C(19)–Au–P, 177.5(2)°; C(20)–C(19)–Au, 176.4(7)°; C(21)–C(20)–C(19), 178.4(8)°] as would be expected for a gold(I) centre.

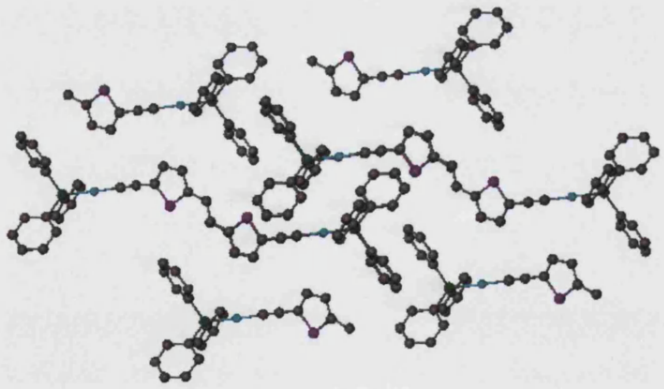

Figure 4.24: Packing diagram of 4.24

Figure 4.24 illustrates how the molecules align in a herring bone pattern in the solid state with π--π stacking between phenyl rings in adjacent molecules. The shortest Au····Au distance between neighbouring molecules (centre of Figure) is 5.337Å, which is too long for an aurophilic interaction to be present as these occur in the range of 2.75 – 3.40 Å.[49]

2,7-Bis(triphenylphosphinegoldethynyl)-3,6-dithia-*as*-indacene **4.25**, the analogous cyclised compound to **4.24**, was prepared in the same manner from **4.17**. There are two singlets observed in the ^{1}H NMR spectrum of **4.25** corresponding to the four protons on the indacene ring, due to the symmetry of the molecule, along with a set of multiplets (7.59 – 7.44 ppm) indicating the presence of the two triphenylphosphine groups.

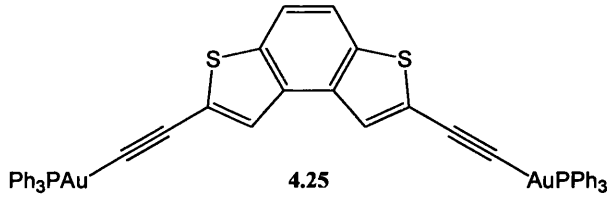

4.25

The $^{13}C\{^1H\}$ NMR spectrum exhibits the expected carbon resonances with the exception of the alkyne quaternary carbons and a singlet is observed in the $^{31}P\{^1H\}$ NMR spectrum at 42.23 ppm. The stretching frequency of the ν(C≡C) stretch is lowered from 2151 cm^{-1} in the trimethylsilyl protected ligand to 2100 cm^{-1} on coordination of the gold phosphine groups.

As with **4.24**, the absorption spectrum of **4.25** shows the strong dependence of ligand centred π–π* transitions from the similar shape and vibrational spacings (~1400 – 1500 cm^{-1}) typical of ν(C=C) stretches. The λ_{max} is observed at 353 nm (ε = 64,200 mol^{-1} dm^3 cm^{-1}) which is red shifted from that of the corresponding ligand **4.17**.

	Absorption λ (nm)* ($\varepsilon/10^4$ mol^{-1} dm^3 cm^{-1})	Emission λ (nm) (excited at λ_{max})	Optical gap (eV)
4.02	281(6.3), 376 sh(4.0), 395(5.5), 419(4.21)	459, 435 sh	2.79
4.17	277(1.7), 295(1.4), 307(2.2), 321(3.5), 336(5.2), 354 (4.1)	363sh, 380, 399sh	3.34
4.24	320(8.4), 392 sh(4.4), 415 (6.5), 441(5.1)	456, 485 sh	2.63
4.25	289(1.7), 304(1.7), 316(2.6), 337(3.9), 353(6.4), 372 (6.2)	378sh, 398, 421sh	3.13

Table 4.7: Absorption and Emission data for $Me_3SiC{\equiv}C\text{-}R\text{-}C{\equiv}CSiMe_3$ and $Ph_3PAuC{\equiv}C\text{-}R\text{-}C{\equiv}CAuPPh_3$ (*CH_2Cl_2, room temperature)

Table 4.7 lists absorption and emission data for $Me_3SiC{\equiv}C\text{-}R\text{-}C{\equiv}CSiMe_3$ compounds **4.02** and **4.17** and $Ph_3PAuC{\equiv}C\text{-}R\text{-}C{\equiv}CAuPPh_3$ compounds **4.24** and **4.25** where R = C_4H_2S-CH=CH-C_4H_2S and $C_{10}H_4S_2$ respectively in each case.

In both series there is a red shift on coordination of the gold phosphine unit again consistent with the conjugation length increasing across the molecule. The cyclic systems are noticeably blue shifted from their unfused analogues by *ca.* 40 nm (30 eV) and this has been observed in the spectra of other fused and unfused thiophene based digold alkynyl complexes reported by Raithby and Khan.[35] As expected the emission spectra are approximate mirror images of the lowest energy absorption bands in each case.

The increase in optical gap on going from **4.02** → **4.17** and from **4.24** → **4.25** is in agreement with expectation due to the cyclised molecules containing a reduced number of 'formal' double bonds as previously discussed. Also the decrease in optical gap on coordination of the gold phosphine suggests the extension of conjugation length across the molecule through the metal centres.

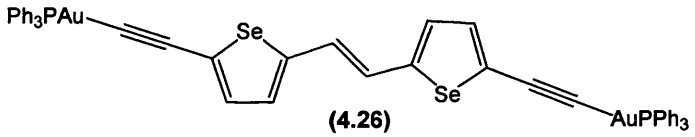

(4.26)

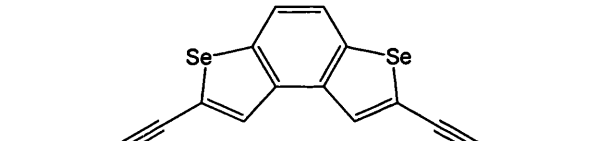

(4.27)

Attempts to prepare the selenium analogues of these gold(I) alkynyl phosphines, 1,2-bis(5'-triphenylphosphinegoldethynyl-2'-selenyl)ethene **4.26** and 2,7-bis(triphenylphosphinegold ethynyl)-3,6-diselena-*as*-indacene **4.27** met with difficulties. The preparation of **4.27** was unsuccessful largely due to solubility problems with the trimethylsilyl protected ligand.

However, reaction of triphenylphosphinegold(I) chloride with **4.06** in a methanol solution of sodium methoxide gave **4.26** as a yellow/orange solid. The ^{1}H NMR spectrum of the unpurified product showed the two doublets and singlet arising from the diselenylethene spacer and a multiplet for the phenyl protons of the triphenyl phosphine groups. A singlet at 42.35 ppm was observed in the $^{31}P\{^{1}H\}$ NMR spectrum along with a small signal at 33.35 ppm assigned to unreacted $Au(PPh_3)Cl$.

Recrystallisation of the solid from methanol/ chloroform gave yellow crystals from which an unexpected structure was determined indicating the yellow crystals are $Ph_3PAuSeH$. The structure consists of a two coordinate gold atom with a triphenylphosphine unit and a selenium atom, which most likely has a hydrogen atom bonded to it in an approximately linear geometry.

An explanation for the formation of this structure could be that the ligand decomposed during recrystallisation and the ejected selenium was scavenged by the gold(I) phosphine. $^1H/^{31}P\{^1H\}$ NMR spectra of the crystals in deuterated chloroform exhibit only the multiplet for the phosphine group protons and a singlet at 33.35 ppm respectively suggesting $Au(PPh_3)Cl$ is reformed in chlorinated solvent.

4.3 Conclusions

In summary, a series of novel heteroaromatic alkynyl ligands have been prepared through a four step synthesis gradually building up the chromophore in the molecule. The optical properties have been studied by solution UV/visible absorption and emission spectroscopies. In the case of each of the non-cyclic ligands, **4.02, 4.06** and **4.08,** and the cyclic ligands, **4.17, 4.18** and **4.19**, the absorption spectra after each synthetic step show a red shift consistent with the increase of conjugation length across the molecule. The absorption spectra of the cyclic ligands show a blue shift in comparison to their non-cyclic analogues due to a reduction in the number of 'formal' double bonds shortening the conjugation length in the molecules.

The replacement of the sulphur with selenium lowers the observed optical gap of these materials due to a lowering of the energy of the LUMO while the energy level of the HOMO is relatively unaffected. This is reflected in the red shift observed on comparison of the absorption spectra in the order of **4.02** → **4.06** → **4.08**.

The dialkynyl gold(I) phosphine complexes **4.24** and **4.25** were readily prepared from their corresponding trimethylsilyl-protected ligands **4.02** and **4.17** respectively. As expected, the absorption spectra show a red shift on coordination of the gold phosphine units consistent with an extension of the conjugation length of the molecule through the metal centres. The general shape of the spectra for the metal complexes are similar to those of the ligands, suggesting the absorption is dominated by intraligand π–π^* transitions.

4.4 References

1. Lin, J. W. P.; Dudek, L. P., *J. Polym. Sci. Pol. Chem.,* 1980, **18**, 2869-2873.
2. Yamamoto, T.; Sanechika, K.; Yamamoto, A., *J. Polym. Sci. C Polym. Lett.,* 1980, **18**, 9-12.
3. Roncali, J., *Chem. Rev.,* 1997, **97**, 173 - 205.
4. McCullough, R. D., *Adv. Mater.,* 1998, **10**, 93 - 116.
5. Nakayama, J.; Fujimori, T., *Heterocycles,* 1991, **32**, 991-1002.
6. McMurry, J. E.; Fleming, M. P., *J. Am. Chem. Soc.,* 1974, **96**, 4708-4709.
7. Horner, L.; Hoffmann, H. M. R.; Wippel, H. G.; Klahre, G., *Chem. Ber.,* 1959, **92**, 2499-2505.
8. Wadsworth, W. S.; Emmons, W. D., *J. Am. Chem. Soc.,* 1961, **83**, 1733-1738.
9. Ozturk, T.; Ertas, E.; Mert, O., *Tetrahedron,* 2005, **61**, 11055-11077.
10. Litvinov, V., *Adv. Heterocycl. Chem.,* 2006, **90**, 125-203.
11. Kellogg, R. M.; Groen, M. B.; Wynberg, H., *J. Org. Chem.,* 1967, **32**, 3093 - 3100.
12. Mallory, F. B.; Wood, C. S.; Gorden, J. T.; Lindquist, L. C.; Savitz, M. L., *J. Am. Chem. Soc.,* 1962, **84**, 4361-4362.
13. Mallory, F. B.; Wood, C. S.; Gordon, J. T., *J. Am. Chem. Soc.,* 1963, **85**, 828 - 829.
14. Mallory, F. B.; Wood, C. S.; Gordon, J. T., *J. Am. Chem. Soc.,* 1964, **86**, 3094 - 3102.
15. Wittig, G.; Geissler, G., *Justus Liebigs Ann. Chem.,* 1953, **580**, 44-57.
16. Wittig, G.; Schöllkopf, U., *Chem. Ber.,* 1954, **87**, 1318-1330.
17. Groen, M. B.; Schadenb.H; Wynberg, H., *J. Org. Chem.,* 1971, **36**, 2797-2809.
18. Tanaka, K.; Osuga, H.; Suzuki, H.; Shogase, Y.; Kitahara, Y., *J. Chem. Soc. Perkin Trans. 1,* 1998, 935-940.
19. Larsen, J.; Bechgaard, K., *Acta Chem. Scand.,* 1996, **50**, 71-76.
20. Tanaka, K.; Shogase, Y.; Osuga, H.; Suzuki, H.; Nakamura, K., *Tetrahedron Lett.,* 1995, **36**, 1675-1678.
21. Tanaka, K.; Suzuki, H.; Osuga, H., *J. Org. Chem.,* 1997, **62**, 4465-4470.
22. Tanaka, K.; Osuga, H.; Kitahara, Y., *J. Org. Chem.,* 2002, **67**, 1795-1801.
23. Caronna, T.; Sinisi, R.; Catellani, M.; Malpezzi, L.; Meille, S. V.; Mele, A., *Chem. Commun.,* 2000, 1139-1140.
24. Caronna, T.; Sinisi, R.; Catellani, M.; Luzzati, S.; Abbate, S.; Longhi, G., *Synth. Met.,* 2001, **119**, 79-80.

25. Maiorana, S.; Papagni, A.; Licandro, E.; Annunziata, R.; Paravidino, P.; Perdicchia, D.; Giannini, C.; Bencini, M.; Clays, K.; Persoons, A., *Tetrahedron,* 2003, **59**, 6481-6488.

26. Tanaka, K.; Osuga, H.; Tsujiuchi, N.; Hisamato, M.; Sakaki, Y., *Bull. Chem. Soc. Jpn.,* 2002, **75**, 551-557.

27. Laquindanum, J. G.; Katz, H. E.; Lovinger, A. J.; Dodabalapur, A., *Adv. Mater.,* 1997, **9**, 36-&.

28. Akimoto, I.; Kan'no, K. I.; Osuga, H.; Tanaka, K., *J. Luminescence,* 2005, **112**, 341-344.

29. Gronowitz, S.; Dahlgren, T., *Chem. Script.,* 1977, **12**, 57-67.

30. Blackburn, E. V.; Timmons, C. J.; Cholerton, T. J., *J. Chem. Soc. Perkin Trans. 2,* 1972, 101-103.

31. Khan, M. S.; Kakkar, A. K.; Long, N. J.; Lewis, J.; Raithby, P.; Nguyen, P.; Marder, T. B.; Wittmann, F.; Friend, R. H., *J. Mater. Chem.,* 1994, **4**, 1227-1232.

32. Beljonne, D.; Wittmann, H. F.; Kohler, A.; Graham, S.; Younus, M.; Lewis, J.; Raithby, P. R.; Khan, M. S.; Friend, R. H.; Bredas, J. L., *J. Chem. Phys.,* 1996, **105**, 3868-3877.

33. Lhost, O.; Toussaint, J. M.; Bredas, J. L.; Wittmann, F. H.; Fuhrmann, K.; Friend, R. H.; Khan, M. S.; Lewis, J., *Synth. Met.,* 1993, **55–57**, 4525–4530.

34. Chawdhury, N.; Kohler, A.; Friend, R. H.; Wong, W. Y.; Lewis, J.; Younus, M.; Raithby, P. R.; Corcoran, T. C.; Al-Mandhary, M. R. A.; Khan, M. S., *J. Chem. Phys.,* 1999, **110**, 4963-4970.

35. Li, P.; Ahrens, B.; Feeder, N.; Raithby, P. R.; Teat, S. J.; Khan, M. S., *Dalton Trans.,* 2005, 874-883.

36. Li, P. Y.; Ahrens, B.; Choi, K. H.; Khan, M. S.; Raithby, P. R.; Wilson, P. J.; Wong, W. Y., *Cryst. Eng. Comm.,* 2002, 405-412.

37. Starcevic, K.; Boykin, D. W.; Karminski-Zamola, G., *Heteroatom Chem.,* 2003, **14**, 218-222.

38. Bouachrine, M.; Lere-Porte, J. P.; Moreau, J. J. E.; Torreilles, C., *J. Chim. Phys. - Chim. Biol.,* 1998, **95**, 1176-1179.

39. Antonov, D. N.; Belenkii, L. I.; Gronowitz, S., *J. Heterocyclic Chem.,* 1995, **32**, 53-55.

40. Yur'ev, Y. K.; Ekkhardt, D., *Zh. Obshch. Khim.,* 1961, **31**, 3298 - 3300.

41. Williams, D. H.; Fleming, I. *Spectroscopic Methods in Organic Chemistry*, 5th ed.; McGraw-Hill: London, 1997.

42. Gronowitz, S.; Dahlgren, T., *Chem. Script.,* 1977, **12**, 97-101.

43. Yoshida, S.; Fujii, M.; Aso, Y.; Otsubo, T.; Ogura, F., *J. Org. Chem.,* 1994, **59**, 3077-3081.

44. Wu, I. Y.; Lin, J. T.; Luo, J.; Li, C. S.; Tsai, C.; Wen, Y. S.; Hsu, C. C.; Yeh, F. F.; Liou, S., *Organometallics,* 1998, **17**, 2188-2198.

45. Migalska-Zalas, A.; Sofiani, Z.; Sahraoui, B.; Kityk, I. V.; Tkaczyk, S.; Yuvshenko, V.; Fillaut, J. L.; Perruchon, J.; Muller, T. J. J., *J. Phys. Chem. B,* 2004, **108**, 14942-14947.

46. Fillaut, J. L.; Perruchon, J.; Blanchard, P.; Roncali, J.; Golhen, S.; Allain, M.; Migalsaka-Zalas, A.; Kityk, I. V.; Sahraoui, B., *Organometallics,* 2005, **24**, 687-695.

47. Sonogashira, K.; Yatake, T.; Tohda, Y.; Takahashi, S.; Hagihara, N., *J.C.S. Chem. Comm.,* 1977, 291 - 292.

48. Marino, G., *Adv. Heterocycl. Chem.,* 1971, **13**, 235-314.

49. Li, J.; Pyykko, P., *Chem. Phys. Lett.,* 1992, **197**, 586-590.

Chapter 5 Experimental

5.1 General

All air-sensitive reactions were carried out under dinitrogen or argon atmospheres using either standard Schlenk line or dry box techniques.[1] Dichloromethane and tetrahydrofuran were dried and degassed under an argon atmosphere over activated alumina columns using an Innovative Technology Solvent Purification System (SPS) and degassed using argon prior to use in air sensitive reactions. All secondary and tertiary amines were purified by distillation using calcium hydride as a drying agent and stored under argon in Young's ampoules over 4 Å molecular sieves.

NMR spectra were recorded on Bruker AV300 or AVANCE 400 spectrometers at 298 K unless otherwise stated. ^{1}H NMR spectra were referenced internally to residual protio-solvent ($CHCl_3$ at 7.26 ppm) and ^{13}C NMR spectra referenced to deuterio-solvent resonance ($CDCl_3$ at 77.0 ppm). ^{31}P NMR spectra were referenced to 85% H_3PO_4 (0.00 ppm), ^{77}Se NMR spectra to selenophene (605.0 ppm), ^{125}Te NMR spectra to tellurophene (776.6 ppm) and ^{195}Pt NMR spectra to K_2PtCl_4 in D_2O (-1607 ppm). Assignments were supported by ^{13}C PENDANT NMR and homo- and hetero-nuclear, one- and two-dimensional experiments as appropriate.

Electronic absorption spectra were recorded using a Perkin Elmer Lambda 650 UV/Visible spectrophotometer in dichloromethane over the range 900 – 200 nm. Samples were prepared in "Grade A" volumetric glassware and analysed in 1.0 cm path length quartz cells at 200 nm/min band pass rate, and spectra recorded as an average of three scans. Emission spectra were recorded using a Perkin Elmer LS55 Luminescence spectrometer, in dichloromethane, by excitation at λ_{max}. Samples were analysed in 1.0 cm path length quartz cells using a 10.0 nm excitation slit width and 240 nm/min band pass rate.

IR spectra were recorded on a Nicolet – Nexus FTIR spectrometer, over the range 4000 – 200 cm^{-1} and averaged over 32 scans, using KBr discs. Elemental analyses were carried out in house using an Exeter Analytical CE 440 elemental analyser.

Bis(tetrahydrofuran)titanium(IV) chloride,[2] 1,2-bis(2'-thienyl)ethene[3], 5-bromo-2-thiophene carbaldehyde[4] and 2,7-diiodo-3,6-dithia-as-indacene[5] were prepared according to literature methods. Some compounds used have been previously reported in the literature, but without their full characterisation being reported.

5.1.1 Preparation of Triethylphosphinegold(I) chloride

Triethylphosphinegold(I) chloride was prepared by adapting a literature procedure.[6] An aqueous solution (10 mL) of hydrogen tetrachloroaurate(III) hydrate (0.64 mmol) was cooled to 0 °C. Triethylphosphine (1 eq) was added dropwise affording a yellow precipitate. The mixture was stirred at 0 °C for one hour affording a white precipitate. The solid was filtered off, washed with water and dried giving a pale grey solid which was recrystallised from methanol to give a white solid in 80% yield.

5.1.2 Synthesis of $Me_3SiC{\equiv}CR$ ligands

Although preparations and characterisations for $Me_3SiC{\equiv}CR$ ligands (where R = 2-C_5H_4N,[7] 3-C_5H_4N,[8] 2-C_4H_3S,[9] 2-$C_6H_4NO_2$,[10] 3-$C_6H_4NO_2$,[11] 4-$C_6H_4NO_2$,[10] 2-C_6H_4CN,[12] 3-C_6H_4CN,[8] 4-C_6H_4CN,[8] 2-C_6H_4OMe,[13] 3-C_6H_4OMe,[13] 4-C_6H_4OMe,[13] 5-$C_4H_3N_2$,[14] (C_6H_4)-$C{\equiv}CSiMe_3$,[15] $(C_6H_4)_2$-$C{\equiv}CSiMe_3$,[10] $C_{14}H_9$,[16] $C_{14}H_8$-$(C{\equiv}CSiMe_3)_2$[16]) have been previously reported, all alkyne and trimethylsilyl protected alkyne ligands were prepared for use from their corresponding bromides following General Procedure A.

5.1.2.1 General Procedure A

Bis(triphenylphosphine)palladium(II) chloride (6 mol%), copper iodide (3 mol%) and the aryl bromide (0.5 g) were placed in a Young's ampoule and dissolved in tetrahydrofuran (10 mL) and triethylamine (10 mL). Trimethylsilylacetylene (1.5 eq) was added and the resulting mixture left to stir overnight (~17 h) under an argon atmosphere at room temperature and in the absence of light. The progress of the reaction was monitored by TLC. On completion of the reaction, the volatiles were removed under reduced pressure. The product was partitioned between diethyl ether and $NaHCO_3$ solution, the aqueous layer removed and the ether solvent washed with water. The organic layer was dried ($MgSO_4$) and volatiles removed under reduced pressure. The resulting solid or oil was purified by column chromatography to afford the desired product.

The trimethylsilyl alkynyl ligands were deprotected to give the corresponding $HC{\equiv}CR$ alkynes by dissolving in methanol/dichloromethane (1:1, v/v, 10 mL) and adding aqueous 2M KOH solution (1.5 eq). The reaction mixture was stirred at room temperature and in the absence of light for several hours.

5.1.3 Preparation of PR_3AuCCR complexes

5.1.3.1 General Procedure B

Gold(I) phosphine chloride was added to a solution of sodium methoxide (1 mmol) in methanol (10 mL). The alkyne ligand (1.1 eq) was added to this mixture and the flask stoppered with a septum. The mixture was stirred overnight (~17 h) at room temperature and in the absence of light. On completion of the reaction, the solvent was then removed under reduced pressure. The resulting solid was washed with water (3 × 10 mL) and dried ($MgSO_4$). Recrystallisation was achieved using methanol or ethanol.

5.1.4 Preparation of phosphonium salts

Triphenyl-thiophen-2-ylmethyl-phosphonium chloride and (5-bromo-thiophen-2-ylmethyl) triphenylphosphonium chloride were prepared by treatment of the methyl alcohols (R-C_4H_2S)-2-CH_2OH (R = H; Br) with thionyl chloride in the presence of anhydrous ether and pyridine, followed by quenching the mixture with saturated aqueous potassium hydroxide and extraction with ether to afford the corresponding 2-chloromethylthiophenes.[17] As the chloromethylthiophenes are prone to polymerisation it was necessary to add toluene (5ml) to the ether extract and selectively remove the ether under reduced pressure leaving the compound in toluene ready for immediate conversion to the phosphonium salt by reaction with triphenylphosphine in refluxing toluene.[18]

5.2 Experimental for Chapter 2

5.2.1 Preparation of 3-(triethylphosphinegoldethynyl)pyridine (2.01)

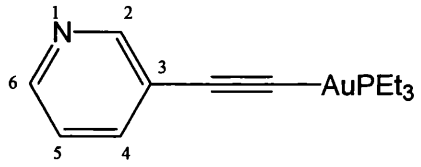

General Procedure B; Triethylphosphinegold(I) chloride (150 mg, 0.429 mmol) and 3-ethynylpyridine (50.6 mg, 0.489 mmol). Recrystallisation from methanol afforded **2.01** as yellow crystals (25.4 mg, 14%).

^{1}H NMR:

8.64	dd, 1H, ^4J 2.2 Hz, ^4J 1.0 Hz	2-Ar*H*
8.33	dd, 1H, ^3J 4.9 Hz, ^3J 1.8 Hz	5-Ar*H*
7.66	ddd, 1H, ^3J 7.8 Hz, ^4J 2.2 Hz, ^3J 1.8 Hz	4-Ar*H*

7.10	ddd, 1H, ^3J 7.8 Hz, ^3J 4.9 Hz, ^4J 1.0 Hz	6-Ar*H*
1.80 – 1.72	m, 6H	$P(CH_2CH_3)_3$
1.19 – 1.10	m, 9H	$P(CH_2CH_3)_3$

$^{13}C\{^1H\}$ NMR:

152.9	CH	2-Ar*C*H	122.2	C_{ipso}	*C*–C≡C–Au
149.3	CH	6-Ar*C*H	100.1	C_{quat}	C≡*C*–Au
139.1	CH	4-Ar*C*H	17.69	CH_2	d, $^1J_{PC}$ 33.1 Hz P(*C*$H_2$$CH_3$)$_3$
122.9	CH	5-Ar*C*H	8.805	CH_3	$P(CH_2CH_3)_3$

$^{31}P\{^1H\}$ NMR: 38.07

UV/Vis (CH_2Cl_2) $\underline{\lambda_{max}}$ [nm] (ε, mol^{-1} dm^3 cm^{-1}):

255 sh (9,040), <u>268</u> (14,340), 280 (13,140), 288 sh (11,140).

Emission (CH_2Cl_2): 454 nm

IR (KBr Disc): 2105 cm^{-1} ν(C≡C)

Elemental Analysis:

Calcd for $C_{13}H_{19}AuNP$ (%): C 37.42; H 4.59; N 3.36. Found (%): C 37.20; H 4.61; N 3.25.

5.2.2 Preparation of 2-(triethylphosphinegoldethynyl)pyridine (2.02)

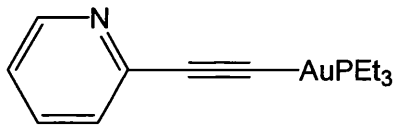

General Procedure B; Triethylphosphinegold(I) chloride (150 mg, 0.429 mmol) and 2-ethynylpyridine (50.4 mg, 0.489 mmol). Recrystallisation from ethyl acetate afforded **2.02** as pale brown crystals (89.7 mg, 50%).

^1H NMR:

8.49	ddd, 1H, ^3J 4.9 Hz, ^4J 2.0 Hz, ^5J 1.0 Hz	6-Ar*H*
7.52	ddd, 1H, ^3J 7.8 Hz, ^3J 7.6 Hz, ^4J 2.0 Hz	4-Ar*H*
7.39	ddd, 1H, ^3J 7.8 Hz, ^4J 1.2 Hz, ^5J 1.0 Hz	3-Ar*H*
7.07	ddd, 1H, ^3J 7.6 Hz, ^3J 4.9 Hz, ^4J 1.2 Hz	5-Ar*H*

1.85 – 1.77	m, 6H	$P(CH_2CH_3)_3$
1.26 – 1.17	m, 9H	$P(CH_2CH_3)_3$

$^{13}C\{^1H\}$ NMR:

149.5	CH	6-Ar*C*H	103.1	C_{ipso}	C≡*C*–Au
144.7	C_{ipso}	*C*–C≡C–Au	102.9	C_{ipso}	*C*≡C–Au
135.5	CH	4-Ar*C*H	17.86	CH_2	d, $^1J_{PC}$ 33.1 Hz $P(CH_2CH_3)_3$
126.9	CH	3-Ar*C*H	8.890	CH_3	$P(CH_2CH_3)_3$
121.2	CH	5-Ar*C*H			

$^{31}P\{^1H\}$ NMR: 38.18

UV/Vis (CH_2Cl_2) λ_{max} [nm] (ε, mol^{-1} dm^3 cm^{-1}):

255 (11,700), 265 (16,420), 289 (16,760), 297 (15,800).

Emission (CH_2Cl_2): 445 nm

IR (KBr Disc): 2106 cm^{-1} ν(C≡C)

Elemental Analysis:

Calcd for $C_{13}H_{19}AuNP$ (%): C 37.42; H 4.59; N 3.36. Found (%): C 36.90; H 4.76; N 3.24.

5.2.3 Preparation of (triethylphosphinegold)phenyl acetylide (2.03)

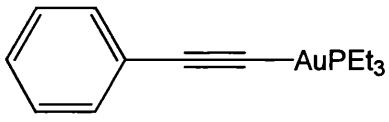

General Procedure B; Triethylphosphinegold(I) chloride (150 mg, 0.429 mmol) and phenylacetylene (0.10 mL, 0.489 mmol). Recrystallisation from ethyl acetate afforded **2.03** as pale yellow crystals (70.3 mg, 39%).

^1H NMR:

7.47	m, 2H	*o*-Ar*H*	Phenyl ring
7.20	m, 3H	m- & p-Ar*H*	Phenyl ring
1.84 – 1.76	m, 6H	$P(CH_2CH_3)_3$	

1.24 – 1.16	m, 9H	$P(CH_2CH_3)_3$

$^{13}C\{^1H\}$ NMR:

132.3	CH	o-Ar*C*H	103.9	C_{quat}	*C*≡C–Au
127.9	CH	p-Ar*C*H	17.81	CH_2	d, $^1J_{PC}$ 33.1 Hz $P(CH_2CH_3)_3$
126.6	CH	m-Ar*C*H	8.836	CH_3	$P(CH_2CH_3)_3$
124.9	C_{ipso}	*C*–C≡C–Au			

$^{31}P\{^1H\}$ NMR: 38.21

UV/Vis (CH_2Cl_2) λ_{max} [nm] (ε, mol^{-1} dm^3 cm^{-1}):

255 sh (12,980), 267 (24,940), 281 (26,140).

Emission (CH_2Cl_2): 421 nm

IR (KBr Disc): 2102 cm^{-1} ν(C≡C)

Elemental Analysis:

Calcd for $C_{14}H_{20}AuP$ (%): C 40.40; H 4.84. Found (%): C 40.40; H 4.79.

5.2.4 Preparation of 1-(triethylphosphinegoldethynyl)-4-nitrobenzene (2.04)

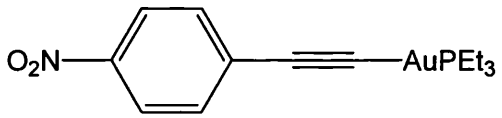

General Procedure B; Triethylphosphinegold(I) chloride (151 mg, 0.429 mmol) and 1-ethynyl-4-nitrobenzene (71.8 mg, 0.489 mmol). Recrystallisation from ethanol afforded **2.04** as orange crystals (86.0 mg, 43%).

^1H NMR:

8.09	d, 2H, ^3J 8.8 Hz	3- & 3'-Ar*H*
7.55	d, 2H, ^3J 8.8 Hz	2- & 2'-Ar*H*
1.87 – 1.79	m, 6H	$P(CH_2CH_3)_3$
1.26 – 1.17	m, 9H	$P(CH_2CH_3)_3$

$^{13}C\{^1H\}$ NMR:

145.8	C_{ipso}	*C*–NO_2	102.3	C_{quat}	*C*≡C–Au	
132.7	CH	2- & 2'-Ar*C*H	17.78	CH_2	d, $^1J_{PC}$ 33.1 Hz	P(*C*$H_2$$CH_3$)$_3$
132.4	C_{ipso}	*C*–C≡C–Au	8.882	CH_3	P(CH_2*C*H_3)$_3$	
123.4	CH	3- & 3'-Ar*C*H				

$^{31}P\{^1H\}$ NMR: 38.13

UV/Vis (CH_2Cl_2) λ_{max} [nm] (ε, mol^{-1} dm^3 cm^{-1}):

337 (21,060)

Emission (CH_2Cl_2): 446 nm

IR (KBr Disc): 2108 cm^{-1} ν(C≡C), 1589 cm^{-1} ν(N=O), 1343 cm^{-1} ν(N=O)

Elemental Analysis:

Calcd for $C_{14}H_{19}AuNO_2P$ (%): C 36.46; H 4.15; N 3.04. Found (%): C 36.50; H 4.30; N 2.95.

5.2.5 Preparation of 1-(triethylphosphinegoldethynyl)-3-nitrobenzene (2.05)

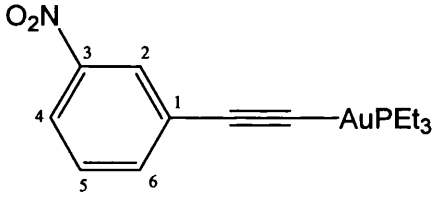

General Procedure B; Triethylphosphinegold(I) chloride (142 mg, 0.406 mmol) and 1-ethynyl-3-nitrobenzene (66 mg, 0.446 mmol). Recrystallisation from ethanol afforded **2.05** as orange crystals (80.5 mg, 43%).

^1H NMR:

8.31	dd, 1H, ^4J 2.4 Hz, ^4J 1.6 Hz	2-Ar*H*
8.03	ddd, 1H, ^3J 8.4 Hz, ^4J 2.4 Hz, ^4J 1.2 Hz	4-Ar*H*
7.74	ddd, 1H, ^3J 8.0 Hz, ^4J 1.6 Hz, ^4J 1.2 Hz	6-Ar*H*
7.39	dd, 1H, ^3J 8.4Hz, ^3J 8.0 Hz	5-Ar*H*
1.88 – 1.80	m, 6H	P(C*H*$_2$$CH_3$)$_3$
1.27 – 1.19	m, 9H	P(CH_2C*H*$_3$)$_3$

$^{13}C\{^1H\}$ NMR:

137.9	CH	6-Ar*C*H	121.3	CH	4-Ar*C*H
128.8	CH	5-Ar*C*H	17.82	CH_2	d, $^1J_{PC}$ 33.1 Hz $P(CH_2CH_3)_3$
127.1	CH	2-Ar*C*H	8.909	CH_3	$P(CH_2CH_3)_3$

$^{31}P\{^1H\}$ NMR: 38.14

UV/Vis (CH_2Cl_2) λ_{max} [nm] (ε, mol^{-1} dm^3 cm^{-1}):

255 sh (19,020), 266 (28,440), 281 (27,800).

IR (KBr Disc): 2104 cm^{-1} ν(C≡C), 1521 cm^{-1} ν(N=O), 1350 cm^{-1} ν(N=O)

Elemental Analysis:

Calcd for $C_{14}H_{19}AuNO_2P$ (%): C 36.46; H 4.15; N 3.04. Found (%): C 36.40; H 4.21; N 2.92.

5.2.6 Preparation of 1-(triethylphosphinegoldethynyl)-2-nitrobenzene (2.06)

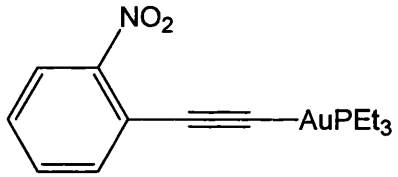

General Procedure B; Triethylphosphinegold(I) chloride (150 mg, 0.429 mmol) and 1-(trimethylsilylethynyl)-2-nitrobenzene (107 mg, 0.471 mmol). Recrystallisation from ethanol afforded **2.06** as yellow crystals (13.7 mg, 7%).

^1H NMR:

7.92	d, 1H, ^3J 8.2 Hz	3-ArH
7.68	d, 1H, ^3J 7.8 Hz	6-ArH
7.45	t, 1H, ^3J 7.8 Hz	5-ArH
7.29	d, 1H, ^3J 8.2 Hz	4-ArH
1.87 – 1.79	m, 6H	$P(CH_2CH_3)_3$
1.26 – 1.18	m, 9H	$P(CH_2CH_3)_3$

$^{13}C\{^1H\}$ NMR:

158.1	C_{ipso}	*C*–NO_2	124.2	CH	3-Ar*C*H

135.9	CH	5-Ar*C*H	17.60	CH_2	d, $^1J_{PC}$ 33.1 Hz	$P(CH_2CH_3)_3$
132.2	CH	6-Ar*C*H	8.845	CH_3	$P(CH_2CH_3)_3$	
126.6	CH	4-Ar*C*H				

$^{31}P\{^1H\}$ NMR: 37.46

UV/Vis (CH_2Cl_2) λ_{max} [nm] (ε, mol^{-1} dm^3 cm^{-1}):

259 (15,100), 279 (11,580), 348 (3,600).

Emission (CH_2Cl_2): 375 nm

IR (KBr Disc): 2108 cm^{-1} ν(C≡C), 1522 cm^{-1} ν(N=O), 1348 cm^{-1} ν(N=O)

5.2.7 Preparation of 1-(triphenylphosphinegoldethynyl)-3-nitrobenzene (2.07)

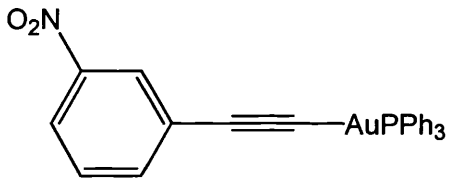

General Procedure B; Triphenylphosphinegold(I) chloride (100 mg, 0.202 mmol) and 1-(trimethylsilylethynyl)-3-nitrobenzene (51.2 mg, 0.222 mmol). Recrystallisation from ethanol/dichloromethane (1:1) afforded **2.07** as yellow crystals (36.2 mg, 30%).

^1H NMR:

8.34	dd, 1H, ^4J 2.4 Hz, ^4J 2.0 Hz	2-Ar*H*
8.04	ddd, 1H, ^3J 8.4Hz, ^4J 2.4 Hz, ^4J 1.2 Hz	4-Ar*H*
7.77	ddd, 1H, ^3J 8.0 Hz, ^4J 2.0 Hz, ^4J 1.2 Hz	6-Ar*H*
7.59 – 7.45	m, 15 H	$P(C_6H_5)_3$
7.40	dd, 1H, ^3J 8.4 Hz, ^3J 8.0 Hz	5-Ar*H*

$^{13}C\{^1H\}$ NMR:

148.1	C_{ipso}	*C*–NO_2		128.8	CH	5-Ar*C*H
137.9	CH	6-Ar*C*H		127.1	CH	2-Ar*C*H
136.7	C_{ipso}	*C*–$P(C_6H_5)_3$		126.8	C_{quat}	*C*–C≡C–$AuPPh_3$
134.3	CH	d, 13.8 Hz	$P(C_6H_5)_3$	121.4	CH	4-Ar*C*H
131.7	CH	d, 2.11 Hz	$P(C_6H_5)_3$	101.7	C_{quat}	*C*≡C–$AuPPh_3$

129.2	CH	d, 11.9 Hz	$P(C_6H_5)_3$	101.4	C_{quat}	$C{\equiv}C$–$AuPPh_3$

$^{31}P\{^1H\}$ NMR: 42.19

UV/Vis (CH_2Cl_2) $\underline{\lambda_{Max}}$ [nm] (ε, $mol^{-1}\ dm^3\ cm^{-1}$):

255 (30,360), <u>268</u> (39,140), 283 (36,740).

Emission (CH_2Cl_2): 298 nm

IR (KBr Disc): 2108 cm^{-1} ν(C≡C), 1521 cm^{-1} ν(N=O), 1346 cm^{-1} ν(N=O)

Elemental Analysis:

Calcd for $C_{26}H_{19}AuNO_2P$ (%): C 51.58; H 3.16; N 2.31. Found (%): C 51.50; H 3.21; N 2.63.

5.2.8 Preparation of 1-(triethylphosphinegoldethynyl)-4-benzonitrile (2.08)

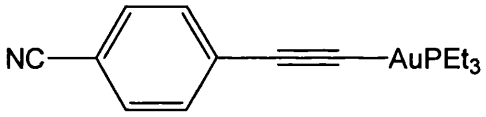

General Procedure B; Triethylphosphinegold(I) chloride (151 mg, 0.429 mmol) and 1-ethynyl-4-benzonitrile (62.8 mg, 0.489 mmol). Recrystallisation from methanol afforded **2.08** as yellow crystals (58.2 mg, 30%).

^1H NMR:

7.51	s, 4H	Ar*H*
1.87 – 1.79	m, 6H	$P(C\mathit{H}_2CH_3)_3$
1.26 – 1.18	m, 9H	$P(CH_2C\mathit{H}_3)_3$

$^{13}C\{^1H\}$ NMR:

132.7	CH	2-Ar*C*H	109.6	C_{ipso}	*C*–C≡N	
131.7	CH	3-Ar*C*H	102.4	C_{quat}	*C*≡C–Au	
130.2	C_{ipso}	*C*–C≡C–Au	17.81	CH_2	d, $^1J_{PC}$ 33.1 Hz	$P(\mathit{C}H_2CH_3)_3$
119.0	C_{quat}	*C*≡N	8.891	$\mathit{C}H_3$	$P(CH_2\mathit{C}H_3)_3$	

$^{31}P\{^1H\}$ NMR: 38.09

UV/Vis (CH_2Cl_2) λ_{max} [nm] (ε, mol^{-1} dm^3 cm^{-1}):

269 sh (12,980), 285 (30,180), 302 (40,600), 325 (5,700).

Emission (CH_2Cl_2): 460 nm

IR (KBr Disc): 2097 cm^{-1} ν(C≡C), 2226 cm^{-1} ν(C≡N)

Elemental Analysis:

Calcd for $C_{15}H_{19}AuNP$ (%): C 40.83; H 4.34; N 3.17. Found (%): C 40.70; H 4.37; N 3.08.

5.2.9 Preparation of 1-(triethylphosphinegoldethynyl)-3-benzonitrile (2.09)

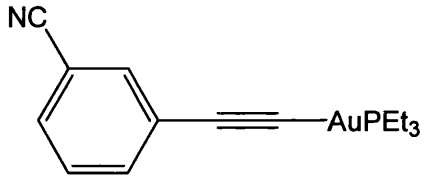

General Procedure B; Triethylphosphinegold(I) chloride (125 mg, 0.357 mmol) and 1-ethynyl-3-benzonitrile (50.0 mg, 0.393 mmol, 1.1 eq). Recrystallisation from ethanol afforded **2.09** as a yellow solid (16.9 mg, 11%).

^{1}H NMR:

7.66	dd, 1H, ^4J 2.2 Hz, ^4J 2.0 Hz	2-Ar*H*
7.60	ddd, 1H, ^3J 8.0 Hz, ^4J 2.0 Hz, ^4J 1.2 Hz	6-Ar*H*
7.39	ddd, 1H, ^3J 7.6 Hz, ^4J 2.2 Hz, ^4J 1.2 Hz	4-Ar*H*
7.28	dd, 1H, ^3J 8.0 Hz, ^3J 7.6 Hz	5-Ar*H*
1.80 – 1.72	m, 6H	$P(CH_2CH_3)_3$
1.12 – 1.11	m, 9H	$P(CH_2CH_3)_3$

^{13}C{^{1}H} NMR:

136.4	CH	6-Ar*C*H	118.6	C_{quat}	*C*≡N
135.6	CH	2-Ar*C*H	112.3	C_{ipso}	*C*–C≡N
129.8	CH	4-Ar*C*H	17.79	CH_2	d, $^1J_{PC}$ 33.1 Hz $P(CH_2CH_3)_3$
128.8	CH	5-Ar*C*H	8.884	CH_3	$P(CH_2CH_3)_3$
126.7	C_{ipso}	*C*–C≡C–Au			

$^{31}P\{^1H\}$ NMR: 38.12

UV/Vis (CH_2Cl_2) λ_{max} [nm] (ε, mol^{-1} dm^3 cm^{-1}):

268 (12,460), 281 (16,320), 310 (1,220).

Emission (CH_2Cl_2): 431 nm

IR (KBr Disc): 2106 ν(C≡C), 2228 ν(C≡N) cm^{-1}

Elemental Analysis:

Calcd for $C_{15}H_{19}AuNP$ (%): C 40.83; H 4.34; N 3.17. Found (%): C 40.80; H 4.28; N 3.34.

5.2.10 Preparation of 1-(triethylphosphinegoldethynyl)-2-benzonitrile (2.10)

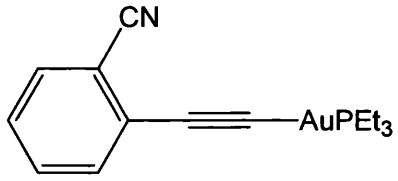

General Procedure B; Triethylphosphinegold(I) chloride (146 mg, 0.417 mmol) and 1-(trimethylsilylethynyl)-2-benzonitrile (109 mg, 0.550 mmol). Recrystallisation from methanol afforded pale yellow crystals (89.0 mg, 48%).

^1H NMR:

7.57 – 7.54	m, 2H	5- & 6-Ar*H*
7.45 – 7.40	m, 1H	3-Ar*H*
7.24 – 7.22	m, 1H	4-Ar*H*
1.86 – 1.78	m, 6H	$P(CH_2CH_3)_3$
1.26 – 1.18	m, 9H	$P(CH_2CH_3)_3$

$^{13}C\{^1H\}$ NMR:

133.1	CH	6-Ar*C*H	118.5	C_{quat}	*C*≡N
132.3	CH	5-Ar*C*H	115.4	C_{ipso}	*C*–C≡N
131.9	CH	3-Ar*C*H	99.41	C_{quat}	*C*≡C–Au
129.4	C_{ipso}	*C*–C≡C–Au	17.75	CH_2	d, $^1J_{PC}$ 33.1 Hz $P(CH_2CH_3)_3$
126.4	CH	4-Ar*C*H	8.845	CH_3	$P(CH_2CH_3)_3$

$^{31}P\{^1H\}$ NMR: 37.62

UV/Vis (CH_2Cl_2) λ_{max} [nm] (ε, mol^{-1} dm^3 cm^{-1}):

265 (14,980), 279 (24,020), 306 (9,000), 316 (9,700), 335 sh (1840).

Emission (CH_2Cl_2): 440 nm

IR (KBr Disc): 2109 cm^{-1} ν(C≡C), 2222 cm^{-1}ν(C≡N).

Elemental Analysis:

Calcd for $C_{15}H_{19}AuNP$ (%): C 40.83; H 4.34; N 3.17. Found (%): C 40.70; H 4.52; N 3.13.

5.2.11 Preparation of 1-(triphenylphosphinegoldethynyl)-3-benzonitrile (2.11)

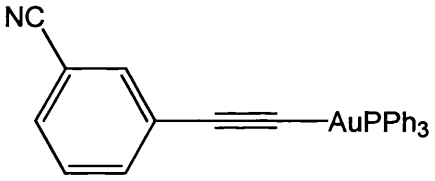

General Procedure B; Triphenylphosphinegold(I) chloride (102 mg, 0.206 mmol) and 1-(trimethylsilylethynyl)-3-benzonitrile (45.5 mg, 0.227 mmol). Recrystallisation from methanol afforded **2.11** as pale brown crystals (33.4 mg, 28%).

^1H NMR:

7.75	t, 1H, 1.37 Hz	6-Ar*H*
7.69	dt, 1H, 7.83 Hz, 1.37 Hz	2-Ar*H*
7.59 – 7.44	m, 16H	$P(C_6H_5)_3$ and 4-Ar*H*
7.34	t, 1H, 7.83 Hz	5-Ar*H*

$^{13}C\{^1H\}$ NMR:

136.4	CH	6-Ar*C*H		129.2	CH	d, 11.0 Hz	$P(C_6H_5)_3$
135.6	CH	2-Ar*C*H		128.9	CH	5-Ar*C*H	
134.9	C_{ipso}	$P(C_6H_5)_3$		118.6	C_{quat}	*C*≡N	
134.3	CH	d, 13.8 Hz	$P(C_6H_5)_3$	112.4	C_{ipso}	*C*–C≡N	
131.7	CH	d, 2.80 Hz	$P(C_6H_5)_3$	101.7	C_{quat}	*C*≡C–$AuPPh_3$	
129.9	CH	4-Ar*C*H		101.4	C_{quat}	C≡*C*–$AuPPh_3$	
129.8	C_{ipso}	*C*–C≡C–$AuPPh_3$					

$^{31}P\{^1H\}$ NMR: 42.21

UV/Vis (CH_2Cl_2) λ_{max} [nm] (ε, mol^{-1} dm^3 cm^{-1}):

269 (27,000), 283 (31,220), 311 (2,340).

Emission (CH_2Cl_2): 431 nm

IR (KBr Disc): 2113 cm^{-1} ν(C≡C), 2226 cm^{-1} ν(C≡N).

Elemental Analysis:

Calcd for $C_{27}H_{19}AuNP$ (%): C 55.40; H 3.27; N 2.39. Found (%): C 55.20; H 3.33; N 2.02.

5.2.12 Preparation of 1-(triethylphosphinegold)-4-methoxyphenylacetylene (2.12)

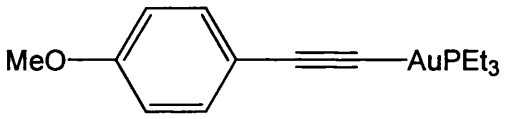

General Procedure B; Triethylphosphinegold(I) chloride (57.6 mg, 0.17 mmol) and 4-(trimethylsilyl)methoxyphenylacetylene (54 mg, 0.27 mmol). Recrystallisation from methanol afforded **2.12** as white crystals (35.2 mg, 48 %).

^1H NMR:

7.42	d, 2H, ^3J 8.8 Hz	2- and 2'-Ar*H*
6.77	d, 2H, ^3J 8.8 Hz	3- and 3'-Ar*H*
3.78	s, 3H	O*CH*$_3$
1.85 – 1.76	m, 6H	P(*CH*$_2$CH$_3$)$_3$
1.25 – 1.17	m, 9H	P(CH$_2$*CH*$_3$)$_3$

$^{13}C\{^1H\}$ NMR:

158.4	C_{ipso}	*C*–OMe	55.17	C_{ipso}	O*CH*$_3$
133.6	CH	2- and 2'-Ar*C*H	17.86	CH_2	d, $^1J_{PC}$ 33.1 Hz P(*CH*$_2$CH$_3$)$_3$
117.3	C_{ipso}	*C*–C≡C–Au	8.845	*C*H$_3$	P(CH$_2$*CH*$_3$)$_3$
113.5	CH	3- and 3'-Ar*C*H			

$^{31}P\{^1H\}$ NMR: 38.18

UV/Vis (CH_2Cl_2) λ_{max} [nm] (ε, mol^{-1} dm^3 cm^{-1}):

258 sh (11,720), 270 (22,280), 281 (29,380), 295 (22,440).

Emission (CH_2Cl_2): 376 nm

IR (KBr Disc): 2094 cm^{-1} ν(C≡C)

Elemental Analysis:

Calcd for $C_{15}H_{22}AuOP$ (%): C 40.20; H 4.96. Found (%): C 40.37; H 4.97.

5.2.13 Preparation of 1-(triethylphosphinegold)-3-methoxyphenylacetylene (2.13)

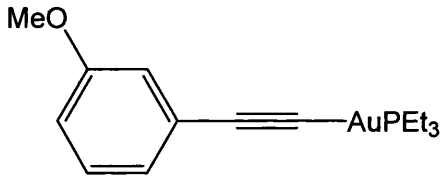

General Procedure B; Triethylphosphinegold(I) chloride (49.9 mg, 0.14 mmol) and 3-(trimethylsilyl)methoxyphenylacetylene (35.8 mg, 0.18 mmol). Recrystallisation from methanol afforded **2.13** as a dark yellow solid (15 mg, 24%).

^{1}H NMR:

7.12	dd, 1H, ^3J 8.22 Hz, ^3J 7.63 Hz	5-Ar*H*
7.08	ddd, 1H, ^3J 7.63 Hz, ^4J 1.37 Hz, ^4J 1.17 Hz	6-Ar*H*
7.03	dd, 1H, ^4J 2.54 Hz, ^4J 1.37Hz	2-Ar*H*
6.76	ddd, 1H, ^3J 8.22Hz, ^4J 2.54 Hz, ^4J 1.17 Hz	4-Ar*H*
3.76	s, 3H	OCH_3
1.85 – 1.77	m, 6H	P($CH_2$$CH_3$)$_3$
1.25 – 1.17	m, 9H	P($CH_2$$CH_3$)$_3$

^{13}C{^{1}H} NMR:

159.0	C_{ipso}	*C*–OMe	113.7	CH	4-Ar*C*H
128.9	CH	5-Ar*C*H	103.9	C_{quat}	*C*≡C–Au
125.9	C_{ipso}	*C*–C≡C–Au	55.16	C_{ipso}	OCH_3
124.9	CH	6-Ar*C*H	17.85	CH_2	d, $^1J_{PC}$ 33.1 Hz P($CH_2$$CH_3$)$_3$
116.8	CH	2-Ar*C*H	8.863	CH_3	P($CH_2$$CH_3$)$_3$

$^{31}P\{^1H\}$ NMR: 38.10

UV/Vis (CH_2Cl_2) λ_{max} [nm] (ε, mol^{-1} dm^3 cm^{-1}):

268 (9,740), 277 (11,820), 294 (5,760), 303 (5,060).

Emission (CH_2Cl_2): 327 nm

IR (KBr Disc): 2105 cm^{-1} ν(C≡C)

Elemental Analysis:

Calcd for $C_{15}H_{22}AuOP$ (%): C 40.20; H 4.96. Found (%): C 40.00; H 4.97.

5.2.14 Preparation of 1-(triethylphosphinegold)-2-methoxyphenylacetylene (2.14)

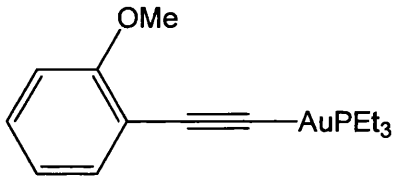

General Procedure B; Triethylphosphinegold(I) chloride (67.4 mg, 0.20 mmol) and 2-(trimethylsilyl)methoxyphenylacetylene (44.2 mg, 0.22 mmol). Recrystallisation from ethanol afforded a pale yellow solid (12.3 mg, 14%).

^1H NMR:

7.48	dd, 1H, ^3J 7.43 Hz, ^4J 1.57 Hz	6-Ar*H*
7.17	ddd, 1H, ^3J 8.41 Hz, ^3J 7.43 Hz, ^4J 1.76 Hz	5-Ar*H*
6.85 – 6.81	m, 2H	3- & 4-Ar*H*
3.86	s, 3H	O*CH*$_3$
1.83 – 1.75	m, 6H	P(*CH*$_2$CH$_3$)$_3$
1.24 – 1.16	m, 9H	P(CH$_2$*CH*$_3$)$_3$

$^{13}C\{^1H\}$ NMR:

134.2	CH	6-Ar*C*H	109.9	CH	3-Ar*C*H
127.8	CH	5-Ar*C*H	55.63	C_{ipso}	O*C*H$_3$
120.1	CH	4-Ar*C*H	17.87	CH_2	d, $^1J_{PC}$ 33.1 Hz P(*C*H$_2$CH$_3$)$_3$
112.3	C_{quat}	*C*≡C–Au	8.808	CH_3	P(CH$_2$*C*H$_3$)$_3$

$^{31}P\{^1H\}$ NMR: 37.75

UV/Vis (CH_2Cl_2) λ_{max} [nm] (ε, mol^{-1} dm^3 cm^{-1}):

260 (9,320), 273 (14,140), 300 (10,460), 310 (12,820).

IR (KBr Disc): 2114 cm^{-1} ν(C≡C)

5.2.15 Preparation of 1-(triphenylphosphinegoldethynyl)-3-methoxyphenylacetylene (2.15)

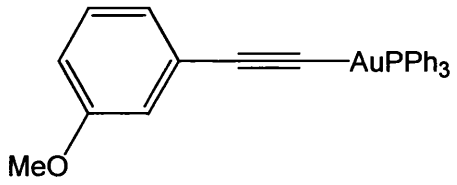

General Procedure B; Triphenylphosphinegold(I) chloride (100 mg, 0.20 mmol) and 3-(trimethylsilyl)methoxyphenylacetylene (45.4 mg, 0.22 mmol). Recrystallisation from methanol/CH_2Cl_2 (1:1) afforded **2.15** as white crystals (89.6 mg, 75%).

^1H NMR:

7.59 – 7.42	(m, 16 H)	Ar*H* and P(C_6H_5)$_3$
7.18	(td, 1H, 7.83 Hz, 1.76 Hz)	Ar*H*
6.79 – 6.76	(m, 2H)	Ar*H*

$^{13}C\{^1H\}$ NMR:

160.5	C_{ipso}	*C*–OCH_3		120.1	CH	6-Ar*C*H
135.9	C_{ipso}	P(C_6H_5)$_3$		114.0	C_{ipso}	*C*–C≡C–$AuPPh_3$
134.4	CH	d, 13.8 Hz	P(C_6H_5)$_3$	109.9	CH	2-Ar*C*H
131.9	CH	5-Ar*C*H		99.64	C_{quat}	*C*≡C–Au
131. 5	CH	d, 1.8 Hz	P(C_6H_5)$_3$	99.37	C_{quat}	C≡*C*–Au
129.1	CH	d, 11.9 Hz	P(C_6H_5)$_3$	55.73	C_{ipso}	O*C*H_3

$^{31}P\{^1H\}$ NMR: 42.45

UV/vis (CH_2Cl_2) λ_{max} [nm] (ε, mol^{-1} dm^3 cm^{-1}):

269 (23,740), 279 (25,140), 295 (14,960), 303 (13,660).

Emission (CH_2Cl_2): 431 nm

IR (KBr Disc): 2115 cm^{-1} $\nu(C{\equiv}C)$

Elemental Analysis:

Calcd for $C_{27}H_{22}AuOP$ (%): C 54.93; H 3.76. Found (%): C 55.00; H 3.72.

5.2.16 Preparation of 1-(triphenylphosphinegoldethynyl)-2-methoxyphenylacetylene (2.16)

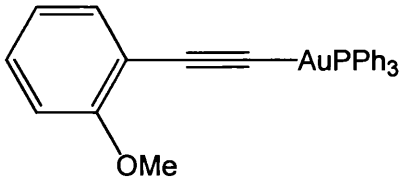

General Procedure B; Triphenylphosphinegold(I) chloride (101 mg, 0.20 mmol) and 2-(trimethylsilyl)methoxyphenylacetylene (47.1 mg, 0.22 mmol). Recrystallisation from methanol afforded **2.16** as a cream solid (83.6 mg, 69%).

^{1}H NMR:

7.59 – 7.42	m, 16 H	6-Ar*H* and $P(C_6H_5)_3$
7.18	ddd, 1H, 8.6 Hz, 7.8 Hz, 1.8 Hz	4-Ar*H*
6.87 – 6.83	m, 2H	3- & 5-Ar*H*

^{13}C{^{1}H} NMR:

160.5	C_{ipso}	*C*–OCH_3		120.1	CH	5-Ar*C*H
135.9	C_{ipso}	$P(C_6H_5)_3$		114.0	C_{quat}	*C*–C≡C–Au
134.4	CH	d, 13.8 Hz	$P(C_6H_5)_3$	109.9	CH	3-Ar*C*H
131.9	CH	6-Ar*C*H		99.64	C_{quat}	*C*≡C–Au
131.5	CH	d, 1.8 Hz	$P(C_6H_5)_3$	99.37	C_{quat}	C≡*C*–Au
129.1	CH	d, 11.9 Hz	$P(C_6H_5)_3$	55.73	C_{ipso}	O*C*H_3

^{31}P{^{1}H} NMR: 42.44

UV/vis (CH_2Cl_2) $\underline{\lambda_{max}}$ [nm] (ε, mol^{-1} dm^3 cm^{-1}):

261 (12,380), <u>275</u> (16,760), 300 (12,100), 311 (15,800).

Emission (CH_2Cl_2): 334 nm

IR (KBr Disc): 2110 cm^{-1} ν(C≡C)

Elemental Analysis:

Calcd for $C_{27}H_{22}AuOP$ (%): C 54.93; H 3.76. Found (%): C 54.80; H 4.26.

5.2.17 Preparation of 5-(triethylphosphinegoldethynyl)pyrimidine (2.17)

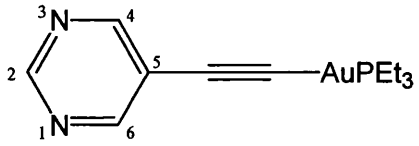

General Procedure B; Triethylphosphinegold(I) chloride (131 mg, 0.37 mmol) and 5-ethynylpyrimidine (43.4 mg, 0.41 mmol). Recrystallisation from methanol afforded **2.17** as long yellow needles (127 mg, 82%).

^{1}H NMR:

8.99	s, 1H	2-Ar*H*
8.77	s, 2H	4- & 6-Ar*H*
1.88 – 1.80	m, 6H	$P(CH_2CH_3)_3$
1.27 – 1.19	m, 9H	$P(CH_2CH_3)_3$

^{13}C{^{1}H} NMR:

159.2	CH	4- & 6-Ar*C*H	96.37	C_{quat}	*C*≡C–Au
155.2	CH	2-Ar*C*H	17.79	CH_2	d, $^1J_{PC}$ 33.1 Hz $P(CH_2CH_3)_3$
121.6	C_{ipso}	*C*–C≡C–Au	8.91	CH_3	$P(CH_2CH_3)_3$

^{31}P{^{1}H} NMR: 38.08

UV/Vis (CH_2Cl_2) $\underline{\lambda_{max}}$ [nm] (ε, mol^{-1} dm^3 cm^{-1}):

256 (12,340), 269 (18,200), <u>283</u> (20,020), 302 (10,220).

Emission (CH_2Cl_2): 460 nm

IR (KBr Disc): 2112 cm^{-1} ν(C≡C)

Elemental Analysis:

Calcd for $C_{12}H_{18}AuN_2P$: C 34.46; H 4.34; N 6.70. Found: C 34.00; H 4.40; N 6.45%.

5.2.18 Preparation of 1-(triphenylphosphinegoldethynyl)-5-pyrimidine (2.18)

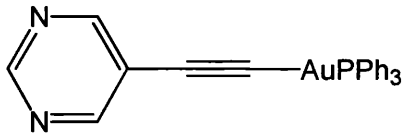

General Procedure B; Triphenylphosphinegold(I) chloride (100 mg, 0.20 mmol) and 1-(trimethylsilylethynyl)-5-pyrimidine (39.1 mg, 0.22 mmol). Recrystallisation from ethyl acetate afforded **2.18** as pale yellow crystals (56.7 mg, 50 %).

^{1}H NMR:

9.02	s, 1H	2-Ar*H*
8.80	s, 2H	4- & 6-Ar*H*
7.56 – 7.45	m, 15H	Ar*H*

^{13}C{^{1}H} NMR:

159.3	CH	4- & 6-Ar*C*H		129.7	C_{ipso}	$P(C_6H_5)_3$	
155.3	CH	2-Ar*C*H		129.3	CH	d, 11.9 Hz	$P(C_6H_5)_3$
134.3	CH	d, 13.8 Hz	$P(C_6H_5)_3$	121.5	C_{ipso}	*C*–C≡C–Au	
131.7	CH	d, 2.11 Hz	$P(C_6H_5)_3$	96.60	C_{quat}	*C*≡C–Au	

^{31}P {^{1}H} NMR: 42.03

UV/vis (CH_2Cl_2) $\underline{\lambda_{max}}$ [nm] (ε, mol^{-1} dm^3 cm^{-1}):

256 (57,600), <u>270</u> (80,400), 285 (70,000).

Emission (CH_2Cl_2): 455 nm

IR (KBr Disc): 2117 cm^{-1} ν(C≡C)

Elemental Analysis:

Calcd for $C_{24}H_{18}AuN_2P$: C 51.26; H 3.23; N 4.98. Found: C 51.40; H 3.30; N 4.85%.

5.2.19 Preparation of 1,4-Bis(triethylphosphinegoldethynyl)benzene (2.19)

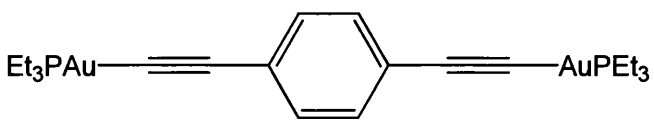

General Procedure B; Triethylphosphinegold(I) chloride (151 mg, 0.43 mmol) and 1,4-diethynylbenzene (27.4 mg, 0.22 mmol). Recrystallisation from methanol afforded **2.19** as yellow crystals (79.6 mg, 49%).

^{1}H NMR:

7.33	s, 4H	Ar*H*
1.84 – 1.76	m, 6H	$P(CH_2CH_3)_3$
1.24 – 1.16	m, 9H	$P(CH_2CH_3)_3$

^{13}C {^{1}H} NMR:

131.9	CH	Ar*C*H	17.84	CH_2	d, $^1J_{PC}$ 33.1 Hz	$P(CH_2CH_3)_3$
123.2	C_{ipso}	*C*–C≡C–Au	8.85	CH_3	$P(CH_2CH_3)_3$	
104.2	C_{quat}	*C*≡C–Au				

^{31}P {^{1}H} NMR: 38.09

UV/Vis (CH_2Cl_2) λ_{Max} [nm] (ε, mol^{-1} dm^3 cm^{-1}):

286 (25,600), 294 (30,000), 303 (62,600), 323 (98,200).

Emission (CH_2Cl_2): 349 nm

IR (KBr Disc): 2106 cm^{-1} ν(C≡C)

Elemental Analysis:

Calcd for $C_{22}H_{34}Au_2P_2$ (%): C 35.03; H 4.54. Found (%): C 34.80; H 4.56.

5.2.20 Preparation of 4,4'-Bis(triethylphosphinegoldethynyl)benzene (2.20)

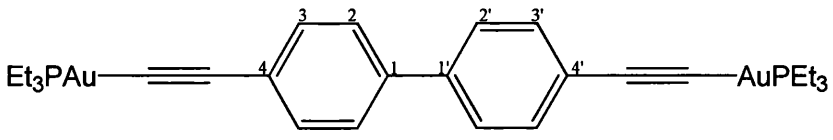

General Procedure B; Triethylphosphinegold(I) chloride (151 mg, 0.43 mmol) and 4,4'-diethynylbenzene (43 mg, 0.22 mmol). Recrystallisation from methanol afforded **2.20** as yellow crystals (93.1 mg, 52%).

^{1}H NMR:

7.52	d, 4H, ^3J8.61 Hz	3- & 3'-Ar*H*

7.46	d, 4H, ^3J 8.61 Hz	2- & 2'-Ar*H*
1.86 – 1.77	m, 6H	$P(CH_2CH_3)_3$
1.26 – 1.18	m, 9H	$P(CH_2CH_3)_3$

^{13}C {^1H} NMR:

132.7	CH	3- & 3'-ArCH (4C)	17.85	CH_2	d, $^1J_{PC}$ 33.1 Hz $P(CH_2CH_3)_3$
126.3	CH	2- & 2'-ArCH (4C)	8.86	CH_3	$P(CH_2CH_3)_3$

^{31}P {^1H} NMR: 38.14

UV/Vis (CH_2Cl_2) λ_{max} [nm] (ε, mol^{-1} dm^3 cm^{-1}):

322 (75400)

Emission (CH_2Cl_2): 358 nm

IR (KBr Disc): 2107 cm^{-1} ν(C≡C)

Elemental Analysis:

Calcd for $C_{28}H_{38}Au_2P_2$ (%): C 40.49; H 4.61. Found (%): C 41.00; H 4.67.

5.2.21 Preparation of 9-(triethylphosphinegoldethynyl)anthracene (2.21)

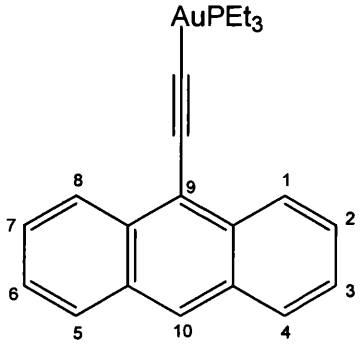

General Procedure B; Triethylphosphinegold(I) chloride (101 mg, 0.29 mmol) and 9-(Trimethylsilylethynyl)anthracene (86.7 mg, 0.32 mmol). The remaining solid after removal of solvent from the reaction mixture was dissolved in dichloromethane (10 mL), washed with water (3 × 20 mL), the solution dried ($MgSO_4$), before the solvent was removed under reduced pressure to give the crude product as an orange solid. Recrystallisation from methanol/CH_2Cl_2 (1:1; v/v) affording **2.21** as a dark yellow solid (47.9 mg) in a 32% yield.

^{1}H NMR:

8.86	d, 2H, ^3J 8.0 Hz	1- & 8-Ar*H*
8.29	s, 1H	10-Ar*H*
7.97	d, 2H, ^3J 8.0 Hz	4- & 5-Ar*H*
7.52 – 7.43	m, 4H	2-,3-,6- & 7-Ar*H*
1.92 – 1.84	m, 6H	$P(CH_2CH_3)_3$
1.31 – 1.23	m, 9H	$P(CH_2CH_3)_3$

^{13}C{^{1}H} NMR:

133.0	C_{ipso}	anthracene	125.3	CH	2-,3-,6- & 7-Ar*C*H
131.3	C_{ipso}	anthracene	99.46	C_{quat}	*C*≡C–Au
128.3	CH	1- & 8-Ar*C*H	17.86	CH_2	d, $^1J_{PC}$ 33.1 Hz $P(CH_2CH_3)_3$
128.1	CH	4- & 5-Ar*C*H	8.90	CH_3	$P(CH_2CH_3)_3$
125.6	CH	10-Ar*C*H			

^{31}P{^{1}H} NMR: 37.81

UV/Vis (CH_2Cl_2) λ_{Max} [nm] (ε, mol^{-1} dm^3 cm^{-1}):

265 (69,980), 357 (3,940), 375 (9,720), 396 (19,720), 419(22,540).

Emission (CH_2Cl_2): 425 nm

IR (KBr Disc): 2088 cm^{-1} ν(C≡C)

Elemental Analysis:

Calcd for $C_{22}H_{24}AuP$ (%): C 51.17; H 4.68. Found (%): C 50.80; H 4.70.

5.2.22 Preparation of 9,10-Bis(triethylphosphinegoldethynyl)anthracene (2.22)

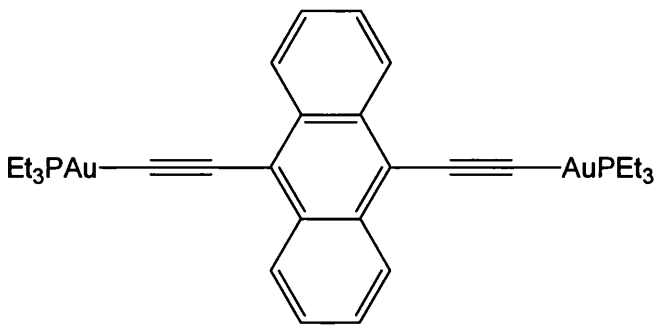

General Procedure B; Triethylphosphinegold(I) chloride (77.2 mg, 0.22 mmol), methanol (40 mL) and 9,10-diethynylanthracene (25.0 mg, 0.11 mmol). The remaining solid after removal of solvent from the reaction mixture was dissolved in CH_2Cl_2 and washed with water (3 × 20 mL), the solution dried ($MgSO_4$), before the solvent was removed under reduced pressure to give an orange solid. Recrystallisation from methanol/dichloromethane (1:1) affording **2.22** as a pale orange solid (11.0 mg, 12%).

^{1}H NMR:

8.82	dd, 4H, ^3J 6.7 Hz, 3.3 Hz	1-,4-,5- & 8-Ar*H*
7.49	dd, 4H, ^3J 6.7 Hz, 3.3 Hz	2-,3-,6- & 7-Ar*H*
1.92 – 1.83	m, 12H	$P(CH_2CH_3)_3$
1.31 – 1.23	m, 18H	$P(CH_2CH_3)_3$

^{13}C{^{1}H} NMR:

132.6	C_{ipso}	anthracene	100.1	C_{quat}	*C*≡C–Au
128.1	CH	1,4,5& 8-Ar*C*H	17.81	CH_2	d, $^1J_{PC}$ 33.1 Hz $P(CH_2CH_3)_3$
125.5	CH	2,3,6 &7-Ar*C*H	8.84	CH_3	$P(CH_2CH_3)_3$
119.1	C_{ipso}	*C*–C≡C–Au			

^{31}P{^{1}H} NMR: 37.80

UV/Vis (CH_2Cl_2) λ_{max} [nm] (ε, mol^{-1} dm^3 cm^{-1}):

277 (70,680), 294 (21,480), 316 (5,660), 387 (4,500), 409 (13,300), 434 (31,880), 461 (44,060).

Emission (CH_2Cl_2): 467 nm

IR (KBr Disc): 2091 cm^{-1} ν(C≡C)

Elemental Analysis:

Calcd for $C_{30}H_{38}Au_2P_2$ (%): C 42.17; H 4.48. Found (%): C 41.50; H 4.42.

5.2.23 Preparation of 9-(triphenylphosphinegoldethynyl)anthracene (2.23)

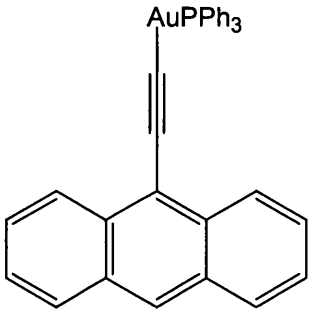

General Procedure B; Triphenylphosphinegold(I) chloride (101 mg, 0.20 mmol) and 9-(Trimethylsilylethynyl)anthracene (63.6 mg, 0.22 mmol). The remaining solid after removal of solvent from the reaction mixture was dissolved in CH_2Cl_2 and washed with water (3 × 20 mL), the solution dried ($MgSO_4$), before the solvent was removed under reduced pressure to give the crude product as an orange solid. Recrystallisation from methanol/CH_2Cl_2 (1:1) affording **2.23** as a yellow solid (109 mg, 81%).

^{1}H NMR:

8.87	d, 2H, ^3J 8.0 Hz	1- and 8-Ar*H*
8.30	s, 1H	10-Ar*H*
7.96	d, 2H, ^3J 8.0 Hz	4- and 5-Ar*H*
7.67 – 7.61	m, 4H	2-,3-,6- & 7-Ar*H*
7.55 – 7.47	m, 15H	$P(C_6H_5)_3$

^{13}C{^{1}H} NMR:

134.4	CH	d, 13.8 Hz	$P(C_6H_5)_3$	128.3	CH	1- and 8-Ar*C*H
133.1	C_{ipso}	anthracene		128.1	CH	4- and 5-Ar*C*H
131.6	CH	d, 2.11 Hz	$P(C_6H_5)_3$	126.9	CH	10-Ar*C*H
131.3	C_{ipso}	anthracene		125.7	CH	2- & 7-Ar*C*H
129.2	CH	d, 11.0Hz	$P(C_6H_5)_3$	125.3	CH	3- & 6-Ar*C*H

^{31}P{^{1}H} NMR: 42.48

UV/Vis (CH_2Cl_2) $\underline{\lambda_{max}}$ [nm] (ε, mol^{-1} dm^3 cm^{-1}):

<u>266</u> (69,880), 357 (3,980), 375 (9,560), 396 (19,240), 419 (22,060).

Emission (CH_2Cl_2): 424 nm

IR (KBr Disc): 2100 cm^{-1} $\nu(C{\equiv}C)$

Elemental Analysis:

Calcd for $C_{34}H_{24}AuP$ (%): C 61.83; H 3.66. Found (%): C 61.90; H 4.01.

5.2.24 Preparation of 9,10-Bis(triphenylphosphinegoldethynyl)anthracene (2.24)

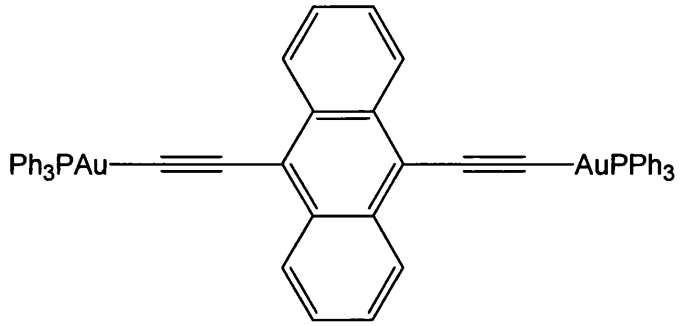

General Procedure B; Triphenylphosphinegold(I) chloride (77.2 mg, 0.22 mmol), Methanol (40 mL) and 9,10-diethynylanthracene (25.0 mg, 0.11 mmol). The remaining solid after removal of solvent from the reaction mixture was dissolved in CH_2Cl_2 and washed with water (3 × 20 mL), the solution dried ($MgSO_4$), before the solvent was removed under reduced pressure to give a dark orange solid. Recrystallisation from methanol/dichloromethane (1:1) affording **2.24** as red crystals (~5 mg, 4%).

^{1}H NMR:

8.87	dd, 4H, ^3J 6.7 Hz, 3.1 Hz	2-, 3-, 6- & 7-Ar*H*
7.62	dd, 4H, ^3J 6.7Hz, 3.1 Hz	1-, 4-, 5- & 8-Ar*H*
7.56 – 7.47	m, 30H	$P(C_6H_5)_3$

^{31}P {^{1}H} NMR: 42.44

5.3 Experimental for Chapter 3

5.3.1 Preparation of 2-(Trimethylsilylethynyl)furan (3.01)

Bis(triphenylphosphine)palladium(II) chloride (143 mg, 0.20 mmol) and copper iodide (19.4 mg, 0.10 mmol) were placed in a Schlenk tube and dissolved in tetrahydrofuran (20

mL) and diethylamine (5 mL). 2-bromofuran (0.30 mL, 3.40 mmol) and trimethylsilylacetylene (0.72 mL, 5.10 mmol) were added and the resulting mixture stirred at room temperature and in the absence of light for 48 h after which time TLC (silica, 4:1, hexane/dichloromethane) showed the reaction to be complete. The volatiles were removed under reduced pressure providing a yellow oil. The crude oil was eluted through a short plug of alumina with 4:1 hexane/dichloromethane as eluant. The volatiles were again removed under reduced pressure and the compound dried affording **3.01** as a colourless oil (0.48 g, 85%).

^{1}H NMR:

7.35	dd, 1H, ^3J 1.8 Hz, ^4J 0.8 Hz	5-Ar*H*
6.60	dd, 1H, ^3J 3.5 Hz, ^3J 0.8 Hz	3-Ar*H*
6.36	dd, 1H, ^3J 3.5 Hz, ^3J 1.8 Hz	4-Ar*H*
0.25	s, 9H	Si(C*H*$_3$)$_3$

^{13}C{^{1}H} NMR:

143.5	CH	5-Ar*C*H	99.53	C_{quat}	*C*≡C–Si(CH$_3$)$_3$
137.1	C_{ipso}	*C*–C≡C–Si	94.15	C_{quat}	C≡*C*–Si(CH$_3$)$_3$
115.7	CH	4-Ar*C*H	-0.30	Si(*C*H$_3$)$_3$	
110.8	CH	3-Ar*C*H			

IR (KBr Disc): 2157 cm^{-1} ν(C≡C)

5.3.2 2-(Trimethylsilylethynyl)thiophene (3.02)

UV (CH_2Cl_2) $\underline{\lambda_{max}}$ [nm] (ε, mol^{-1} dm^3 cm^{-1}):

252 sh (7,680), 259 sh (9,260), <u>277</u> (12,560), 289 sh (9,280).

5.3.3 Preparation of 2-(Trimethylsilylethynyl)selenophene (3.03)

Bis(triphenylphosphine)palladium(II) chloride (80.2 mg, 0.11 mmol) and copper iodide (10.9 mg, 0.06 mmol) and were placed in a Schlenk tube and dissolved in tetrahydrofuran (20 mL) and diethylamine (5 mL). 2-bromoselenophene[19] (400 mg, 1.91 mmol) and

trimethylsilylacetylene (0.40 mL, 2.86 mmol) were added and the resulting mixture stirred at room temperature and in the absence of light for 1 hour after which time TLC (silica, hexane) showed the reaction to be complete. The volatiles were removed under reduced pressure providing a yellow oil. The crude oil was eluted through a short plug of alumina with hexane as eluant. The volatiles were again removed under reduced pressure and the compound dried affording **3.03** as a colourless oil (0.42 g, 98%).

^{1}H NMR:

7.96	dd, 1H, ^{3}J 5.7 Hz, ^{4}J 1.2 Hz, $^{2}J_{SeH}$ 46Hz	5-Ar*H*
7.42	dd, 1H, ^{3}J 3.9 Hz, ^{4}J 1.2 Hz	3-Ar*H*
7.18	dd, 1H, ^{3}J 5.7 Hz, ^{3}J 3.9 Hz	4-Ar*H*
0.24	s, 9H	Si(CH_3)$_3$

^{13}C{^{1}H} NMR:

134.9	CH	5-Ar*C*H	100.5	C_{quat}	*C*≡C–Si(CH$_3$)$_3$
133.2	CH	4-Ar*C*H	99.63	C_{quat}	C≡*C*–Si(CH$_3$)$_3$
129.3	CH	3-Ar*C*H	-0.15	CH_3	Si(*C*H$_3$)$_3$
127.5	C_{ipso}	*C*–C≡C–Si			

^{77}Se{^{1}H} NMR: 692.6 ppm

^{77}Se NMR: 692.7 dt, $^{2}J_{SeH}$ 46.3 Hz, $^{3}J_{SeH}$ 12.9 Hz

UV (CH_2Cl_2) $\underline{\lambda_{max}}$ [nm] (ε, mol^{-1} dm^3 cm^{-1}):

<u>271</u> (12,960), 286 (11,680), 301 sh (9,060).

Emission (CH_2Cl_2): 369 nm

IR (Neat): 2138 cm^{-1} ν(C≡C)

5.3.4 Preparation of 2-(Trimethylsilylethynyl)tellurophene (3.04)

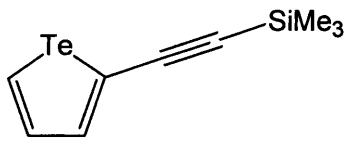

Bis(triphenylphosphine)palladium(II) chloride (63.2 mg, 0.09 mmol) and copper iodide (10.0 mg, 0.05 mmol) were placed in a Schlenk tube and dissolved in tetrahydrofuran (20 mL) and diethylamine (5 mL). 2-bromotellurophene[20] (387 mg, 1.50 mmol) and trimethylsilylacetylene (0.32 mL, 2.25 mmol) were added and the resulting mixture stirred at room temperature and in the absence of light overnight (~17 h) after which time TLC (silica, hexane) showed the reaction to be complete. The volatiles were removed under reduced pressure providing a yellow oil. The crude oil was eluted through a short plug of alumina with hexane as eluant. The volatiles were again removed under reduced pressure and the compound dried affording **3.04** as a yellow oil (0.41 g, 98%).

^{1}H NMR:

8.95	dd, 1H, ^{3}J 6.9 Hz, ^{4}J 1.4 Hz, $^{2}J_{TeH}$ 95.7 Hz	5-Ar*H*
8.82	dd, 1H, ^{3}J 4.1 Hz, ^{4}J 1.4 Hz	3-Ar*H*
7.66	dd, 1H, ^{3}J 6.9 Hz, ^{3}J 4.1 Hz	4-Ar*H*
0.23	s, 9H	Si(C*H*$_3$)$_3$

^{13}C{^{1}H} NMR:

143.3	CH	5-Ar*C*H	104.2	C_{quat}	*C*≡*C*–Si(CH$_3$)$_3$
137.1	CH	4-Ar*C*H	101.8	C_{quat}	C≡*C*–Si(CH$_3$)$_3$
129.9	CH	3-Ar*C*H	-0.14	CH_3	Si(*C*H$_3$)$_3$

^{125}Te{^{1}H} NMR: 959.9

^{125}Te NMR: 959.9 ddd, $^{2}J_{TeH}$ 95.7 Hz, $^{3}J_{TeH}$ 15.5 Hz, $^{3}J_{TeH}$ 11.4 Hz

UV (CH_2Cl_2) $\underline{\lambda_{max}}$ [nm] (ε, mol^{-1} dm^3 cm^{-1}):

288 (8,960), <u>295</u> (9,020), 320 (5,460).

Emission (CH_2Cl_2) λ_{max}: 375 nm

IR (KBr Disc): 2132 cm^{-1} ν(C≡C)

5.3.5 Preparation of 2-ethynylselenophene (3.05)

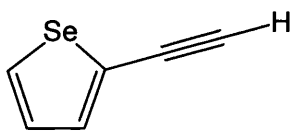

3.03 (206 mg, 0.91 mmol) was dissolved in dichloromethane /methanol (1:1, v/v, 10 mL). 2.0 M KOH solution (0.68 mL, 1.36 mmol) was added drop wise and the mixture stirred at room temperature in the absence of light overnight. The volatiles were removed under reduced pressure providing a yellow oil which was dissolved in dichloromethane and washed with water (3 × 20 mL). The dichloromethane layer was dried ($MgSO_4$) and the volatiles removed under reduced pressure providing a yellow oil. The crude oil was eluted through a short plug of silica with diethyl ether as eluant. The volatiles were again removed under reduced pressure and the compound dried affording **3.05** as a yellow oil (52.4 mg, 38%).

^{1}H NMR:

7.99	dd, 1H, ^3J 5.7 Hz, ^4J 1.2 Hz $^2J_{SeH}$ 46.6 Hz	*H* in 5-position
7.48	ddd, 1H, ^3J 3.7, ^4J 1.2, ^5J 0.39 Hz	*H* in 3-position
7.21	dd, 1H, ^3J 5.7, ^3J 3.7 Hz	*H* in 4-position
3.51	s, 1H, $^4J_{SeH}$ 4.1 Hz	C≡C–*H*

^{13}C{^{1}H} NMR:

135.5	CH	5-Ar*C*H	126.4	C_{ipso}	*C*–C≡C–H
133.4	CH	4-Ar*C*H	82.92	C_{quat}	*C*≡C–H
129.3	CH	3-Ar*C*H	79.10	CH	C≡*C*–H

^{77}Se{^{1}H} NMR: 693.2

5.3.6 Preparation of 2-ethynyltellurophene (3.06)

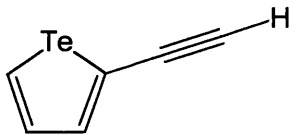

3.04 (100 mg, 0.36 mmol) was dissolved in dichloromethane /methanol (1:1, v/v, 10 mL). 2.0 M KOH solution (0.36 mL, 0.72 mmol) was added drop wise and the mixture stirred at room temperature in the absence of light overnight. The volatiles were removed under reduced pressure providing a yellow oil which was dissolved in dichloromethane and washed with water (3 × 20 mL). The dichloromethane layer was dried ($MgSO_4$) and the volatiles removed under reduced pressure providing a yellow oil. The crude oil was eluted through a short plug of silica with diethyl ether as eluant. The volatiles were again

removed under reduced pressure and the compound dried affording **3.06** as a yellow oil (51.6 mg, 70%).

^{1}H NMR:

8.98	dd, 1H, ^3J 7.0 Hz, ^4J 1.2 Hz, $^2J_{TeH}$ 97 Hz	*H* in 5-position
7.90	ddd, 1H, ^3J 3.9 Hz, ^4J 1.2 Hz, ^5J 0.6 Hz	*H* in 3-position
7.69	dd, 1H, ^3J 7.0 Hz, ^3J 3.9Hz	*H* in 4-position
3.70	s, 1H, $^4J_{TeH}$ 8.9 Hz	C≡C–*H*

^{13}C{^{1}H} NMR:

143.9	CH	5-Ar*C*H	122.0	C_{ipso}	*C*–C≡C–H
137.0	CH	4-Ar*C*H	84.23	C_{quat}	*C*≡C–H
130.4	CH	3-Ar*C*H	83.59	CH	C≡*C*–H

^{125}Te NMR: 961.5 ddt, $^2J_{TeH}$ 97 Hz, $^3J_{TeH}$ 15.4 Hz, $^4J_{TeH}$ 8.9 Hz

5.3.7 Preparation of *trans*-[Pt(PBu$_3$)$_2$(C≡C-C$_4$H$_3$O)$_2$] (3.07)

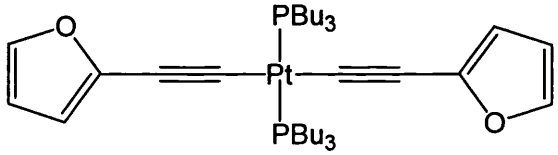

Trans-bis(tributylphosphine)platinum(II) chloride (250 mg, 0.37 mmol), copper iodide (~5 mg) and sodium methoxide (60 mg, 1.1 mmol) were placed in a Young's ampoule. Dichloromethane (10 mL), diisopropylamine (5 mL), **3.01** (153 mg, 0.93 mmol) and methanol (5 mL) were added and the resulting mixture left to stir at room temperature and in the absence of light for 15 h. Volatiles were removed under reduced pressure and the resulting pale orange solid eluted through a short plug of alumina with 4:1 hexane/ethyl acetate as eluant. The ^{1}H and ^{31}P NMR spectra of the resultant orange solid were recorded before recrystallisation from heptane attempted. Volatiles were again removed under reduced pressure leaving a yellow/brown oil which was purified by column chromatography (silica, 2:1, dichloromethane/hexane) affording **3.07** as a yellow solid (208 mg) in a 72% yield.

^{1}H NMR:

7.20	dd, 2H, ^3J 1.8 Hz, ^4J 0.8 Hz	5-Ar*H*

6.28	dd, 2H, ^3J 3.3 Hz, ^3J 1.8 Hz	4-Ar*H*
6.11	dd, 2H, ^3J 3.3 Hz, ^4J 0.8 Hz	3-Ar*H*
2.14 – 2.08	m, 12H	$P(CH_2CH_2CH_2CH_3)_3$
1.63 – 1.53	m, 12H	$P(CH_2CH_2CH_2CH_3)_3$
1.49 – 1.40	m, 12H	$P(CH_2CH_2CH_2CH_3)_3$
0.92	t, 18H, 7.24 Hz	$P(CH_2CH_2CH_2CH_3)_3$

$^{13}C\{^1H\}$ NMR:

141.4 C_{ipso}	*C*–C≡C–Pt	98.37 C_{quat}	*C*≡C–Pt
140.4 CH	5-Ar*C*H	26.31 CH_2	$P(CH_2CH_2CH_2CH_3)_3$
113.3 C_{quat}	C≡*C*–Pt	24.29 CH_2	$P(CH_2CH_2CH_2CH_3)_3$
110.2 CH	4-Ar*C*H	23.89 CH_2	$P(CH_2CH_2CH_2CH_3)_3$
109.3 CH	3-Ar*C*H	13.74 CH_3	$P(CH_2CH_2CH_2CH_3)_3$

$^{31}P\{^1H\}$ NMR: 5.42 ($^1J_{PtP}$ 2327 Hz)

$^{195}Pt\{^1H\}$ NMR: -4713 ($^1J_{PtP}$ 2327 Hz)

UV (CH_2Cl_2) $\underline{\lambda_{max}}$ [nm] (ε, mol^{-1} dm^3 cm^{-1}):

263 (24,800), 284 (19,700), <u>340</u> (32,600).

5.3.8 Preparation of *trans*-[$Pt(PBu_3)_2(C{\equiv}C\text{-}C_4H_3S)_2$] (3.08)

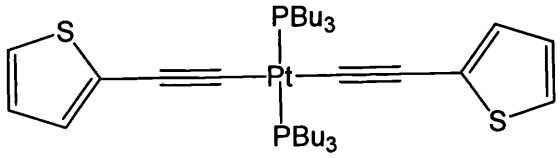

Trans-bis(tributylphosphine)platinum(II) chloride (250 mg, 0.37 mmol), copper iodide (5 mg) and sodium methoxide (60 mg, 1.1 mmol) were placed in a Young's ampoule. Dichloromethane (10 mL), diisopropylamine (5 mL), 2-(trimethylsilyl ethynyl)thiophene (146 mg, 0.81 mmol) and methanol (5 mL) were added and the resulting mixture left to stir at room temperature and in the absence of light for 48 h. Volatiles were removed under reduced pressure and the resulting yellow solid eluted through a short plug of alumina with 4:1 hexane/ethyl acetate as eluant. Recrystallisation from heptane afforded **3.08** as pale yellow crystals (243 mg) in an 80% yield.

^{1}H NMR:

6.97	dd, 2H, ^3J 5.3 Hz, ^4J 1.2 Hz	5-Ar*H*
6.86	dd, 2H, ^3J 5.3 Hz, ^3J 3.5 Hz	4-Ar*H*
6.84	dd, 2H, ^3J 3.5 Hz, ^4J 1.2 Hz	3-Ar*H*
2.15 – 2.08	m, 12H	$P(CH_2CH_2CH_2CH_3)_3$
1.64 – 1.55	m, 12H	$P(CH_2CH_2CH_2CH_3)_3$
1.51 – 1.42	m, 12H	$P(CH_2CH_2CH_2CH_3)_3$
0.93	t, 18H, 7.20 Hz	$P(CH_2CH_2CH_2CH_3)_3$

^{13}C{^{1}H} NMR:

129.9	C_{ipso}	*C*–C≡C–Pt	100.9	C_{quat}	*C*≡C–Pt
126.9	CH	5-Ar*C*H	26.23	CH_2	$P(CH_2CH_2CH_2CH_3)_3$
126.4	CH	4-Ar*C*H	24.37	CH_2	$P(CH_2CH_2CH_2CH_3)_3$
122.5	CH	3-Ar*C*H	23.97	CH_2	$P(CH_2CH_2CH_2CH_3)_3$
113.6	C_{quat}	C≡*C*–Pt	13.81	CH_3	$P(CH_2CH_2CH_2CH_3)_3$

^{31}P{^{1}H} NMR: 5.73 ($^1J_{PtP}$ 2339 Hz)

^{195}Pt{^{1}H} NMR: -4702 ($^1J_{PtP}$ 2339 Hz)

UV (CH_2Cl_2) $\underline{\lambda_{max}}$ [nm] (ε, mol^{-1} dm^3 cm^{-1}):

268 (15,200), 295 (20,600), <u>349</u> (33,100).

Emission (CH_2Cl_2): 371 nm

IR (KBr Disc): 2093 cm^{-1} ν(C≡C)

Elemental Analysis:

Calcd for $C_{36}H_{60}P_2PtS_2$ (%): C 53.12; H 7.43. Found (%): C 53.3; H 7.51.

5.3.9 Preparation of *trans*-[Pt(PBu$_3$)$_2$(C≡C-C$_4$H$_3$Se)$_2$] (3.09)

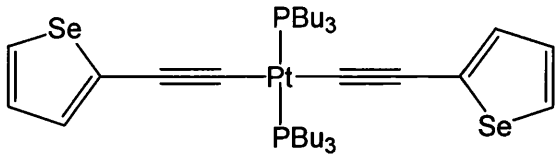

Trans-bis(tributylphosphine)platinum(II) chloride(250 mg, 0.37 mmol), copper iodide (5 mg) and sodium methoxide (60 mg, 1.11 mmol) were placed in a Young's ampoule.

Dichloromethane (10 mL), diisopropylamine (5 mL), **3.03** (212 mg, 0.93 mmol) and methanol (5 mL) were added and the resulting mixture left to stir at room temperature and in the absence of light for 48 h. Volatiles were removed under reduced pressure and the resulting yellow/brown oil eluted through a short plug of alumina with 4:1 hexane/ethyl acetate as eluant. Recrystallisation was attempted from ethanol/chloroform, no solid afforded. Volatiles were again removed under reduced pressure leaving a yellow/brown oil which was purified by column chromatography (silica, 2:1, dichloromethane/hexane) affording **3.09** as a yellow solid (259 mg) in a 77% yield.

^{1}H NMR:

7.66	dd, 2H, ^{3}J 5.7 Hz, ^{4}J 1.0 Hz, $^{2}J_{SeH}$ 44 Hz	5-Ar*H*
7.08	dd, 2H, ^{3}J 5.7 Hz, ^{3}J 3.7 Hz	4-Ar*H*
6.97	dd, 2H, ^{3}J 3.7 Hz, ^{4}J 1.0 Hz	3-Ar*H*
2.12 – 2.06	m, 12H	$P(CH_2CH_2CH_2CH_3)_3$
1.62 – 1.55	m, 12H	$P(CH_2CH_2CH_2CH_3)_3$
1.49 – 1.42	m, 12H	$P(CH_2CH_2CH_2CH_3)_3$
0.93	t, 18H, 7.20 Hz	$P(CH_2CH_2CH_2CH_3)_3$

^{13}C{^{1}H} NMR:

134.6	C_{ipso}	*C*–C≡C–Pt		103.7	C_{quat}	($^{2}J_{PtC}$ 275 Hz) *C*≡C–Pt
129.1	CH	5-Ar*C*H		26.35	CH_2	$P(CH_2CH_2CH_2CH_3)_3$
128.8	CH	4-Ar*C*H		24.39	CH_2	$P(CH_2CH_2CH_2CH_3)_3$
127.8	CH	J_{SeC} 114 Hz	3-Ar*C*H	23.82	CH_2	$P(CH_2CH_2CH_2CH_3)_3$
116.8	C_{quat}	C≡*C*–Pt		13.83	CH_3	$P(CH_2CH_2CH_2CH_3)_3$

^{31}P{^{1}H} NMR: 5.91 $^{1}J_{PtP}$ 2338 Hz

^{195}Pt{^{1}H} NMR: -4688 $^{1}J_{PtP}$ 2338 Hz, $^{4}J_{PtSe}$ 27.0 Hz

^{77}Se NMR: 665.7 $^{2}J_{SeH}$ 44 Hz, $^{3}J_{SeH}$ 7 Hz, $^{5}J_{SeP}$ 4.7 Hz, $^{4}J_{PtSe}$ 27.0 Hz

UV (CH_2Cl_2) $\underline{\lambda_{Max}}$ [nm] (ε, mol^{-1} dm^{3} cm^{-1}):

269 (28,600), 298 (23,000), 343 sh (36,600), <u>357</u> (42,100)

Emission (CH_2Cl_2): 379 nm

IR (KBr Disc): 2082 cm^{-1} ν(C≡C)

5.3.10 Preparation of *trans*-[Pt(PBu$_3$)$_2$(C≡C-C$_4$H$_3$Te)$_2$] (3.10)

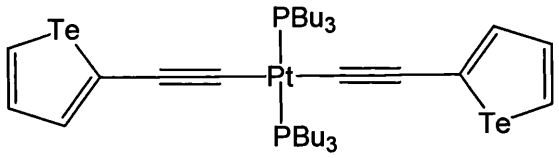

Trans-bis(tributylphosphine)platinum(II) chloride (150 mg, 0.22 mmol), copper iodide (5 mg) and sodium methoxide (36 mg, 0.67 mmol) were placed in a Young's ampoule. Dichloromethane (10 mL), diisopropylamine (5 mL), **3.04** (154 mg, 0.56 mmol) and methanol (5 mL) were added and the resulting mixture left to stir at room temperature and in the absence of light for 48 h. Volatiles were removed under reduced pressure and the resulting yellow/brown oil eluted through a short plug of alumina with hexane/ethyl acetate (4:1) as eluant. Volatiles were removed under reduced pressure again and the yellow oil purified by column chromatography (silica, 2:1, dichloromethane/hexane) affording **3.10** as a yellow solid (164 mg) in a 74% yield.

^{1}H NMR:

8.59	dd, 2H, ^3J 6.9 Hz, ^4J 0.4 Hz, $^2J_{TeH}$ 92.5 Hz	5-Ar*H*
7.51	dd, 2H, ^3J 6.9 Hz, ^3J 3.9 Hz	4-Ar*H*
7.32	dd, 2H, ^3J 3.9 Hz, ^4J 0.4 Hz	3-Ar*H*
2.09 – 2.02	m, 12H	P(C*H*$_2$CH$_2$CH$_2$CH$_3$)$_3$
1.62 – 1.54	m, 12H	P(CH$_2$C*H*$_2$CH$_2$CH$_3$)$_3$
1.50 – 1.41	m, 12H	P(CH$_2$CH$_2$C*H*$_2$CH$_3$)$_3$
0.94	t, 18H, 7.20 Hz	P(CH$_2$CH$_2$CH$_2$C*H*$_3$)$_3$

^{13}C{^{1}H} NMR:

137.1	CH	5-Ar*C*H	109.0	C_{quat}	*C*≡C–Pt
136.9	CH	4-Ar*C*H	26.34	CH_2	P(*C*H$_2$CH$_2$CH$_2$CH$_3$)$_3$
131.0	C_{ipso}	*C*–C≡C–Pt	24.48	CH_2	P(CH$_2$*C*H$_2$CH$_2$CH$_3$)$_3$
123.2	CH	$^2J_{TeC}$ 302 Hz 3-Ar*C*H	23.83	CH_2	P(CH$_2$CH$_2$*C*H$_2$CH$_3$)$_3$
119.7	C_{quat}	C≡*C*–Pt	13.91	CH_3	P(CH$_2$CH$_2$CH$_2$*C*H$_3$)$_3$

^{31}P{^{1}H} NMR: 6.29 $^1J_{PtP}$ 2343 Hz

^{195}Pt{^{1}H} NMR: -4671 $^1J_{PtP}$ 2343 Hz, $^4J_{PtTe}$ 56.6 Hz

^{125}Te NMR: 890.5 $^2J_{TeH}$ 92.5 Hz, $^3J_{TeH}$ 15.0 Hz, $^5J_{TeP}$ 9.3 Hz, $^4J_{PtTe}$ 56.6 Hz

UV (CH_2Cl_2) λ_{max} [nm] (ε, mol^{-1} dm^3 cm^{-1}):

275 (21,300), 298 (21,800), 361 (26,900), 371 (26,800).

Emission (CH_2Cl_2): 403 nm

IR (KBr Disc): 2074 cm^{-1} ν(C≡C)

5.3.11 Preparation of $Ph_3PAuCC\text{-}2\text{-}C_4H_3S$ (3.11)

General Procedure B; Triphenylphosphinegold(I) chloride (100 mg, 0.202 mmol) and 2-(trimethylsilylethynyl) thiophene (40.1 mg, 0.222 mmol, 1.1 eq). Recrystallisation from methanol afforded **3.11** as pale yellow needles (81.9 mg, 72%).

^{1}H NMR:

7.58 – 7.43	m, 15 H	$P(C_6H_5)_3$
7.16	dd, 1H, ^3J 3.5 Hz, ^4J 1.2 Hz	5-Ar*H*
7.09	dd, 1H, ^3J 5.3 Hz, ^3J 1.2 Hz	3-Ar*H*
6.89	dd, 1H, ^3J 5.3 Hz, ^4J 3.5 Hz	4-Ar*H*

$^{13}C\{^1H\}$ NMR:

134.4	CH	d, 13.8 Hz	$P(C_6H_5)_3$	129.3	C_{ipso}	*C*–C≡C–Au	
131.5	CH	d, 1.80 Hz	$P(C_6H_5)_3$	129.1	CH	d, 11.0 Hz	$P(C_6H_5)_3$
131.1	CH	3-Ar*C*H		126.5	CH	4-Ar*C*H	
129.9	C_{ipso}	$P(C_6H_5)_3$		125.1	CH	5-Ar*C*H	

$^{31}P\{^1H\}$ NMR: 42.28

UV (CH_2Cl_2) λ_{max} [nm] (ε, mol^{-1} dm^3 cm^{-1}):

268 sh (16,900), 276 sh (20,400), 287 sh (23,940), 297 (29,300), 310 sh (21,480).

Emission (CH_2Cl_2): 368 nm

IR (KBr Disc): 2104 cm^{-1} ν(C≡C)

Elemental analysis:

Calcd for $C_{24}H_{18}AuPS$ (%): C 50.89; H 3.20. Found (%): C 50.90; H 3.26.

5.3.12 Preparation of $Ph_3PAuCC\text{-}2\text{-}C_4H_3Se$ (3.12)

General Procedure B: Triphenylphosphinegold(I) chloride (107 mg, 0.20 mmol) and **3.03** (52.0 mg, 0.22 mmol). Recrystallisation from methanol/chloroform (1:1) afforded **3.12** as orange crystals (53.7 mg, 40%).

^{1}H NMR:

7.80	dd, 1H, ^3J 5.7 Hz, ^4J 1.0 Hz, $^2J_{SeH}$ 45.2 Hz	5-Ar*H*
7.58 – 7.43	m, 15H	P(C_6H_5)$_3$
7.34	dd, 1H, ^3J 3.7 Hz, ^4J 1.0 Hz	3-Ar*H*
7.12	dd, 1H, ^3J 5.7 Hz, ^3J 3.7 Hz	4-Ar*H*

^{13}C{^{1}H} NMR:

134.3	CH	d, 13.8 Hz	P(C_6H_5)$_3$	129.4	C_{ipso}	*C*–C≡C–Au	
133.4	CH	3-Ar*C*H		129.2	CH	5-Ar*C*H	
131.6	CH	d, 1.80 Hz	P(C_6H_5)$_3$	129.1	CH	d, 11.0 Hz	P(C_6H_5)$_3$
130.7	CH	4-Ar*C*H		98.43	C_{quat}	*C*≡C–Au	
129.9	C_{ipso}	P(C_6H_5)$_3$					

^{31}P{^{1}H} NMR: 42.38

^{77}Se{^{1}H} NMR: 689.0

UV (CH_2Cl_2) $\underline{\lambda_{max}}$ [nm] (ε, mol^{-1} dm^3 cm^{-1}):

269 (13,740), 275 (14,260), <u>305</u> (20,080), 319 (16,820).

Emission (CH_2Cl_2): 361 nm

IR (KBr Disc): 2090 cm^{-1} ν(C≡C)

Elemental Analysis:

Calcd for $C_{24}H_{18}AuPSe$ (%): C 47.00; H 2.96. Found (%): C 46.60; H 2.95.

5.3.13 Preparation of 2-(triethylphosphinegoldethynyl)thiophene (3.13)

General Procedure B; Triethylphosphinegold(I) chloride (103 mg, 0.294 mmol) and 2-ethynythiophene (38.2 mg, 0.350 mmol). Recrystallisation from methanol afforded **3.13** as pale yellow crystals (48.5 mg, 39%).

^{1}H NMR:

7.13	dd, 1H, ^3J 3.5 Hz, ^4J 1.0 Hz	5-Ar*H*
7.07	dd, ^3J 5.5 Hz, ^3J 1.0 Hz	3-Ar*H*
6.87	dd, ^3J 5.5 Hz, ^4J 3.5 Hz	4-Ar*H*
1.85 – 1.77	m, 6H	$P(CH_2CH_3)_3$
1.25 – 1.16	m, 9H	$P(CH_2CH_3)_3$

^{13}C{^{1}H} NMR:

130.9	CH	3-Ar*C*H	95.98	C_{quat}	*C*≡C–Au
126.5	CH	4-Ar*C*H	17.84	CH_2	d, $^1J_{PC}$ 33.1 Hz $P(CH_2CH_3)_3$
125.4	C_{ipso}	*C*–C≡C–Au	8.810	CH_3	$P(CH_2CH_3)_3$
124.9	CH	5-Ar*C*H			

^{31}P{^{1}H} NMR: 38.19

UV (CH_2Cl_2) $\underline{\lambda_{max}}$ [nm] (ε, mol^{-1} dm^3 cm^{-1}):

255 sh (12,140), 265 (16,920), <u>289</u> (17,220), 297 sh (16,220).

Emission (CH_2Cl_2): 446 nm

IR (KBr Disc): 2093 cm^{-1} ν(C≡C)

Elemental analysis:

Calcd for $C_{12}H_{18}AuPS$ (%): C 34.13; H 4.30. Found (%): C 33.80; H 4.34.

5.4 Experimental for chapter 4

5.4.1 Preparation of 1,2-Bis(5'-Bromo-2'-thienyl)ethene (4.01)

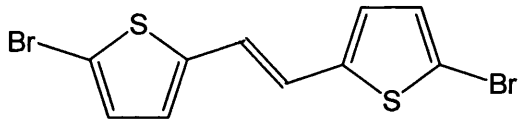

(Tetrahydrofuran)titanium(IV) chloride[2] (6.01 g, 18.0 mmol) was placed in a Schlenk tube and dissolved in tetrahydrofuran (60 mL). The solution was cooled to –18 °C, 5-bromo-2-thiophenecarbaldehyde[4] (1.80 mL, 15.0 mmol) added and the resulting mixture left to stir at – 18 °C for 30 min. Zinc powder (2.34 g, 36.0 mmol) was carefully added in small amounts, the mixture again left to stir at – 18 °C for 30 min then allowed to warm to room temperature. The mixture was heated at 60 °C overnight (~15 h), after this time TLC (silica, 2:1 (v/v), hexane/dichloromethane) showed the reaction to be complete. The mixture was poured onto ice (100 mL) and the resulting light brown precipitate filtered. The solid was dissolved in dichloromethane and filtered to leave insoluble inorganic salts behind. Volatiles were removed under reduced pressure leaving a pale yellow/orange solid. Recrystallisation from methanol afforded **4.01** as a pale yellow/brown solid (1.65 g, 63%; mp 119 – 121 °C).

^{1}H NMR:

6.94	d, 2H, ^3J 3.7 Hz	thiophene 4-C*H*
6.80	s, 2H	alkene C*H*
6.77	d, 2H, ^3J 3.7 Hz	thiophene 3-C*H*

^{13}C{^{1}H} NMR:

143.6	C_{ipso}	*C*–CH=CH	121.1	CH	thiophene 3-*C*H
130.6	CH	thiophene 4-*C*H	111.5	C_{quat}	*C*–Br
126.5	CH	*C*H=*C*H			

UV (CH_2Cl_2) $\underline{\lambda_{max}}$ [nm] (ε, mol^{-1} dm^3 cm^{-1}):

261 (6,780), 343 sh (31,620), <u>359</u> (39,180), 377 sh (27,580).

Emission (CH_2Cl_2): 421 nm

IR (KBr Disc): 1442 cm^{-1} ν(C=C), 804 cm^{-1} (C–Br)

5.4.2 Preparation of 1,2-Bis(5'-Trimethylsilylethynyl-2'-thienyl)ethene (4.02)

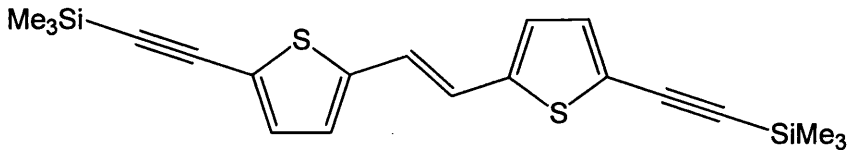

4.01 (699 mg, 2.00 mmol), bis(triphenylphosphine) palladium(II) chloride (85.2 mg, 0.12 mmol) and copper iodide (11.4 mg, 0.06 mmol) were placed in a Young's ampoule. Tetrahydrofuran (20 mL), triethylamine (10 mL) and trimethylsilylacetylene (0.62 mL, 4.40 mmol) were added and the resulting mixture left to stir at room temperature and in the absence of light for one hour. After this time, TLC (silica, 4:1 (v/v), hexane/dichloromethane) showed the reaction to be complete. Volatiles were removed under reduced pressure leaving a yellow/brown solid, which was eluted through a short plug of alumina with hexane/ethyl acetate (4:1) as eluant. Volatiles were again removed under reduced pressure leaving a bright yellow solid. Recrystallisation from heptane afforded **4.02** as yellow gold flakes (626 mg, 81%; mp 199 – 201 °C).

^{1}H NMR:

7.10	d, 2H, ^3J3.7 Hz	thiophene 4-C*H*
6.96	s, 2H	alkene C*H*=C*H*
6.88	d, 2H, ^3J3.7 Hz	thiophene 3-C*H*
0.25	s, 18H	Si(C*H*$_3$)$_3$

^{13}C {^{1}H} NMR:

143.5	C_{ipso}	*C*–CH=CH	121.8	CH	thiophene 3-*C*H
133.4	CH	*C*H=*C*H	100.5	C_{quat}	*C*≡C–Si
126.4	CH	thiophene 4-*C*H	97.71	C_{quat}	C≡*C*–Si
122.1	C_{ipso}	*C*–C≡C–Si	-0.167	CH_3	Si(*C*H$_3$)$_3$

UV (CH_2Cl_2) λ_{max} [nm] (ε,mol^{-1} dm^3 cm^{-1}):

281 (6,320), 376 sh (40,200), 395 (54,520), 419 (41,720).

Emission (CH_2Cl_2): 459 nm, 435 nm (sh).

IR (KBr Disc): 2141 cm^{-1} ν(C≡C), 1457 cm^{-1} ν(C=C)

Elemental Analysis:

Calcd for $C_{20}H_{24}S_2Si_2$ (%): C 62.44; H 6.29. Found (%): C 62.66; H 6.26.

5.4.3 Preparation of 1,2-Bis(5'-Ethynyl-2'-thienyl)ethene (4.03)

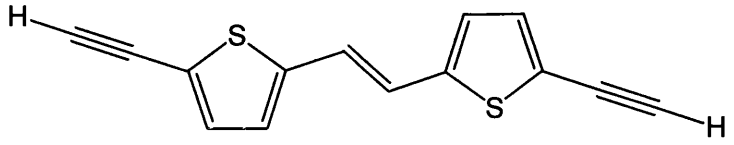

4.02 (249 mg, 0.650 mmol) was dissolved in methanol/dichloromethane (1:1, v/v, 10 mL). 2.0 M potassium hydroxide solution (1 mL, 2 mmol) was added and the resulting mixture left to stir at room temperature and in the absence of light for one hour. After this time, TLC (silica, 4:1, hexane/dichloromethane) showed the reaction to be complete. Volatiles were removed under reduced pressure and the product extracted with dichloromethane. The CH_2Cl_2 layer was dried ($MgSO_4$) and volatiles again removed under reduced pressure leaving a brown solid which was eluted through a short plug of silica with hexane/dichloromethane (4:1) as eluant. Volatiles were removed under reduced pressure affording **4.03** as an orange solid (120 mg, 77 %).

^{1}H NMR:

7.08	d, 2H, ^3J 3.7 Hz	thiophene 4-C*H*
6.87	s, 2H	alkene C*H*=C*H*
6.84	d, 2H, ^3J 3.7 Hz	thiophene 3-C*H*
3.36	s, 2H	alkyne C–*H*

^{13}C{^{1}H} NMR:

143.6	C_{ipso}	*C*–CH=CH	120.9	C_{ipso}	*C*–C≡C–H
133.8	CH	*C*H=*C*H	82.55	CH	C≡*C*–H
126.3	CH	thiophene 4-*C*H	77.14	C_{quat}	*C*≡C–H
121.8	CH	thiophene 3-*C*H			

Elemental Analysis:

Calcd for $C_{14}H_8S_2$ (%): C 69.96; H 3.36. Found (%): C 69.90; H 3.36.

5.4.4 Preparation of 5-Bromoselenophene-2-carbaldehyde (4.04)

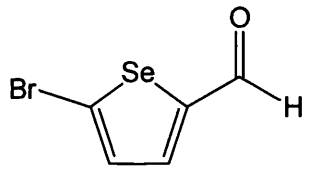

2,5-Dibromoselenophene[19] (1.00 g, 3.46 mmol) was dissolved in tetrahydrofuran (30 mL) and the solution cooled to -78 °C. To this mixture was added ^{n}butyllithium (2.62 M in hexane, 1.32 mL). After 5 min stirring at -78 °C the mixture was allowed to come to -10 °C for 10 min before returning to -78 °C. *N,N*-dimethylformamide (0.40 mL, 5.19 mmol) was added drop wise and the resulting mixture left to stir for 30 min at -78 °C before it was allowed to warm to room temperature. After stirring overnight (~ 15 h) TLC (silica, hexane) showed the reaction to be complete. The reaction mixture was quenched with saturated aqueous ammonium chloride (10 mL) and volatiles removed under reduced pressure. The resulting yellow oil was washed with further saturated ammonium chloride and the product extracted with ether. The ether layer was dried ($MgSO_4$), filtered and volatiles again removed under reduced pressure leaving an orange oil which was purified by column chromatography (silica, 2:1, hexane/dichloromethane) affording **4.04** as a yellow oil (282 mg, 34%).

^{1}H NMR:

9.71	s, $^{3}J_{SeH}$ 8.4 Hz	aldehyde CO*H*
7.71	d, ^{3}J 4.3 Hz	selenophene 3-C*H*
7.43	d, ^{3}J 4.3 Hz	selenophene 4-C*H*

^{13}C {^{1}H} NMR:

183.3	CH	aldehyde *C*OH	139.2	CH	selenophene 4-*C*H
151.7	C_{ipso}	*C*–COH	134.5	CH	selenophene 3-*C*H

^{77}Se{^{1}H} NMR: 684

5.4.5 Preparation of 1,2-Bis(5'-Bromo-2'-selenyl)ethene (4.05)

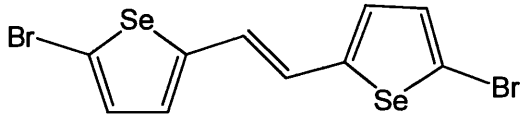

(Tetrahydrofuran)titanium(IV) chloride (421 mg, 1.26 mmol) was placed in a Schlenk tube and dissolved in tetrahydrofuran (30 mL). The solution was cooled to –18 °C, **4.04** (223 mg, 0.94 mmol) added and the resulting mixture left to stir at – 18 °C for 30 min. Zinc powder (165 mg, 2.52 mmol) was carefully added in small amounts, the mixture again left to stir at – 18 °C for 30 min then allowed to warm to room temperature. The mixture was heated at 60 °C overnight (~15 h), after this time TLC (silica, 1:2, hexane/dichloromethane) showed the reaction to be complete. The mixture was poured onto ice (100 mL) and the resulting yellow/orange precipitate filtered. The solid was dissolved in dichloromethane and filtered to leave insoluble inorganic salts behind. Volatiles were removed under reduced pressure leaving a pale yellow/orange solid which was eluted through a short plug of silica with hexane/dichloromethane (1:2) as eluant affording **4.05** as a green solid (68 mg, 42%; mp 157 – 159 °C).

^{1}H NMR:

7.12	d, 2H, ^{3}J 4.1 Hz, $^{3}J_{SeH}$ 25.6 Hz	selenophene 4-C*H*
6.87	d, 2H, ^{3}J 4.1 Hz	selenophene 3-C*H*
6.75	s, 2H	alkene C*H*=C*H*

^{13}C{^{1}H} NMR:

149.8	C_{ipso}	*C*–CH=CH	124.7	CH	selenophene 4-*C*H
133.7	CH	selenophene 4-*C*H	114.2	*C*–Br	
129.0	CH	alkene *C*H=*C*H			

^{77}Se{^{1}H} NMR: 648.0

UV (CH_2Cl_2) $\underline{\lambda_{max}}$ [nm] (ε, mol^{-1} dm^3 cm^{-1}):
<u>279</u> (3,420), 324 (2,500).

Emission (CH_2Cl_2): 333 nm (sh), 357 nm, 375 nm (sh)

IR (KBr Disc): 1452 cm^{-1} ν(C=C), 802 cm^{-1} (C–Br)

5.4.6 Preparation of 1,2-Bis(5'-Trimethylsilylethynyl-2'-selenyl)ethene (4.06)

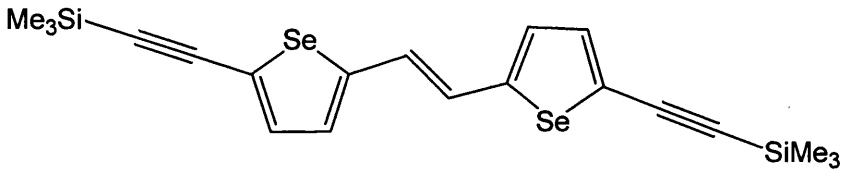

4.05 (50 mg, 0.11 mmol), bis(triphenylphosphine) palladium(II) chloride (9.5 mg, 0.01 mmol)) and copper iodide (2 mg, 0.01 mmol) were placed in a Young's ampoule. Tetrahydrofuran (15 mL), diethylamine (5 mL) and trimethylsilylacetylene (0.10 mL, 0.34 mmol) were added and the resulting mixture left to stir at room temperature and in the absence of light overnight. After this time, TLC (silica, 4:1, hexane/ethyl acetate) showed the reaction to be complete. Volatiles were removed under reduced pressure leaving a yellow/brown solid, which was eluted through a short plug of alumina with hexane/ethyl acetate (4:1) as eluant. Volatiles were again removed under reduced pressure leaving a yellow/orange solid. Recrystallisation from heptane/dichloromethane (1:1) afforded **4.06** as gold flakes (40.3 mg, 75%; 224 – 226 °C).

^{1}H NMR:

7.26	d, 2H, ^{3}J 3.9 Hz	selenophene 4-C*H*
7.03	d, 2H, ^{3}J 3.9 Hz	selenophene 3-C*H*
6.87	s, 2H	alkene C*H*=C*H*
0.25	s, 18H	Si(CH_3)$_3$

^{13}C{^{1}H} NMR:

149.9	C_{ipso}	*C*–CH=CH	125.3	CH	selenophene 3-*C*H
135.9	CH	selenophene 4-*C*H	102.4	C_{quat}	*C*≡C–Si(CH$_3$)$_3$
129.3	CH	alkene *C*H=*C*H	99.86	C_{quat}	C≡*C*–Si(CH$_3$)$_3$
125.7	C_{ipso}	*C*–C≡C–Si	-0.167	Si(*C*H$_3$)$_3$	

^{77}Se{^{1}H} NMR: 655.6

UV (CH_2Cl_2) $\underline{\lambda_{max}}$ [nm] (ε, mol^{-1} dm^3 cm^{-1}):

<u>307</u> (17,260), 357 (13,080), 386 (14,320), 408 (15,580), 435 (10,820).

Emission (CH_2Cl_2): 461 nm

IR (KBr Disc): 2134 ν(C≡C), 1463 cm^{-1} ν(C=C).

Elemental Analysis:

Calcd for $C_{20}H_{24}Se_2Si_2$ (%): C 50.20; H 5.06. Found (%): C 50.80; H 5.06.

5.4.7 Preparation of 1-(5-bromo-2-thienyl)-2-(5-bromo-2-selenyl)ethene (4.07)

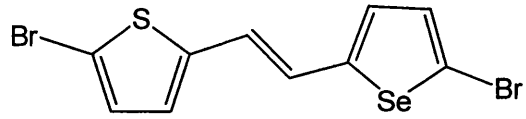

Triphenyl-(5-bromo-2-thienyl)phosphonium chloride (227 mg, 0.63 mmol) and **4.04** (125 mg, 0.53 mmol) were placed in a flask and dissolved in anhydrous methanol solution (20 mL). The resulting mixture was heated to boiling under a flow of N_2 and sodium methoxide (30 mg, 0.56 mmol) in methanol (2 mL) was added. The yellow mixture was heated under reflux overnight after which time TLC (silica, 4:1, hexane/dichloromethane) showed the reaction to be complete. On cooling an orange precipitate formed. Volatiles were removed under reduced pressure and the resulting orange solid was eluted through a short plug of silica with hexane/dichloromethane (4:1) as eluant. ^{1}H NMR showed unreacted aldehyde. Solid was redissolved in anhydrous methanol (20 mL). Triphenyl-(5-bromo-2-thienyl)phosphonium chloride (120 mg, 0.33 mmol) and sodium methoxide (30 mg, 0.56 mmol) were added and the mixture heated under reflux overnight. The yellow mixture was allowed to cool yielding a pale orange precipitate which was filtered and dried affording **4.07** as pale orange flakes (130 mg, 63%; mp 133 – 135 °C).

^{1}H NMR:

7.13	d, 1H, ^3J 4.1 Hz	selenophene 4-C*H*
6.93	d, 1H, ^3J 3.9 Hz	thiophene 4-C*H*
6.87	d, 1H, $^3J_{trans}$ 15.9 Hz	alkene C*H*–selenophene
6.86	d, 1H, ^3J 4.1 Hz	selenophene 3-C*H*
6.77	d, 1H, ^3J 3.9 Hz	thiophene 3-C*H*
6.68	d, 1H, $^3J_{trans}$ 15.9 Hz	alkene C*H*–thiophene

^{13}C{^{1}H} NMR:

149.8	C_{ipso}	*C*–CH=CH (selenophene)	126.6	CH	selenophene 3-*C*H
143.6	C_{ipso}	*C*–CH=CH (thiophene)	123.8	CH	alkene *C*H–thiophene
133.6	CH	selenophene 4-*C*H	122.1	CH	thiophene 3-*C*H
130.6	CH	thiophene 4-*C*H	114.1	C_{ipso}	*C*–Br thiophene ring
128.9	CH	alkene *C*H–selenophene	111.5	C_{ipso}	*C*–Br selenophene ring

$^{77}Se\{^{1}H\}$ NMR: 647

UV (CH_2Cl_2) λ_{max} [nm] (ε, mol^{-1} dm^3 cm^{-1}):

274 (5,100), 348 (18,940), 365 (23,800), 383 (17,040).

Emission (CH_2Cl_2): 429 nm

IR (KBr Disc): 1447 cm^{-1} ν(C=C), 803 cm^{-1} (C–Br)

Elemental Analysis:

Calcd for $C_{10}H_6Br_2SSe$ (%): C 30.25; H 1.52. Found (%): C 30.60; H 1.63.

5.4.8 Preparation of 1-(5-trimethylsilylethynyl-2-thienyl)-2-(5-trimethylsilylethynyl-2-selenyl)ethene (4.08)

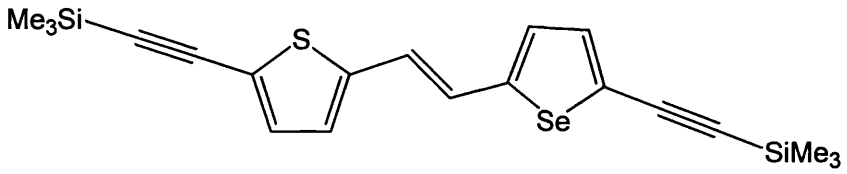

4.07 (51.0 mg, 0.13 mmol), bis(triphenylphosphine)palladium(II) chloride (11.0 mg, 0.02 mmol) and copper iodide (2 mg, 0.01 mmol) were placed in a Young's ampoule and dissolved in tetrahydrofuran (10 mL) and diethylamine (5 mL). Trimethylsilylacetylene (0.05 mL, 0.32 mmol) was added and the resulting mixture left to stir at room temperature and in the absence of light overnight. Volatiles were removed under reduced pressure leaving a yellow/gold solid, which was eluted through a short plug of alumina with hexane/ethyl acetate (9:1) as eluant affording **4.08** as a yellow/gold solid (53.0 mg, 96%; 205 – 208 °C).

^{1}H NMR:

7.09	d, 1H, ^{3}J 3.7 Hz	selenophene 4-C*H*
7.02	d, 1H, ^{3}J 4.1 Hz	thiophene 4-C*H*
6.99	d, 1H, ^{3}J 4.1 Hz	thiophene 3-C*H*
6.97	d, 1H, $^{3}J_{trans}$ 15.7 Hz	alkene C*H*-selenophene
6.88	d, 1H, ^{3}J 3.7 Hz	selenophene 3-C*H*
6.81	d, 1H, $^{3}J_{trans}$ 15.7 Hz	alkene C*H*-thiophene
0.25	s, 9H	$Si(CH_3)_3$
0.24	s, 9H	$Si(CH_3)_3$

$^{13}C\{^1H\}$ NMR:

149.9	C_{ipso}	*C*–CH=CH (selenophene)	122.6	CH	thiophene 3-*C*H
143.6	C_{ipso}	*C*–CH=CH (thiophene)	122.1	C_{ipso}	*C*–C≡C (thiophene)
135.8	CH	selenophene 4-*C*H	102.3	C_{quat}	C–*C*≡C–Si (selenophene)
133.5	CH	thiophene 4-*C*H	100.5	C_{quat}	selenophene-C≡*C*–Si(CH_3)$_3$
129.2	CH	alkene *C*H–selenophene	99.83	C_{quat}	C–*C*≡C–Si (thiophene)
126.4	CH	selenophene 3-*C*H	97.72	C_{quat}	thiophene-C≡*C*–Si(CH_3)$_3$
125.7	C_{ipso}	*C*–C≡C (selenophene)	-0.171	CH_3	Si(*C*H_3)$_3$
124.5	CH	alkene *C*H–thiophene			

$^{77}Se\{^1H\}$ NMR: 653.6

UV (CH_2Cl_2) λ_{max} [nm] (ε, mol^{-1} dm^3 cm^{-1}):

301 (8,460), 382 (13,920), 402 (17,180), 427 (12,500).

Emission (CH_2Cl_2): 447 nm (sh), 469 nm.

IR (KBr Disc): 2142 cm^{-1} ν(C≡C), 1454 cm^{-1} ν(C=C)

Elemental Analysis:

Calcd for $C_{20}H_{24}SSeSi_2$ (%): C 55.66; H 5.60. Found (%): C 55.30; H 5.55.

5.4.9 Preparation of Selenophene-2-carbaldehyde (4.09)

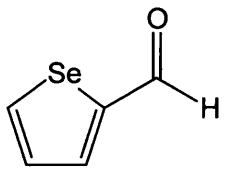

Selenophene (0.82 mL, 9.50 mmol) was dissolved in tetrahydrofuran (30 mL) and the solution cooled to -78 °C. To this mixture was added ^{n}butyllithium (2.62 M in hexane, 3.60 mL). After 5 min stirring at -78 °C the mixture was allowed to come to -10 °C for 10 min before returning to -78 °C. *N,N*-dimethylformamide (1.10 mL, 14.3 mmol) was added drop wise and the resulting mixture left to stir for 30 min at -78 °C before it was allowed to warm to room temperature. After stirring overnight (~ 15 h) TLC (silica, 4:1, hexane/dichloromethane) showed the reaction to be complete. The reaction mixture was quenched with saturated aqueous ammonium chloride (10 mL) and volatiles removed under reduced pressure. The resulting yellow oil was washed with further saturated

ammonium chloride and the product extracted with ether. The ether layer was dried ($MgSO_4$), filtered and volatiles again removed under reduced pressure affording **4.09** as a yellow oil (1.38 g, 91%). ^{1}H NMR was in accordance with literature.[21]

^{77}Se{^{1}H} NMR: 614.9

5.4.10 Preparation of 1,2-Bis(2'-selenyl)ethene (4.10)

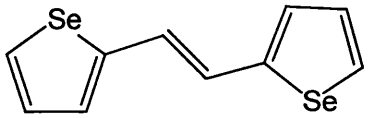

(Tetrahydrofuran)titanium(IV) chloride (2.52 g, 7.55 mmol) was placed in a Schlenk tube and dissolved in tetrahydrofuran (30 mL). The solution was cooled to –18 °C, **4.09** (1.00 g, 6.29 mmol) added and the resulting mixture left to stir at – 18 °C for 30 min. Zinc powder (0.99 g, 15.1 mmol) was carefully added in small amounts, the mixture again left to stir at – 18 °C for 30 min then allowed to warm to room temperature. The mixture was heated at 60 °C overnight (~15 h), after this time TLC (silica, 4:1, hexane/dichloromethane) showed the reaction to be complete. The mixture was poured onto ice (100 mL) and the resulting yellow precipitate filtered. The solid was dissolved in dichloromethane and filtered to leave insoluble inorganic salts behind. Volatiles were removed under reduced pressure leaving a yellow/orange solid. Recrystallisation from cyclohexane afforded **4.10** as an orange solid (0.497 g, 55%; mp 155 °C).

^{1}H NMR:

7.83	dd, 2H, ^3J5.5 Hz, ^4J 1.2 Hz, $^2J_{SeH}$ 48.5 Hz	selenophene 5-C*H*
7.21	dd, 2H, ^3J 5.5 Hz, ^3J 3.7 Hz	selenophene 4-C*H*
7.18	dd, 2H, ^3J3.7 Hz, ^4J 1.2 Hz	selenophene 3-C*H*
6.99	s, 2H	alkene C*H*

^{13}C{^{1}H} NMR:

148.4	C_{ipso}	*C*–CH=CH	128.8	CH	selenophene 4-*C*H
130.2	CH	alkene *C*H	125.1	CH	selenophene 3-*C*H
128.9	CH	$^2J_{CSe}$ 114.0 Hz 5-*C*H			

^{77}Se{^{1}H} NMR: 578

^{77}Se NMR: 578 (d, 47.9 Hz)

UV (CH_2Cl_2) $\underline{\lambda_{max}}$ [nm] (ε, mol^{-1} dm^3 cm^{-1}):

286 (10,300), 339 sh (22,520), <u>356</u> (29,040), 373 sh (21,100).

Emission (CH_2Cl_2): 420 nm

5.4.11 Preparation of 1-(2-thienyl)-2-(2-selenyl)ethene (4.11)

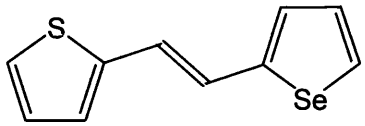

Triphenyl-thiophen-2-ylmethyl-phosphonium chloride (500 mg, 1.39 mmol) and **4.09** (288 mg, 1.81 mmol) were placed in a flask and dissolved in anhydrous methanol (20 mL). The mixture was heated to boiling under a flow of N_2 and sodium methoxide (75 mg, 1.39 mmol) in methanol (2 mL) was added. The yellow mixture was heated under reflux for 15 h and the progress of the reaction monitored by TLC. After 15 h the reaction had not progressed further than after the first hour and further Sodium methoxide (75 mg, 1.39 mmol) was added. The mixture was left heating under reflux for a further 15 h at which point the solution became orange. TLC (silica, 4:1, hexane/ dichloromethane) showed the reaction to be complete. On cooling a yellow precipitate formed. Volatiles were removed under reduced pressure and the resulting pale peach solid, was dissolved in diethyl ether and washed with water (3 × 20 mL) and dried ($MgSO_4$). Volatiles were again removed under reduced pressure and the resulting solid eluted through a short plug of silica with hexane/dichloromethane (4:1) as eluant. Recrystallisation from methanol afforded **4.11** as a pale yellow solid (237 mg, 71%; mp 142 °C).

^{1}H NMR:

7.82	d, 1H, ^3J 5.5 Hz, $^2J_{SeH}$ 48.1 Hz	selenophene 5-C*H*
7.21	dd, 1H, ^3J 5.5 Hz, ^3J 3.7 Hz	selenophene 4-C*H*
7.19 – 7.18	m, 2H	selenophene 3-C*H* & thiophene 5-C*H*
7.09	d, 1H, $^3J_{trans}$ 15.7 Hz	alkene C*H* (selenophene)
7.04	d, 1H, ^3J 3.5 Hz	thiophene 3-C*H*
6.99	dd, 1H, ^3J 5.1 Hz, ^3J 3.5 Hz	thiophene 4-C*H*
6.95	d, 1H, $^3J_{trans}$ 15.7 Hz	alkene C*H* (thiophene)

^{13}C{^{1}H} NMR:

148.4	C_{ipso}	selenophene*C*–CH=CH	127.7	CH	thiophene 5-*C*H

142.4	C_{ipso}	thiophene*C*–CH=CH	126.1	CH	selenophene 3-*C*H
137.9	CH	selenophene 4-*C*H	124.3	CH	alkene *C*H (thiophene)
130.2	CH	alkene *C*H (selenophene)	123.9	CH	thiophene 4-*C*H
128.8	CH d, $^2J_{CSe}$ 114 Hz	selenophene 5-*C*H	122.6	CH	thiophene 3-*C*H

^{77}Se NMR: 576.7 (ddd, $^2J_{SeH}$ 48.2 Hz, $^3J_{SeH}$ 18.4 Hz, $^3J_{SeH}$ 6.9 Hz)

UV (CH_2Cl_2) $\underline{\lambda_{max}}$ [nm] (ε, mol^{-1} dm^3 cm^{-1}):

283 (8,180), 334 (26,440), <u>349</u> (32,720), 365 (23,400).

Emission (CH_2Cl_2): 408 nm

IR (KBr Disc): 1441 cm^{-1} ν(C=C)

Elemental Analysis:

Calcd for $C_{10}H_8SSe$ (%): C 50.21; H 3.37. Found (%): C 50.40; H 3.41.

5.4.12 Preparation of 3,6-Dithia-*as*-indacene (4.12)

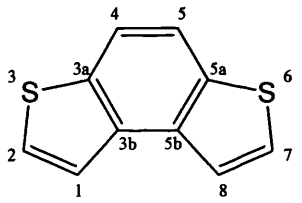

1,2-Bis(2'-thienyl)ethene[3] (205 mg, 1.07 mmol) was dissolved in benzene in a 100 mL capacity immersion photolysis vessel and irradiated for 2 h at room temperature by a broadband UV light source. After this time, iodine (136 mg, 0.54 mmol, 0.5 eq) was added and the mixture irradiated for 22 h at room temperature with a flow of air through the solution. Excess iodine was quenched by the addition of with aqueous saturated sodium thiosulphate solution (20 mL), the phases separated, the organic layer washed with water (3 × 30 mL) and dried ($MgSO_4$). Volatiles were removed under reduced pressure leaving a brown solid, which was sublimed at 40 °C (5 × 10^{-4} mbar). Recrystallisation from methanol afforded **4.12** as white flakes (155 mg, 77%). ^{1}H/^{13}C NMR consistent with literature.[22]

UV (CH_2Cl_2) $\underline{\lambda_{max}}$ [nm] (ε, mol^{-1} dm^3 cm^{-1}):

252 (20,180), 257 (17,820), 268 (11,580), 279 (16,200), <u>289</u> (24,200), 300 (19,140), 317 (3,540).

Emission (CH_2Cl_2): 333 nm

5.4.13 Preparation of 3-Thia-6-selena-*as*-indacene (4.13)

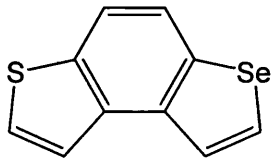

4.11 (100 mg, 0.421 mmol) and iodine (53.4 mg, 0.210 mmol) was dissolved in benzene in a 100 mL capacity immersion photolysis vessel and the resulting mixture irradiated for 22 h at room temperature by a broadband UV light source with a flow of air through the solution. Excess iodine was quenched by the addition of with aqueous saturated sodium thiosulphate solution (20 mL), the phases separated, the organic layer washed with water (3 × 30 mL) and dried ($MgSO_4$). Volatiles were removed under reduced pressure leaving a yellow/brown oil which was eluted through a short plug of silica with diethyl ether as eluant affording 4.13 as a yellow/brown solid (78.5mg, 79%; mp 112 – 115 °C).

^{1}H NMR:

8.15	d, 1H, ^3J 6.0 Hz, $^2J_{SeH}$ 47.5 Hz	indacene 7-C*H*
8.00	d, 1H, ^3J 6.0 Hz	indacene 8-C*H*
7.88	d, 1H, ^3J 8.4 Hz	indacene 5-C*H*
7.79	d, 1H, ^3J 8.4 Hz	indacene 4-C*H*
7.72	d, 1H, ^3J 5.6 Hz	indacene 2-C*H*
7.55	d, 1H, ^3J 5.6 Hz	indacene 1-C*H*

^{13}C{^{1}H} NMR:

138.2	C_{ipso}	indacene 3a-*C*	125.6	CH	indacene 8-*C*H
136.8	C_{ipso}	indacene 3b-*C*	122.1	CH	indacene 1-*C*H
136.3	C_{ipso}	indacene 5a-*C*	121.5	CH	indacene 5-*C*H
129.5	CH	indacene 7-*C*H	118.8	CH	indacene 4-*C*H
126.4	CH	indacene 2-*C*H			

^{77}Se NMR: 536.9 ddt, $^2J_{SeH}$ 47.1 Hz, $^3J_{SeH}$ 8.14, $^3J_{SeH}$ 5.52 Hz

UV (CH_2Cl_2) $\underline{\lambda_{max}}$ [nm] (ε, mol^{-1} dm^3 cm^{-1}):

<u>257</u> (11,060), 263 (10,800), 272 (7,260), 294 (10,020), 323 (3,380).

Emission (CH_2Cl_2): 372 nm

Elemental Analysis:

Calcd for $C_{10}H_6SSe$ (%): C 50.64; H 2.55. Found (%): C 51.10; H 3.04.

5.4.14 Preparation of 3,6-diselena-*as*-indacene (4.14)

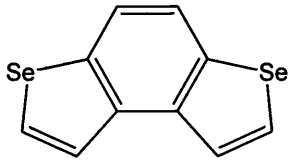

4.10 (100 mg, 0.35 mmol) and iodine (44.4 mg, 0.18 mmol) was dissolved in benzene in a 100 mL capacity immersion photolysis vessel and the resulting mixture irradiated for 22 hours at room temperature by a broadband UV light source with a flow of air through the solution. Excess iodine was quenched by the addition of with aqueous saturated sodium thiosulphate solution (20 mL), the phases separated, the organic layer washed with water (3 × 30 mL) and dried ($MgSO_4$). Volatiles were removed under reduced pressure leaving a green solid, which was eluted through a short plug of silica with hexane/dichloromethane (4:1) as eluant affording **4.14** as a yellow/brown solid (69.3 mg, 70%).

^{1}H NMR:

8.12	d, 2H, ^3J5.9 Hz, $^2J_{SeH}$ 47.2 Hz	indacene 2- & 7-C*H*
8.01	d, 2H, ^3J5.9 Hz	indacene 1- & 8-C*H*
7.84	s, 2H	indacene 4- & 5-C*H*

^{13}C{^{1}H} NMR:

138.5	C_{ipso}	indacene 3a- & 5a-*C*	125.9	CH	indacene 4- & 5-*C*H
129.4	CH	indacene 2- & 7-*C*H	121.7	CH	indacene 1- & 8-*C*H

^{77}Se NMR: 534.8 (dd, $^2J_{SeH}$ 47.1 Hz, $^3J_{SeH}$ 8.4 Hz)

UV/Vis (CH_2Cl_2) $\underline{\lambda_{max}}$ [nm] (ε, mol^{-1} dm^3 cm^{-1}):

263 (16,540), <u>269</u> (18,560), 289 (12,140), 299 (17,860), 311 (14,400), 329 (2,620).

Emission (CH_2Cl_2): 350 nm

Elemental Analysis:

Calcd for $C_{10}H_6Se_2$ (%): C 42.28; H 2.13. Found (%): C 42.10; H 2.16.

5.4.15 Preparation of 2,7-Diiodo-3-thia-6-selena-*as*-indacene (4.15)

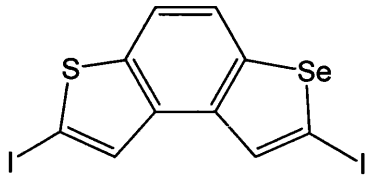

N,N,N',N'-Tetramethylethylenediamine (0.05 mL, 0.32 mmol) was placed in a Young's ampoule and dissolved in tetrahydrofuran (20 mL) and the solution cooled to –78 °C. ^{n}Butyllithium (2.59 M in hexane, 0.26 mL) was added drop wise and the mixture stirred for 10 min at –78 °C before addition of **4.13** (69.0 mg, 0.29 mmol) in tetrahydrofuran (10 mL) and the resulting mixture left to stir for a further 30 min at –78 °C. A tetrahydrofuran solution (10 mL) of iodine (210 mg, 0.83 mmol) was added slowly and the mixture allowed to warm to room temperature. After stirring overnight, TLC (silica, 4:1, hexane/dichloromethane) showed the reaction to be complete. Excess iodine was quenched by addition of saturated sodium thiosulphate solution (10 ml). Diethyl ether (10 mL) was added and the organic layer washed with water (3 × 30 mL) and dried ($MgSO_4$). Volatiles were removed under reduced pressure and the resulting yellow/brown oil eluted through a short plug of silica with diethyl ether as eluant affording **4.15** as a brown solid (69.1 mg, 49%).

^{1}H NMR:

8.14	s, 1H	indacene 8-C*H*
7.81	s, 1H	indacene 1-C*H*
7.69	d, 1H, ^3J 8.6 Hz	indacene 5-C*H*
7.63	d, 1H, ^3J 8.6 Hz	indacene 4-C*H*

^{13}C{^{1}H} NMR:

143.8	C_{ipso}	indacene 5a-*C*	120.6	CH	indacene 5-*C*H
141.8	C_{ipso}	indacene 5b-*C*	117.7	CH	indacene 4-*C*H
136.8	C_{ipso}	indacene 3a-*C*	78.46	C_{quat}	indacene 7-*C*–I
135.8	CH	indacene 8-*C*H	77.84	C_{quat}	indacene 2-*C*–I
131.9	CH	indacene 1-*C*H			

$^{77}Se\{^1H\}$ NMR: 659.4

UV (CH_2Cl_2) λ_{max} [nm] (ε, mol^{-1} dm^3 cm^{-1}):

258 (10,520), 270 sh (9,060), 282 (8,340), 297 sh (9,000), 309 (9,860), 324 (7700).

Emission (CH_2Cl_2): 317 nm (sh), 417 nm, 433 nm (sh).

Elemental Analysis:

Calcd for $C_{10}H_4SSe$ (%): C 24.56; H 0.82. Found (%): C 25.02; H 0.97.

5.4.16 Preparation of 2,7-Diiodo-3,6-diselena-*as*-indacene (4.16)

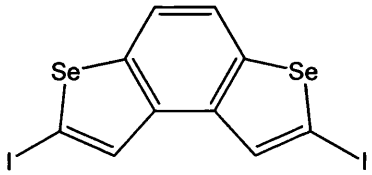

N,N,N',N'-Tetramethylethylenediamine (0.10 mL, 0.39 mmol) was placed in a Young's ampoule and dissolved in tetrahydrofuran (20 mL) and the solution cooled to –78 °C. ^{n}Butyllithium (2.59 M in hexane, 0.31 mLl) was added drop wise and the mixture stirred for 10 min at –78 °C before addition of **4.14** (100 mg, 0.35 mmol) in tetrahydrofuran (10 mL) and the resulting mixture left to stir for a further 30 min at –78 °C. A tetrahydrofuran solution (10 mL) of iodine (254 mg, 1 mmol) was added slowly and the mixture allowed to warm to room temperature. After stirring overnight, TLC (silica, hexane) showed the reaction to be complete. Excess iodine was quenched by addition of saturated sodium thiosulphate solution. Diethyl ether (10 mL) was added and the organic layer washed with water (3 × 30 mL) and dried ($MgSO_4$). Volatiles were removed under reduced pressure and the resulting dark green solid eluted through a short plug of silica with diethyl ether as eluant affording **4.16** as a pale yellow/brown solid (104 mg, 55%; mp decomposes above 160 °C).

^1H NMR:

8.14	s, 2H	indacene 1- & 8-C*H*
7.67	s, 2H	indacene 4- & 5-C*H*

$^{13}C\{^1H\}$ NMR:

144.0	C_{ipso}	indacene 3a- & 5a-*C*	120.9	CH	indacene 4- & 5-*C*H
138.0	C_{ipso}	indacene 3b- & 5b-*C*	77.83	C_{quat}	*C* – I

136.1 CH indacene 1- & 8-*C*H

^{77}Se NMR: 657.6 dd, $^{3}J_{SeH}$ 5.54 Hz, $^{3}J_{SeH}$ 2.59 Hz

UV (CH_2Cl_2) λ_{max} [nm] (ε, mol^{-1} dm^3 cm^{-1}):

264 (23,360), 275 (22,760), 287 (21,000), 302 (23,660), 313 (28,080), 328 (24,060).

Emission (CH_2Cl_2): 378 nm

Elemental Analysis:

Calcd for $C_{10}H_4I_2Se_2$ (%): C 22.41; H 0.75. Found (%): C 22.50; H 1.70.

5.4.17 Preparation of 2,7-Bis(trimethylsilylethynyl)-3,6-dithia-*as*-indacene (4.17)

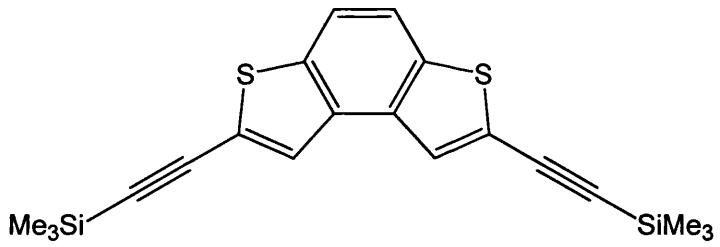

2,7-diiodo-3,6-dithia-as-indacene[5] (200 mg, 0.452 mmol), copper iodide (5.0 mg, 0.027 mmol) and bis(triphenylphosphine)palladium(II) chloride (38.0 mg, 0.054 mmol) were placed in a Schlenk tube and dissolved in tetrahydrofuran (20 mL) and diethylamine (5 mL). Trimethylsilylacetylene (0.14 mL, 0.995 mmol) was added and the resulting mixture left to stir overnight at room temperature and in the absence of light. Volatiles were removed under reduced pressure leaving an orange solid, which was eluted through a short plug of alumina with hexane/ethyl acetate (10:1) as eluant. Volatiles were again removed and the resulting orange solid purified by column chromatography (silica, 7:1, hexane/dichloromethane) affording **4.17** as a white solid (0.1276 g, 74%; 174 °C).

^{1}H NMR:

7.75	s, 2H	indacene 1- and 8-C*H*
7.70	s, 2H	indacene 4- and 5-C*H*
0.30	s, 18H	Si(CH_3)$_3$

^{13}C{^{1}H} NMR:

137.3 C_{ipso} indacene 3a- & 5a-*C* 119.5 CH indacene 4- & 5-*C*H

133.7	C_{ipso}	indacene 3b- & 5b-*C*	101.7	C_{quat}	*C*≡C–Si
127.2	CH	indacene 1- & 8-*C*H	97.58	C_{quat}	C≡*C*–Si
123.8	C_{ipso}	*C*–C≡C–Si	-0.207	CH_3	Si(*C*H_3)$_3$

UV (CH_2Cl_2) $\underline{\lambda_{max}}$ [nm] (ε,mol^{-1} dm^3 cm^{-1}):

266 (12,480), 277 (17,260), 295 (13,980), 307 (21,780), 321 (35,060), <u>336</u> (52,140), 354 (41,120).

Emission (CH_2Cl_2): 363 nm (sh), 380 nm, 399 nm (sh)

IR (KBr Disc): 2151 cm^{-1} ν(C≡C)

Elemental Analysis:

Calcd for $C_{20}H_{22}S_2Si_2$ (%): C 62.77; H 5.79. Found (%): C 62.40; H 5.74.

5.4.18 Preparation of 2,7-Bis(trimethylsilylethynyl)-3-thia-6-selena-*as*-indacene (4.18)

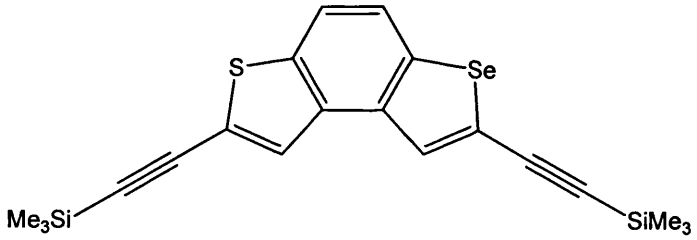

4.15 (49.6 mg, 0.10 mmol), bis(triphenylphosphine)palladium(II) chloride (8.5 mg, 0.01 mmol) and copper iodide (1 mg, 0.01 mmol) were placed in a Young's ampoule and dissolved in tetrahydrofuran (10 mL) and diethylamine (5 mL). Trimethylsilylacetylene (0.05 mL, 0.25 mmol) was added and the resulting mixture left to stir overnight (~15 h) at room temperature and in the absence of light. After this time TLC (silica, hexane) showed the reaction to be incomplete and further trimethylsilylacetylene (0.05 mL) was added and the mixture left to stir for a further 15 h. Volatiles were removed under reduced pressure leaving a brown oil, which was eluted through a short plug of alumina with hexane/ethyl acetate (4:1) as eluant. The resulting orange/brown oil was eluted through a short plug of silica with diethyl ether as eluant affording **4.18** as an orange solid (41.4 mg, 94%).

^{1}H NMR:

7.98	s, 1H	indacene 8-C*H*
7.75	s, 1H	indacene 1-C*H*

7.74	d, 1H, ^3J 8.6 Hz	indacene 5-C*H*
7.67	d, 1H, ^3J 8.6 Hz	indacene 4-C*H*
0.30	s, 9H	$Si(CH_3)_3$
0.29	s, 9H	$Si(CH_3)_3$

$^{13}C\{^1H\}$ NMR:

139.4	C_{ipso}	indacene 5a-*C*H	122.4	CH	indacene 1-*C*H
135.9	C_{ipso}	indacene 3a-*C*H	119.5	CH	indacene 4-*C*H
130.8	CH	indacene 8-*C*H	99.55	C_{quat}	*C*≡C–Si
127.5	CH	indacene 5-*C*H	-0.196	$Si(CH_3)_3$	

$^{77}Se\{^1H\}$ NMR: 617.1

UV (CH_2Cl_2) λ_{max} [nm] (ε, mol^{-1} dm^3 cm^{-1}):

268 (16,060), 274 (15,900), 281 (16,500), 312 (13,780), 326 (17,580), 342 (23,220), 360 (18000).

Emission (CH_2Cl_2): 375 nm (sh), 389 nm, 411 nm (sh)

IR (KBr Disc): 2142 cm^{-1} ν(C≡C)

5.4.19 Preparation of 2,7-Bis(trimethylsilylethynyl)-3,6-diselena-*as*-indacene (4.19)

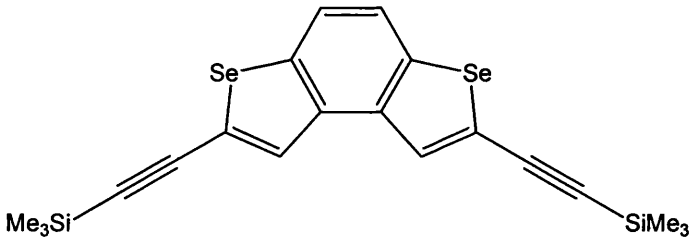

4.16 (100 mg, 0.190 mmol), bis(triphenylphosphine)palladium(II) chloride (16.0 mg, 0.023 mmol) and copper iodide (2.0 mg, 0.011 mmol) were placed in a Young's ampoule and dissolved in tetrahydrofuran (20 mL) and diethylamine (5 mL). Trimethylsilylacetylene (0.10 mL, 0.475 mmol) was added and the resulting mixture left to stir overnight at room temperature and in the absence of light. Volatiles were removed under reduced pressure and the resulting brown solid eluted through a short plug of alumina with hexane/ethyl acetate (4:1) as eluant. The resulting brown oil was eluted through a short plug of silica

with hexane/dichloromethane (2:1) as eluant affording **4.19** as a dark orange/red solid (76.9 mg, 85 %; mp 95 – 97 °C).

^{1}H NMR:

7.99	s, 2H	indacene 1- & 8-C*H*
7.71	s, 2H	indacene 4- & 5-C*H*
0.29	s, 18H	Si(C*H*$_3$)$_3$

^{13}C{^{1}H} NMR:

139.9	C_{ipso}	indacene 3a- & 5a-*C*	122.5	CH	indacene 4- & 5-*C*H
137.7	C_{ipso}	indacene 3b- & 5b-*C*	103.3	C_{quat}	*C*≡C–Si(CH$_3$)$_3$
131.1	CH	indacene 1- & 8-*C*H	99.59	C_{quat}	C≡*C*–Si(CH$_3$)$_3$
125.6	C_{ipso}	*C*–C≡C–Si	-0.195	CH_3	Si(*C*H$_3$)$_3$

^{77}Se{^{1}H} NMR: 614.0

UV (CH_2Cl_2) λ_{max} [nm] (ε, mol^{-1} dm^3 cm^{-1}):

272 (6,740), 284 (7,160), 318 (7,820), 330 (11,100), 346 (15,820), 365 (13,040).

Emission (CH_2Cl_2) λ_{max}: 379 nm (sh), 398 nm, 416 nm

IR (KBr Disc): 2134 cm^{-1} ν(C≡C)

Elemental Analysis:

Calcd for $C_{20}H_{22}Se_2Si_2$ (%): C 50.41; H 4.65. Found (%): C 52.60; H 5.17.

5.4.20 Preparation of 2,7-Diethynyl-3,6-dithia-*as*-indacene (4.20)

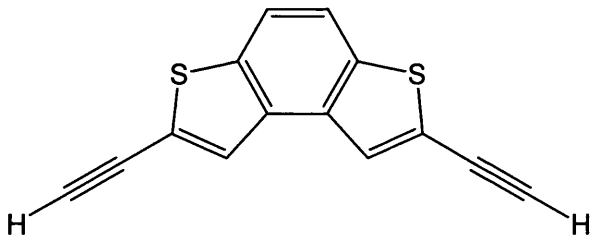

4.17 (76.0 mg, 0.20 mmol) was dissolved in dichloromethane /methanol (1:1, v/v, 10 mL). 2.0M Potassium hydroxide solution (0.30 mL, 0.60 mmol) was added drop wise and the resulting mixture left to stir at room temperature and in the absence of light overnight. After this time, TLC (silica, 4:1, hexane/dichloromethane) showed the reaction to be

complete. Volatiles were removed under reduced pressure and the product extracted with dichloromethane. The CH_2Cl_2 layer was dried ($MgSO_4$) and volatiles again removed under reduced pressure affording **4.20** as a pale yellow solid (40.7 mg, 86%).

^{1}H NMR:

7.81	s, 2H	indacene 1- & 8-C*H*
7.73	s, 2H	indacene 4- & 5-C*H*
3.51	s, 2H	alkyne C≡C–*H*.

^{13}C{^{1}H} NMR:

137.4	C_{ipso}	indacene 3a- & 5a-*C*	119.6	CH	indacene 4- & 5-*C*H
133.6	C_{ipso}	indacene 3b- & 5b-*C*	83.53	CH	C≡*C*–H
127.7	CH	indacene 1- & 8-*C*H	77.07	C_{quat}	*C*≡C–H
122.8	C_{ipso}	*C*–C≡C–H			

5.4.21 Preparation of 2,5-Bis(2-(5-bromothiophen-2-yl)-vinyl)selenophene (4.21)

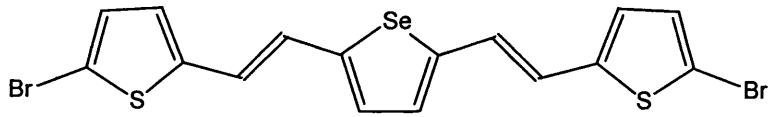

Triphenyl-(5-bromo-2-thienyl)phosphonium chloride (141 mg, 0.32 mmol) and selenophene-2,5-carbaldehyde[23] (30 mg, 0.16 mmol) were placed in a flask and dissolved in anhydrous methanol solution (20 mL). The resulting mixture was heated to boiling under a flow of N_2 and sodium methoxide (17 mg, 0.32 mmol) in methanol (2 mL) was added. The yellow mixture was heated under reflux overnight after which time TLC (silica, 1:1, hexane/dichloromethane) showed the reaction to be complete. On cooling a bright yellow precipitate formed which was filtered and dried. The yellow solid was eluted through a short plug of silica with hexane/dichloromethane (4:1) as eluant to remove remaining triphenylphosphine oxide. Volatiles were removed under reduced pressure affording **4.21** as a yellow solid (62.2 mg, 77%; 150 – 151 °C).

^{1}H NMR:

7.04	s, 2H	selenophene C*H*
6.94	d, 2H, ^3J 3.8 Hz	thiophene 4-C*H*
6.90	d, 2H, $^3J_{trans}$ 15.5 Hz	alkene C*H* (selenophene)
6.78	d, 2H, ^3J 3.8 Hz	thiophene 3-C*H*

6.75 d, 2H, $^3J_{trans}$ 15.5 Hz alkene C*H* (thiophene)

$^{13}C\{^1H\}$ NMR:

146.3	C_{ipso}	selenophene	130.3	CH	alkene *C*H (thiophene)
144.1	C_{ipso}	thiophene	126.5	CH	selenophene *C*H
133.0	C_{quat}	*C*–Br	124.3	CH	thiophene *C*H
130.7	CH	alkene *C*H (selenophene)	122.2	CH	thiophene *C*H

UV (CH_2Cl_2) $\underline{\lambda_{max}}$ [nm] (ε, mol^{-1} dm^3 cm^{-1}):

274 (9240), 311 (8180), 407 sh (27,960), <u>429</u> (37,920), 457 (29,560).

Emission (CH_2Cl_2): 512 nm, 545 nm (sh)

IR (KBr Disc): 1265, 1422 cm^{-1} ν(C=C)

5.4.22 Preparation of 2,5-Bis(2-(5-trimethylsilylethynylthiophen-2-yl)-vinyl) selenophene (4.22)

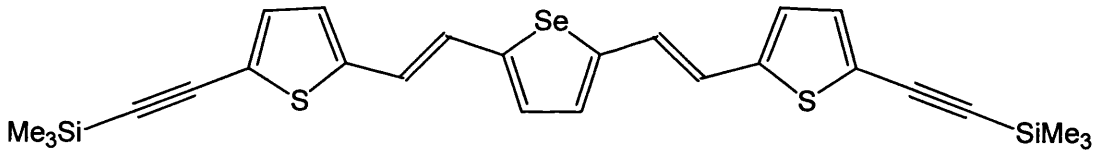

4.21 (35.0 mg, 0.07 mmol), bis(triphenylphosphine)palladium(II) chloride (8.0 mg, 0.01 mmol) and copper iodide (1.0 mg, 0.01 mmol) were placed in a Young's ampoule and dissolved in tetrahydrofuran (10 mL) and diethylamine (5 mL). Trimethylsilylacetylene (0.05 mL, 0.35 mmol) was added and the resulting mixture left to stir at room temperature and in the absence of light overnight. Volatiles were removed under reduced pressure leaving an orange/red solid, which was eluted through a short plug of alumina with hexane/ethyl acetate (4:1) as eluant affording **4.22** as an orange/red solid (40.9 mg, 77%; 173 -175 °C).

^1H NMR:

7.10	d, 2H, ^3J 3.9 Hz	thiophene 4-C*H*
7.06	s, 2H	selenophene C*H*
6.99	d, 2H, $^3J_{trans}$ 15.3 Hz	alkene C*H* (selenophene)
6.88	d, 2H, ^3J 3.9 Hz	thiophene 3-C*H*
6.78	d, 2H, $^3J_{trans}$ 15.3 Hz	alkene C*H* (thiophene)

0.06 s, 18H $Si(CH_3)_3$

$^{13}C\{^1H\}$ NMR:

146.6	Ar q*C* in selenophene ring	122.4	*m*-Ar*C*H on thiophene ring
143.9	Ar q*C* in thiophene ring	121.9	Ar q*C* in thiophene ring
133.5	Alkene *C*H (thiophene)	100.5	Acetylide q*C* bonded to thiophene ring
130.5	Alkene *C*H (selenophene)	97.80	Acetylide q*C* bonded to $Si(CH_3)_3$
126.1	*m*-Ar*C*H on selenophene	-0.159	$Si(CH_3)_3$
124.8	*m*-Ar*C*H on thiophene ring		

$^{77}Se\{^1H\}$ NMR: 620.6

UV (CH_2Cl_2) $\underline{\lambda_{max}}$ [nm] (ε, mol^{-1} dm^3 cm^{-1}):

296 (12,040), 358 (7,800), 431 (39,740), <u>455</u> (53,600), 484 (40,700).

Emission (CH_2Cl_2): 547 nm.

IR (KBr Disc): 2140 cm^{-1} ν(C≡C), 1251 cm^{-1} ν(C=C)

Elemental Analysis:

Calcd for $C_{26}H_{28}S_2SeSi_2$ (%): C 57.86; H 5.23. Found (%): C 57.90; H 5.68.

5.4.23 Preparation of 1,2-Bis(5'-platinumphenyltriethylphosphineethynyl-2'-thienyl)ethene (4.23)

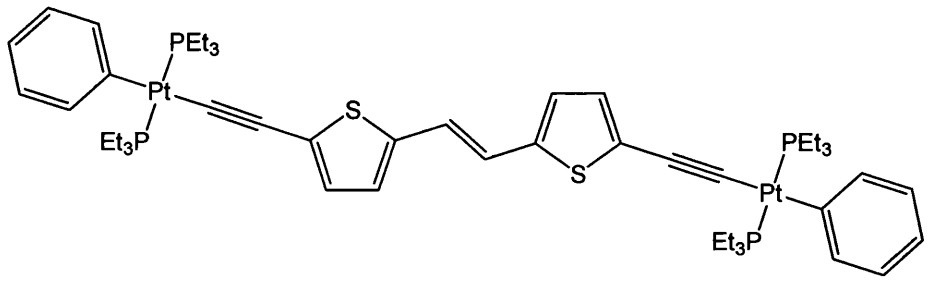

4.03 (39.6 mg, 0.17 mmol), copper iodide (5 mg) and platinum(II)(triethylphosphine) phenyl chloride (182 mg, 0.33 mmol) were placed in a Schlenk tube and dissolved in dichloromethane (10 mL) and diisopropylamine (5 mL). The resulting mixture was left to stir at room temperature and in the absence of light for one hour. Volatiles were removed and the resulting orange solid eluted through a short plug of alumina with ethyl acetate as eluant. Recrystallised from heptane afforded **4.23** as an orange solid (151 mg, 73%).

^{1}H NMR:

7.31	d, 4H, 7.4 Hz	Ar*H* phenyl ring
6.97	t, 4H, 7.4 Hz	Ar*H* phenyl ring
6.80	t, 4H, 7.4 Hz	Ar*H* phenyl ring
6.79	s, 2H	alkene C*H*=C*H*
6.74	d, 2H, 3.7 Hz	thiophene 4-C*H*
6.70	d, 2H, 3.7 Hz	thiophene 3-C*H*
1.78 – 1.70	m, 24H	$P(CH_2CH_3)_3$
1.13 – 1.06	m, 36H	$P(CH_2CH_3)_3$

^{13}C{^{1}H} NMR:

139.5	C_{ipso}	*C*–C≡C–Pt	121.3	CH	C_6H_5
139.1	CH	C_6H_5	120.4	CH	*C*H=*C*H
127.5	CH	thiophene 3-*C*H	102.9	C_{quat}	*C*≡C–Pt
127.3	CH	C_6H_5	15.15	CH_2	$P(CH_2CH_3)_3$
125.9	CH	thiophene 4-*C*H	8.032	CH_3	$P(CH_2CH_3)_3$

^{31}P{^{1}H} NMR: 10.15 ($^1J_{PtP}$ 2629 Hz)

UV (CH_2Cl_2) λ_{Max} [nm] (ε,mol^{-1} dm^3 cm^{-1}):

345 (7,000), 406 sh (42,200), 432 (67,200), 458 (60,800).

Emission (CH_2Cl_2): 479nm, 509 nm (sh)

IR (KBr Disc): 2081 cm^{-1} ν(C≡C), 1457 cm^{-1} ν(C=C)

Elemental Analysis:

Calcd for $C_{50}H_{76}P_4Pt_2S_2$ (%): C 47.84; H 6.10. Found (%): C 47.40; H 6.05.

5.4.24 Preparation of 1,2-Bis(5'-goldtriethylphosphineethynyl-2'-thienyl)ethene (4.24)

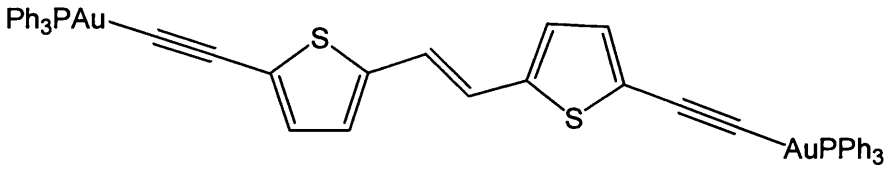

4.02 (63.4 mg, 0.17 mmol), sodium methoxide (1 mmol) and triphenylphosphinegold(I) chloride (165 mg, 0.33 mmol) were placed in a round bottom flask and dissolved in methanol (10 mL). The resulting mixture was left to stir at room temperature and in the absence of light overnight (~ 17 h). The volatiles were removed under reduced pressure and the resulting orange solid dissolved in dichloromethane, washed with water (3 × 20 mL) and dried ($MgSO_4$). Recrystallisation from methanol/dichloromethane (1:1, v/v) afforded **4.24** as a red/orange solid (154 mg, 40%).

^{1}H NMR:

7.58 – 7.43	m, 30H	$P(C_6H_5)_3$
7.02	d, 2H, ^3J 3.7 Hz	thiophene 4-C*H*
6.86	s, 2H	alkene C*H*=C*H*
6.81	d, 2H, ^3J 3.7 Hz	thiophene 3-C*H*

^{13}C {^{1}H} NMR:

141.9	C_{ipso}	*C*–C≡C–Au		129.4	C_{ipso}	*C*–CH=CH	
134.3	CH	d, 13.8 Hz	$P(C_6H_5)_3$	129.2	CH	d, 11 Hz	$P(C_6H_5)_3$
132.1	CH	thiophene 3-*C*H		126.1	CH	thiophene 4-*C*H	
131.6	CH	$P(C_6H_5)_3$		121.3	CH	*C*H=*C*H	
129.9	C_{ipso}	$P(C_6H_5)_3$		96.69	C_{quat}	*C*≡C–Au	

^{31}P{^{1}H} NMR: 42.30

UV (CH_2Cl_2) $\underline{\lambda_{max}}$ [nm] (ε, mol^{-1} dm^3 cm^{-1}):

320 (8,420), 392 sh (44,000), <u>415</u> (65,380), 441 (51,080).

Emission (CH_2Cl_2): 456 nm, 485 nm (sh).

IR (KBr Disc): 2090 cm^{-1} ν(C≡C)

5.4.25 Preparation of 2,7-Bis(triphenylphosphinegoldethynyl)-3,6-dithia-*as*-indacene (4.25)

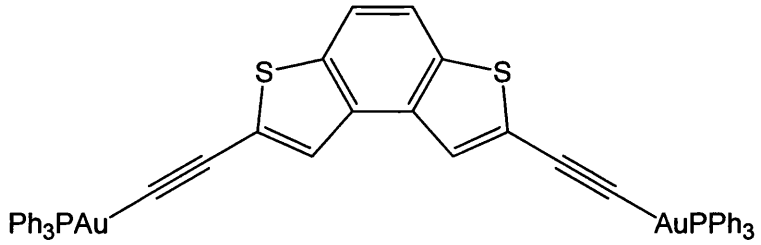

Triphenylphosphinegold(I) chloride (176 mg, 0.360 mmol), **4.17** (68.2 mg, 0.18 mmol) and sodium methoxide (54.0 mg, 1 mmol) were placed in a round bottom flask and dissolved in methanol (10 mL). The flask was stoppered with a septum and the mixture left to stir for 48 h at room temperature and in the absence of light. The volatiles were removed under reduced pressure and the resulting orange solid dissolved in dichloromethane, washed with water (3 × 20 mL) and dried ($MgSO_4$). Recrystallisation from methanol/dichloromethane (1:1) afforded **4.25** as an orange solid (151.9 mg, 74 %).

^{1}H NMR:

7.68	s, 2H	indacene 1- & 8-C*H*
7.57	s, 2H	indacene 4- & 5-C*H*
7.59 – 7.44	m, 30H	P(C_6H_5)$_3$

^{13}C{^{1}H} NMR:

136.4	C_{ipso}	indacene 3a- & 5a-*C*		129.2	CH	d, 11.7 Hz	P(C_6H_5)$_3$
134.3	CH	d, 13.8 Hz	P(C_6H_5)$_3$	126.0	CH	indacene 1- & 8-*C*H	
134.0	C_{ipso}	indacene 3b- & 5b-*C*		125.5	C_{ipso}	*C*–C≡C–Au	
131.6	CH	d, 1.7 Hz	P(C_6H_5)$_3$	118.6	CH	indacene 4- & 5-*C*H	
129.9	C_{ipso}	P(C_6H_5)$_3$					

^{31}P{^{1}H} NMR: 42.23

UV (CH_2Cl_2) $\underline{\lambda_{max}}$ [nm] (ε, mol^{-1} dm^3 cm^{-1}):

276 (16,200), 289 (17,400), 304 (17,160), 316 (25,880), 337 (39,060), <u>353</u> (64,200), 372 (62,240).

Emission (CH_2Cl_2): 378 nm (sh), 398 nm, 421 nm (sh).

IR (KBr Disc): 2100 cm^{-1} ν(C≡C)

Elemental Analysis:

Calcd for $C_{50}H_{34}Au_2P_2S_2$ (%): C 52.00; H 2.97. Found (%): C 49.90; H 3.18.

5.4.26 Attempted preparation of 1,2-Bis(5'-triphenylphosphinegoldethynyl-2'-selenyl)ethene (4.26)

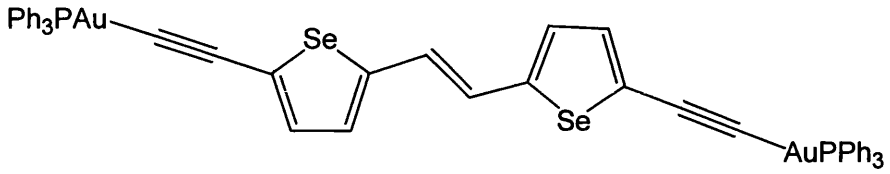

General Procedure B; **4.06** (25.4 mg, 0.053 mmol), methanol (15 mL) and triphenylphosphinegold(I) chloride (52.5 mg, 0.106 mmol). Recrystallisation from methanol/chloroform afforded **4.26** as yellow crystals (~ 10 mg).

^{1}H NMR:

7.56 – 7.45 m $P(C_6H_5)_3$

$^{31}P\{^1H\}$ NMR: 33.35

5.4.27 Attempted preparation of 2,7-Bis(triphenylphosphinegoldethynyl)-3,6-diselena-*as*-indacene (4.27)

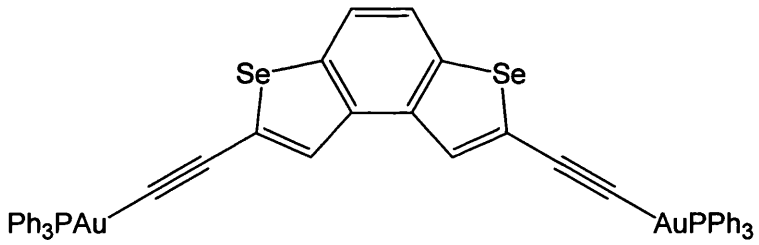

General Procedure B; **4.19** (50.0 mg, 0.105 mmol), triphenylphosphinegold(I) chloride (109 mg, 0.210 mmol) and methanol (40 mL). ^{1}H and $^{31}P\{^1H\}$ NMR show only triphenylphosphinegold(I) chloride and uncoordinated ligand.

5.5 References

1. Errington, R. J. *Advanced Practical Inorganic and Metalorganic Chemistry*; Blackie Academic and Professional: London, 1997.
2. Manzer, L. E., *Inorg. Synth.*, **21**, 135 - 136.
3. Starcevic, K.; Boykin, D. W.; Karminski-Zamola, G., *Heteroatom Chem.,* 2003, **14**, 218-222.
4. Buu-Hoï, N. P.; Lavit, D., *J. Chem. Soc.,* 1958, 1721 - 1723.
5. Yoshida, S.; Fujii, M.; Aso, Y.; Otsubo, T.; Ogura, F., *J. Org. Chem.,* 1994, **59**, 3077-3081.
6. Yang, Y.; Ramamoorthy, V.; Sharp, P. R., *Inorg. Chem.,,* 1993, **32**, 1946 - 1950.
7. Woodgate, P. D.; Sutherland, H. S., *J. Organomet. Chem.,* 2001, **629**, 131 - 144.
8. Musso, D. L.; Clarke, M. J.; Kelley, J. L.; Boswell, G. E.; Chen, G., *Org. Biomol. Chem.,* 2003, **1**, 498 - 506.
9. Wang, F.; Kaafarani, B. R.; Neckers, D. C., *Macromolecules,* 2003, **36**, 8225 - 8230.
10. Takahashi, S.; Kuroyama, Y.; Sonogashira, K.; Hagihara, N., *Synthesis,* 1980, **8**, 627-630.
11. Tomioka, H.; Sawai, S., *Org. Biomol. Chem.,* 2003, **1**, 4441 - 4450.
12. Hirsch, K. A.; Wilson, S. R.; Moore, J. S., *J. Am. Chem. Soc.,* 1997, **119**, 10401 - 10412.
13. Erdelyi, M.; Gogoll, A., *J. Org. Chem.,* 2001, **66**, 4165 - 4169.
14. Eckert, T.; Ipaktschi, J., *Monatsh. Chem.,* 1998, **129**, 1035 - 1048.
15. Pelter, A.; Jones, D. E., *J. Chem. Soc. Perkin Trans. 1,* 2000, **14**, 2289 - 2294.
16. John, J. A.; Tour, J. M., *Tetrahedron,* 1997, **53**, 15515 - 15534.
17. Kirner, W. R., *J. Am. Chem. Soc.,* 1928, **50**, 1955 - 1961.
18. Yur'ev, Y. K.; Ekkhardt, D., *Zh. Obshch. Khim.,* 1961, **31**, 3298 - 3300.
19. Keegstra, M. A.; Brandsma, L., *Synthesis,* 1988, 890 - 891.
20. Inoue, S.; Jigami, T.; Nozoe, H.; Aso, Y.; Ogura, F.; Otsubo, T., *Heterocycles,* 2000, **52**, 159 - 170.
21. Antonov, D. N.; Belenkii, L. I.; Gronowitz, S., *Journal of Heterocyclic Chemistry,* 1995, **32**, 53-55.
22. Larsen, J.; Bechgaard, K., *Acta Chem. Scand.,* 1996, **50**, 71-76.
23. Lash, T. D.; Colby, D. A.; Graham, S. R.; Chaney, S. T., *J. Org. Chem.,* 2004, **69**, 8851-8864.

Chapter 6 Polymer-Supported Organometallics

6.1 Introduction

Though group eight metal cluster carbonyls have received much attention over the years, the harsh conditions required for substitution had been a hindrance to early studies of these compounds. Iron carbonyls are largely available in the forms: $Fe(CO)_5$, $Fe_2(CO)_9$ and $Fe_3(CO)_{12}$, the latter two having bridging as well as terminal carbonyls. In the case of ruthenium and osmium, the most common complexes comprising solely the metal and carbonyl ligands, are of the general formula $M_3(CO)_{12}$ with no bridging carbonyls (Figure 6.1).

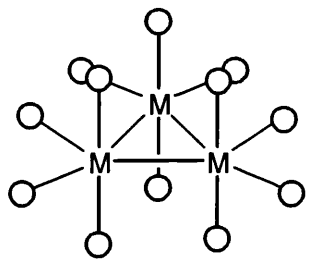

Figure 6.1: Schematic drawing of $M_3(CO)_{12}$ where M = Ru, Os.

Substitution reactions of ruthenium and osmium clusters proved difficult as they required high temperatures (80 - 100°C) and vigorous conditions. These reactions were made more accessible by Johnson *et al*[1] who found that acetonitrile readily substitutes for carbonyl ligands in $Os_3(CO)_{12}$ under mild conditions. A dichloromethane solution of $Os_3(CO)_{12}$ was reacted with trimethylamine N-oxide, in methanol, in the presence of a small amount of acetonitrile at room temperature to yield $[Os_3(CO)_{11}(MeCN)]$. This complex was then treated with a series of donor ligands to give $Os_3(CO)_{11}L$ (where L = CO, PPh_3, C_2H_4, C_5H_5N, $CH_3C_6H_4SO_2CH_2NC$-p).[2] The further treatment of $[Os_3(CO)_{11}(MeCN)]$ with Me_3NO produces the bis–acetonitrile complex $[Os_3(CO)_{10}(MeCN)_2]$.

Shapley reported the preparation of the bis-substituted complex starting from $Os_3(CO)_{10}(C_8H_{14})_2$.[3] The precursor is formed by the reaction of $H_2Os_3(CO)_{10}$ with ethene in cyclooctene solutions. Addition of acetonitrile to the solution of $Os_3(CO)_{10}(C_8H_{14})_2$ produces $[Os_3(CO)_{10}(MeCN)_2]$. In the presence of a strong donor ligand high yields of $Os_3(CO)_{12}L_2$

were isolated (Scheme 1). A wide range of examples of substitution of both $[Os_3(CO)_{11}(MeCN)]$ and $[Os_3(CO)_{10}(MeCN)_2]$ have been reviewed.[4]

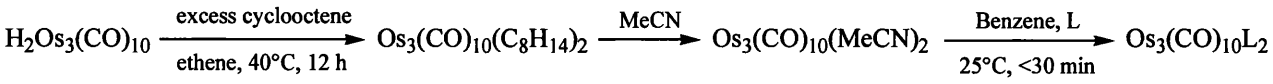

(L = PPh_3, PPh_2Me, $P(OMe)_3$, MeCN, $PhCH_2CN$)

Scheme 1

Johnson and co-workers extended their approach to $Ru_3(CO)_{12}$.[5] Dichloromethane solutions of $Ru_3(CO)_{12}$ were reacted with trimethylamine N-oxide in the presence of acetonitrile at – 78 °C and the mixture allowed to slowly warm to room temperature. The formation of $[Ru_3(CO)_{11}(NCMe)]$ is indicated by a colour change of the solution from light orange to dark orange. Again the bis-substituted complex can be prepared stoichiometrically from ruthenium carbonyl or by further treatment of $[Ru_3(CO)_{11}(NCMe)]$ with Me_3NO. Substitution reactions of these complexes in the presence of donor ligands were then possible in dichloromethane solutions at -78°C (Scheme 2).

$[Ru_3(CO)_{11}(MeCN)]$ and $[Ru_3(CO)_{10}(MeCN)_2]$ are less stable, more reactive, than their osmium analogues. Hence lower temperatures are required to prevent formation of $Ru_3(CO)_{12}$ and higher nuclearity clusters.

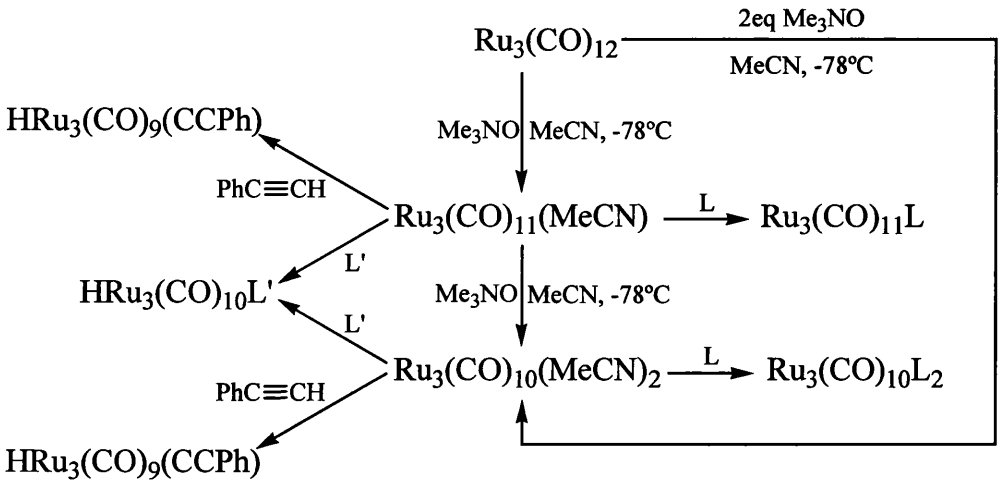

(L = PPh_3, $P(OMe)_3$; L' = CH_3CH_2SH, Py)

Scheme 2

6.1.1 Photochemistry

One of the most effective and often highly selective routes to synthesis of organometallic compounds is through photochemistry. In the case of metal carbonyl compounds a simple dissociation of CO from a mononuclear system, e.g. $Mo(CO)_6$, in the presence of a ligand, L, can be effected, thus leading to a substituted product (Scheme 3a). In a polynuclear system, such as $Ru_3(CO)_{12}$, along with loss of CO, the formation of mononuclear fragments can be effected by cleavage of a metal-metal bond *via* a photofragmentation mechanism (Scheme 3b).

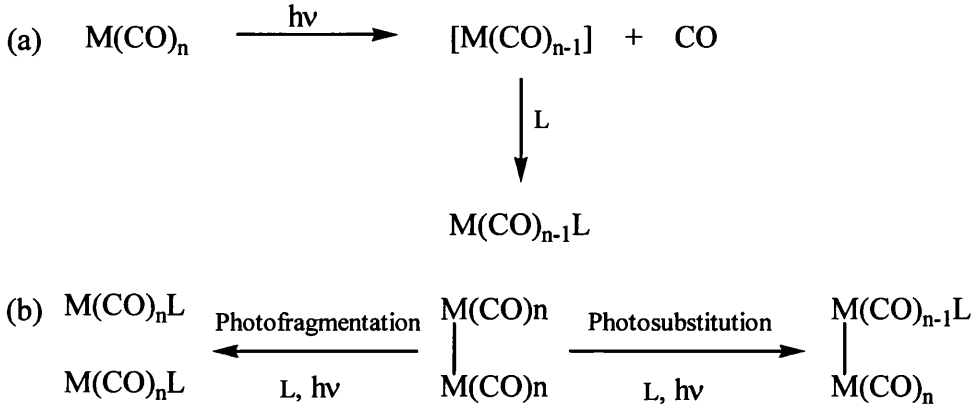

Scheme 3

Considering that M–M bonded dimers can undergo homolytic bond cleavage upon photoexcitation[6] it was postulated that the primary photoprocess in the fragmentation mechanism of $Ru_3(CO)_{12}$ was the formation of a diradical species as a result of homolysis of a single Ru–Ru bond (Scheme 4).

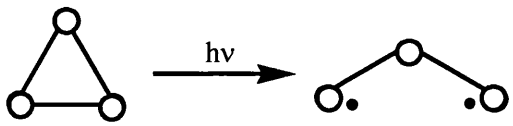

Scheme 4

If this were the case then photolysis of $Ru_3(CO)_{12}$ in the presence of a chlorocarbon would trap the diradical forming chlorocarbonylruthenium products as seen in the metal – dimer systems. The validity of this postulation was investigated by photolysis of octane solutions of the ruthenium cluster in presence and absence of CCl_4.[7] It was found that the photofragmentation yields in both cases were not significantly different. Under a CO atmosphere, reactions in the presence of CCl_4 showed the formation of $Ru(CO)_5$ which then underwent a secondary

thermal reaction to produce chloro derivatives. These observations led to the conclusion that the mechanism does not proceed *via* homolytic bond cleavage and a diradical intermediate.[8]

The presence of π – acid ligands such as CO, ethene, activated olefins and tertiary phosphines in hydrocarbon solutions produce substituted mononuclear species (eq 1) in modest yields. Whereas, whether used as solvent or an addition to hydrocarbon solutions, with harder donor ligands such as THF, diglyme or 2-methyltetrahydrofuran, virtually no photoactivity is observed.

$$Ru_3(CO)_{12} + 3L \xrightarrow{h\nu} 3Ru(CO)_4L \qquad (1)$$

All this information combined led to the proposal that the mechanism must proceed *via* the formation of a coordinatively unsaturated intermediate which is an isomeric form of the starting cluster.[9] This is achieved by heterolytic cleavage of a Ru – Ru bond and subsequent movement of a terminal carbonyl into a bridging site in order to maintain the electrical charge neutrality of both Ru atoms. Thus one of the Ru atoms would be a 16 electron centre (i.e. electron deficient) and capable of coordinating a two electron donor (Scheme 5) to give $[Ru_3(CO)_{12}L]$ a precursor to fragmentation products.

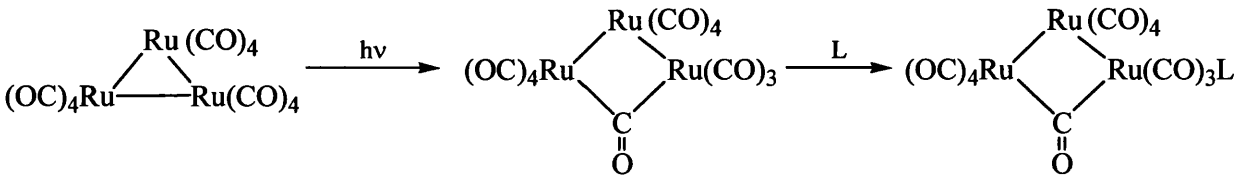

Scheme 5

The formation of intermediates of the type $[Ru_3(CO)_{12}L]$ has been proved by kinetic flash photolysis experiments.[7] $[Ru_3(CO)_{12}L]$ decays by fragmentation when L = $P(OMe)_3$ or PPh_3 but when the ligand used is cyclohexene or THF the loss of ligand, L, regenerating the starting material is the predominant process. There is a correlation between the photofragmentation rate and the π–acceptor/σ–donor properties of the ligand present. The fastest rates are observed for strong π–acceptors and weak σ–donors.

Similarly, information about the photosubstitution mechanism has been obtained from flash photolysis experiments[10,11] along with matrix isolation techniques.[12] Flash photolysis of THF solutions of $Ru_3(CO)_{12}$ show the existence of a transient species, most likely a THF adduct of

the form $Ru_3(CO)_{11}S$ (where S = solvent). Initially there is a photochemical labilisation of CO which forms $[Ru_3(CO)_{11}]$ (eq. 2). This intermediate is solvated producing $Ru_3(CO)_{11}S$ (eq. 3) which can either react with free CO to regenerate the starting cluster (eq. 4) or in the presence of another two electron donor, L, form $Ru_3(CO)_{11}L$ (eq. 5).

$$Ru_3(CO)_{12} \xrightarrow{h\nu} [Ru_3(CO)_{11}] + CO \qquad (2)$$

$$[Ru_3(CO)_{11}] \underset{-S}{\overset{+S}{\rightleftharpoons}} [Ru_3(CO)_{11}S] \qquad (3)$$

$$[Ru_3(CO)_{11}S] + CO \longrightarrow Ru_3(CO)_{12} \qquad (4)$$

$$[Ru_3(CO)_{11}S] + L \longrightarrow [Ru_3(CO)_{11}L] \qquad (5)$$

The use of solvent, ligand and wavelength all have an effect on the photochemical pathway and so these factors may be used to control the reactions in order to obtain the desired product.

Desrosiers *et. al*[7] investigated the effects of solvent on the photoreactions of $Ru_3(CO)_{12}$ and studied quenching of the photofragmentation pathway under a CO atmosphere. While photophysical studies show that irradiation of $Ru_3(CO)_{12}$ by wavelengths of approximately 390 nm favours the photofragmentation pathway and the formation of fragments of lower nuclearity, irradiating the compound with shorter wavelengths (typically 310 nm) allows the domination of the photosubstitution pathway and its products.

When using a broad band UV source to irradiate the trinuclear cluster the choice of solvent is an important factor in the control of which process predominates. Solvents such as diethyl ether, ethyl acetate and acetonitrile are known to quench the photofragmentation process[13] producing high yields of substituted products. When hexane or dichloromethane are used as the photolysis media along with a two-electron donor, for instance triphenylphosphine, high fragmentation product yields are obtained.

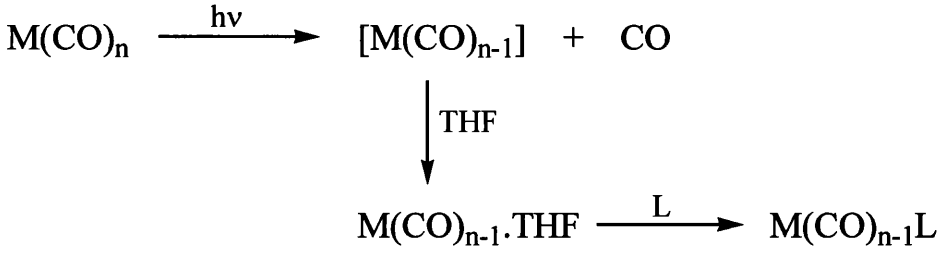

Scheme 7

Due to the short lifetimes of intermediates formed in photolysis reactions (in the order of ns / ms) ligands are required to react quickly. The intermediate can also be stabilised by solvent interaction (Scheme 7).

Lewis and co-workers[14] first reported the photofragmentation of $Ru_3(CO)_{12}$ **1** to produce the mononuclear ruthenium species $Ru(CO)_5$ **2** in 1974. $Ru(CO)_4(\eta^2$ – olefin) complexes were prepared by the irradiation of n-heptane solutions of $Ru_3(CO)_{12}$ in the presence of an olefin under an argon atmosphere at low temperature. Using ethene they produced colourless solutions with IR absorptions at 2104m, 2021vs, and 1995s cm^{-1} believed to be due to $Ru(CO)_4(C_2H_4)$ **3**. Ruthenium carbonyl was also irradiated with triphenylphosphine under argon to give a mixture of two monomers: $Ru(CO)_4PPh_3$ **4** and *trans*-$Ru(CO)_3(PPh_3)_2$ **5** in a 2:1 molar ratio. It was found that in the presence of CO the major product is **4**. A summary of these results is shown (Scheme 8).

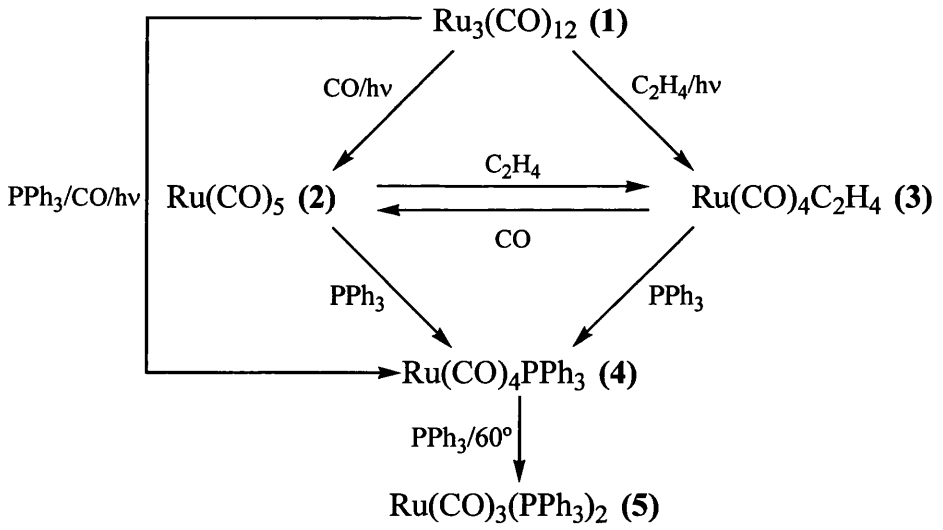

Scheme 8

Ethene is commonly used in these reactions as the resultant $Ru(CO)_4(\eta^2 - C_2H_4)$ is a stabilised form of the $[Ru(CO)_4]$ fragment. This complex has found use as a starting material for a variety of different synthetic reactions[15] and has the potential of use as a capping agent[16] to prepare target ruthenium containing clusters due to the ease of olefin loss.

$M(CO)_4(\eta^2 -$ olefin) complexes generally exhibit four bands in the carbonyl region of the IR spectrum. Occasionally there are only three bands observed as a consequence of the two central peaks overlapping as in the case of the ethene complex. This indicates that the olefin occupies an equatorial site in the trigonal bipyramidal structure (Scheme 9).

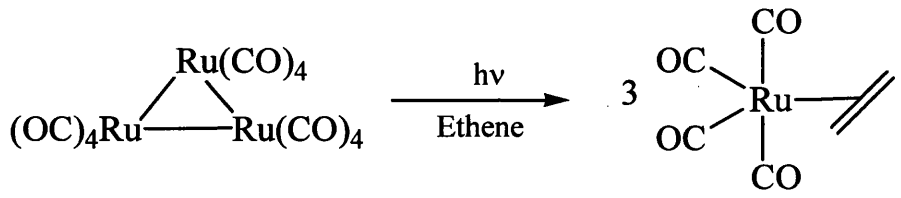

Scheme 9

As well as the photochemical preparation of these metal carbonyl – (η^2- olefin) complexes, the use of ligand exchange reactions to prepare substituted olefin complexes has been investigated[17] resulting in the ordering of relative stabilities as follows: olefins with electron withdrawing groups > olefins with halogen substituents > olefins with hydrocarbon substituents. From this it can be seen that methyl acrylate, an example of an olefin containing an electron withdrawing group, will form more stable complexes with metal carbonyl fragments than ethene. This is due to the increase in back bonding between the metal and olefin π^* orbitals.

Wrighton and co-workers[18] have studied the photochemistry of $M(CO)_n(C_2H_4)_{5-n}$ complexes (where M = Fe, Ru; n = 4, 3, 2) in an extension to their work on alkene isomerisation catalysis. A summary of the photochemical reactions for the ruthenium carbonyl complexes is shown below (Scheme 10).

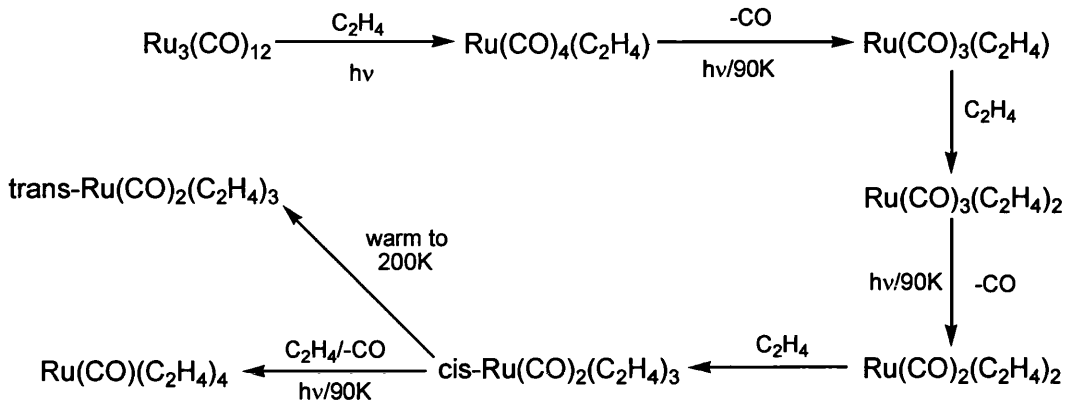

Scheme 10

Subsequently $Ru(CO)_3(C_2H_4)_2$ and $Ru(CO)_2(C_2H_4)_3$ were found to be catalytically active in the isomerisation of 1-pentene.

Grevels *et al* have used photochemistry as a tool to quantitatively synthesise (η^2-olefin) tetracarbonylruthenium complexes,[19] where the products are screened from any further reaction by a cut-off filter ($\lambda \geq 370$ nm), and also to yield bis(η^2-methyl acrylate) tricarbonylruthenium.[20] The lability of the olefin ligand means that it may be substituted for other ligands.

6.1.2 Solid Phase Synthesis

The area of solid phase synthesis (SPOS) has continued to grow due to its use not only in synthetic organic but biological and pharmaceutical chemistry to build compound libraries. In general it is organic compounds that are generated on polymeric supports. Organometallic molecules tend to be immobilised for use as synthetic intermediates rather than as target molecules themselves. A recent surge of interest has expanded the applications of solid phase methods to include immobilisation of catalysts.[21-23]

Solid phase methods have many advantages over their solution phase analogues. The immobilised product can easily be separated from the reaction mixture at the end of the reaction by filtration. There are fewer purification steps required; only a resin washing step and purification of the final cleavage product is necessary. Solid phase synthesis allows the use of high concentrations of reagents in order to push the reaction through to completion though the presence of excess reagents in solution can be problematic to structure

determination. Characterisation of molecules 'on–bead' is hindered by interference produced by the polymer backbone. On–bead analysis also suffers from a limited number of analytical techniques available for the task. A few of the tools that can be used are: gel-phase NMR, high-resolution magic angle spinning NMR (hr-MAS) and perhaps the most useful tool, FTIR spectroscopy. With FTIR systems it is necessary for a "reporter" ligand such as a carbonyl group to be present so that the progress of the reaction can be monitored. Of course once the target molecule is cleaved from the support characterisation becomes much easier but recently a mass spectrometric technique has been developed to monitor solid phase reactions without the need for cleavage.[24]

In the case of organometallic compounds, such as catalysts, solid phase synthesis has further advantages. The problem with using transition metal catalysts is that the product becomes contaminated with metal, which is difficult to remove. Immobilising the catalyst makes use and extraction a simpler task and also opens the possibility for re-use. Recyclability can be thought of as a 'green' chemistry approach as it reduces the amount of waste material and depletion of transition metal sources. Unfortunately there can still be some leaching of metal off the support and the catalyst can show a reduction in activity as it is recycled. Considering all of this, it is surprising that, with a few exceptions,[25-27] organometallic and inorganic synthetic chemists have largely overlooked the use of solid phase synthesis.

Heinze[28] has reported a solid-phase organometallic synthetic approach to molybdenum tricarbonyl complexes. The ligand used was a bidentate nitrogen base with a phenolic hydroxy group, which enabled attachment to the polystyrene support for solid phase reactions, and to a TMS protecting group for analogous solution phase reactions. To acetonitrile solutions of 1a/2a were added $[Mo(CO)_3(NCCH_3)_3]$ at room temperature to give 1b/2b, which have an intense blue colour (Scheme 11). The lability of the acetonitrile ligand was used to carry out ligand exchange reactions with several different ligands (L = carbon monoxide, *t*-butyl isonitrile and triphenylphosphine) forming 1c-e/2c-e.

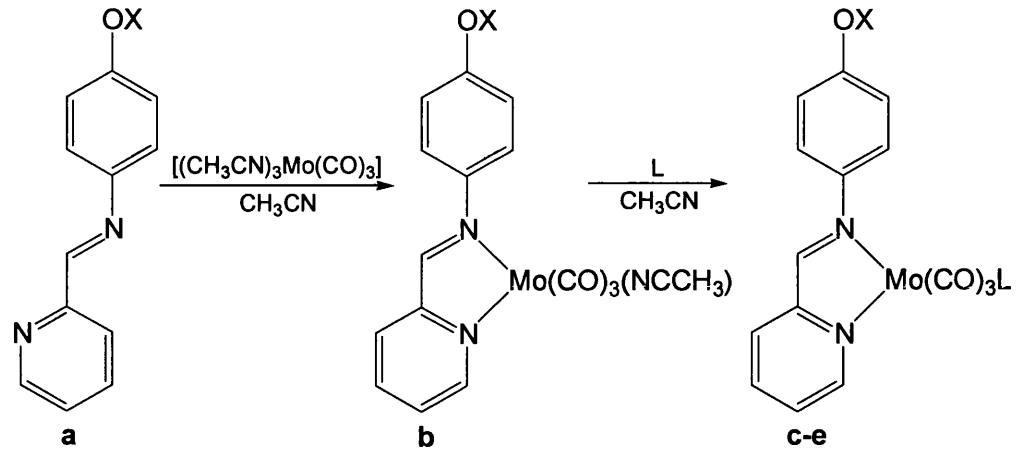

Scheme 11

The polystyrene resin was functionalised with a silyl chloride group prior to loading with the ligand (1a) under basic conditions to form yellow 3a. Though dichloromethane proved to be a good solvent to swell the resin it was shown in the homogeneous reactions to promote the formation of "$Mo(CO)_4$" rather than the tricarbonyl complex and therefore the solid phase reactions were performed in pure acetonitrile. Similarly, addition of tris(acetonitrile) molybdenumtricarbonyl to the swollen resin at room temperature produces a deep blue colour indicating the formation of the immobilised complex. The result of using acetonitrile was low yields and so the heterogeneous ligand exchange reactions were run in toluene. It was found that the stability of both soluble and insoluble complexes to ligand exchange follow the trend: MeCN > PPh_3 > CO > C*n*Bu.

Oxidative elimination reactions between 1c/3c and phenyltin trichloride both resulted in a seven-coordinate molybdenum complex (Scheme 12).

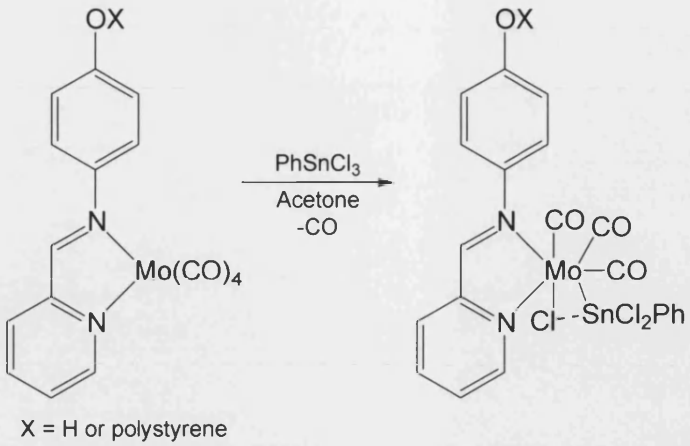

Scheme 12

6.1.3 Objectives for this Chapter

The aim of the work in this area was to prepare a range of metal carbonyl olefin complexes starting from $Ru_3(CO)_{12}$ and $Mo(CO)_6$. This was carried out homogeneously firstly to provide spectral data for comparison with later heterogeneous reactions utilising the corresponding alkene functionalised polymeric supports. The olefin complexes are usually only synthesised just before required for use as many are air and moisture sensitive and easily decompose. Immobilisation on polymer-supports would not only stabilise these complexes put provide a potentially storable source of these organometallic fragments for synthesis. To assess whether the metal can be removed from the polymer-support, a series of ligand exchange reactions were run using triphenylphosphine (Scheme 13).

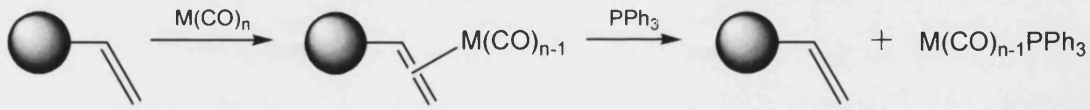

Scheme 13

6.2 Results and discussion

6.2.1 Photochemistry

Transition metal carbonyl olefin complexes, of the type $M(CO)_n(\eta^2$- olefin), are useful in synthesis of organometallic molecules as they are a potential source of $M(CO)_n$ fragments due to the lability of the olefin ligands. However, these olefin complexes tend to be air and moisture sensitive. They are only stable at low temperatures and in solution as removal of solvent leads to decomposition.

Immobilisation of metal complexes on polymer supports can reduce the air sensitivity of the organometallic fragment and overcome the difficulty of isolation making their use in synthesis more approachable. Another advantage of using solid-phase chemistry is the potential preparation of a storable source of the metal fragment. It is necessary to test that the metal fragment can be removed from the support for use in synthetic transformations. The polymer support can be removed by a simple filtration step at the end of the synthesis and re-used (Scheme 14).

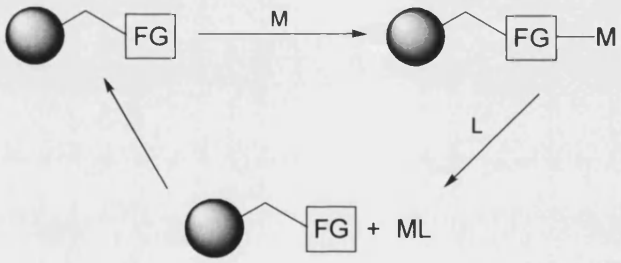

Scheme 14

It is the aim of our work in this area to prepare a range of transition metal olefin complexes both in solution and on solid phase focussing on $Ru_3(CO)_{12}$ and $Mo(CO)_6$ complexes incorporating ethene and methyl acrylate as these both have solid-phase analogues, 3-butenyl polystyrene (**1**) and REM resin (**2**) respectively. The loading of alkene functionality for **1** is 3.9 mmol g^{-1} and 1.1 mmol g^{-1} for **2**.

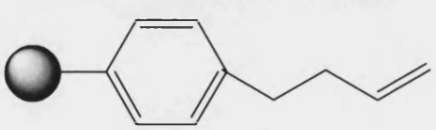

(1)

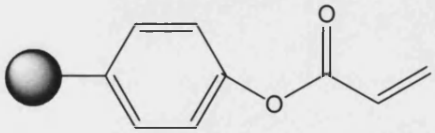

(2)

Due to the nature of the bonding between metal and olefin in $M(CO)_n(\eta^2$ – olefin) complexes, i.e. forward donation from a filled olefin π orbital to an empty metal p – orbital and back donation from the filled metal d – orbitals into the olefin π^* orbital, olefins with electron withdrawing groups increase the amount of metal back donation and in doing so stabilise the complex. $M(CO)_n(\eta^2$ – olefin) complexes where the olefin has an electron withdrawing group present are therefore more stable than complexes consisting of olefins with hydrocarbon substituents. It is expected that the solid-phase analogues will follow the same trend.

6.2.2 Photolysis of $Ru_3(CO)_{12}$

6.2.2.1 Homogeneous preparations

Firstly, in order to gather spectral data, it is necessary to carry out homogeneous reactions. These solution phase reactions not only provide useful spectral data for comparison with results from solid-phase reactions but also act as a control for the subsequent ligand exchange reactions with triphenylphosphine.

$$Ru_3(CO)_{12} \xrightarrow[3PPh_3]{h\nu} 3\ Ru(CO)_4(PPh_3) \quad \textbf{(3)}$$

$Ru(CO)_4(PPh_3)$ **3** may be prepared directly by irradiation of $Ru_3(CO)_{12}$ with three equivalents of triphenylphosphine. The solution IR spectrum of this complex shows three bands at: 2061(s), 1987(m) and 1955(vs) cm^{-1}. The presence of three bands in the IR spectrum suggests a C_{2v} arrangement where the phosphine is in an equatorial position. Irradiating the mixture for too long can lead to formation of the *bis*-substituted complex $Ru(CO)_3(PPh_3)_2$ which, from its IR spectrum, has a D_{3h} arrangement with both phosphines occupying axial positions.

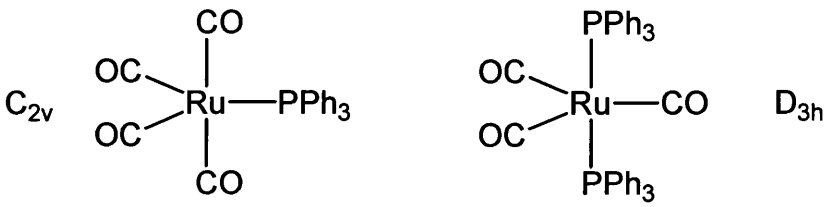

6.2.2.1.1 Preparation of $Ru(CO)_4(H_2C{=}CR)$

Methyl acrylate was added to a HPLC grade DCM solution of $Ru_3(CO)_{12}$ and the mixture irradiated to form a colourless solution of $Ru(CO)_4(H_2C{=}CHCO_2Me)$ **4**.

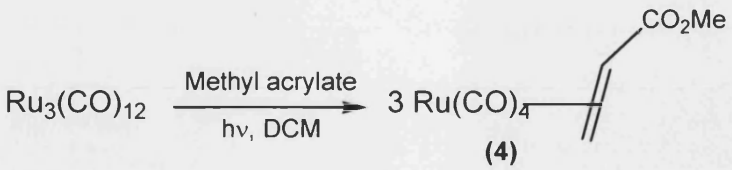

(4)

This complex is usually formed by reactions carried out in hydrocarbon solutions such as hexane but the resin beads will not swell in hexane therefore it was necessary to find a way of producing the olefin complex homogeneously in the same solvent, i.e. dichloromethane, used for heterogeneous reactions. It was found that one of the stabilising additives of dichloromethane was acting as a photofragmentation quencher and therefore HPLC grade dichloromethane without the stabiliser was used. As isolation is difficult due to the sensitivity of the complex it was characterised by its solution IR spectrum which shows four bands which agree with literature values.[17]

A similar reaction was performed using 1-octene to form $Ru(CO)_4(H_2C{=}CHC_6H_{13})$ to provide information for solid-phase reactions using **1**, though due to the low stability of this complex and its rapid decomposition, ligand exchange reactions in solution phase were inconclusive.

6.2.2.2 Heterogeneous Preparations

6.2.2.2.1 Synthesis of Polymer-supported $Ru(CO)_4(H_2C{=}CR)$

For both polymer-supports this was achieved by pre-swelling **1** or **2** in dichloromethane and irradiating in the presence of $Ru_3(CO)_{12}$ for 35 min forming **5** and **6** respectively. Using single bead FTIR spectroscopy, the completion of these reactions was confirmed by the appearance of ν(CO) bands which correspond to the solution phase analogues. In the case of **5**, three bands are observed, as is the case with solution phase ethene complexes where the central two bands overlap (Figure 6.2). Four bands in the ν(CO) region are seen in the IR spectrum of **6** in correlation with the spectrum of **4**.

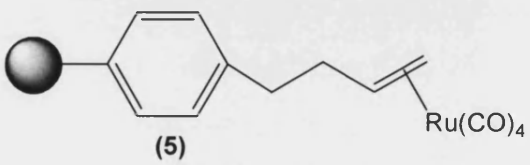

(5)

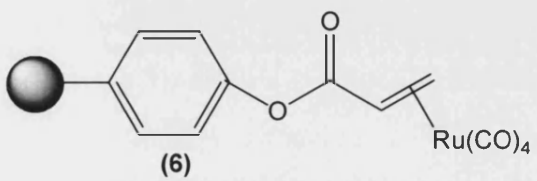

(6)

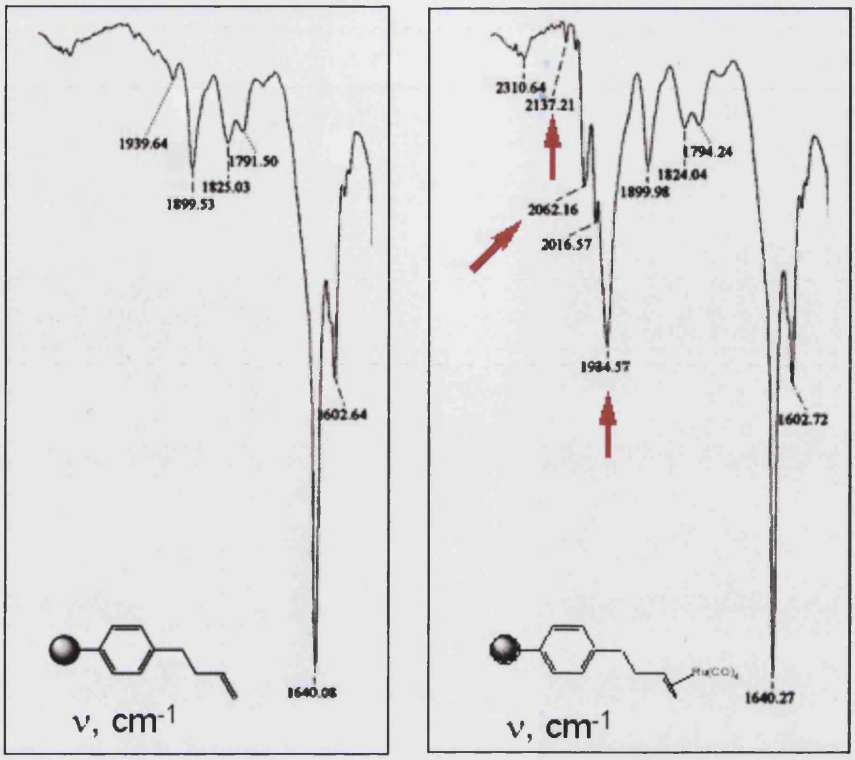

Figure 6.2: IR spectra of 3-butenyl polystyrene and 5

Metal loadings have been determined by mass increase measurements. These calculations give approximate loadings of $[Ru(CO)_4]$ on the support as 0.117 mmol g^{-1} and 0.216 mmol g^{-1} for **5** and **6** respectively. Both of these supported $[Ru(CO)_4]$ fragments are stable in air at room temperature and may be stored by refrigeration under nitrogen for several weeks.

In order to assess the reactivity of these supported complexes and thus the validity of their use as storable sources of $[Ru(CO)_4]$, each where tested in a ligand exchange reaction using triphenylphosphine (Scheme 15).

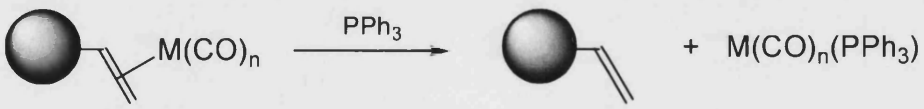

Scheme 15

The supported complex was pre-swollen in dichloromethane and one equivalent of triphenylphosphine was added. The mixture was stirred overnight at room temperature. Along with the formation of product, IR spectra confirm that the metal is coming off the support due to the change in peaks in the carbonyl region.

In this case **5** seemed to give a better result, 30% of the ruthenium came off the support giving $Ru(CO)_4(PPh_3)$, as identified by IR and ^{31}P NMR spectra, in comparison to just 20% of ruthenium removed from support **6**. These results do not bode well for these supported complexes to be used as efficient transfer agents with so little metal coming off the support. It was found that stirring the mixtures overnight while gently warming (40°C) produced much improved results, **5** still showing a slightly better result with 80% of the ruthenium coming off in contrast to 75% from **6**. Solution-phase reactions run alongside their solid phase analogues mirrored the improved result at 40°C.

6.2.3 Photolysis of $Mo(CO)_6$

6.2.3.1 Homogeneous Preparations

6.2.3.1.1 Preparation of $Mo(CO)_5(H_2C{=}CR)$

Methyl acrylate was added to a hexane solution of $Mo(CO)_6$ and the mixture irradiated to form $Mo(CO)_5(H_2C{=}CHCO_2Me)$ **7**. The progress of the reaction was monitored by solution IR spectroscopy and the appearance of peaks corresponding to the formation of **7** was observed after 5 min.

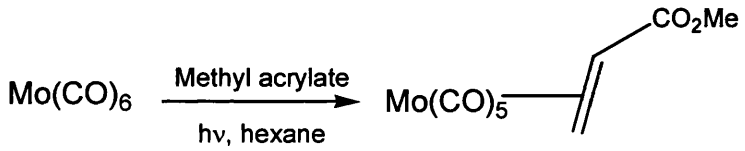

$Mo(CO)_5(H_2C{=}CHC_6H_{13})$ was also prepared by irradiation of $Mo(CO)_6$ in the presence of 1-octene and subsequently used in a ligand exchange reaction.

6.2.3.2 Heterogeneous Preparations

6.2.3.2.1 Synthesis of Polymer-supported $Mo(CO)_5(H_2C{=}CR)$

$[Mo(CO)_5]$ was supported on **1** and **2** to give **8** and **9**, respectively. The polymer-support was pre-swollen in dry dichloromethane and irradiated in the presence of $Mo(CO)_6$ for 25 min. As previously, mass measurements lead us to approximate $[Mo(CO)_5]$ loadings of 0.065 mmol g^{-1} for **8** and 1.06 mmol g^{-1} for **9**.

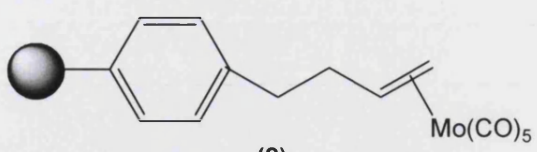

(8)

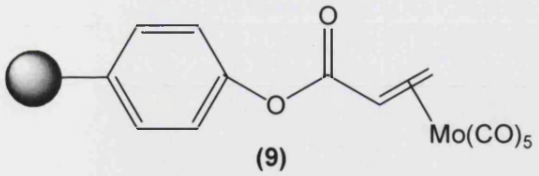

(9)

Similarly to the supported ruthenium, completion of the reaction was confirmed by appearance of bands in the carbonyl region of the IR spectrum (Figure 6.3). These supported molybdenum fragments are less stable than their ruthenium counterparts and are kept refrigerated when not in use. Ligand substitution reactions using **8** give very poor results, less than ten percent of the metal removed at room temperature and only 42% after overnight reaction at 40°C. This is a reflection of the low stability of the supported $[Mo(CO)_5]$ fragment. In contrast, the ligand exchange reactions using **9** show 23% of the metal removed at room temperature and, as with the polymer supported $[Ru(CO)_4]$, greatly improved results at 40°C with 85% of the metal coming off the support. In each case, IR spectra of the resins after metal transfer experiments showed no signs of thermal decomposition.

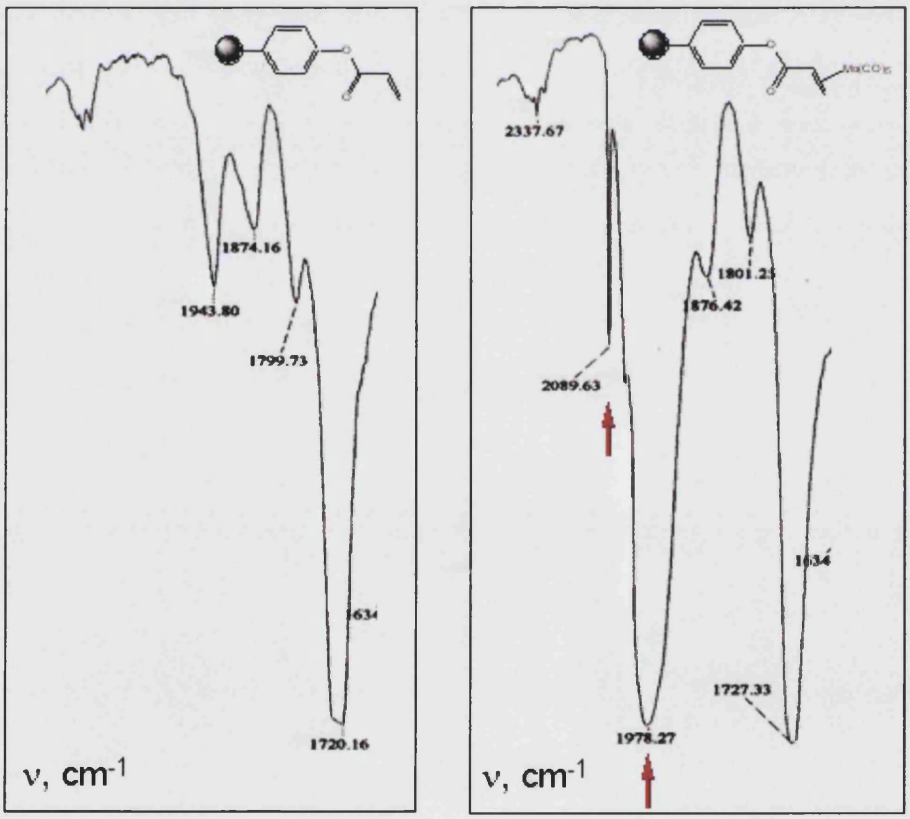

Figure 6.3: IR spectra of REM resin and 9

6.2.4 Polymer-supported diene

In an extension to this work, both $Ru_3(CO)_{12}$ and $Mo(CO)_6$ were reacted with polymer-supported cyclooctadiene **10** (diene functionality loading of 0.9 mmol g^{-1}) to form sources of $[Ru(CO)_3]$ and $[Mo(CO)_4]$ (Scheme 16).

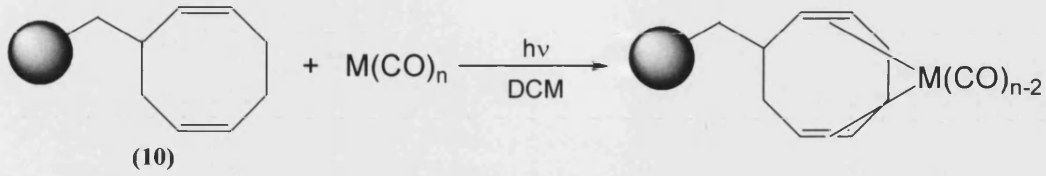

(10)

Scheme 16

6.2.4.1 Photolysis of $Ru_3(CO)_{12}$

The cyclooctadiene resin was pre-swollen in dichloromethane and irradiated in the presence of $Ru_3(CO)_{12}$. Bands in the carbonyl region of the IR spectrum showed that the reaction was complete after 35 min. The beads then underwent ligand exchange reactions as before with triphenylphosphine at room temperature and 40°C.

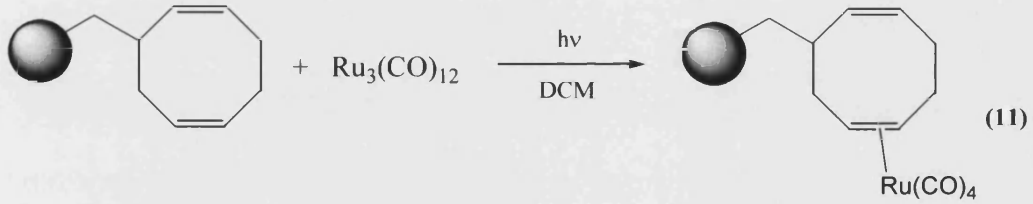

(11)

Scheme 17

The resultant IR and ^{31}P NMR spectra at both temperatures show the presence of $Ru(CO)_4(PPh_3)$ suggesting that the ruthenium fragment is bound to the resin in an η^2 fashion rather than in an η^4 manner as expected (Scheme 17).

6.2.4.2 Photolysis of $Mo(CO)_6$

Immobilisation of $[Mo(CO)_4]$ met with more success than with $[Ru(CO)_3]$ which may be attributed to the greater reactivity of $Mo(CO)_6$ than the ruthenium cluster. Cyclooctadiene resin was pre-swollen in dry dichloromethane and irradiated in the presence of $Mo(CO)_6$ for 25 min to form **12** with a mass increase of 24 mg on the resin *i.e.* approximately a full loading. **12** was then reacted with triphenylphosphine to assess removal of the fragment from the

support (Scheme 18). The formation of $Mo(CO)_4(PPh_3)_2$ is clearly evident from IR and ^{31}P NMR spectra which correspond with the literature.[29]

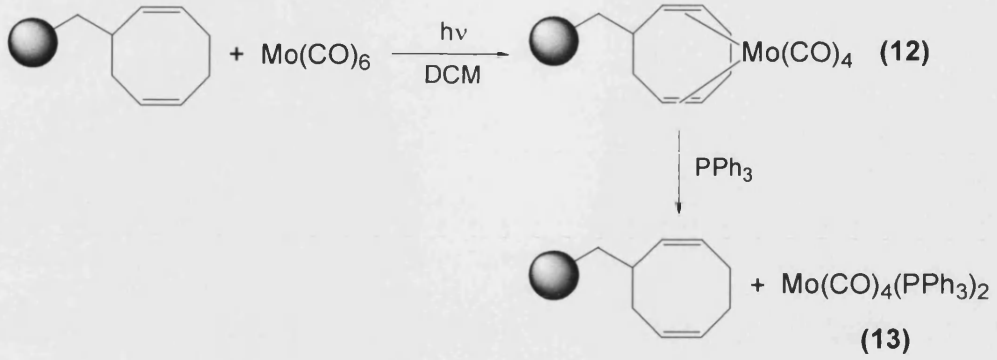

Scheme 18

6.3 Conclusions

The organometallic fragments $[Ru(CO)_4]$ and $[Mo(CO)_5]$ were successfully supported on two different alkene functionalised polymer supports providing a storable source of these fragments for use in synthetic transformations. Reactions were carried out homogeneously using 1-octene and methyl acrylate to gather data which could be used to aid the monitoring of analogous solid phase reactions with 3-butenyl polystyrene and REM resin, respectively. It was possible to correlate spectra from the heterogeneous reactions with those from the solution phase and in so doing confirm the formation of polymer-supported organometallic fragments.

The ability to remove the fragments from the support for use in synthesis was then investigated by a series of ligand exchange reactions using triphenylphosphine. From solution phase studies we know that olefins with electron withdrawing groups present form more stable complexes than those with hydrocarbon substituents and this was reflected in the results of our solid phase reactions.

For the ruthenium fragments, $[Ru(CO)_4]$ on 3-butenyl polystyrene **(5)** showed greater reactivity in substitution reactions than the fragment supported on REM resin **(6)**. The REM resin supported $[Mo(CO)_5]$ fragment **(9)** was also found to be a more stable complex, though the molybdenum fragments proved to be much less stable than their ruthenium counterparts, which could be left in air for a couple of days without decomposition.

Ligand exchange reactions at room temperature showed that only small amounts of metal are removed from the support (~30%) but it was found that gently warming the reaction to 40°C overnight increased the percentage of metal removal to around 80% making these supported organometallics much more efficient as transfer agents.

In an extension to this work a resin functionalised with cyclooctadiene was reacted with $Ru_3(CO)_{12}$ and $Mo(CO)_6$ in an attempt to prepare a source of $[Ru(CO)_3]$ and $[Mo(CO)_4]$, respectively. In the case of the former the reaction went against our expectations and formed an η^2 complex rather than the desired η^4 complex as evidenced by the formation of $Ru(CO)_4(PPh_3)$ in subsequent ligand exchange reactions. $Mo(CO)_6$ is highly reactive and supporting $[Mo(CO)_4]$ seems to be more achievable according to the formation of $Mo(CO)_4(PPh_3)_2$ as observed from IR and ^{31}P NMR spectra. Very little of the organometallic

fragment was removed from the support in ligand exchange reactions at room temperature and 40°C and this needs to be investigated further.

In all reactions, were IR spectroscopy confirmed the formation of desired products in ligand exchange reactions, ^{31}P NMR shows that in most cases there is unreacted triphenylphosphine present. This may be due to low metal loadings which so far have been approximated.

6.4 Experimental

All reagents were used as acquired and all reactions carried out under a nitrogen atmosphere unless otherwise stated. Infrared spectra were recorded on a Perkin Elmer 'Spectrum One' FTIR spectrometer using either a solution cell (NaCl, 0.5 mm) or a diamond compression cell accessory for single bead FTIR measurements. All data is given in wavenumbers (cm^{-1}) and using the following abbreviations: vs. – very strong, s – strong, m – medium, br – broad, sh – shoulder.

^{13}C, ^{31}P and ^{1}H NMR spectra were recorded on a Bruker 400MHz Fourier-transform NMR spectrometer using $CDCl_3$ as solvent. Data reported using chemical shift, δ (ppm), relative to the TMS internal standard for ^{1}H and phosphoric acid for ^{31}P. Photochemical reactions were performed using a 125W mercury arc broadband UV lamp. The photolysis vessel was wrapped in aluminium foil to maximise efficiency.

6.4.1 Polymer-Supported Organometallics (Alkene functionality)

6.4.1.1 Photolysis of $Ru_3(CO)_{12}$ – Homogeneous reactions

6.4.1.1.1 Preparation of $Ru(CO)_4(H_2C{=}CHCO_2Me)$ (4)

To an HPLC grade dichloromethane solution (100 ml) of $Ru_3(CO)_{12}$ (20.4 mg, 0.03 mmol) was added methyl acrylate (1 ml, 11.1 mmol). The mixture was irradiated with a UV source whilst bubbling nitrogen through the photolysis vessel. The progress of this reaction was monitored using solution IR spectroscopy with spectra recorded at 5 min intervals. Disappearance of starting material peaks observed after 10 min.

Solution IR (CH_2Cl_2): υ(CO)cm^{-1}: 2120w, 2062sh, 2033vs, 2006w.

Triphenylphosphine (10.7 mg, 0.04 mmol) was added to the solution and the mixture stirred overnight at room temperature.

Solution IR (CH_2Cl_2): υ(CO)cm^{-1}: *$Ru(CO)_4PPh_3$* – 2063w, 1985s, 1943vs,br.

6.4.1.1.2 Preparation of $Ru(CO)_4(H_2C{=}CHC_6H_{13})$

To an HPLC grade dichloromethane solution (100 ml) of $Ru_3(CO)_{12}$ (21.8 mg, 0.03 mmol) was added 1-octene (3.65mg, 1 eq, 0.03 mmol). The mixture was irradiated with a UV source

whilst bubbling nitrogen through the photolysis vessel. Further 1-octene (1 ml, 6.37 mmol) was added after 10 min. The progress of this reaction was monitored using solution IR spectroscopy with spectra recorded at 5 min intervals. Complete disappearance of starting material peaks was found after 25 min.

Solution IR (CH_2Cl_2): υ(CO)cm^{-1}: 2136w, 2075sh, 2050s, 2015m.

Triphenylphosphine (10 mg, 0.038 mmol) was added to the solution and the mixture stirred overnight.

Solution IR (CH_2Cl_2): υ(CO)cm^{-1}: 2063w, 1985s, 1943br.

6.4.1.2 Photolysis of $Ru_3(CO)_{12}$ – Heterogeneous reactions

6.4.1.2.1 Preparation of polymer-supported $Ru(CO)_4(HC{=}CR)$ (5)

To a dry DCM solution (100 ml) of $Ru_3(CO)_{12}$ (53.0 mg, 0.08 mmol) was added **1** (99.5 mg, 0.39 mmol, resin loading 3.9 mmol g^{-1}). The mixture was irradiated with a UV source for 35 min whilst bubbling nitrogen through the photolysis vessel. The beads (0.102g) were filtered and washed with DCM and hexane sequentially and then dried under reduced pressure.

IR: beads after reaction, υ(CO)cm^{-1}: 2104w, 2020s, 1985vs.

2.5 mg of $Ru(CO)_4$ on 0.1 g resin $\Rightarrow$ 0.012 mmol on 0.1 g $\Rightarrow$ 0.117 mmol $Ru(CO)_4$ per g of resin.

6.4.1.2.2 Ligand substitution with (5) at Room Temperature

5 (26 mg, 0.003 mmol, assuming resin loading 0.117 mmol g^{-1}) were swollen in dry DCM (10 ml), and to this suspension was added triphenylphosphine (1 ml of solution of PPh_3 (4 mg) in dry DCM (10 ml), 0.8 mg, 1 eq, 0.003 mmol). The mixture was left to stir overnight at room temperature. The beads were then filtered and washed with DCM and hexane sequentially and then dried under reduced pressure. The filtrate was concentrated under reduced pressure and a solution IR spectrum recorded. The solvent was removed under reduced pressure and remaining solid (0.004 g) dissolved in $CDCl_3$ to obtain a ^{31}P NMR spectrum.

IR (beads): υ(CO) cm^{-1}: 2054m, 1982m.

Solution IR (CH_2Cl_2): υ(CO) cm^{-1}: 2059s, 1995s.

^{31}P NMR: NMR spectrum of all of concentrated filtrate: 30.4 [$Ph_3P(O)$], 18.2 [$Ru(CO)_4(PPh_3)$], -4.2 [PPh_3].

6.4.1.2.3 Ligand substitution with (5) at 40°

As above using **5** (25.2 mg, 0.003 mmol, assuming resin loading 0.117 mmol g^{-1}) and the mixture was left to stir overnight at 40°C. The remaining solid (0.007g) dissolved in $CDCl_3$ for ^{31}P NMR.

IR (beads): υ(CO) cm^{-1}: 2052m, 1982m.

Solution IR (CH_2Cl_2): υ(CO) cm^{-1}: 2057vs, 1995vs.

^{31}P NMR: NMR spectrum of all of concentrated filtrate: 30.5 [$Ph_3P(O)$], 18.2 [$Ru(CO)_4(PPh_3)$], -4.2 [PPh_3]

6.4.1.2.4 Preparation of polymer-supported $Ru(CO)_4(HC{=}CR)$ (6)

To a dry DCM solution (100 ml) of $Ru_3(CO)_{12}$ (30.0 mg, 0.05 mmol) was added **2** (102 mg, 0.11 mmol, resin loading 1.06 mmol g^{-1}). The mixture was irradiated with a UV source for 35 min whilst bubbling nitrogen through the photolysis vessel. The beads (0.1064g) were filtered and washed with DCM and hexane sequentially and then dried under reduced pressure.

IR: beads after reaction, υ(CO)cm^{-1}: 2115w, 2034vs, 2001s, 1961m.

4.6 mg of $Ru(CO)_4$ on 0.1 g resin $\Rightarrow$ 0.022 mmol on 0.1 g $\Rightarrow$ 0.216 mmol $Ru(CO)_4$ per g of resin.

6.4.1.2.5 Ligand substitution with (6) at Room Temperature

6 (26.4 mg, 0.01 mmol, assuming resin loading 0.216 mmol g^{-1}) were swollen in dry DCM (10 ml), and to this suspension was added triphenylphosphine (1 ml of solution of 14.4 mg PPh_3 in dry DCM (10 ml), 1.44 mg, 1 eq, 0.01 mmol). The mixture was left to stir overnight at room temperature. The beads (26 mg) were then filtered and washed with DCM and hexane sequentially and then dried under reduced pressure. The filtrate was concentrated under reduced pressure and a solution IR spectrum recorded. The solvent was removed under

reduced pressure and remaining solid (0.002 g) dissolved in $CDCl_3$ to obtain a ^{31}P NMR spectrum.

IR (beads): υ(CO) cm^{-1}: 2115w, 2033s, 2000m, 1950m.

Solution IR (CH_2Cl_2): υ(CO) cm^{-1}: 2057s, 1994br, 1955s.

^{31}P NMR: NMR spectrum of all of concentrated filtrate, 30.5 [$Ph_3P(O)$], 18 [$Ru(CO)_4(PPh_3)$], -4.3 ppm [PPh_3].

6.4.1.2.6 Ligand substitution with (6) at 40°

As above using **6** (26.2 mg, 0.01 mmol, assuming resin loading 0.216 mmol g^{-1}) and the mixture left to stir overnight at 40°C. The remaining solid (0.002 g) dissolved in $CDCl_3$ for ^{31}P NMR.

IR (beads): υ(CO) cm^{-1}: 2115w, 2032s, 2001m, 1953br.

Solution IR (CH_2Cl_2): υ(CO) cm^{-1}: 2058s, 1995s.

^{31}P NMR: NMR spectrum of all of concentrated filtrate, 30.5 [$Ph_3P(O)$], 18.2 [$Ru(CO)_4(PPh_3)$], -4.2 ppm [PPh_3].

6.4.1.3 Photolysis of $Mo(CO)_6$ – Homogeneous Preparations

6.4.1.3.1 Preparation of $Mo(CO)_5(H_2C{=}CHCO_2Me)$ (7)

To a hexane solution (100 ml) of $Mo(CO)_6$ (20.5 mg, 0.08 mmol) was added methyl acrylate (0.1 ml, 1.11 mmol). The mixture was irradiated with a UV source whilst bubbling nitrogen through the photolysis vessel. The progress of this reaction was monitored using solution IR spectroscopy with spectra recorded at 5 min intervals. Further methyl acrylate (0.1 ml, 1.11 mmol) was added after 5 min. Disappearance of starting material peaks observed after 10 min.

Solution IR (hexane): υ(CO)cm^{-1}: 2091w, 1979m, 1967m.

The reaction mixture was split equally between two flasks. Triphenylphosphine (10.2 mg, 0.04 mmol) was added to each solution and the mixture stirred overnight at room temperature and 40°C.

Solution IR(hexane): υ(CO)cm^{-1}: 1991m, 1950vs,br.

^{31}P NMR: NMR spectrum of all of concentrated filtrate: 39.1 [$Mo(CO)_4(PPh_3)_2$], -4 ppm [PPh_3].

6.4.1.3.2 Preparation of $Mo(CO)_5(H_2C{=}CHC_6H_{13})$

To a hexane solution (100 ml) of $Mo(CO)_6$ (40.0 mg, 0.15 mmol) was added 1-octene (1 ml, 6.37 mmol). The mixture was irradiated with a UV source whilst bubbling nitrogen through the photolysis vessel. The progress of this reaction was monitored using solution IR spectroscopy with spectra recorded at 5 min intervals. Further 1-octene (0.50 ml, 3.19 mmol) was added after 15 and 20 min. Disappearance of starting material peaks observed after 25 min.

Solution IR (hexane): υ(CO)cm^{-1}: 2081 w, 1967 m.

The reaction mixture was split equally between two flasks. Triphenylphosphine (19.9 mg, 0.15 mmol) was added to each solution and the mixture stirred overnight at room temperature and 40°C.

Solution IR(hexane): υ(CO)cm^{-1}: 2073m, 1988m, 1951vs,br.

^{31}P NMR: NMR spectrum of all of concentrated filtrate, 39.1 [$Mo(CO)_4(PPh_3)_2$], - 4 ppm [PPh_3].

6.4.1.4 Photolysis of $Mo(CO)_6$ – Heterogeneous Preparations

6.4.1.4.1 Preparation of polymer-supported $Mo(CO)_5(HC{=}CR)$ (8)

To a dry DCM solution (100 ml) of $Mo(CO)_6$ (100 mg, 0.38 mmol) was added **1** (101 mg, 0.39 mmol, resin loading 3.9 mmol g^{-1}). The mixture was irradiated with a UV source for 25 min whilst bubbling nitrogen through the photolysis vessel. The dark brown beads (0.116 g) were filtered and washed with DCM and hexane sequentially and then dried under reduced pressure.

IR: beads after 25 min irradiation, υ(CO)cm^{-1}: 2079 m, 1984 vs, 1957 vs,br.

15.4 mg of $Mo(CO)_5$ on 0.1 g resin ⇒ 0.065 mmol on 0.1 g ⇒ assume full loading of 0.653 mmol $Mo(CO)_5$ per g of resin.

6.4.1.4.2 Ligand Substitution with (8) at Room Temperature

8 (26.8 mg, 0.02 mmol, assuming resin loading 0.653 mmol g^{-1}) were swollen in dry DCM (10 ml), and to this suspension was added triphenylphosphine (4.1 mg, 1 eq, 0.02 mmol). The mixture was left to stir overnight at room temperature. The light brown beads (26.5 mg) were then filtered and washed with DCM and hexane sequentially and then dried under reduced pressure. The filtrate was concentrated under reduced pressure and a solution IR spectrum recorded. The solvent was removed under reduced pressure and remaining off white solid (0.004 g) dissolved in $CDCl_3$ to obtain a ^{31}P NMR spectrum.

IR (beads): υ(CO) cm^{-1}: 2043w, 1986m, 1944vs.

Solution IR (CH_2Cl_2): υ(CO) cm^{-1}: *$Mo(CO)_5(PPh_3)$* – 2072s, 1945vs.

^{31}P NMR: NMR spectrum of all of concentrated filtrate, 38.9 $[Mo(CO)_4(PPh_3)_2]$, 30.3 $[Mo(CO)_5(PPh_3)]$ ppm.

6.4.1.4.3 Ligand Substitution with (8) at 40°

As above using **8** (26.2 mg, 0.02 mmol, assuming resin loading 0.653 mmol g^{-1}) and the mixture was left to stir overnight at 40°C. The remaining solid (0.006 g) dissolved in $CDCl_3$ to obtain a ^{31}P NMR spectrum.

IR (beads): υ(CO) cm^{-1}: 2043vw, 1983w, 1944vs.

Solution IR (CH_2Cl_2): υ(CO) cm^{-1}: *$Mo(CO)_5(PPh_3)$* – 2072s, 1945vs.

^{31}P NMR: NMR spectrum of all of concentrated filtrate, 30.4 $[Mo(CO)_5(PPh_3)]$; 38.9 ppm $[Mo(CO)_4(PPh_3)_2]$.

6.4.1.4.4 Preparation of polymer-supported $Mo(CO)_5(HC{=}CR)$ (9)

To a dry DCM solution (100 ml) of $Mo(CO)_6$ (27.9 mg, 0.11 mmol) was added **2** (100 mg, 0.11 mmol, resin loading 1.06 mmol g^{-1}). The mixture was irradiated with a UV source for 25 min whilst bubbling nitrogen through the photolysis vessel. The dark brown beads (0.126 g)

were filtered and washed with DCM and hexane sequentially and then dried under reduced pressure.

IR: beads after 25 min irradiation, υ(CO)cm^{-1}: 2089m, 2032w, 1978vs,br.

25.5 mg of $Mo(CO)_5$ on 0.1 g resin $\Rightarrow$ 0.108 mmol on 0.1 g $\Rightarrow$ assume full loading of 1.06 mmol $Mo(CO)_5$ per g of resin.

6.4.1.4.5 Ligand substitution with (9) at Room Temperature

9 (24.5 mg, 0.03 mmol, assuming resin loading 1.06 mmol g^{-1}) were swollen in dry DCM (10 ml), and to this suspension was added triphenylphosphine (6.8 mg, 1 eq, 0.03 mmol). The mixture was left to stir overnight at room temperature. The light brown beads (23.7 mg) were then filtered and washed with DCM and hexane sequentially and then dried under reduced pressure. The filtrate was concentrated under reduced pressure and a solution IR spectrum recorded. The solvent was removed under reduced pressure and remaining off white solid (0.008g) dissolved in $CDCl_3$ to obtain a ^{31}P NMR spectrum.

IR (beads): υ(CO) cm^{-1}: 2031w, 1993s.

Solution IR (CH_2Cl_2): υ(CO) cm^{-1}: *$Mo(CO)_5(PPh_3)$* – 2072m, 1945vs.

^{31}P NMR: NMR spectrum of all of concentrated filtrate, 30.3 [$Mo(CO)_5(PPh_3)$], 38.9 [$Mo(CO)_4(PPh_3)_2$], – 4.2 ppm [PPh_3].

6.4.1.4.6 Ligand substitution with (9) at 40°

As above using **9** (25.4 mg, 0.03 mmol, assuming resin loading 1.06 mmol g^{-1}) and the mixture was left to stir overnight at 40°C. The remaining solid (0.013g) dissolved in $CDCl_3$ to obtain a ^{31}P NMR spectrum.

IR (beads): υ(CO) cm^{-1}: 2027w, 1986sh.

Solution IR (CH_2Cl_2): υ(CO) cm^{-1}: *$Mo(CO)_5(PPh_3)$* – 2072m, 1946vs.

^{31}P NMR: NMR spectrum of all of concentrated filtrate, 30.6 [$Mo(CO)_5(PPh_3)$], 38.9 [$Mo(CO)_4(PPh_3)_2$], – 4.18 ppm [PPh_3].

6.4.2 Polymer-Supported Organometallics (Diene functionality)

6.4.2.1 Photolysis of $Ru_3(CO)_{12}$

6.4.2.1.1 Preparation of polymer-supported $Ru(CO)_3$ (11)

To a dry DCM solution (100 ml) of $Ru_3(CO)_{12}$ (19.3 mg, 0.03 mmol) was added **10** (94.8 mg, 0.09 mmol, resin loading 0.9 mmol g^{-1}). The mixture was irradiated with a UV source for 35 min whilst bubbling nitrogen through the photolysis vessel. The beads (0.113g) were filtered and washed with DCM and hexane sequentially and then dried under reduced pressure.

IR: beads after reaction, υ(CO)cm^{-1}: 2055w, 1978sh, 1964br.

18.5 mg of $Ru(CO)_3$ on 0.1 g resin $\Rightarrow$ 0.1 mmol on 0.1 g $\Rightarrow$ *suggests full loading* 0.9 mmol $Ru(CO)_3$ per g of resin.

6.4.2.1.2 Ligand Substitution using (11) at Room Temperature

11 (26 mg, 0.02 mmol, assuming resin loading 0.9 mmol g^{-1}) were swollen in dry DCM (10 ml), and to this suspension was added triphenylphosphine (13.1 mg, 2 eq, 0.04 mmol). The mixture was left to stir overnight at room temperature. The beads (25 mg) were then filtered and washed with DCM and hexane sequentially and then dried under reduced pressure. The filtrate was concentrated under reduced pressure and a solution IR spectrum recorded. The solvent was removed under reduced pressure and remaining solid (0.013 g) dissolved in $CDCl_3$ to obtain a ^{31}P NMR spectrum.

IR (beads): υ(CO) cm^{-1}: 2049w, 2026w, 1983sh, 1953s.

Solution IR (CH_2Cl_2): υ(CO) cm^{-1}: (*PPh_3* – 1957s.) 2058s, 1994br $\Rightarrow$ $Ru(CO)_4(PPh_3)$

^{31}P NMR: NMR spectrum of all of concentrated filtrate, 30.4 [$Ph_3P(O)$], 18.3 [$Ru(CO)_4(PPh_3)$], -4.2 ppm [PPh_3].

6.4.2.1.3 Ligand Substitution using (11) at 40°

As above using **11** (24.6 mg, 0.02 mmol, assuming resin loading 0.9 mmol g^{-1}) and the mixture was left to stir overnight at 40°C. The remaining solid (0.017 g) dissolved in $CDCl_3$ to obtain a ^{31}P NMR spectrum.

IR (beads): υ(CO) cm^{-1}: 2049w, 2026w, 1980sh, 1947s.

Solution IR (CH_2Cl_2): υ(CO) cm^{-1}: *$Ru(CO)_4(PPh_3)$* - 2058s, 1995br. *PPh_3* – 1957s

^{31}P NMR: NMR spectrum of all of concentrated filtrate, 30.4 [$Ph_3P(O)$], 18.3 [$Ru(CO)_4(PPh_3)$], -4.2 ppm [PPh_3].

6.4.2.2 Photolysis of $Mo(CO)_6$

6.4.2.2.1 Preparation of polymer-supported $Mo(CO)_4$ (12)

To a dry DCM solution (100 ml) of (24.4 mg, 0.09mmol) was added **10** (101.2 mg, 0.09 mmol, resin loading 0.9 mmol g^{-1}). The mixture was irradiated with a UV source for 25 min whilst bubbling nitrogen through the photolysis vessel. The beads (0.125g) were filtered and washed with DCM and hexane sequentially and then dried under reduced pressure for several hours.

IR: beads after reaction, υ(CO)cm^{-1}: 2034s, 1983sh, 1939vs, 1891s

24 mg of $Mo(CO)_4$ on 0.1 g resin ⇒ *assume full loading* 0.9 mmol $Mo(CO)_4$ per g of resin.

6.4.2.2.2 Ligand Substitution using (12) at Room Temperature

12 (26.2 mg, 0.02mmol, assuming resin loading 0.9 mmol g^{-1}) were swollen in dry DCM (10 ml), and to this suspension was added triphenylphosphine (14.7 mg, ~2 eq, 0.03 mmol). The mixture was left to stir overnight at room temperature. The beads (26 mg) were then filtered and washed with DCM and hexane sequentially and then dried under reduced pressure. The filtrate was concentrated under reduced pressure and a solution IR spectrum recorded. The solvent was removed under reduced pressure and remaining solid (0.015 g) dissolved in $CDCl_3$ to obtain a ^{31}P NMR spectrum.

IR (beads): υ(CO) cm^{-1}: 2034m, 1939s, 1891s.

Solution IR (CH_2Cl_2): υ(CO) cm^{-1}: *$Mo(CO)_4(PPh_3)_2$* – 2021m, 1919sh, 1906vs,br, 1884sh.

^{31}P NMR: NMR spectrum of all of concentrated filtrate, 39.3 [$Mo(CO)_4(PPh_3)_2$], 30.5 [$Mo(CO)_5(PPh_3)$], -4.2 ppm [PPh_3].

6.4.2.2.3 Ligand Substitution using (12) at 40°

As above using **12** (24.6 mg, 0.02 mmol, assuming resin loading 0.9 mmol g^{-1}) and the mixture was left to stir overnight at 40°C. The remaining solid (0.014 g) dissolved in $CDCl_3$ to obtain a ^{31}P NMR spectrum.

IR (beads): υ(CO) cm^{-1}: 2034m, 1939s, 1888w.

Solution IR (CH_2Cl_2): υ(CO) cm^{-1}: 2021m, 1919sh, 1904vs,br, 1884sh.

^{31}P NMR: NMR spectrum of all of concentrated filtrate: 39.3 $[Mo(CO)_4(PPh_3)_2]$, 30.5 $[Mo(CO)_5(PPh_3)]$, -4.2 ppm $[PPh_3]$.

6.5 References

1. Johnson, B. F. G.; Lewis, J.; Pippard, D., *J. Organomet. Chem.,* 1978, **160**, 263-274.
2. Johnson, B. F. G.; Lewis, J.; Pippard, D. A., *J. Chem. Soc. Dalton Trans.,* 1981, 407-412.
3. Tachikawa, M.; Shapley, J. R., *J. Organomet. Chem.,* 1977, **124**, C19-C22.
4. Schriver, D. F.; Bruce, M. I. In *Comprehensive Organometallic Chemistry II*; Pergamon: New York, 1995; Vol. 7; pp. 843.
5. Foulds, G. A.; Johnson, B. F. G.; Lewis, J., *J. Organomet. Chem.,* 1985, **296**, 147-153.
6. Wrighton, M. S.; Ginley, D. S., *J. Am. Chem. Soc.,* 1975, **97**, 4246-4251.
7. Desrosiers, M. F.; Wink, D. A.; Trautman, R.; Friedman, A. E.; Ford, P. C., *J. Am. Chem. Soc.,* 1986, **108**, 1917-1927.
8. Desrosiers, M. F.; Ford, P. C., *Organometallics,* 1982, **1**, 1715-1716.
9. Malito, J.; Markiewicz, S.; Poe, A., *Inorg. Chem.,* 1982, **21**, 4335-4337.
10. Dibenedetto, J. A.; Ryba, D. W.; Ford, P. C., *Inorg. Chem.,* 1989, **28**, 3503-3507.
11. Grevels, F. W.; Klotzbucher, W. E.; Schrickel, J.; Schaffner, K., *J. Am. Chem. Soc.,* 1994, **116**, 6229-6237.
12. Bentsen, J. G.; Wrighton, M. S., *J. Am. Chem. Soc.,* 1987, **109**, 4530-4544.
13. Leadbeater, N. E., *J. Organomet. Chem.,* 1999, **573**, 211-216.
14. Johnson, B. F. G.; Lewis, J.; Twigg, M. V., *J. Organomet. Chem.,* 1974, **67**, C75-C76.
15. Leadbeater, N. E., *J. Chem. Soc. Dalton Trans.,* 1995, 2923-2934.
16. Edwards, A. J.; Leadbeater, N. E.; Lewis, J.; Raithby, P. R., *J. Organomet. Chem.,* 1995, **503**, 15-20.
17. Leadbeater, N. E., *Inorg. Chem. Commun.,* 2001, **4**, 395-397.
18. Wuu, Y. M.; Bentsen, J. G.; Brinkley, C. G.; Wrighton, M. S., *Inorg. Chem.,* 1987, **26**, 530-540.
19. Grevels, F. W.; Reuvers, J. G. A.; Takats, J., *J. Am. Chem. Soc.,* 1981, **103**, 4069-4073.
20. Grevels, F. W.; Reuvers, J. G. A.; Takats, J., *Angew. Chem. Int. Edit. Engl.,* 1981, **20**, 452-460.
21. Boussie, T. R.; Coutard, C.; Turner, H.; Murphy, V.; Powers, T. S., *Angew. Chem.-Int. Edit.,* 1998, **37**, 3272-3275.
22. Boussie, T. R.; Murphy, V.; Hall, K. A.; Coutard, C.; Dales, C.; Petro, M.; Carlson, E.; Turner, H. W.; Powers, T. S., *Tetrahedron,* 1999, **55**, 11699-11710.

23. Clapham, B.; Reger, T. S.; Janda, K. D., *Tetrahedron,* 2001, **57**, 4637-4662.
24. Heinze, K.; Winterhalter, U.; Jannack, T., *Chem. Eur. J.,* 2000, **6**, 4203-4210.
25. Reginato, G.; Taddei, M., *Farmaco,* 2002, **57**, 373-384.
26. Leadbeater, N. E.; van der Pol, C., *Chem. Commun.,* 2001, 599-600.
27. Kerr, W. J.; Lindsay, D. M.; Watson, S. P., *Chem. Commun.,* 1999, 2551-2552.
28. Heinze, K., *Chem.-Eur. J.,* 2001, **7**, 2922-2932.
29. Varshney, A.; Gray, G. M., *Inorg. Chim. Acta,* 1988, **148**, 215-222.